



Immune modulation in the prevention of pathologies relating to diet-induced obesity

Thesis submitted for the degree of
Doctor of Philosophy
at the University of Leicester

By

Ramiar Kamal Kheder

(BSc, MSc)

Department of Infection, Immunity, and Inflammation

University of Leicester

June 2017

Abstract

Immune modulation in the prevention of pathologies relating to diet-induced obesity

Ramiar Kamal Kheder

Non-alcoholic fatty liver disease (NAFLD) results from accumulation of fat in liver, so-called steatosis. Fatty liver may lead to the development of inflammation (steatohepatitis). This study analysed the role of high fat diet, Vitamin D, and complement properdin in mouse models of high fat diet. Properdin knockout mice, and properdin wild type mice on LDLR^{-/-} and LDLR^{+/+} background were fed a high fat –high sugar diet or Western (high fat) diet. Body weight, fat pad weight, liver histopathology, immunohistochemistry were analysed. Hepatic expression of candidate genes (TNF- α , srebp-1c, TLR4, HMGCR, SR-B1, PPAR- γ) was performed by qPCR. ELISA was used to quantify serum insulin, Adiponectin, MDA. Liver function test, endotoxin, complement activation, Western blot were evaluated. *in vivo* results showed that a high fat–high sugar diet and so-called Western diet led to the development steatosis, inflammation, and properdin has a role in the prevention of obesity, and metabolic syndrome diseases. Vitamin D given to mice fed high fat –high sugar diet led to the prevention of obesity, and associated complications. Exercising mice combined with supplemented Vitamin D had a better effect to prevent metabolic syndrome diseases. *in vitro* results shown that DHA, Vitamin D, and Allicin had anti-inflammatory roles by reducing TNF- α to LPS stimulation.

Statement of originality

This accompanying thesis submitted for the degree of PhD entitled “Immune modulation in the prevention of pathologies relating to diet-induced obesity.” is based on work conducted by the author at the University of Leicester mainly during the period between November 2013 and October 2016.

All the work recorded in this thesis is original unless otherwise acknowledged in the text or by references.

None of the work has been submitted for another degree in this or any other University.

Signed: _____

Date: _____

Dedicated to the soul of my father

Acknowledgement

“Thanks to Allah for all his mercy, blessing and help throughout my life”

I would like to offer my deepest thanks, respect and gratitude to my PhD supervisor Dr Cordula Stover. Many thanks and higher gratitude for proposing this interesting study and for her supervision, advice, guidance and support throughout the time spent on this project. In addition, I would like to present my thanks to Dr Michael Browning, my second supervisor, for his encouragement and support. Heartiest thanks to Dr James Hobkirk as an external supervisor.

My thanks and appreciations are also offered to my sponsor Kurdistan region government under human capacity development programme.

Also I would thank my progress review panel members, Professor Nigel Brunskill and Dr Nicholas Lynch for their positive feedback and advice.

My thanks would be extended to my postgraduate tutor Dr Caroline Beardsmore.

I would like to thank Natalie Allcock of the electron microscopy laboratory for processing my samples for transmission electron microscopic and for providing me with such lovely images, and my thanks must go to Dr Michael Kelly for running MRI liver samples.

I would like to thank Dr Izzat Al-Rayahi for his support and guidance during my PhD study.

It is a pleasure to extend my special thanks to Dr Dr Simon Byrne, Dr Marwah Aldriwesh and all PhD students in lab 211b.

My special gratitude and thanks to my wonderful mother Khadija, my grandmother Safia and my brothers Mahmood and Masoud and sisters Nazifa and Faiza for giving me all the help and support I needed. My thanks go out to my cousins and friends for their unfailing friendship.

I would like to express my deep gratitude to my wife Mryam for her enormous support, and patience during my PhD study and our children Rabwn, Rahand, Rega, Renma and Aga who constantly reminded me of the truly important gifts in life and enabled me to keep my work in the right perspective.

With love,

Ramiar

Publications arising from this thesis

1. Kheder, R.K., Hobkirk, J. and Stover, C.M., 2016. **In vitro Modulation of the LPS-Induced Pro-inflammatory Profile of Hepatocytes and Macrophages- Approaches for Intervention in Obesity?** *Frontiers in Cell, and Developmental Biology*, 4.

A full version of the article can be found at the following link:
<http://journal.frontiersin.org/article/10.3389/fcell.2016.00061/full>

2- Kheder, R., Hobkirk, J., Saeed, Z., Janus, J., Carroll, S., Browning, M.J. and Stover, C., 2017. **Vitamin D3 supplementation of a high fat high sugar diet ameliorates prediabetic phenotype in female LDLR^{-/-} and LDLR^{+/+} mice.** *Immunity, Inflammation and Disease*.

A full version of the article can be found at the following link:
<http://onlinelibrary.wiley.com/doi/10.1002/iid3.154/full>

Seminar and Posters

1. Ramiar Kheder, Michael Browning, Cordula Stover. **The role of complement properdin in fatty liver disease. Poster presentation.** Fourth European Congress of Immunology (ECI 2015), Austria- Vienna. (Appendix I)

2- Ramiar Kheder and Cordula. **Approaches to refine animal experimentation in fatty liver disease model.** 3Rs Conference, Leicester UK. March 2016. Selected as one of the best posters (awarded prize). (Appendix II)

3- Ramiar Kheder, James Hobkirk, Michael Browning, Cordula Stover. **The role of Vitamin D3 in high fat diet induced fatty liver disease and Obesity.** 84th European Atherosclerosis Society Congress. 2016. Austria, Innsbruck. (Appendix III)

4- Ramiar Kheder, James Hobkirk, Michael Browning, Cordula Stover. **The role of Vitamin D3 and properdin in fatty liver disease.**

Presentation (Talk).The seventh annual postgraduate student conference, University of Leicester, Leicester, UK, April 2015.

5- Ramiar Kheder, James Hobkirk, Michael Browning, Cordula Stover. **The benefit of Vitamin D3 in high fat diet induced fatty liver disease and obesity.** Presentation (Talk).The 8th annual postgraduate student conference, University of Leicester, Leicester, UK, April 2016.

Table of contents

ABSTRACT.....	I
STATEMENT OF ORIGINALITY.....	II
ACKNOWLEDGEMENT.....	IV
TABLE OF CONTENTS.....	VI
LIST OF FIGURES.....	XI
LIST OF TABLES.....	XVII
CHAPTER 1 INTRODUCTION.....	1
1.1 Overview.....	2
1.2 Obesity and diet-induced complications.....	2
1.3 Obesity associated inflammation.....	5
1.4 Liver manifestation of diet-induced obesity.....	6
1.5 Triglyceride and fatty acid metabolism in the liver.....	10
1.6 The role of complement in metabolism.....	11
1.6.1 The complement system.....	11
1.6.2 Properdin and its role in complement system.....	12
1.6.3 Generation and function of complement C3a-desarg.....	14
1.7 Mouse model using LDLR ^{-/-}	18
1.8 Nutritional and lifestyle intervention in fatty liver disease.....	19
1.9 Hypotheses.....	20
1.10 Aims and objectives.....	21

CHAPTER 2	MATERIALS AND METHODS	22
2.1	Materials	23
2.1.1	Animals	23
2.1.2	HepG2 cell line	26
2.1.3	J774 cell line	26
2.2	Methods	27
2.2.1	Polymerase chain reaction (PCR).....	27
2.2.1.5	PCR.....	28
2.2.1.6	Agarose gel electrophoresis.....	29
2.2.2	Real-time quantitative polymerase chain reaction (RT-qPCR).....	29
2.2.3	Liver section staining	34
2.2.4	Electron microscopy (EM).....	35
2.2.5	Immunohistochemistry.....	36
2.2.5.1	Anti-F4/80 and C5L2 antibodies	36
2.2.6	Immunofluorescence for C5L2 antibody	38
2.2.7	Western blotting.....	39
2.2.7.1	Pierce™ 660nm protein assay	39
2.2.7.2	Adipose lysate preparation.....	39
2.2.7.3	Liver lysate preparation.....	39
2.2.7.4	Preparation of SDS-PAGE gels.....	40
2.2.7.5	SDS-PAGE gels staining.....	42
2.2.8	Investigation of iron storage by Prussian blue staining	42
2.2.8.2	Prussian blue staining	43
2.2.9	Limulus ameocyte lysate (LAL) endotoxin measurement.....	43
2.2.10	Glucose measurement	44
2.2.11	Insulin ELISA test.....	44
2.2.12	Liver function tests	45
2.2.13	Adiponectin ELISA test.....	46
2.2.14	Malondialdehyde (MDA) assay	46
2.2.15	Pro-inflammatory parameters.....	47
2.2.15.1	IL-6 ELISA.....	47
2.2.15.2	TNF- α ELISA test, supernatant and mice serum.....	48

2.2.16	C5a ELISA level	49
2.2.17	Lipid measurements	50
2.2.18	NEFA Measurement.....	51
2.2.19	Measurement of glycated haemoglobin in mouse serum (Ghb A 1C) 51	
2.2.20	Vitamin D serum mice measurement	52
2.2.21	Complement activation.....	52
2.2.22	Procedure of Mouse XL cytokine array kit.....	54
2.2.23	Microarray for adipose tissue	55
2.2.24	Detection of apoptosis by cytochemical method	56
2.2.25	HepG2 cells by Oil Red O staining.....	57
2.2.25.1	Intracellular lipid content assessment.....	57
2.2.25.2	Oil Red O staining measurement by spectrophotometer.....	57
2.2.26	Stimulation of macrophages <i>in vitro</i>	59
2.2.26.1	Using J774 cell line	59
2.2.26.2	Bone marrow derived macrophages.....	59
2.2.27	Data analysis.....	60
CHAPTER 3 CHARACTERISTICS OF COMMON NUTRIENT ADDITIVES WITH BENEFICIAL DIETARY EFFECT.....		
		62
3.1	Introduction	63
3.1.1	Anti-inflammatory Role of Allicin	63
3.1.2	Anti-inflammatory Role of Omega 3.....	64
3.1.3	Anti-inflammatory Role of Vitamin D	67
3.2	Result.....	67
3.2.1	The effect of anti-inflammatory agents (DHA, Vitamin D, Allicin) on LPS-induced TNF- α mRNA expression, and protein <i>in vitro</i>	67
3.2.2	Anti-inflammatory effect of Vitamin D on HepG2 cells	73
3.2.3	Stimulation of J774 cells with LPS, and Tunicamycin (ER stress marker) by using Oil Rd O staining method.....	74
3.2.4	Allicin has anti-inflammatory role on J774	75
3.3	Discussion.....	79

CHAPTER 4 THE EFFECTS OF VITAMIN D3 AS A NUTRACEUTICAL DURING HIGH FAT DIETS.....	82
4.1 Introduction	83
4.2 Results.....	88
4.2.1 Ten weeks study.....	88
4.2.2 Effect of Vitamin D on fatty liver disease in ten weeks.....	88
4.2.3 The effects of Vitamin D3 as a nutraceutical during high fat diets on Five weeks' diets	132
4.2.4 Effect of Vitamin D on Fatty liver disease in male mice	132
4.2.4.1.1 Electron microscopic analysis	132
4.3 Discussion.....	144
CHAPTER 5 THE ROLE OF PROPERDIN IN FATTY LIVER DISEASE ...	148
5.1 Introduction	149
5.2 Results.....	151
5.2.1 Effect of properdin on fatty liver disease in 10 weeks given diet.....	151
5.2.1.5 Analysis of measurements of Liver function	172
5.2.1.10 Lipid peroxidation product, and Vcam-1 mRNA as indicators of inflammatory endothelial damage.....	185
5.2.1.13 Analysis of adipokinins in epididymal fat pads	193
5.2.1.14 Apoptosis in liver	195
5.2.2 Effect of properdin on Fatty liver disease in five weeks diet.....	208
5.2.2.1 Histopathology of livers from male LDLR ^{-/-} mice in relation to properdin	208
5.3 Discussion.....	219
CHAPTER 6 THE ROLE OF EXERCISE AND VITAMIN D ON MICE INDUCED OBESITY	224
6.1 Introduction	225

6.2	Specific materials and methods	228
6.3	Result.....	229
6.3.1	Effect of exercise, and Vitamin D on fatty liver disease	229
6.3.1.3	Fat pad weight (g)	232
6.4	Discussion.....	249
CHAPTER 7 GENERAL DISCUSSION.....		252
7.1	Introduction	253
7.2	Characteristics of common nutrient additives with beneficial dietary effect 253	
7.3	The effects of Vitamin D3 as a nutraceutical during high fat diets.....	255
7.4	The role of properdin in fatty liver disease	262
7.5	The role of Exercise and Vitamin D on mice induced obesity	268
7.6	Limitations.....	270
7.7	Conclusions	271
7.8	Future plan.....	273
APPENDIX.....		274
REFERENCES.....		294

LIST OF FIGURES

Figure 1-1: High fat diet-induced complications: mechanisms of induction of insulin resistance.....	4
Figure 1-2: Pathophysiology of non-alcoholic fatty liver disease from steatosis to NASH.	10
Figure 1-3: A simplified overview of triggers and effects of complement activation and properdin functions.....	13
Figure 1-4: The proposed contributions of complement system activation products to the development of obesity and associated pathologies.	16
Figure 2-1 Genotyping of wildtype and properdin deficient mice by PCR.	25
Figure 2-2: SYBR Green-based RT-qPCR amplification chart.	30
Figure 2-3: Melting curve analysis confirming specific amplification from qPCR using SYBR green.....	31
Figure 2-4: 1 Kb Plus DNA Ladder in 1% agarose gel electrophoresis.1 Kb Plus DNA Ladder in 1% agarose gel electrophoresis, GAPDH size=130bp.	31
Figure 3-1 Mechanism action of DHA in macrophage, and adipocyte.....	66
Figure 3-2 DHA (16µg/ml), Vitamin D (4 µg/ml) preconditioning for 5 days.....	69
Figure 3-3 Vitamin D preconditioning for 1 day at different concentrations.	72
Figure 3-4 TNF-α mRNA expression in HepG2 cell.	73
Figure 3-5 Oil Red O staining in J774 stimulation with Tunicamycin and LPS. 74	
Figure 3-6 Using J774 cells to investigate TNF-α mRNA expression in the presence of Allicin.	75
Figure 3-7 Using Allicin as treating J774 cells after stimulation with LPS 100ng/ml.	76
Figure 3-8 ELISA test to investigate TNF-α protein in the presence of, Vitamin D, DHA and Allicin.....	78
Figure 4-1 Vitamin D3 synthesis and metabolism.	84
Figure 4-2 Proposed model of action of Vitamin D3 on macrophage or adipocyte.....	86
Figure 4-3 Proposed model of action of Vitamin D3 on muscle cells.	87

Figure 4-4 The effect of Vitamin D supplemented high fat high sugar diet compared to high fat high sugar diet in mice sera on Vitamin D levels.	90
Figure 4-5 The percentage of body weight gain in female mice.	92
Figure 4-6 Liver weights both in grams (g), and percentage of liver weight (%) in female mice.	93
Figure 4-7 The Epididymal fat pad (g) in male LDLR ^{-/-} mice.	94
Figure 4-8 Haematoxylin and eosin staining of paraffin embedded liver sections obtained from LDLR ^{-/-} mice.	97
Figure 4-9 Haematoxylin and eosin staining of paraffin embedded liver sections obtained from LDLR ^{+/+} mice	98
Figure 4-10 The effect of high fat high sugar diet with and without Vitamin D diet on liver function.	103
Figure 4-11 The effect of mice fed high fat high sugar diet with, and without Vitamin D diet on insulin, adiponectin, and HbA1c test.	107
Figure 4-12 The effect of mice fed high fat high sugar diet with, and without Vitamin D diet on hepatic gene expression of TNF- α , IL-6, and ELISA IL-6... ..	109
Figure 4-13 The effect of mice fed high fat high sugar diet with, and without Vitamin D diet on hepatic gene expression of TLR4 and serum endotoxin level.	111
Figure 4-14 The effect of mice fed high fat high sugar diet with, and without Vitamin D diet on hepatic gene expression of Srebp-1c.	112
Figure 4-15 The effect of mice fed high fat high sugar diet with, and without Vitamin D diet on triglyceride (TG) and NEFA serum level.	114
Figure 4-16 The effect of mice fed high fat high sugar diet with, and without Vitamin D diet on serum MDA level and aortic Vcam-1 mRNA expression.	116
Figure 4-17 Immunohistochemistry of liver paraffin sections of mice fed high fat high sugar diet with, and without Vitamin D.	118
Figure 4-18 The effect of mice fed high fat high sugar diet with, and without Vitamin D diet on splenic gene expression of iNOS and Arginase -1.	120
Figure 4-19 The effect of mice fed high fat high sugar diet with, and without Vitamin D diet on hepatic gene expression of iNOS and Arginase -1.	121
Figure 4-20 Prussian blue staining of splenocytes of mice fed high fat high sugar diet with, and without Vitamin D.	123

Figure 4-21 The effect of mice fed high fat high sugar diet with, and without Vitamin D diet on hepatic gene expression of genes involved in cholesterol metabolism.....	125
Figure 4-22 Mouse adipokine array detects multiple protein analyses in adipose tissue of mice.	127
Figure 4-23 The effect of mice fed high fat high sugar diet with, and without Vitamin D diet on functional complement residual activities.	129
Figure 4-24 Electron micrograph showing lipid droplets from livers of mice fed high fat diet with, and without Vitamin D.	133
Figure 4-25 Electron micrograph showing mitochondria from livers from mice fed high fat-high sugar diet with, and without Vitamin D.....	134
Figure 4-26 Electron micrograph showing mega mitochondria from livers of mice fed high fat -high sugar diet without Vitamin D.	135
Figure 4-27 Electron micrograph showing nuclei from livers of mice fed high fat-high sugar without Vitamin D.....	136
Figure 4-28 Haematoxylin and eosin staining of paraffin embedded liver sections obtained from mice.....	138
Figure 5-1 Roles of complement in lipid metabolism.....	150
Figure 5-2 The effect of properdin on body weight gain in female mice.	153
Figure 5-3 The effect of properdin on liver weight and the percentage of liver weight in female mice.....	156
Figure 5-4 The effect of properdin on liver weight and the percentage of liver weight in female mice.....	157
Figure 5-5 Haematoxylin, and eosin staining of paraffin embedded liver sections obtained from female LDLR ^{-/-} mice.....	159
Figure 5-6 Haematoxylin, and eosin staining of paraffin embedded liver sections obtained from female LDLR ^{+/+} mice.	160
Figure 5-7 Haematoxylin, and eosin staining of paraffin embedded liver sections obtained from male LDLR ^{-/-} mice.....	161
Figure 5-8 Haematoxylin, and eosin staining of paraffin embedded liver sections obtained from male LDLR ^{+/+} mice.....	162
Figure 5-9 Olive green stain in LDLR ^{+/+} mice.	166
Figure 5-10 Electron micrograph from liver LDLR ^{+/+} mice fed low fat diet. ...	167
Figure 5-11 Electron micrograph from liver LDLR ^{+/+} mice fed Western diet. ...	168

Figure 5-12 Electron micrograph showing lipid droplets from liver LDLR+/+ mice fed Western diet.....	169
Figure 5-13 Electron micrograph showing mitochondria from liver LDLR+/+ mice fed Western diet.....	170
Figure 5-14 The effect of properdin on hepatic gene expression of Srebp-1c.....	171
Figure 5-15 The effect of properdin on AST activity in female mice.....	173
Figure 5-16 The effect of properdin on AST and ALT activity in female and male mice.....	174
Figure 5-17 The effect of properdin on insulin and adiponectin protein in female mice sera.....	176
Figure 5-18 The effect of properdin on insulin, adiponectin, HbA1 activity in female and male mice sera.....	177
Figure 5-19 The effect of properdin on hepatic TNF- α IL-6 mRNA expression, IL-6 protein in female and male mice sera.....	179
Figure 5-20 The effect of properdin on hepatic TLR4 mRNA expression, endotoxin in female and male mice sera.....	181
Figure 5-21 The effect of properdin on triglyceride in female and male mice sera.....	183
Figure 5-22 The effect of properdin on NEFA in female and male mice sera.....	184
Figure 5-23 The effect of properdin on MDA assay test, and Vcam-1 in aorta.....	187
Figure 5-24 The effect of properdin on hepatic and splenic gene expression of iNOS.....	189
Figure 5-25 The effect of properdin on hepatic and splenic gene expression of Arginase-1.....	190
Figure 5-26 The effect of properdin on hepatic gene expression of SR-B1, HMGCR and PPAR γ	192
Figure 5-27 The Mouse adipokine array detects multiple protein analyses in adipose tissue of wildtype and deficient mice.....	194
Figure 5-28 Apoptosis test for liver sections of western diet.....	195
Figure 5-29 Body mass index (BMI), functional complement residual activities of human serum.....	197
Figure 5-30 The effect of properdin on complement classical pathway activation in female mice sera.....	199

Figure 5-31 The effect of properdin on complement alternative pathway activation and C5a in mice sera.	200
Figure 5-32 The effect of properdin on Vitamin D level of mice sera.....	201
Figure 5-33 mRNA expression of C5L2 in adipose tissue.....	204
Figure 5-34 Western blot of C5L2 protein presence in adipose tissue.	205
Figure 5-35 Western blot of C5L2 protein presence in livers.....	205
Figure 5-36 Immunohistochemistry of C5L2 adipose tissue of mice fed high sugar-high fat diet, and western diet.	206
Figure 5-37 Immunohistochemistry staining of livers of mice fed Western diet.	207
Figure 5-38 Immunofluorescent for adipose tissue of mice fed Western diet.	207
Figure 5-39 Immunofluorescent for livers of mice fed Western diet.	207
Figure 5-40 Electron micrograph showing fat droplets from livers of mice fed high fat diet for five weeks.....	209
Figure 5-41 Electron micrograph showing mitochondria from livers of mice fed high fat diet for five weeks.....	210
Figure 5-42 Haematoxylin and eosin staining of paraffin embedded liver sections obtained from mice.....	212
Figure 5-43 Percentage fat fraction using MRI of mouse livers from male mice (regardless diet).	213
Figure 6-1 Proposed model of action of exercise on muscle cells.....	228
Figure 6-2 The effect of exercise and Vitamin D on body weight measurement.	230
Figure 6-3 The effect of exercise and Vitamin D on liver weight measurement.	231
Figure 6-4 The effect of exercise and Vitamin D on epididymal fat pad weight measurement.	233
Figure 6-5 Haematoxylin and eosin staining of paraffin embedded liver sections obtained from mice.....	235
Figure 6-6 The effect of exercise and Vitamin D on TNF- α and IL-6 ELISA... ..	238
Figure 6-7 The effect of exercise and Vitamin D on NEFA assay in C57BL/6 mice sera.....	239
Figure 6-8 The effect of exercise and Vitamin D on Insulin ELISA in C57BL/6 mice sera.....	240

Figure 6-9 The effect of exercise and Vitamin D on functional classical and alternative complement pathway.....	242
Figure 6-10 Muscle cytokines array protein membrane spots (A) and representative examples (B).	245
Figure 6-11 Effect of exercise and Vitamin D on muscle cytokines.....	248
Figure 7-1 Roles of properdin in lipid metabolism.	272

List of tables

Table 2.1: Different diet components	25
Table 2.2 Sequences of primer pairs (with their annealing temperatures) used in this study for mouse.	33
Table 2.3 Sequences of primer pairs (with their annealing temperatures) used in this study for human.	34
Table 2.4 Primary and secondary antibodies for immunohistochemistry.	38
Table 2.5 Primary, and secondary antibody for Western blotting.	38
Table 2.6: Preparation of buffers for Western blot.....	41
Table 4.1 Lobular inflammation scores, and steatosis scores in LDLR ^{-/-} mice.	100
Table 4.2 Lobular inflammation scores, and steatosis scores in LDLR ^{+/+} mice.	101
Table 4.3 Male mice given high fat-high sugar diet with and without supplemented Vitamin D (58R3± Vitamin D) for five weeks.	141
Table 4.4 Female mice given high fat-high sugar diet with and without supplemented Vitamin D (58R3± Vitamin D) for five weeks.	142
Table 5.1 The effect of properdin on body weight, fat pad (weight gain and the percentage) in female and male mice.	154
Table 5.2 The effect of properdin on body weight, fat pad (weight gain and the percentage) in female and male mice.	154
Table 5.3 The effect of properdin on percentage body weight and fat pad weight (g) in female and male mice.	155
Table 5.4 Lobular inflammation (A) scores and steatosis scores (B) for male LDLR ^{-/-} PWT/PKO mice.....	163
Table 5.5 Lobular inflammation (A) scores, and steatosis scores (B) for female LDLR ^{+/+} PWT/PKO mice.....	164
Table 5.6 Lobular inflammation (A) scores, and steatosis scores (B) for male LDLR ^{+/+} PWT/PKO mice.....	164
Table 5.7 Lobular inflammation (A) scores, and steatosis scores (B) for male LDLR ^{-/-} PWT/PKO mice.....	165
Table 5.8 MRI of mouse livers from female, and male mice.	213
Table 5.9 Male mice, mice given high fat-high sugar diet for five weeks.....	216
Table 5.10 Female mice given high fat-high sugar diet for five weeks.	217

Table 5.11 Male mice given high fat-high sugar diet, and Western diet for five weeks.....	217
Table 5.12 Male mice given Western diet for five weeks.	218
Table 6.1 Scoring system in liver mice fed high fat-high sugar diet for five weeks.....	236
Table 6.2 All proteins detected in the microarray.	246

LIST OF ABBREVIATIONS

%: Percent
°C: Degree Celsius
ALT: Alanine Transaminase
AST: Aspartate Aminotransferase
BMDM: Bone marrow derived macrophages
BSA: Bovine serum albumin
C5aR: C5a receptors
CD: Cluster differentiation
cDNA: Complementary DNA
DHA: Docosahexaenoic acid
DNA: Deoxyribonucleic acid
EDTA: Ethylene diaminetetraacetic acid
e.g: example
ELISA: Enzymen-Linked immunosorbent assay
f: female
FCS: Fetal calf serum
FFA: Free fatty acid
GAPDH: Glyceraldehyde 3-phosphate dehydrogenase
GLUT4: Glucose transporter type 4
GM-CSF: Granulocyte/Macrophage Colony-Stimulating Factor
HbA1C: Glycated haemoglobin
HFD: High fat diet
58R3: high fat-high sugar diet
5TJN: Wester diet (high fat diet)
58R1: Low fat diet
HepG2: Human liver cell line
HRP: Horse reddish peroxidase
IGFBP: Insulin-like growth factor binding protein
IL: Interleukin
IMS: Industrial methylated spirit
J774: Macrophage cell line
Kb: kilo base
kDa: Kilo dalton
LAL: Limulus amebocyte Lysate
LDLR^{-/-}: Low density lipoprotein receptor knockout
LDLR^{+/+}: Low density lipoprotein receptor knockout
LFD: Low fat diet
LPS: Lipopolysaccharide
MCP-1: Monocyte Chemoattractant Protein-1
BM: Bone marrow
m: Male

mM: Milimolar
mm: millimetres.
mRNA: Messenger Ribonucleic acid
N=number of mice
NAFLD: Non-alcoholic fatty liver disease
NASH: Non-alcoholic steatohepatitis
NEFA: Non-esterified free fatty acid
ng: Nanogram
OD: Optical Density
PBS: Phosphate buffered saline
PCR: Polymerase Chain Reaction
PD mice: Name of Mice in the cage
PKO: properdin deficient mice
PWT: Properdin wild type mice
PPAR γ : Peroxisome proliferator-activated receptor γ
QPCR: Real-time Polymerase Chain Reaction
RNA: Ribonucleic acid
RNA: Ribonucleic acid
ROS: reactive oxygen species
RPMI: Roswell Park Memorial Institute medium
RT: Room temperture
SDS: Sodium Dodecyl Sulphate
TBS: Tris buffered saline
TEMED: N, N, N', N'-tetramethyl ethylene diamine
TG: Triglyceride
TLR: Toll like Receptor
TNF- α : Tumour Necrosis Factor Alpha
VLDL: very low density lipoprotein
v/v: volume/volume
w/v: weight/volume
WT: Wild-type
 μ l: Microliter
 μ m: Micrometer
 μ g: Microgram
MDA: Malondialdehyde
VD: Vitamin D

Chapter 1 Introduction

1.1 Overview

Insulin resistance, impaired postprandial lipid metabolism and the development or progression of non-alcoholic fatty liver disease (NAFLD) are metabolic syndrome diseases caused by increased fat intake, as in Western diets (Martins et al., 2015). Consumption of sugar in the form soft drinks contributes to the increased incidence of diabetes and associated cardiovascular disease. One of the WHO (World Health Organization) guidelines advises to reduce sugar intake by 5-10 % of the daily calorie intake to reduce metabolic syndrome diseases, because sugar is a major factor for developing diabetes mellitus type 2 (Zhang et al., 2012) and fatty liver disease (Lim et al., 2010). Fructose promotes *de novo* lipogenesis, hepatic, and skeletal insulin resistance (Lim et al., 2010). In the USA, obese adult people will increase to 11 million, and 65 million in the UK by 2030 (Wang et al., 2011). The third most common disease after cancer and cardiovascular disease is fatty liver disease, which increases mortality by 1.7-fold (Farrell and Larter, 2006).

1.2 Obesity and diet-induced complications

Obesity refers to an excess of body fat or adiposity, the extent of which is determined by calculating the so-called body mass index (BMI; in kg/m^2). It is a weight-for-height index that has correlation with adiposity. BMI of underweight ($\text{BMI} < 18.5 \text{ kg/m}^2$), normal weight ($18.5\text{--}24.9 \text{ kg/m}^2$), overweight ($25.0\text{--}29.9 \text{ kg/m}^2$) and obese ($\geq 30.0 \text{ kg/m}^2$) (Nuttall, 2015).

Chronic low-grade inflammation is a feature of obesity. Obesity is a main factor that develops NAFLD (Paschos and Paletas, 2009). There is a link between obesity, and inflammation; the pro-inflammatory cytokine tumor-necrosis factor (TNF)- α was expressed in adipose tissue (AT) of obese mice, and linked to insulin resistance (IR) (Hotamisligil et al., 1993). Adipose tissue, liver, and skeletal muscle play a significant role in glucose uptake, glucose production, and glucose processing (Hashimoto et al., 2012). Hepatic gluconeogenesis and lipogenesis were increased due to hepatic insulin resistance in mice and human (Perry et al., 2014). Free fatty acids (FFAs) accumulation develops into hepatic steatosis, and disruption of insulin signalling (Fabbrini et al., 2010). There is a link between dysfunctional glycogen synthesis, insulin resistance, and

dysregulation of fatty acid metabolism in skeletal muscle which results in impaired insulin signalling (Fabbrini et al., 2010). Adipose tissue is a lipid storage organ, which is composed of white and brown adipose tissue. The former is involved in insulin resistance and obesity, but the latter plays a positive function on insulin action. White adipose tissue expands due to weight gain; as the result, inflammatory cytokines are increased (McArdle et al., 2013). Insulin resistance develops in the obese state due to white adipose tissue expansion and immune cell recruitment, because white adipose tissue plays in the release of FFA, dysregulation of FFA metabolism, and insulin stimulated–glucose uptake (McArdle et al., 2013). Adipocyte fraction of obese mice showed elevation of IL-6, inducible nitric oxide synthase (iNOS), and MCP-1 (Weisberg et al., 2003). Obesity goes along with dysfunctional lipid metabolism, and impaired insulin signaling; thus, circulating free fatty acids (FFAs) play a negative effect on insulin target tissues. FFAs act through the activation of inflammatory pathways, via cell surface pattern recognition receptors (PRRs) (Shi et al., 2006). In addition, diacylglycerol (DAG), and ceramides, which are fatty acid metabolites, play a negative role on insulin action (Schenk et al., 2008). Central obesity and over-nutrition are features of non-alcoholic fatty liver disease (NAFLD), and type 2 diabetes (Farrell and Larter, 2006). Metabolic complications, including fasting hyperglycaemia, the elevation of serum lipids, and high blood pressure, are a key point to develop fatty liver disease (Farrell and Larter, 2006). Mice given high fat diet during pregnancy and lactation period induced metabolic abnormalities in the offspring (Kruse et al., 2013). Mice given high fat diet changed multiple molecular factors that act synergistically to increase the risk of colon cancer associated with obesity (Padidar et al., 2012). Colon cancer can be induced in rats given a high fat diet, and low dietary intakes of calcium, Vitamin D and folic acid, which was designed to mimic the human Western diet (Newmark et al., 2001).

Dietary food releases FFA after the meals. Insulin enters circulation via the portal blood stream Insulin, which is released from pancreatic β cells, acts on lipid metabolism in both liver, and adipose tissues (Saltiel and Kahn, 2001). In adipose tissue, high levels of insulin causes the initiation of triglyceride biosynthesis from FFAs (Parekh and Anania, 2007). In the liver through SREBP-1c expression and through PPAR γ in muscle, insulin promotes

lipogenesis, and increases lipid export (Kersten, 2001). Hepatic steatosis is caused by increased import and decreased export or oxidation of fatty acids. The actual mechanisms associated with development of NAFLD are de novo lipogenesis, increased adipose tissue lipolysis, increased dietary FFA levels, impaired β -oxidation, and impaired VLDL synthesis. These have a role in increasing accumulation of triglycerides, leading to NAFLD (Lau et al., 2017).

Liver FFAs are either comes from adipocytes lipolysis which store triglyceride or from dietary FFA. FFA may lead to β -oxidation in mitochondria to produce energy for cells and ketone bodies. In addition, FFA produce triglyceride which either it can be stored as lipid droplets or can be exported via very low-density lipoproteins (Sattiel and Kahn, 2001). In addition, in obesity, which causes insulin resistance, triglyceride levels in circulation are elevated because there is no VLDL inhibition (Parekh and Anania, 2007).

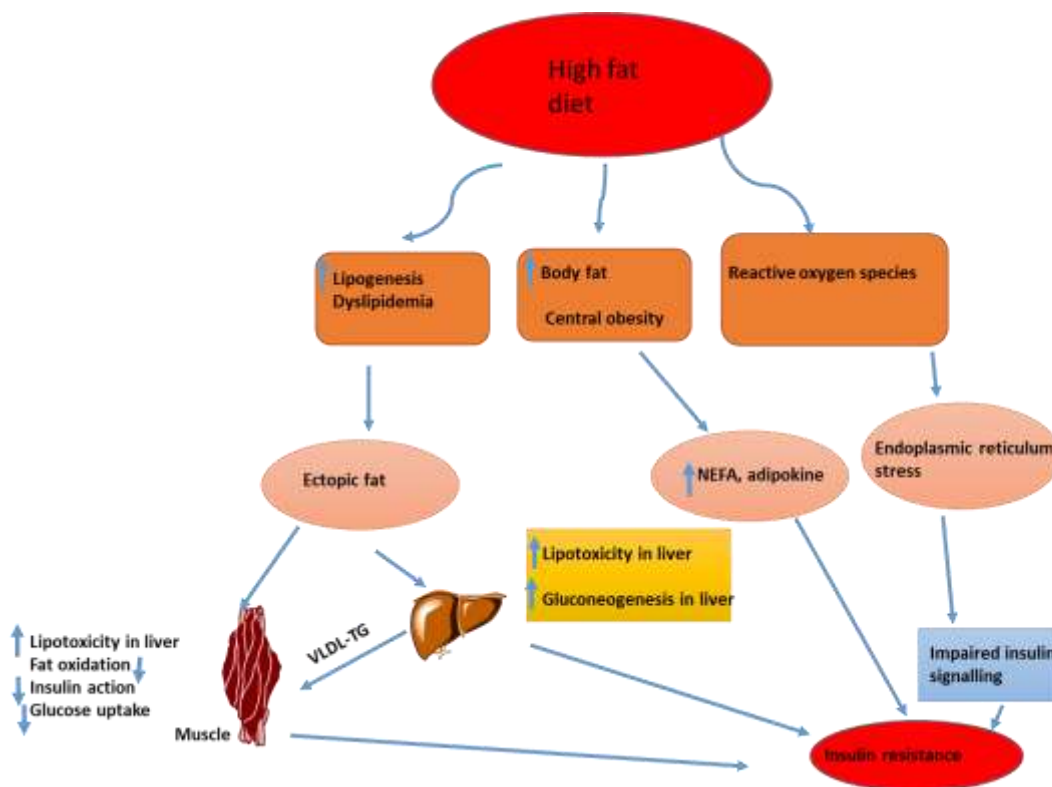


Figure 1-1: High fat diet-induced complications: mechanisms of induction of insulin resistance.

Long term consumption of a high fat diet sets off sequential mechanisms across many organ systems, and cells.

1.3 Obesity associated inflammation

Fatty liver disease occurs in the obese. There are many features that are related to increased obesity; one of the most common causes is the chronic state of inflammation. Characteristically, chemoattraction of immunocytes, such as monocytes, plays a role and circulating free fatty acids which are deleterious to membrane integrity, but may function as endogenous ligands for TLR (Toll-like receptor) binding. Tumour necrosis factor, interleukin-6 and monocyte chemoattractant protein-1 are examples of inflammatory cytokines that are enhanced in obesity. The increase in the size of adipocytes may cause hypoxia; as a result, this may lead to the necrosis of fat cells (Hursting and Hursting, 2012).

Rudolph Virchow was the first to discover the relationship between cancer and inflammation. He observed white blood cells in neoplastic tissue (Hursting and Hursting, 2012). The link between chronic inflammation and cancer is now accepted, because inflammatory lesions tend to produce or increase the risk of cancer. Steatohepatitis can be repaired by activation of progenitor cells; however, more reactivation of progenitor cells may progress to cancer (Lade et al., 2014).

In a model of chemically induced hepatocellular carcinoma, the presence of Toll-like receptor 4 (TLR4) was shown to have a protective role by eliciting an inflammatory response within the treated liver (Wang et al., 2013). By contrast, Dapito and colleagues, conclude that the presence of TLR4 enhances the development of hepatocellular carcinoma in the presence of endotoxemia (Dapito et al., 2012).

Macrophages determine progression of inflammation. This is because macrophages in liver produce inflammatory mediators such as tumour necrosis factor, interleukin-1, and reactive oxygen species (ROS) in non-alcoholic steatohepatitis (Miura et al., 2012). These inflammatory mediators further stimulate hepatocytes and hepatic satellite cells, to induce hepatocyte steatosis and fibrosis. Macrophages encourage development of steatohepatitis because of the interaction of chemokine-chemokine receptors on liver cells, and Kupffer cells. Depletion of Kupffer cells will progress to ameliorate steatohepatitis (Miura et al., 2012). TNF- α has a role in activating Kupffer cells, and thereby

promoting inflammation of liver. It was shown that steatosis, liver injury, and pro-inflammatory monocyte infiltration were reduced as a result of depletion of Kupffer cells (Tosello-Tramont et al., 2012). T-helper 17 (Th17) cells protect body against foreign particles, autoimmune disease, and their functions are well mediated by production some cytokines, for example IL-17 which increased in expression in liver diseases. Expression of IL-17 receptors is present in liver parenchymal, and non-parenchymal cells, and it has a role in liver inflammation by promoting non-parenchymal liver cells to produce pro-inflammatory cytokines (Lafdil et al., 2010). A previous study showed that, in the absence of properdin, IL-17 mRNA expression in unstimulated spleen is significantly reduced compared to wildtype, and is not upregulated to the levels observed in wildtype during infection (Dupont et al., 2014).

1.4 Liver manifestation of diet-induced obesity

Steatosis is the accumulation of fat in hepatocytes which can lead to an overall increase in liver size, so-called hepatomegaly. Accumulation of lipids may lead to inflammation. This is called non-alcoholic steatohepatitis (NASH), to differentiate the disease from alcohol-induced liver injury, either of which can progress to cirrhosis (Brown and Kleiner, 2016). It is estimated that there is evidence of non-alcoholic steatohepatitis in up to a third of populations in the developed world (Preiss and Sattar, 2008), (Asrih and Jornayvaz, 2015). Chronic liver inflammation can also be caused by genotoxic agents, hepatic viral or parasitic infection, and autoimmune reaction, and leads to hepatocellular carcinoma. Mechanisms involved are lymphocytic infiltration, immune recognition, and oxidative stress (Kang et al., 2011). Endoplasmic reticulum stress in oxidative conditions leads to further cell damage (Stauffer et al., 2012). NAFLD is started by accumulation of triglyceride (TG) droplets, and may be associated with other expressions of metabolic disease such as diabetes mellitus type 2 (Anstee et al., 2013). In adipose tissue, several pro inflammatory adipokines such as IL-6, IL-8, IL-1 β , and TNF- α , and monocyte chemoattractant protein-1, and also hormones such as leptin, adiponectin and resistin are produced. Furthermore, pro inflammatory adipokines lead to liver inflammation. The actual mechanism for this is that pro inflammatory adipokines stimulate

production TNF-alpha, IL-6, reactive oxygen species, and the increase adipocyte lipolysis (Scorletti and Byrne, 2013). If fatty acids and cytokines enter the liver, then it will cause the increase endoplasmic reticulum stress, and Kupffer cell activation. As a result, liver inflammation is triggered by endoplasmic reticulum stress, and Kupffer cells activation that will promote NASH development (Scorletti and Byrne, 2013). NAFLD is linked to the reduction of cellular responses to insulin, termed insulin resistance. This is described as the “first hit” resulting in the accumulation fat in liver (steatosis) (Anstee et al., 2013).

Furthermore, in liver cells, it will lead to the increase of gluconeogenesis, the uptake of FFA, changes in the removal of triglyceride for instance, VLDL, and β -oxidation inhibition. This alteration of lipid metabolism is the main cause in the fatty liver disease development (Anstee et al., 2013). The “second hit” of NAFLD is oxidative stress development in hepatocytes, which is promoted by fructose (Lim et al., 2010) then is followed by steatohepatitis, and liver cirrhosis (Vonghia et al., 2013).

NAFLD is obesity associated metabolic syndrome disease, ranging from non-alcoholic fatty liver (NAFLD), nonalcoholic steatohepatitis (NASH), liver fibrosis, and to liver carcinoma. Steatosis is a characterization of NAFLD while, in NASH steatosis, lobular inflammation, and hepatocellular ballooning were detected, NASH also will lead to the development of liver fibrosis and liver carcinoma (Paschos and Paletas, 2009).

Mice fed a high fat diet develop NAFLD because of increased dietary FFA levels. The increase of oxidative stress and proinflammatory cytokines are associated with the progression of steatosis to steatohepatitis. The main factors associated with NAFLD are obesity and insulin resistance. In the obese state, proinflammatory cytokine TNF- α (which may be elevated due to concomitant elevation of endotoxins) inhibits the phosphorylation of insulin receptor; this leads to the development of insulin resistance. The association between insulin resistance and liver steatosis is as follows: when insulin sensitivity is lost, insulin is not able to inhibit the hormone sensitive lipase which promotes the increase FFA release from adipocytes to the circulation and redirects these to the liver. Insulin resistance is described by hyperinsulinemia and hyperglycaemia. Hepatic de novo lipid synthesis ensues by upregulation of the membrane-bound

transcription factor sterol regulatory element-binding protein-1c (SREBP-1c) and carbohydrate response element-binding protein (ChREBP). In addition, hyperinsulinemia plays as the inhibition of β -oxidation of FFAs (Lau et al., 2017).

In muscle and adipose tissue, Insulin enters glucose via glucose transporter-4. It is estimated 60-70 % of body insulin and 10% can be taken in muscle and adipose tissue respectively. Insulin plays a significant role in glycogen synthesis via glycogen synthase. However, insulin is not able to produce glycogen in muscle during insulin resistance and it leads to decreased intracellular glucose translocation. There is a relation between insulin resistance and endothelial dysfunction which causes atherosclerosis via elevated triglycerides and increased foam cell formation (Wilcox, 2005).

Endotoxemia coincides with the development of NASH. The pattern recognition molecule CD14 that associates with LPB-bound endotoxin is combined with toll-like receptors to form (TLR4-CD14) complex. Lipopolysaccharide activates, and stimulates toll-like receptors, and as a result, inflammatory mediators such as IL-6, leptin, and tumour necrosis factor- α are induced (Harte et al., 2010). Endotoxin clearance is performed in liver by initiation of acute phase response. Residential liver Kupffer cells have an important role in absorbing endotoxin; it is secreted in small amount from intestinal lumen in non-infectious state. Elevation amount of endotoxin may result in NAFLD and an insulin resistant state. A high fat diet has a role in the increased translocation of LPS into the blood (Harte et al., 2010). In mice, high fat - high fructose diet plays role in the development of NASH, and the amount of endotoxin may depend on the type of bacteria: In the obese state, bacterial flora of gut will change for both, humans, and mice. Bacterial overgrowth, increased gut permeability, and intestinal dysmotility are characteristics of patients with NAFLD and NASH. Endotoxin level in NAFLD patients was higher (10.6 EU/mL) compared to control patients (3.9 EU/mL) (Harte et al., 2010).

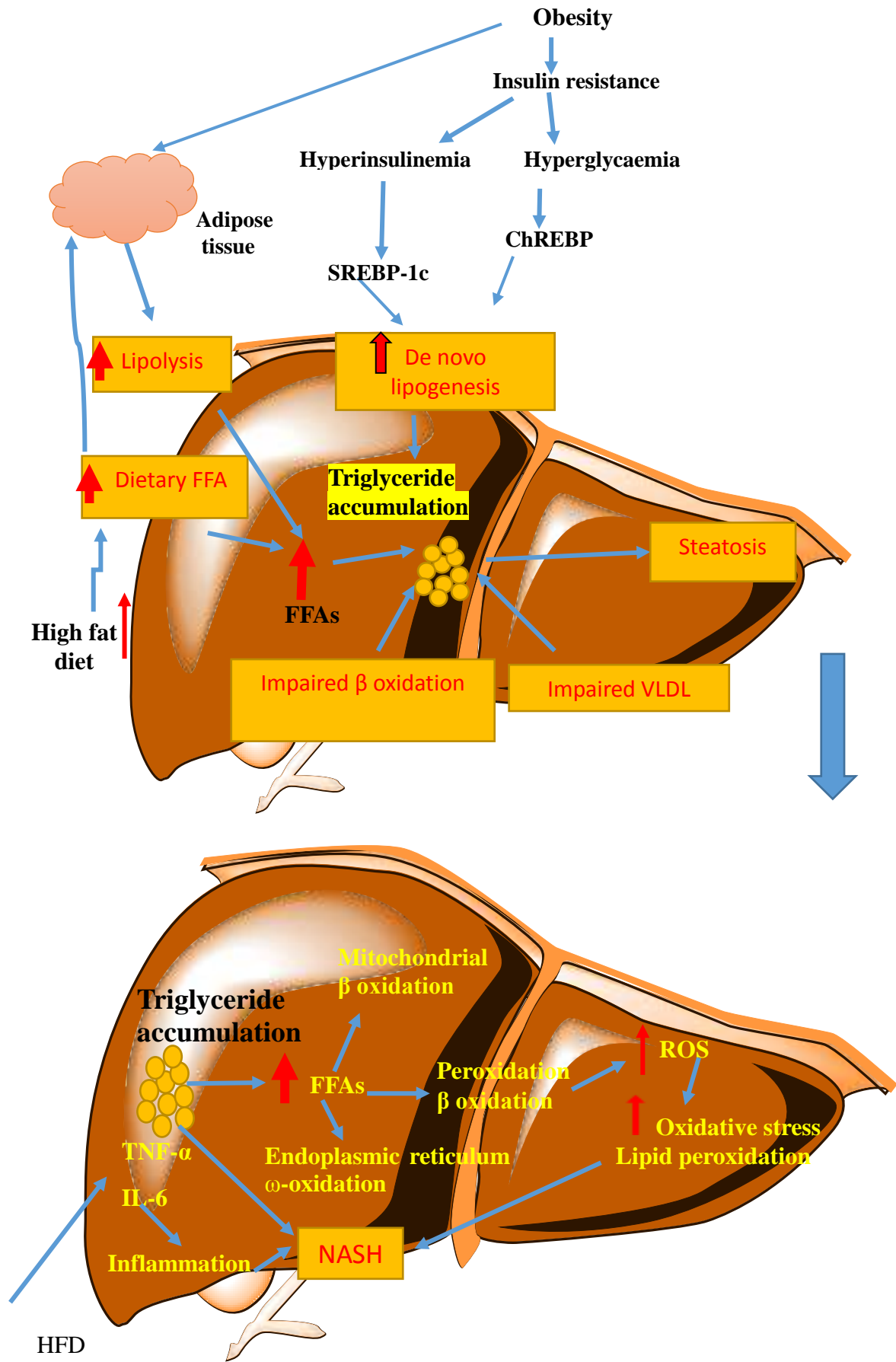


Figure 1-2: Pathophysiology of non-alcoholic fatty liver disease from steatosis to NASH.

Obesity is a main factor to develop insulin resistance. This leads to hyperinsulinemia and hyperglycaemia which promote hepatic *de novo* lipid synthesis by upregulation of the membrane-bound transcription factor sterol regulatory element-binding protein-1c (SREBP-1c) and carbohydrate response element-binding protein (ChREBP), respectively. Hyperinsulinemia plays as the inhibition of β -oxidation of FFAs. Some factors are related to NAFLD including *de novo* lipogenesis, increased adipose tissue lipolysis, increased dietary FFA levels, impaired β -oxidation, and impaired VLDL synthesis. These have a role in the increase of triglyceride accumulation resulting NAFLD. Oxidative stress and pro-inflammatory cytokines increases with the progression of steatosis to steatohepatitis. The red arrows indicate increase (pointing upward). FFA, free fatty acids; TG, triglyceride; VLDL, very-low-density lipoprotein, HFD: high fat diet.

1.5 Triglyceride and fatty acid metabolism in the liver

Triglyceride and fatty acid metabolism occur in the liver. In fatty liver disease, triglyceride is initiated as the result of free fatty acid combination, and glycerol. Free fatty acid formation sources are dietary foods, which enter the liver via intestinal chylomicrons, adipose tissue lipolysis process, and liver synthesis of fatty acid via *de novo* lipogenesis (Donnelly et al., 2005).

Dietary lipids act as a source of liver fat deposition. In the duodenum and proximal jejunum, long free fatty acids are taken up by intestinal enterocytes, where they are esterified to triglycerides. As the result, they enter the circulation as a chylomicron. In proximal small intestine, medium free fatty acids also are taken to the liver directly by entering in to plasma NEFA pool (Westerbacka et al., 2005). FFA biosynthesis process is also developed by *de novo* lipogenesis in liver, and adipose tissue as a respondent to dietary carbohydrate after a meal.

Serum non esterified fatty acid, which is a major source of fatty acids, and *de novo* lipogenesis caused triglyceride liver synthesis (Timlin and Parks, 2005). Liver steatosis and inflammation is associated with several alterations in lipid metabolism process steps especially lipid production and removal in liver. The factors that lead to the increase of triglyceride accumulation are the increase of dietary source, adipose tissue lipolysis, oxidation of free fatty acids, and the decrease of lipid removal via low density lipoprotein (Tiniakos et al., 2010).

1.6 The role of complement in metabolism

1.6.1 The complement system

The complement system is part of the innate immune system, and consists of more than 30 proteins. They can be present as soluble protein in blood or as membrane associated proteins. There are three pathways (classical, lectin, and alternative) which lead to production of complement activation products C3a, C5a (anaphylatoxins), opsonins (C3b), and formation of membrane attack complex (C5b-9) (Hourcade, 2006).

The classical pathway is activated when immune complexes are formed by binding IgG or IgM antibodies to pathogens, antigens, and non-self-antigens. C1q complement protein in complex with C1r, and C1s binds to the Fc region of antibody attached to antigen, activating C1r, and C1s, which cleave C4, and C2 to form C4bC2a (C3 convertase). The Lectin pathway is activated by binding of mannan-binding lectin (MBL) or ficolin to carbohydrates on a pathogen's surface. MBL is a carbohydrate-binding serum protein, which circulates in complex with serine proteases known as mannan-binding lectin associated serine proteases (MASPs) (Petersen et al., 2001). Their activation leads to cleaving of C4, and C2. The classical and lectin pathway C3 convertase is the C4bC2a, which cleaves C3 into C3b, and C3a. C3b can associate with C4bC2a to form the C5 convertase of the classical and lectin pathways, C4bC2aC3b. The alternative pathway (AP) is activated when C3 undergoes spontaneous hydrolysis, C3 (H₂O) (functionally similar to C3b). AP C3 (H₂O) Bb (C3 convertase), is initiated by binding factor Bb (which is initiated due to cleavage to Bb, and Ba by factor D) with C3 (H₂O). The basis of an amplification loop is formed by C3 (H₂O) Bb, which starts to cleave C3 to C3a, and C3b. The C3b that is formed then binds to factor Bb yielding C3Bb (AP C3convertase). The complex is stabilised by properdin complement, which is also called factor P. The C3a via the enzyme carboxypeptidase is converted to C3adesArg. C5 convertase is formed when C3b binds to C3 convertase, and its activity leads to the production of C5a, and C5b. C5b is part of the membrane attack complex (Merle et al., 2015).

1.6.2 Properdin and its role in complement system

Properdin is a 53kDa protein which binds to C3b, and plays a role in alternative pathway activation as follows: properdin complement acts as the only positive regulator of alternative pathway (Figure 1.3, B). It stabilizes C3, and C5 convertase by interaction with factor B bound C3b, as a result more cleavage of C3 and C5 are initiated (Blatt et al., 2016). Decay of the convertase, which is accelerated by factor H, and I, is decreased by properdin, thereby extending the half- life of the convertase (Blatt et al., 2016).

Properdin, in addition to its stabilising role provides a point to assembly C3bBb on a surface, and may amplify the C3 convertase formation by binding to membrane bound C3b, iC3b or other ligands to form a C3b-properdin complex. This complex can increase the association of factor B to C3b, and further C3Bb is initiated. As a result, properdin may direct activation of C3 on the surface of targets (Hourcade, 2006). iC3b (C3b degradative product) has a continual role in complement activation due to its affinity for properdin complement, and if it is not degraded as a result it leads to the accumulation iC3b on the cell surface, either causing damage to the cell or contributing to pathogenicity, but C3dg, and C3c (degradative product of iC3b by factor I, and complement receptor 1) cannot lead to complement activation because they do not bind to properdin (Hourcade, 2006).

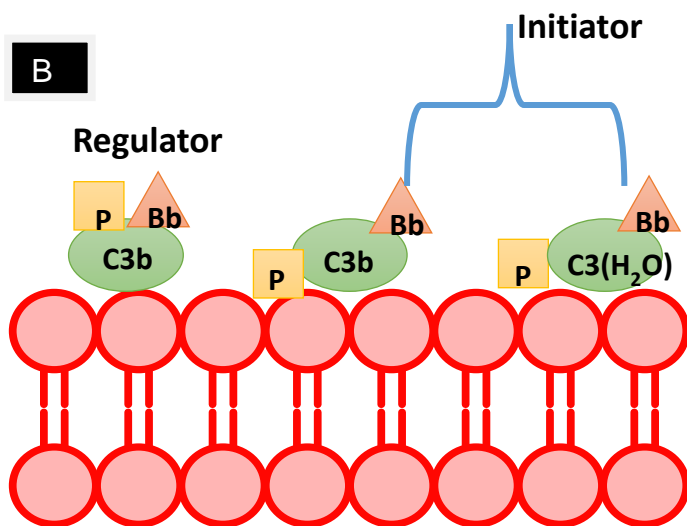
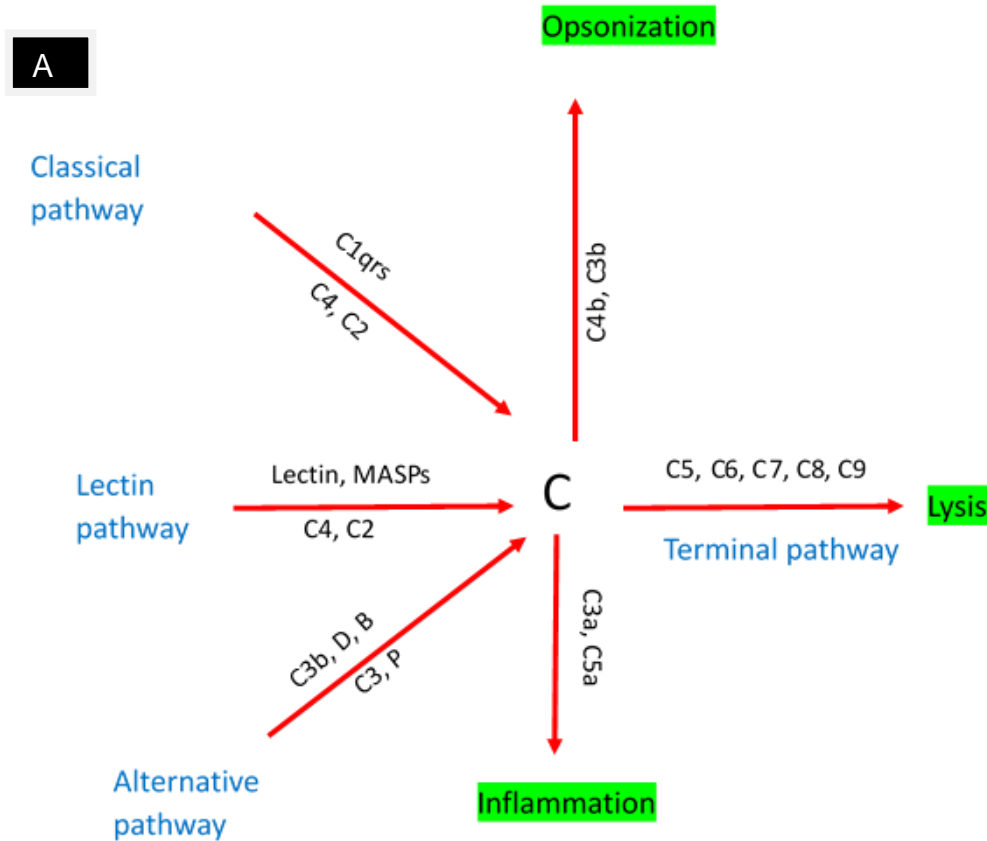


Figure 1-3: A simplified overview of triggers and effects of complement activation and properdin functions.

Complement triggers and effects of complement activation and functions (A). Properdin functions (B), it is regulator and initiator of alternative pathway. Properdin act as positive regulate by stabilizing the alternative pathway C3 and C5 Convertases. It also binds to specific surface and recruits C3H₂O and C3b to initiate alternative pathway, which increases alternative pathway activity 5-10-fold. P=Properdin, C2,3-C9, =complement proteins.

1.6.3 Generation and function of complement C3a-desarg

The complement system bridges the innate and adaptive immune response. In addition, complement activation works to shape cellular responses (Kemper and Hourcade, 2008). Recent studies have assigned a role for complement in metabolism, aside from its importance in the innate and adaptive immune defense. Acylation stimulating protein, which is an enzymatically modified complement system activation product (anaphylatoxin C3a without C terminal arginine residue, so-called C3a-desarg), leads to the increase glucose-stimulated insulin secretion by acting directly on β -cells, resulting in glucose disposal (Ahren et al., 2003).

Adipsin, which is produced in adipocytes, is complement factor D. Two other components of the alternative pathway, C3 and factor B, can be synthesised by adipocytes (Choy et al., 1992). Therefore, adipose tissue may contribute to complement activation. Adipocytes respond to C3a-desArg. There is a positive correlation between Acylation stimulation protein (ASP) level and NEFA and cholesterol. ASP enhances lipogenesis triglyceride (TG) synthesis via elevated diacylglycerol acyltransferase activity, and binds to C5L2 to enhance triglyceride synthesis in adipocytes (Paglialunga et al., 2008). The lack of ASP in C3, and factor B deficient mice led to glucose intolerance, and delayed triglyceride, and NEFA clearance (Paglialunga et al., 2007). However, according to Munkonda and colleagues, in C3 deficient mice fed high fat diet given ASP increased adipose tissue inflammation, and insulin resistance (Munkonda et al., 2012). Therefore, increased levels of C3, and ASP together with ongoing inflammation, may enhance adipose tissue dysfunction, and provoke insulin resistance. The exact roles of ASP and C3 in lipid metabolism, and insulin resistance are not fully understood.

ASP is a serum protein capable of stimulating triglyceride synthesis in cultured fibroblasts, and adipocytes. ASP is identical to C3adesArg. Inactive form of complement anaphylatoxin peptide is called C3a. ASP acts as adipocyte autocrine factor which plays a significant role in metabolism of adipocytes (Kildsgaard et al., 1999).

After a meal, in normal situation, half of free fatty acid enters adipocytes, and half of it binds to albumin which enters the liver. In capillaries of adipose tissue,

chylomicrons (TG rich lipoprotein) attach to endothelial cells, lipoprotein lipase hydrolyse, and TGs, and the membrane bound to lipoprotein lipase will lead to the release of NEFA. NEFA will either enter adipocytes to be absorbed as *de novo* TG synthesized or they may enter the general circulation bound to plasma albumin. ASP acts on adipocytes by two mechanism. Firstly it causes glucose entry via stimulating translocation of glucose transporters (GLUT 1, GLUT 2, GLUT 3 and GLUT 4). Secondly, ASP acts on last enzyme involved at TG synthesis, diacylglycerol transferase, due to increasing activity of ASP (Kildsgaard et al., 1999).

It has been suggested that C5L2 acts as a receptor for ASP and possibly C5a (Kalant et al., 2005). Because there was not a direct interaction between C5L2 and ASP, so there was a doubt to assure the binding ASP to C5L2 (Johswich et al., 2006). Noticeably, delayed postprandial TG clearance and reduced adipocyte size were shown in C5L2-deficient mice fed a diabetogenic diet. Also, some insulin resistance features and inflammation were detected, including higher glucose uptake, and lipid deposition in the liver (Paglialunga et al., 2007). It can be determined that that C5L2 deficiency may develop the increase of C5a-C5aR which leads to the enhancement of adipose tissue inflammation, and insulin resistance (Lim et al., 2013). In a study performed on rats, using antagonists of C3aR, and C5aR, they caused the decrease of body weight and improvement of insulin sensitivity (Lim et al., 2013). Mice deficient in the receptor for anaphylatoxin C3a (C3aR) led to the improvement of insulin sensitivity, and decreased diet-induced macrophage accumulation in the adipose tissue (Mamane et al., 2009). It can be concluded that there was a variation in adipose tissue receptors of complement components ASP, C3a, C5a, so further studies are needed.

The liver is a main source for plasma complement production that includes factors for activation complement pathways (classical, lectin, and alternative pathway). Complement receptors C3a receptor, C5a receptor, and C5L2 are expressed by parenchymal cells (hepatocytes, and non- parenchymal cells (Kupffer cells, stellate, and sinusoidal endothelial cells) (Phieler et al., 2013). Local complement activation is present in patients with NAFLD compared to healthy controls. It therefore appears that complement activation associates with the progression of NAFLD. For example, the cleavage of complement

proteins to trigger C5a and C3a leads to neutrophil infiltration in tissues, and increase of pro-inflammatory markers such as IL-6, TNF- α , and IL-8 by activated Kupffer cells (Rensen et al., 2009b). In livers of patients who have NAFLD, C3, IL-6 mRNA, IL-8 mRNA were more highly expressed, and also neutrophil infiltration, and apoptosis were increased compared to normal people (Phieler et al., 2013). In NASH patients', gene expression of C3 in liver is increased, but in liver cirrhosis C3 is lower in serum, due to abnormal liver function. Mice given a high fat diet increase their hepatic expression of complement Factor D, which is a key component of the alternative pathway, and may play a direct role in the development NAFLD (Phieler et al., 2013).

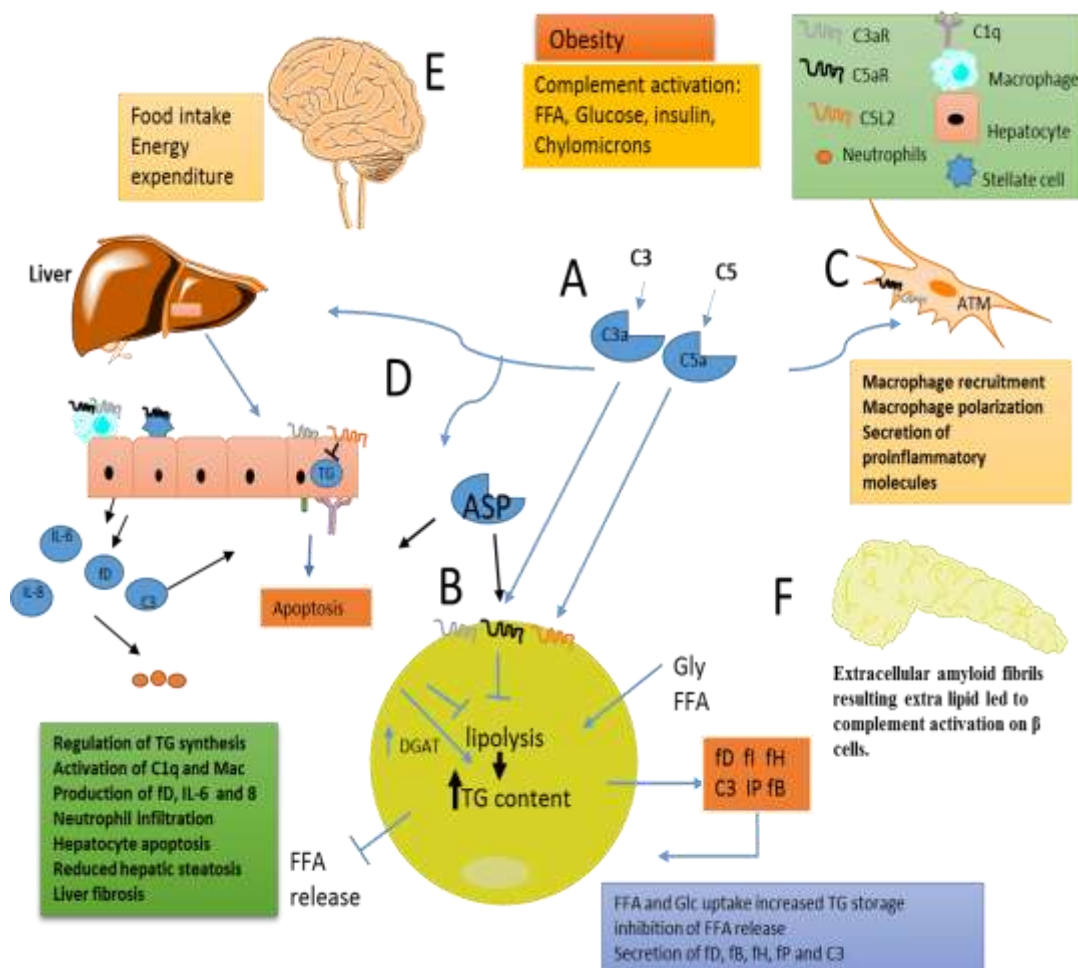


Figure 1-4: The proposed contributions of complement system activation products to the development of obesity and associated pathologies.

Anaphylotoxins C3a, C5a, and C3adesArg (ASP) are increased, both locally, and systemically during obesity, resulting in the increase of plasma and tissue concentrations of free fatty acids (FFA), glucose (Glc), insulin, and chylomicrons (Figure 1.4, A). C3a, and C5a binding to their respective receptors C3aR, and C5aR, complement components could enhance triglyceride (TG) formation by lipolysis inhibition, enhanced Glc, and FFA uptake, and the decrease of FFA release indirectly. Furthermore, C5L2 was shown to stimulate lipid incorporation into TG via diglyceride acyltransferase (DGAT) activation. Several complement factors, including factor D (adipsin), fP (properdin), factor B, factor H, and C3, can be produced by adipocytes in the obese adipose tissue (B). Anaphylatoxin C3a, and potentially C5a can stimulate adipose tissue macrophage (ATM) recruitment, macrophage polarization to a pro-inflammatory phenotype, pro-inflammatory factors, contributing to obesity induced insulin resistance (C). C3a can potentially regulate TG accumulation in hepatocytes, and hepatic steatosis. C3 was linked to C1q, and membrane attack complex (MAC) deposition as well as hepatocyte apoptosis. In addition, hepatocytes can enhance neutrophil recruitment via pro-inflammatory factors such as IL-6, and IL-8, as well as complement activation. Moreover, C5a was implicated in liver fibrosis development (D). Food intake, and energy expenditure impairment was implicated by complement through acting on the central nervous system (E). Extracellular amyloid produced by the increase of NEFA, and cholesterol during obesity as a result complement activation occurred on β cells which leads to the β cell death (F).

1.7 Mouse model using LDLR^{-/-}

The combination of steatosis and inflammation can lead to the development of liver fibrosis, and cirrhosis. LDLR^{-/-} mice develop steatohepatitis after 3 months of high fat high cholesterol (HFC) diet (Bieghs *et al.*, 2012), and there is increased sensitivity for oxLDL uptake by bone marrow derived macrophages in the absence of LDLR^{-/-} mice (Bieghs *et al.*, 2012).

mRNA expression for inflammatory mediators such as MCP-1, TNF, and of CD68 (macrophage marker) were increased after 7, and 21 days high fat diet (HFD) in LDLR^{-/-} mice, while there was no inflammation in wild type mice on HFD and even normal chow (Wouters *et al.*, 2008). There was more inflammation in livers of LDLR^{-/-} mice compared with wild type mice. There was greater plasma total cholesterol and an accumulation of lipid droplets in LDLR^{-/-} mice fed HFD liver sectioned samples, consistent with NASH, compared to wild type.

Male LDLR^{-/-} mice had increased steatosis, and inflammation. Characteristically, there was an increase of infiltrating macrophages, T cells, and monocytes. Also inflammatory cytokines, such as TNF- α , and MCP1 (inflammatory mediators), and CD68 (macrophage marker) were increase at the 7 days feeding HFC compared with chow diet, and HFC wild type mice. In male LDLR^{-/-} mice there was steatosis, and fibrosis at the 3 months feeding HFC; this was investigated by performing the gene expression of *Tgf β* , *Mmp-9*, *Collal*, *Timpl*, and α SMA. In addition, apoptosis was only seen in LDLR^{-/-} mice group, this was investigated by performing apoptotic markers such as *Bax*, *Bcl-2*, *Traf1*, *BFI 1*, and *chop*. Lipid-related genes expression such as *CD-68*, *Sr-a*, *LPI*, *Abca1*, and *Ppary* were more increased in LDLR^{-/-} HFC mice. Oil Red O staining test shows that hepatic steatosis had appeared in LDLR^{-/-} in three months feeding HCF; the level of IL6 (stimulates B and T cells) CD36 (uptakes of oxidised cholesterol, and transduction of inflammatory signal) and after oxLDL loading, was more abundantly expression in LDLR^{-/-} bone marrow derived macrophages compared to control (Bieghs *et al.*, 2012).

1.8 Nutritional and lifestyle intervention in fatty liver disease

Lack of dietary Omega 3 associates with the development of insulin resistance, fatty liver disease and dyslipidaemia (Scorletti and Byrne, 2013). Atherosclerosis, and its clinical manifestations of myocardial infarction, sudden death, and stroke are likely to be prevented by Omega 3 (Mori and Beilin, 2004). Vitamin D deficiency has been found in NAFLD patients. It therefore appears that lower Vitamin D is more likely to increase susceptibility to develop NAFLD (Stein and Shane, 2011). Body weight, and central obesity decreased by giving garlic in a group of people with NAFLD (Soleimani et al., 2016). Exercise training has a role in the decrease or inhibition of inflammation by switching of M1 macrophage to M2 macrophage. TNF- α , and F4/80 mRNA expression in adipose tissue mice was reduced a result of the exercise training. A M1 macrophage marker, CD11c, increased in high fat diet; however, mRNA expression was decreased in the exercise training high fat diet fed mice. However, CD163, M2 macrophage marker, decreased in high fat diet; while, there was increased mRNA expression in adipose tissue of the exercise mice training. The mRNA expression of Toll like receptor 4 was decreased in adipose tissue of the exercise mice training (Kawanishi et al., 2010).

1.9 Hypotheses

1. LPS-induced inflammatory effect on hepatocytes and macrophages in vitro is aggravated by Nonesterified fatty acids and ameliorated by Vitamin D, DHA or allicin.
2. Dietary Vitamin D significantly improves obesity induced inflammation in vivo.
3. Complement properdin has a significant role on the development of fatty liver disease in vivo.
4. The addition of exercise to dietary consumption of Vitamin D improves high fat diet-induced disease.

1.10 Aims and objectives

The overall aim of the current study was to identify modulation of the inflammatory response to development of diet induced obesity. Therefore, this study investigated the role of Vitamin D in diet induced obesity and liver disease in mice on a LDLR^{-/-} background (prone to develop metabolic syndrome), and LDLR^{+/+}. This study also investigated the role of properdin in diet induced obesity and liver disease, by comparing properdin deficient and wild type mice on a LDLR^{-/-} / LDLR^{+/+} background. Furthermore, also test the anti-inflammatory role of Vitamin D, DHA, and Allicin. Finally, this study investigates an additional positive effect of voluntary exercise on the beneficial effect of Vitamin D added to our high fat high sugar diet. Therefore, the specific objectives of my study were:

- *In vitro*, using J774 and HepG2 cells to study anti-inflammatory role of Vitamin D, DHA and Allicin (measuring TNF- α). In addition, using markers of relevance in profibrotic (TGF β), and lipogenic response (SREBP-1c, PPAR- α).
- To establish a fatty liver disease model and prediabetic phenotype *in Vivo*, LDLR^{-/-} and LDLR^{+/+} mouse lines were used by giving high fat-high sugar diet and Western diet to mice for ten weeks and five weeks.
- To understand the role of Vitamin D and complement properdin in developing metabolic syndrome disease, a variety of readouts were used (Body weight, Fat pad weight, liver histology, qPCR for liver and adipose tissue, ELISA, liver functions, endotoxin assay, immunohistochemistry for liver and adipose tissue, protein array, Western blot for C5L2 in liver and adipose tissue, serum complement activation).
- To investigate beneficial effect of supplemented Vitamin D with access to exercises, body weight, fat pad weight, liver histology, Insulin ELISA, TNF- α , IL-6 and NEFA, complement activation assay were analysed.

Chapter 2 Materials and Methods

2.1 Materials

2.1.1 Animals

For this work a mouse line was used, which is described in an atherosclerosis model (Steiner et al., 2014), and was part of a study conducted during a British Heart Foundation-funded grant period at University of Leicester and University of Sheffield. As part of this work, a novel mouse line was generated by intercrossing commercially available LDLR^{-/-} mice (Ldlr^{tm1Her/J}; Jackson Laboratories), and a previously generated Properdin-deficient (PKO) mouse line Cfp^{tm1Cmst} (Stover et al., 2008), which is owned by the University of Leicester. Properdin deficient, and wild type mice were also used.

Mice were maintained in a barrier facility on 5LF2 (14% protein, 6% fat, 65% carbohydrate). At 3 months of age, they were randomised to two groups fed for 10 weeks the formulated (cholesterol free) diet 58R3 (20% protein, 36% fat, 35% carbohydrate, rich in sucrose) differing in the content of admixed Vitamin D3 (1 IU/g vs 10 IU/g) (test diet), and also 5TJN (western diet) were fed to mice for 10 weeks (18% protein, 19.3% fat, 58% carbohydrate). Animal experimentation was performed in accordance with UK Home Office regulations, and institutional guidelines. Mice were weighed weekly. LDLR^{-/-} : model of familial hypercholesterolaemia, LDLR^{+/+}: inbred, but not congenic WT control.

2.1.1.1 Genotyping of wildtype and properdin deficient mice

The aim of this experiment was to confirm the genotype of the mice. This method involves the analysis of DNA extracted from tail snip biopsies using polymerase chain reaction.

For each sample to be tested, 120µl of 0.5M EDTA solution (pH 8.0) was added to 500µl of nuclear lysis solution in a centrifuge tube followed by chilling the mixture on ice. The next step was to add 0.5-1.0 cm of thawed mouse tail to a 1.5 ml microcentrifuge tube followed by adding 600 µl of EDTA/nuclei lysis solution previously prepared to the tube. Then 17.5µl of 20mg/ml proteinase K was added followed by overnight incubation at 55 °C with gentle shaking. In the next day the sample was allowed to reach room temperature for 5 minutes, then 3µl of RNaseA (4mg/ml) was added to the nuclear lysate followed by mixing the sample by inverting the tube 2-5 times. The mixture was incubated for 15-30

minutes at 37 °C. Then 200µl of protein precipitation solution was added followed by vortexing vigorously at high speed for 20 seconds. After that the samples were chilled on ice for 5 minutes and centrifuged at 13000-16000g for 4 minutes. The supernatant (containing the DNA) was removed carefully and transferred to a clean 1.5ml microcentrifuge tube containing 600µl of room temperature isopropanol. Then the mixture was incubated at room-temperature for 5 minutes. After incubation, the mixture was centrifuged at 15,500g for 4 minutes. After centrifugation, the supernatant was decanted and 200µl of 70% ethanol was added to the pellet, then the mixture was centrifuged as before. After centrifugation, the supernatant was decanted and the pellet left to dry, then 200µl of 0.2XTE performed (Tris EDTA buffer) was added. Polymerase chain reaction was done using the following primer pairs:

For the wildtype gene:

WT antiproperdin 5'-GGATTATCACATACTCGTTGACGG-3'

PCAS 5'-CTCTTGAGTGGCAGCTACAG-3'

For the targeted gene (KO specific):

OCP665'-CGTGCAATCCATCTTGTTC-3'

Neoend anti5'-CAAGGCAGTCTGGAGCATGC-3'

A mixture containing 2µl of 25 mM MgCl₂, 0.5µl of genomic DNA (1/200 dilution), 2.5µl of 10X buffer, 4.0µl of dNTPs(1.25mM), 0.5µl of sense primers, 0.5µl of antisense primers and 0.2µl of Thermoprime Taq polymerase were added to a nuclease free microcentrifuge tube. The reaction was made up to 24.5µl with sterile distilled water. The following cycling conditions were applied: initial denaturation at 94 °C for 2 minutes and 30 seconds, thirty cycles of denaturation at 94 °C 45 seconds, annealing at 59 °C for 30 seconds and extension at 72 °C for 1 minute and 30 seconds. The final extension was 72 °C for 10 minutes, finally the sample was held at 15 °C. The size of the PCR product was analysed using 1% agarose gel electrophoresis. The wildtype genotype should show a 1000bp band while the properdin deficient genotype should show a 500bp band.

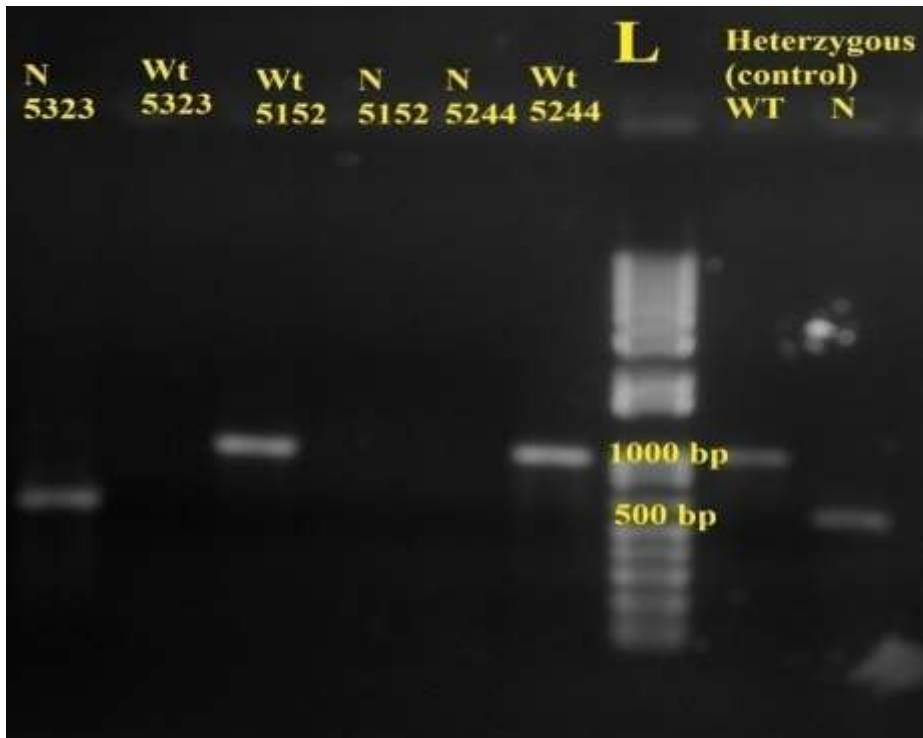


Figure 2-1 Genotyping of wildtype and properdin deficient mice by PCR.

Numbers indicate ID numbers of experimental mice. Products from PCR reaction were loaded in 1% agarose. A 1000bp fragment was seen in the wildtype mice, while a 500bp fragment seen in the properdin deficient mice (representative image). (Wt= wildtype gene amplification; N=knockout specific gene amplification). Lane N 5152, 5244, did not work.

Table 2.1: Different diet components

Nutritional profile	Erodent diet %14 (Normal chow diet) (5LF2)	Western diet for rodents (HFD) (5TJN)	High fat diet –high fructose (58R3)
% Protein	14.3	18	20.2
% Fat	5.8	19.8	36
% Sucrose	0.94	7.8	17.4
Soybean meal (Phytoestrogens)	Up to 20%	Not included	Not included

2.1.2 HepG2 cell line

This is a human liver carcinoma cell line that was used to investigate steatosis, inflammation when Vitamin D3 was added. Dulbecco's modified Eagle's medium supplemented with 10% fetal calf serum, 2mM L-glutamine, and 100 U/ml penicillin 100µg/ml streptomycin was used to maintain HepG2 cell line. Incubation was at 37°C with 5% CO₂ in a humidified chamber. Cells were counted and adjusted to 40,000/ml for HepG2 in 25cm² flasks (5ml) and treated when 70%confluent.

2.1.3 J774 cell line

This is a macrophage cell line that was used to investigate changing M1 to M2 macrophages. RPMI (Roswell Park Memorial Institute medium) (Gibco) with 10% fetal calf serum, 2mM L-glutamine, 100U/ml penicillin, 100 µg/ml streptomycin was used to maintain J774 cell line. Incubation was at 37°C with 5% CO₂ in a humidified chamber. Cells were counted and adjusted to 60,000/ml for J774, in 25cm² flasks (5ml) and treated when 70%confluent.

2.2 Methods

2.2.1 Polymerase chain reaction (PCR)

2.2.1.1 Ribonucleic acid (RNA) isolation of liver cells

RNA was isolated following the instructions in the TRI Reagent[®] Protocol. The livers are homogenised by using a dounce homogeniser with 100mg tissue per 1ml of Trizol then incubated for 5 minutes at room temperature. The homogenate centrifuged was done for 15 minutes 12,000 xg at room temperature, and the supernatant collected. 200µl of chloroform was added, and the tubes were shaken for 5 seconds, and incubated for 5 minutes. After centrifugation for 15 minutes at 12,000 xg, the aqueous phase was collected in new tubes. The aqueous phase was added 500µl of isopropanol to precipitate the nucleic acids, and incubated for 5 minutes at room temperature. Centrifugation for 10 minutes at 12,000 xg, and the supernatant was discarded. 1 ml of 75% ethanol was added to wash the RNA, and centrifugation at 7,500 xg for 5 minutes, the ethanol was removed, and the pellet was air dried. The RNA pellet was suspended by diethyl-pyrocabonate 0.2% (v/v)-treated water. The RNA samples were measured by using a Nano drop spectrophotometer.

2.2.1.2 RNA isolation of adipose tissue

RNA was prepared using RNeasy[®] Lipid Tissue Mini Kit (Qiagen, Manchester UK). The adipose tissues are homogenised by using a homogeniser with 100mg tissue per 1ml of QIAzol lysis reagent, then incubated for 5 minutes at room temperature, 200µl of chloroform was added, and the tubes were shaken for 15 seconds, and incubated for 3 minutes. After centrifugation for 15 minutes at 12,000 xg, the aqueous phase was collected in new tubes, then 75% ethanol were added, up to 700µl of samples were transferred to RNeasy mini spin column 2 ml collection tubes. After centrifugation for 15 seconds at 8,000 x g, the flow-through was discarded. To repeat the former step, same collection tubes were used. The 700µl buffer RW1 was added to RNeasy column. After centrifugation for 15 seconds at 8,000 xg, the flow-through was discarded. The 500µl buffer RPE was added to RNeasy column. Centrifugation was performed for 2 minutes at 8,000 xg, after RNeasy column was put in a 1.5ml new tube then 50 µl RNase-free water was added. Later, Centrifugation was performed

for 1 minute at 8,000 xg. Finally, the RNA samples were measured by using a Nano drop spectrophotometer

2.2.1.3 Purification of RNA

To ensure that the final amplification product mirrored true mRNA expression, isolated RNA was digested with DNase I (5 U for 10µg RNA preparation, 37 °C, and 30min). This step removes contaminating genomic DNA, and is important when using primers which do not span an intron. After the digest, and renewed precipitation, and washing, the concentration of nucleic acids was determined using Nanodrop spectrophotometer.

2.2.1.4 Synthesis of complementary deoxyribonucleic acid (cDNA)

cDNA was synthesised following this programme: 65°C for 5 minutes, 42°C for 1 hour, and 72°C for 10 minutes. A 12µl mixture was prepared by adding 5µg RNA, 1µl of Oligo (dT)18 primer, and DEPC-H₂O was added up to 12µl after 5 minutes incubation at 65°C then the tube was put on an ice box. A master mix was added in the ice box which formed by adding 5x reaction buffer (4µl), RiboLock RNase Inhibitor (20u/µl), 10mM dNTP Mix (1µl), and RevertAid H Minus M-MuL V Reverse Transcriptase (200U/µl), the final volume was made to 20µl. The Mixture was heated at 42°C for 1 hour, and then heated at 72°C for ten minutes to inactivate enzymes. cDNA was kept frozen at -20°C.

2.2.1.5 PCR

A master mix was formed by adding the following components. 2.5µl of 10x buffer, 4µl dNTP 1.25mM, 0.5µM of reverse primer (100 µM stock), 0.5µM of forward primer (100µM stock), 25mM Magnesium Chloride, 10.8 µl of deionised H₂O, and 0.2µl of DNA polymerase. 23µl from master mix was added to a PCR tube plus 2µl of cDNA. The final volume was 25µl for each PCR reaction. The following programme was applied:

95°C for 2 minutes: Initial denaturation

94°C for 1 minute: Denaturation

Determined individually for the sequences of primers: Annealing

72 °C for 1 minute: Extension

72 °C for 10 minutes: Final extension

Followed by 30 cycles. After PCR, the samples were run in gel electrophoresis.

2.2.1.6 Agarose gel electrophoresis

Basically, 1% (w/v) agarose gel was prepared in 0.5X TBE (Tris boric acid EDTA). It includes 1 g agarose plus 100ml TBE in 0.5X, and 0.5µg/ml ethidium bromide. After melting, the gel was cast in a prepared plastic gel tray in order to make the wells. After the gel had set then it was put in running tank which was immersed with 0.5X TBE. The loading dye (reagent) was added in to each sample DNA then the samples were loaded to each well, and 1kb plus DNA ladder was loaded which includes bands from 100 to 1200 base pair. The electrophoresis was set at 90V, for 1 hour. The negatively charged DNA, is attracted toward the anode (positive charges). UV transilluminator was used to visualise the DNA bands in the gel, and the image was documented using DC 120 digital camera.

2.2.2 Real-time quantitative polymerase chain reaction (RT-qPCR)

Total RNA was isolated, and extracted with Trizol, and cDNA was synthesised as described in section 2.2.1.4. After cDNA was synthesised from extracted RNA from each sample was used as templates in qPCR using SYBR Green PCR kit (SensiMix™ SYBR Kit, Cat.QT605).

cDNA was diluted (1:4) in d.H₂O. The master mix was made as follows: 10 µl of SYBR Green I dye (SensiMix™ SYBR Kit, Cat.QT605), 2µL reverse primer (5µm), 2µL forward primer (5µm), and 3µl dH₂O. 3 µl of diluted cDNA +17 µl master mix to get 20µl/reaction. Real time PCR was used to quantify the relative changes in gene expression by 2^{-ΔΔCt} method. Derivation of 2^{-ΔΔCt} has been described (Livak and Schmittgen, 2001). In 2^{-ΔΔCt} method,

amplification efficiencies of target, and reference must be equal. Primer efficiency was previously performed in our lab for the primers used in this study. For each test sample/ the following cycling conditions were used:

Cycle: hold at 95°C 10 minutes

Cycle point: Step 1 at 95°C, hold 15 seconds

Step 2 at 55°C (Determined individually for the sequences of primers), hold 15 seconds

Step 3 at 72°C, hold 15 seconds, acquiring to Cycling

Melt (55-95°C), hold a second on the 1st step, hold 5 seconds on next steps

The number of cycles was 45 cycles.

Figure 2.1 shows the amplification of one gene in 5 samples, and each sample was run in duplicate. Threshold line determined the cycle threshold (Ct) for each sample. This threshold line represents the fractional cycle number at which the amount of amplified target reaches a fixed threshold, and also it is a dividing point that separates the auto-fluorescent signal (background levels) from the real fluorescent signal that radiates from cDNA templates. Indirect proportion is presented between Ct levels, and the amount of the target template in the sample. In this amplification curve, Ct values for all 5 samples between 8 to 15, while the non-template sample (negative control) reached the threshold after 23 cycles.

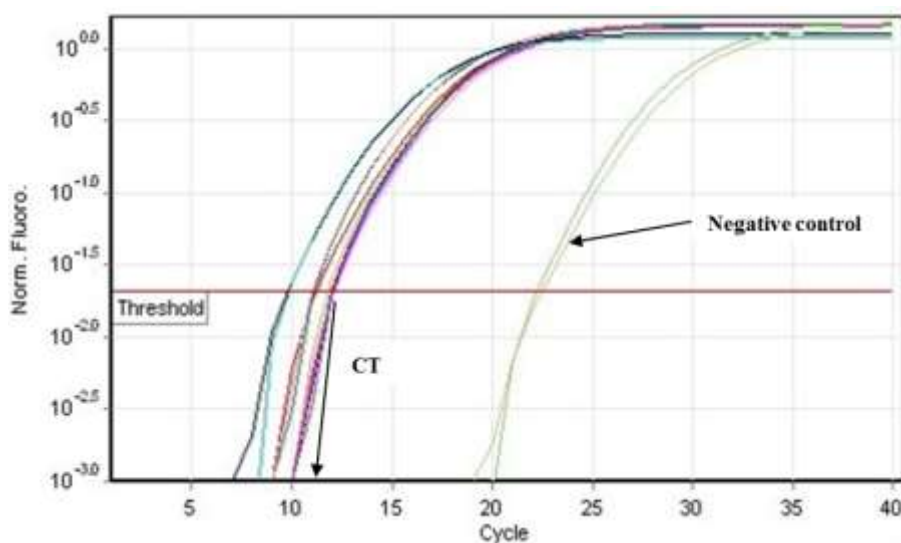


Figure 2-2: SYBR Green-based RT-qPCR amplification chart.

Black squares represent the number of cycles required by the fluorescent signal to cross the threshold (background). Ct = cycle threshold

All sample amplicons dissociated at the same time, and this is confirmed by their curves which reach the peak together at 87°C (Figure 2.2).

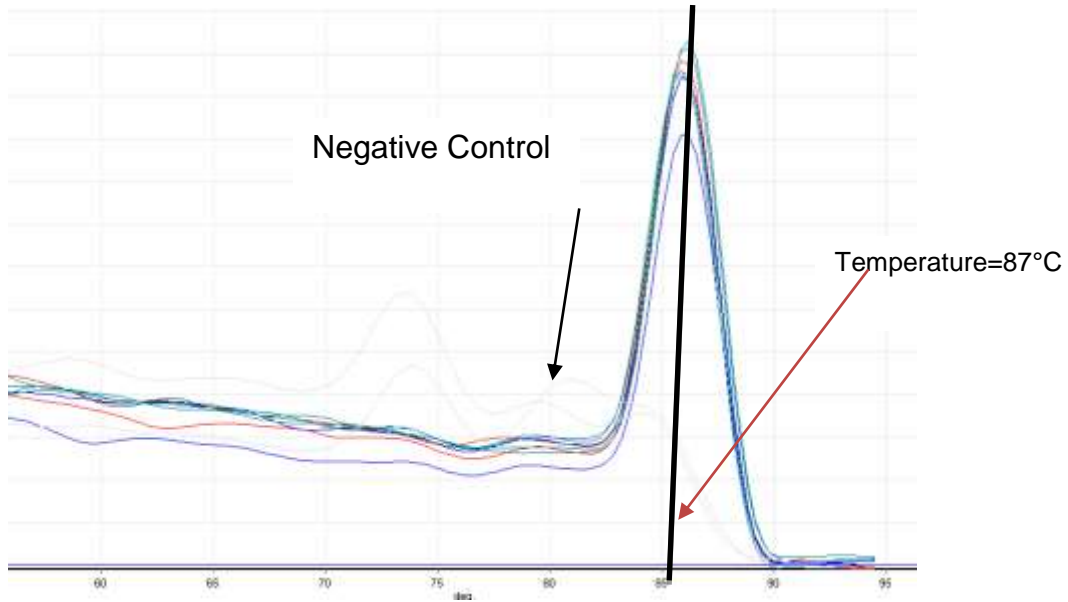


Figure 2-3: Melting curve analysis confirming specific amplification from qPCR using SYBR green.

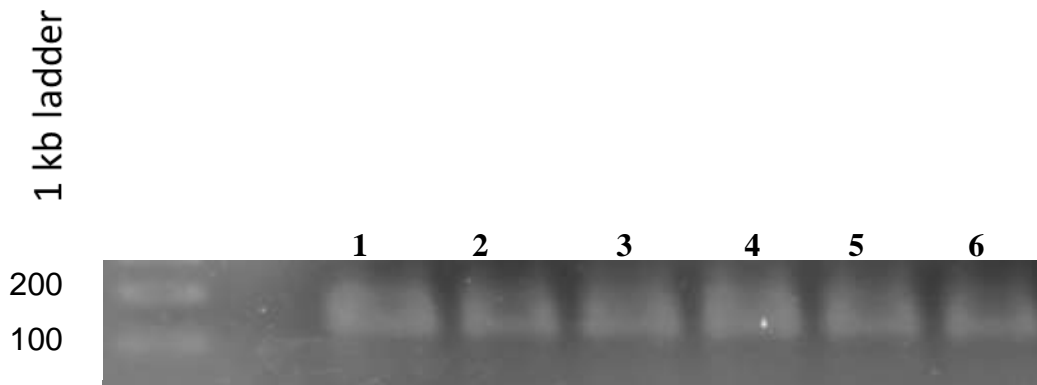


Figure 2-4: 1 Kb Plus DNA Ladder in 1% agarose gel electrophoresis. 1 Kb Plus DNA Ladder in 1% agarose gel electrophoresis, GAPDH size=130bp.

Semi-quantitative RT-PCR product for mRNA GAPDH. 1-J774, 2- J774+LPS 100ng/ml, 3- J774+ LPS 1000ng/ml 4- 774+Vitamin D 2 µg/ml LPS 100ng/ml, 5- 774+Vitamin D 2 µg/ml+ LPS 1000ng/ml, 6- J774

GAPDH was used as housekeeping gene (Matouskova et al., 2014), Ct value showed that the expression level of GAPDH was consistent and also the samples were run on gel electrophoresis, and the results there showed

comparable mRNA expressions (Figure 2.3). Next, for each sample was performed GAPDH (as a house keeping gene), and a target gene (TNF- α as an example) for stimulated, and unstimulated J774 in order know how much TNF- α is synthesised above the normal state. Untreated control was used as calibrator by using $2^{-\Delta\Delta C_t}$ as follows: the data is presented as the fold change in gene expression normalized to an endogenous reference gene, and relative to untreated control. $\Delta\Delta C =$ Zero in unstimulated control sample. While, for treated samples $2^{-\Delta\Delta C_t}$ indicates the fold change in gene expression relative to the untreated control. Then samples were analysed as follows: mean of GAPDH expression of each sample, and mean of CT target gene-mean of reference gene (GAPDH) as housekeeping gene ΔC_t sample = C_t target gene – C_t reference gene. Then, $\Delta\Delta C_t = \Delta C_t$ sample - ΔC_t control. After that, the expression of target gene normalised to reference gene, and relative to normal condition (control) was determined by calculation of $2^{-\Delta\Delta C_t}$

Table 2.2 Sequences of primer pairs (with their annealing temperatures) used in this study for mouse.

Target	Forward sequences 5'-3'	Reverse sequences 5'-3'	Annealing Temp.
GAPDH	F:CCTGGAGAAACCTGC CAAGTATG	AGAGTGGGAGTTGCTGTTGAAG TC	55
TNF-α	GGCAGGTCTACTTTGGA GTCATTCC	ACATTCGAGGCTCCAGTGAATT CGG	60
IL-6	GACAACTTTGGCATT	ATGCAGGGATGATGT	53
β2M	GTTCCGGCTTCCCATTCT CC	GGTCTTTCTGGTGCTTGTCTCA	55
Vcam-1	GTCACGGTCAAGTGTTT GGC	AGATCCGGGGGAGATGTCAA	56
TLR4	CGCTTTCACCTCTGCCT TCACTACAG	ACACTACCACAATAACCTTCCG GCTC	55
HMGC R	TGGCAGGACGCAACCT CTAT	TGACGGCTTCACAAACCACA	55
PPAR- G	GATGGAAGACCACTCG CATT	AACCATTGGGTCAGCTCTTG	55
SR-B1	TCCCCATGAACTGTTCT GTGAA	TGCCCGATGCCCTTGACA	55
INOS	GGCAGGCCTGTGAGAC CTTTG	GAAGCGTTTCGGGATCTGAA	60
ARG-1	GGGAATCTGCATGGGC AAC	GCAAGCCAATGTACACGATGTC	60
SREBP 1-C	TCTGCCTTGATGAAGTG TGG	AGCAGCCCCTAGAACAACA	55
C5L2	GCCTACCTCATAGTCCT GCT	CAGTGGTGATGGTAACTTCC	55
Vitamin D R	TACATCCGCTGCCGCCA CCCGC	TCAGGAGTCTCATTGCC	55
Insulin R	TTTGTGATGGATGGAGG CTA	CCTCATCTTGGGGTTGAACT	55

Table 2.3 Sequences of primer pairs (with their annealing temperatures) used in this study for human.

Target	Forward sequences 5'-3'	Reverse sequences 5'-3'	Annealing Temp.
TNF-α	GGACCTCTCTCTAATCA GCCCTC	TCGAGAAGATGATCTGACTGCC	55
PPAR-α	GCAGAAACCCAGAACTC AGC	ATGGCCCAGTGTAAGAAACG	55
SREBP-1C	GGATTGCACTTTTCAAG ACATG	ACTCTGGACCTGGGTGTGCAAG	55
TLR4	AGGATGATGCCAGGAT GATGTC	TCAGGTCCAGGTTCTTGTTGA G	55
GAPDH	TCCCTGAGCTGAACGG GAAG	GGAGGAGTGGGTGTCGCTGT	55
Vitamin D R	CTCATCTGTCAGAATGA ACTCCTTCA	TCACCAAGGACAACCGACG	55
Insulin R	AACCAGAGTGAGTATGA GGAT	CCGTTCCAGAGCGAAGTGCTT	60

2.2.3 Liver section staining

2.2.3.1 Haematoxylin and Eosin staining

Sections were cut by microtome at 4 μ m, and sections were floated on 52°C in water bath, then the sections were put on the slides. After being dried the wax was removed by rinsing in xylene for 2-3 minutes. The slides were rinsed in 100% IMS (industrial methylated spirit) for 5 minutes (2 times) then immersed in 70% IMS for 5 minutes then washed with water for 5 minutes. Hematoxylin stain was added to the slides for 5 minutes after that washed with water for 5 minutes to remove the excess of stain. After using Eosin stain for 2 minutes then the slides were rinsed in water for 50 seconds. Water was removed by rinsing in IMS (2 times) 100% for 2 minutes. After putting in Xylene for 1 minute then the slides were put DPX with cover slips.

2.2.3.2 Olive green Oil

Olive green stain: Epoxy embedded, Osmicated.

Livers were sectioned on an ultra-microtome at 400nm. Sections were transferred to glass slides, and dried at 92°C on a hot-plate. Sections were then stained with 1% Toluidine blue in 1% borax for 30 seconds at the same temperature (92°C). Excess stain was washed off with distilled water at room temperature. Slides were dried briefly on the hot plate, and viewed with a X10 or X40 objectives.

2.2.3.3 Alcian blue staining

Sections of sample were cut by microtome at 4µm, and sections were floated at 52°C in water bath, then the sections were put on the slides then paraffin brought to water as above. Carmalum (differentiate in acid alcohol) was added for 5 minutes. After slides were washed with water (running water) for 2 minutes then Alcian blue (0.5% Alcian blue in 0.5% Acetic acid) was added by filter syringe after that washed with water for 2 minutes (rinse in tap water). After IMS was added for 50 seconds then Xylene 50 seconds. DPX was put on coverslips then put on the slides. As an alternative method to increase staining intensity, sections were stained with Haematoxylin. After slides were rinsed with water (running water) for 10 seconds then rinsed in acid alcohol (1% HCl plus 70% IMS). The sections were washed with water for 10 minutes then rinsed in D.W for 10 seconds. Filtered Gomoris' 1 step Trichrome was added for 5 minutes; rinsed in 0.2% acetic acid for 5 seconds then blotted on a filter paper. After IMS was added for 50 seconds then Xylene 50 seconds. DPX was put on coverslips then put on the slides.

2.2.4 Electron microscopy (EM)

Liver samples were placed in fixative buffer 2% (v/v) formaldehyde / 4% (v/v) glutaraldehyde / 0.1M Sodium Cacodylate buffer / 2mM Calcium chloride pH 7.4) processed by Natalie Allcock, EM Facility University of Leicester according to established methods, as follows:

Samples were washed in PBS, and stored at 4°C. After that with same washing buffer samples were washed 3 times for 20 minutes, and then washed 2 times for 20 minutes in distilled de-ionised water. Samples were secondary fixed with 1% Osmium tetroxide for 2.5 hours. Then samples were washed 3 times for 20

minutes in distilled de-ionised water followed with serial alcohols, 25% Ethanol 15 minutes, 50% Ethanol 15 minutes, 75% Ethanol 15 minutes, 70% Ethanol stored overnight at 4°C, 90% Ethanol 30 minutes, 100% Analytical Grade ethanol for 30 minutes for 3 times. Cells were transferred through 25%, 50%, and 75% Agar low viscosity resin in propylene oxide, 3 times for 10 minutes, followed by 100% Agar Low Viscosity Resin for 30 minutes, and again for overnight after that Fresh Agar Low Viscosity Resin was added for 3 hours 2 times. Finally, the samples were embedded, and polymerised at 60 for 16 hours. Samples sectioned were embedded using a Reichert Ultracut S ultramicrotome. Then samples sections of approximately 90 nm thickness were cut from each sample, and were collected onto copper mesh grids after that were counterstained with 2% Uranyl Acetate and Reynold's Lead citrate. Samples were viewed on the JEOL 1400 TEM with an accelerating voltage of 100kV. Images were captured using Mageview III digital camera with iTEM software.

2.2.5 Immunohistochemistry

2.2.5.1 Anti-F4/80 and C5L2 antibodies

Liver or adipose sections were cut at 4µm, and de-waxed by rinsing in xylene for 5 minutes (2 times). The slides were rinsed in 100% ethanol for 5 minutes (2 times) then immersed in 95% ethanol for 5 minutes. Slides were rinsed 70% ethanol for 5 minutes then washed with water for 5 minute. To do antigen retrieval, the sections were put in in 10mM citrate buffer for 20 minutes in a water bath at 95°C, and then they were put in 10mM citrate buffer at room temperature for 20 minutes. Later, the slides were washed with 10% H₂O₂ for 15 minutes, and then they were washed with 1xPBS (5 times, 5 minutes. To block endogenous peroxidase activity sections, 30 % of Hydrogen peroxide was diluted in PBS (1ml from hydrogen peroxide was mixed with 9 ml PBS) then added to the sections for 15 minutes then washed 3 times (5 minutes each) in 1xPBS. Blocking in goat serum 10% for 1 hour (the serum that secondary antibody raised in) then washed for 5 minutes. Primary antibody (F480: RAT anti mouse F4/80 Bio Rad) (C5L2: rabbit polyclonal antibody Sc-368572, Santacruz Biotechnolog) (1:100 dilution) (was added for 1 hours in room temperature or 24 hours in cold room then washed 3 times (15 minutes each) (it

was performed with magnetic bar in stirring machine). Secondary antibody (Goat anti Rat Santacruz for F480) (Poly clonal swine Anti Rabbit Immunoglobulin HRP, Dako) (1:200 dilution) was added for 30 minutes in room temperature then washed 3 times (15 minutes each). DAB Substrate was prepared, and added to sections for 10 minutes. The substrate was prepared by (0.2 M Tris/HCl-pH 7.5 10 ml which was prepared by mixing 2 ml Tris HCl with 8ml H₂O), 10mg DAB (1mg/ml DAB), and (10 µl H₂O₂). The sections were put in 70%, 90%, 100% ethanol, and 100% Xylene for 5minutes each. The sections were added DPX with cover slips.

2.2.5.2 Anti-C3, CD68, and iNOS antibodies

Liver sections were cut by cryostat (freezing microtome) at 7µm. Slides were prepared after being dried for 10 minutes at room temperature, then the sections were fixed in (Acetone-methanol 1:1) for 10 minutes. The slides were rinsed in 1:10 H₂O₂ in methanol (10 ml H₂O₂ with 90ml methanol) for 10 minutes. The slides were rinsed in 70% IMS (2 minutes). The rest of the procedure for CD68, C3, and iNOS antibodies was same as above, except primary, and secondary antibodies concentration were shown in the Table below (Table 2.4).

Table 2.4 Primary and secondary antibodies for immunohistochemistry.

Primary antibody	Dilution	Secondary antibody	Dilution
Rat anti-mouse F4/80	1:100	Goat anti-rat IgG	1:200
C5L2: rabbit polyclonal antibody (Sc-368572), (Sc-368572), Santa Cruz Biotechnology.	1:100	Poly clonal swine Anti Rabbit Immunoglobulin HRP, Dako	1:200
Anti-C3 antibody Abcam (ab11887)	1:100	Goat anti-Rat IgG	1:200
iNOS Thermo Fisher Catalog#: PA3-030A	1:100	Polyclonal swine anti-Rabbit Dako	1:100

Table 2.5 Primary, and secondary antibody for Western blotting.

Primary antibody	Dilution	Secondary antibody	Dilution
C5L2: rabbit polyclonal antibody (Sc-368572), Santacruz Biotechnology.	1:1000	Polyclonal swine Anti Rabbit Immunoglobulin HRP, Dako.	1:2000
β -actin: mouse monoclonal beta actin.	1:5000	Goat anti-mouse antibody Life technologies-Molecular probe.	1:10000

2.2.6 Immunofluorescence for C5L2 antibody

Sections were cut by cryostat (freezing microtome) at 7 μ m. Sections were fixed in (acetone-methanol 1:1) for 10 minutes. The slides were fixed in acetone, and methanol (1:1) for 10 minutes. They were washed with 1xPBS (3 times, 5 minutes) to remove the fixative. The 10% bovine serum albumin (BSA) were added for each section to block non-specific labelling, and incubated for 30 minutes at room temperature. The primary antibody (C5L2 rabbit polyclonal antibody) was added to each section, and incubated at room temperature for 1h. After the incubation period, the sections were washed with 1xPBS (3 times, 10 minutes). Secondary, antibody (anti-goat anti-rabbit Immunoglobulin FITC conjugated, Alexa Fluor 488, Thermo Fisher; 1:200 dilution) was added for 30 minutes in room temperature then washed 3 times (15 minutes each). Fluoroshield Mounting Medium with DAPI was added to each section and covered with coverslips. Finally, the slides were viewed under the confocal microscope (OLYMPUS microscope, and the software's name is FLUOVIEW).

2.2.7 Western blotting

2.2.7.1 Pierce™ 660nm protein assay

Pierce™ 660nm protein assay is a colorimetric method that is used to measure protein concentration. To determine the protein concentration, it was necessary to make a protein standard curve. Bovine serum albumin (BSA), 2000 µg/ml was used as a standard protein. A range of BSA concentrations were prepared for the standard curve (2000, 1500, 1000, 750, 500, 250, 125, 50, 25 and 0 µg/ml) by dissolving in PBS. A microplate 96 well was used to perform the procedure, to each well was added 150 µl Pierce Assay reagent, and 10µl of the dilution, protein that was of unknown concentration and a blank (PBS only). The microplate was covered, and put on plate shaker for 1 minute, and then incubated for 5 minutes at room temperature; it was read at 660 nm using spectrophotometer (Thermo Scientific, MULTISKAN FC). To know protein concentration a standard curve was made by plotting the optical density readings against the known concentration.

2.2.7.2 Adipose lysate preparation

The method of extracting proteins from fat tissue was developed by Dr S. Byrne: 400 mg epididymal fat pad were homogenised in 400 microbutan-1-ol: Diisopropylether (2:3) with added Oil red O (take upper, red phase), and 200 microl PBS using a glass homogeniser. After centrifugation (1200 xg 5 min), the top, pink phase is discarded, more butan-1-ol: with added Oil Red O to colour the organic phase and, the tube shaken, centrifuged, the top phase discarded. This procedure is repeated twice, and needs to occur in the fume hood. 100 µl sample buffer was mixed with 100 µl protein sample then the samples were heated at 95°C for 3 minutes. Each well was loaded with 20 µl sample (4 mg /ml).

2.2.7.3 Liver lysate preparation

One hundred milligram of liver was added 1ml cell/tissue extraction lysis buffer (180 mMTris/HCL PH 6.8, 29% (v/v) glycerol, 5.7% (w/v) SDS, bromophenol blue, and dH₂O). The samples were centrifuged then the supernatant was collected into a new tube. Reducing sample buffer was prepared by adding 900µl Laemmli to 100µl 1M dithiothreitol (DTT). 200µl sample buffer was mixed

with 200µl protein sample then the samples were heated in 95°C for 3 minutes. Each well was loaded with 20µl sample.

2.2.7.4 Preparation of SDS-PAGE gels

12% SDS-PAGE gel was prepared as described in Table 2.6. After the gel was poured between glass plates, the gel polymerised then stacking gel was added in to the top gel. 5% stacking gel was prepared by mixing H₂O 2.1ml with 30% acrylamide mix 0.5ml, 1.5M Tris (pH 8.8), 380µl, 10% SDS 30µl, 10% ammonium persulfate 30µl, and TEMED 3µl. Then the samples were heated in 95°C for 3 minutes. Each well was loaded with 20µl sample.

Table 2.6: Preparation of buffers for Western blot.

Solution	Preparation
2x Loading Buffer	4ml dH ₂ O, (1ml) 0.5M pH 6.8 Tris-HCL, 800µl Glycerol, 1.6ml 10% sodium dodecyl sulfate (SDS) (Fisher) (w/v) in H ₂ O, Bromophenol blue, and 200mM Dithiothreitol (DTT) (Sigma).
SDS-PAGE gel	12% Resolving Buffer: H ₂ O, 30% Acrylamide/Bis solution, 1.5M pH 8.8 Tris, 10% SDS, 10% Ammonium persulfate (APS) (Sigma A-3678), and 10µlTEMED (Sigma T9281). 5% Stacking Buffer: H ₂ O, 30% Acrylamide/Bis solution, 1M pH 6.8 Tris, 10%SDS, 10% APS, and 6µl TEMED (Sigma T9281).
10 x Running buffer	30g Tris-Base, 144g Glycine (Fisher), and 10g SDS in 1L dH ₂ O (for 1x Running buffer diluted 1:10 in dH ₂ O).
1 x Blotting Buffer	5.9g Tris-Base, 2.9g Glycine, 100ml Methanol, and 3.4ml 10%SDS, and 1L dH ₂ O.

The protein samples were prepared for SDS-PAGE analysis by mixing 20µg from each sample with 2x loading buffer (Table 2.6) 1:2 dilution into new reaction tubes, and heated at 95C° for 5 minutes to denature the protein to the primary structure for protein. Then the samples were centrifuged in 16,000 xg for 5 seconds to remove insoluble debris, and the supernatants were used. After that the protein samples were run in 12% SDS-PAGE gel with a 5µl protein marker in 1x running buffer 60mA for 1-1.5 hour (Table 2.6). The separated proteins on the gel were electrophoretically transferred to a methanol activated PVDF membrane (GF Heath care Life Science, AmershamTmHybondTm 0.2µm PVDF, 1060006), using 1x blotting buffer (transfer buffer). After blotting at 250mA for 1hour, the membrane was washed in PBS, and blocked with 20ml of 5% (w/v) dried skimmed milk in PBS for 2 hour on the shaker at RT. Then the membrane was washed three times in PBS-0.05% (v/v) Tween for 10min with shaking. After that, the membrane was

probed with the primary antibody (Table 2.5) diluted in 5% skimmed milk in PBS (w/v) overnight at 4°C, washed as above, and probed with a second antibody (Table 2.5) diluted in 5% skimmed milk in PBS (w/v) for 2 hour maximum at RT with shaking. Finally, the membrane was washed as described previously, and the face of the membrane exposed to Enhanced chemiluminescence (ECL) (Pierce™ ECL Western Blotting Substrate, 32106) reagents, wrapped in cling film, and exposed to x-ray film (Bio-Max Light, Sigma) in a light-tight cassette. Then the film was submerged in developing solution for 2min until antibody-reactive bands appeared, then were washed in water, then submerged in a Fixer solution, washed in water again, and then the film was left to dry.

2.2.7.5 SDS-PAGE gels staining

Proteins separated in SDS-PAGE gel were detected by staining the gel with Coomassie brilliant blue R-250 (3g stain in 100ml acetic acid, 450ml IMS, 450ml H₂O) then the stain was removed by de-staining solution (50ml IMS, 100ml acetic acid, 850ml H₂O).

2.2.8 Investigation of iron storage by Prussian blue staining

2.2.8.1 Splenocyte preparation

Spleen was placed into a reaction tube of RPMI medium, then spleen was placed into the cell strainer. The plunger end of the syringe was used to mash the spleen through the cell strainer into a 50ml falcon tube. Cell strainer was rinsed with 5mL RPMI medium. Cell suspension was transferred to 15ml tube, and centrifuged at 300 xg for 5 minutes. Supernatant was discarded, and pellet was re-suspended in 1mL RBC lysis buffer per spleen (0.15M NH₄Cl, 1 mM KHCO₃, EDTA 0.1mM), followed by incubation at room temperature for ~1 minute. 5mL RPMI was added, and centrifuged as described in the previous step. Supernatant was discarded, and pellet re-suspended in 1mL RPMI medium per spleen. Hemocytometer was used to count splenocyte viable cells by adding 10µL cell suspension in trypan blue. Splenocytes with the media were placed in six well plate, and coverslips were inserted into the wells, after 24 hours Prussian blue staining was performed.

2.2.8.2 Prussian blue staining

Cells were rinsed twice with PBS then fixed 5 minutes in 4% paraformaldehyde in PBS, equal parts of 20% HCl and 10% potassium ferrocyanide was mixed, and immediately performed before starting. Slides were immersed in this solution for 20 minutes then washed three times in distilled water. Counter stain step was performed by using nuclear fast red for 5 minutes. Slides were rinsed in distilled water two times. The sections were immersed in 95% alcohol, and 2 changes of 100% alcohol. Xylene, 2 changes, 3 minutes each. Finally, slides were placed by DPX with cover slips.

2.2.9 Limulus amoebocyte lysate (LAL) endotoxin measurement

LAL is a quantitative method to detect bacterial endotoxin. LAL was lyophilised lysate prepared from amoebocytes in horseshoe crab. The activation of proenzymes in the modified LAL is catalysed by bacterial endotoxin, and the splitting of p-Nitroaniline (PNA) from the colourless substance is catalyzed by the activated pro enzyme. The rate of activation, and colour intensity is relative to the concentration of endotoxin amount.

A 96-well microplate well was placed in a heating block for 10 minutes at 37°C. 50µl standard, and unknown samples were added to the microplate wells then the plate was covered with the lid. After incubation for 5 minutes at 37°C, 50µl of LAL was added to each well, the plate was covered with the lid then it was gently shaken on a plate shaker for 10 seconds. After incubation for 10 minutes at 37°C, 100 µl of substrate solution was added to each well, the covered plate with the lid was gently shaken on a plate shaker for 10 seconds, and incubated for 10 minutes at 37°C. 50 µl of a stop reagent (%25 acetic acid) was added in to the plate, covered with the lid, and put on the plate shaker for 10 seconds then incubated at 37°C for 10 minutes. The plate absorbance was measured by a plate reader at 405-410nm. A standard curve was made in EU/mL between blank-corrected absorbance against concentration to know unknown concentration of endotoxin samples. Activity of samples was expressed as IE/ml with the help of the standard curve.

2.2.10 Glucose measurement

Blood glucose was measured by using glucose meter. Approximately 5µl of serum was put on testing strip after it was inserted in to the blood glucose meter then the result was shown in 5 seconds. Serum glucose was measured by using glucose meter. To ensure a good result OneTouch® Ultra control solution was used, this is performed as following: shaking it, and first drop was discarded then a drop inserted in to testing strip. In order to check whether it is working or not, human plasma was checked twice then our serum samples were tested. Approximately 2µl serum sample was pipetted on testing strip after it was inserted into the blood glucose meter then the result was shown in 5 seconds.

2.2.11 Insulin ELISA test

Sandwich ELISA method was performed by utilizing the wide range mouse insulin immunoassay kit (catalogue number: orb54821). 5µl of standard or sample was added in duplicate to its corresponding well without sample dilution. 100µl of 1x detection antibody solution was added per well. The plate was sealed with a plate cover after incubation for 1 hour and half at room temperature then shaking the plate at 600rpm on a horizontal micro-plate shaker. The content was discarded, and the plate was tapped on a clean paper towel to remove residual solution. 300µl of 1x wash buffer was added to each well. The well plate was incubated at room temperature for 20 seconds. To remove residual wash buffer, the 1x wash buffer was discarded. The washing step was repeated for a total 4 washes. The rest steps as follows: 100 µl of the provided substrate solution was added to each well for 15 minutes at room temperature. 100µl of stop solution was added to each well. To ensure thorough mixing, gently tap the plate frame for a few seconds. The well plate was measured at 450nm absorbance.

2.2.12 Liver function tests

2.2.12.1 Alanine transaminase activity (ALT)

ALT assay (Abcam: catalogue number 105134) was used according to the manufacturer's instructions. Serum samples were diluted in 1:5 dilution, and also standard curve was prepared from 0nmol/well to 10nmol/well. 20 μ L of standard dilutions or unknown samples were performed in duplicate, then 100 μ L of the reaction mix was added. Concentration of pyruvate in the unknown samples was calculated as follows:

$$\text{ALT activity} = (B / \Delta T \times V) D.$$

$$\text{ALT activity} = \text{nmol/min/mL} = \text{mU/mL}.$$

B = Amount of pyruvate from pyruvate standard curve.

ΔT = reaction time (min).

V = original sample volume added into the reaction well (mL).

D = sample dilution factor.

2.2.12.2 Aspartate Aminotransferase activity (AST)

AST assay (Abcam: catalogue number 105135) was used according to the manufacturer's instructions. Serum samples were diluted in 1/5 dilution, and also standard curve was prepared from 0nmol/well to 10nmol/well. 50 μ L standard dilutions for standard wells, and 50 μ L samples for sample wells were performed in duplicate then reaction mix 100 μ L was added. Concentration of glutamate in the test samples was calculated:

$$\text{AST activity} = B / (T2 - T1) \times V = \text{nmol/min/ml} = \text{mU/ml} \text{ Where:}$$

B is the glutamate amount (nmol) calculated from the standard curve.

T1 is the time of the first reading (A1) (min).

T2 is the time of the second reading (A2) (min).

V is the original sample volume added into the reaction well (ml).

2.2.13 Adiponectin ELISA test

Serum samples were required to be diluted at least 2000-fold in Calibrator Diluent RD5-26 (1:4) (20ml of calibrator diluent RD5-26 + 60ml dH₂O). A suggested 2000-fold dilution was performed by creating a 100-fold dilution of 10 µL of sample and 990µL of Calibrator Diluent RD5-26 (1:4). Further dilute 20-fold with 10µL of the 100-fold diluted sample and 190 µL of Calibrator Diluent RD5-26 (1:4). Standard was prepared from 0.16ng-10ng. 50µL of Assay Diluent RD1W was added to each well then the diluted standard, and serum samples were added to the wells in duplicate, the rest steps are shown in manufacturer's instructions of ELISA Mouse Adiponectin/Acp30, R&D systems.

2.2.14 Malondialdehyde (MDA) assay

MDA assay was performed according to manufacturer's instructions (ab118970 Lipid Peroxidation). Serum samples were diluted as follow: 10µL serum was mixed gently with 500µL of 42mM H₂SO₄ in an eppendorf tube then 125µL of phosphotungstic acid solution was added. Standard dilutions were used from 0nmol-2nmol. MDA-TBA adduct was made by adding 600 µL of TBA, 200µL standard, and 200µL sample. 200µL of diluted standard or serum samples were added in duplicate. Concentration of MDA in the unknown samples was calculated as follows:

Concentration of MDA = (A/ml) x 4 x D

A = Amount of MDA in sample from the standard curve (nmol).

ml = Original serum volume used in ml.

4 = correction for using 200 µL of the 800 µL reaction mix.

D = Sample dilution factor.

2.2.15 Pro-inflammatory parameters

2.2.15.1 IL-6 ELISA

Murine IL-6 ELISA kit (Peprotech) was used according to manufacturer's instructions. To prepare the ELISA plate, capture antibody was diluted with PBS to a concentration of 2µg/ml, and immediately 100µl were added to each well (41µg of antigen –affinity purified goat anti IL-6 and 0.5mg D-mannitol) in 210µl H₂O. It was done in 96-well plate in 1:100 dilution (1ml of stock and 99ml PBS). The plates were sealed, and incubated overnight at room temperature. Subsequently, the plate wells were aspirated to remove liquid, and washed 4 times using 300µl of wash buffer (0.05% (v/v) Tween-20 in PBS) per well. After the last wash, the plates were inverted to remove the residual buffer, and were blotted on paper towels. Then 300µl of the block buffer (1% (w/v) BSA in PBS) were added to each well, and incubated for at least 1 hour at room temperature after that the plate was aspirated, and washed 4 times.

Murine IL-6 standard was diluted starting from 4 ng/ml to zero, in diluent (0.05% (v/v) Tween-20, 0.1% BSA in PBS). Then immediately, 100µl of standard or sample were added (serum samples was diluted 1/10) to each well in duplicate, and incubated at room temperature for at least 2 hours. The plate was aspirated, and washed 4 times by using wash buffer. Biotinylated detection antibody was diluted in diluent to a concentration of 0.25µg/ml, and then 100µl were added per well, and incubated at room temperature for 2 hours. After that, the plate was aspirated, and washed 4 times using a wash buffer. 5.5µl of Avidin-HRP conjugate was diluted 1:2000 in diluent for total volume of 11ml, and 100µl were added per well, and incubated 30 minutes at room temperature. The plate was aspirated, and washed 4 times, and 100µl of substrate solution ABTS, 2, 2'-azino-bis (3-ethylbenzothiazoline-6-sulphonic acid) (Sigma) were added to each well, and incubated at room temperature for colour development. After colour developed stopping solution (Sulfuric acid 6.6ml and d.H₂O 4ml). Colour development was monitored using an ELISA plate reader (680 Microplate Absorbance Reader) at 405 nm wavelength.

2.2.15.2 TNF- α ELISA test, supernatant and mice serum

Murine TNF- α ELISA kit (Peprotech) was used according to manufacturer's instructions. To prepare the ELISA plate, capture antibody was diluted with PBS to a concentration of 2 μ g/ml, and immediately 100 μ l were added to each well (41 μ g of antigen –affinity purified goat anti TNF- α +0.5mg D-mannitol) in 210 μ l H₂O. The 96 well plates were sealed, and incubated overnight at room temperature. Subsequently, the plate wells were aspirated to remove liquid, and washed 4 times using 300 μ l of wash buffer (0.05% (v/v) Tween-20 in PBS) per well.

After the last wash, the plates were inverted to remove the residual buffer, and were blotted on paper towels. Then 300 μ l of the blocking buffer (1% (w/v) Bovine Serum Albumin (BSA) in PBS) were added to each well, and incubated for at least 1 hour at room temperature. After that the plate was aspirated, and washed 4 times.

TNF- α standard was diluted starting from 2 ng/ml to zero, in diluent (0.05% (v/v) Tween-20, 0.1% BSA in PBS). Then immediately, 100 μ l of standard, and supernatant samples were added to each well (serum was 1/5 dilution) in duplicate, and incubated at room temperature for at least 2 hours. The plate was aspirated, and washed 4 times by using wash buffer. Detection antibody was diluted in diluent to a concentration of 0.25 μ g/ml, and then 100 μ l were added per well, and incubated at room temperature for 2 hours. After that, the plate was aspirated, and washed 4 times using a wash buffer. 5.5 μ l of Avidin-HRP conjugate was diluted 1:2000 in diluent for total volume of 11ml, and 100 μ l were added per well, and incubated 30 minutes at room temperature. The plate was aspirated, and washed 4 times, and 100 μ l of substrate solution ABTS, 2,2'-azino-bis (3-ethylbenzothiazoline-6-sulphonic acid) (Sigma) were added to each well, and incubated at room temperature for colour development. After colour development, stopping solution (Sulfuric acid 6.6ml+ D.W 4.4ml) was added, and plate was read using an ELISA plate reader (680 Microplate Absorbance Reader) at 405 nm wavelength.

2.2.16 C5a ELISA level

To prepare the ELISA plate, capture antibody (purified rat anti-mouse C5a (152-1486 BD Pharmingen) was diluted with PBS to a concentration of 10µg/ml, and immediately 100µl were added to each well (96 well plate). The plates were sealed, and incubated overnight at room temperature. Subsequently, the plate wells were aspirated to remove liquid, and washed 5 times using 300µl of wash buffer (0.05% (v/v) Tween-20 in PBS) per well.

After the last wash the plates were inverted to remove the residual buffer, and were blotted on paper towels. Then 200µl of the block buffer (1% (w/v) Bovine Serum Albumin (BSA) in PBS) were added to each well, and incubated for at least 1 hour at room temperature after that the plate was aspirated, and washed 5 times. After that the plate was washed as above.

Standards (purified recombinant mouse C5a; BD) was diluted to 60, 30, 15, 7.5, 3.7, 1.87, 0.935, 0.467, and 0ng/ml in dilution (0.05% (v/v) Tween buffer (v/v) 20, 1% (w/v) BSA in PBS). Then immediately, 100µl of standard or sample were added (serum samples were diluted 1/20) to each well in triplicate, and incubated at room temperature for at least 2 hours. The plate was aspirated, and washed 5 times by using wash buffer. Detection antibody (purified biotinylated rat anti-mouse C5a (152-1486 BD Pharmingen) was diluted in diluent to a concentration of 2µg/ml, and then 100µl were added per well, and incubated at room temperature for 2 hours. After that, the plate was aspirated, and washed 5 times using a wash buffer. One hundred microliters of Streptavidin-peroxidase conjugate (from Sigma-Aldrich) diluted 1:100 was added to each well followed by incubation for 30 minutes. The plate was aspirated, and washed 5 times. Then 100µl of substrate solution (TNB, R&D, and USA) was added to each well. The plate was incubated at room temperature for colour development. After that, stop solution was added, and the results were obtained by reading absorbance at 450nm.

2.2.17 Lipid measurements

2.2.17.1 Triglyceride quantification assay for mouse liver

100 mg liver tissue was homogenized with 1mL of 5%NP-40/ddH₂O by using a Dounce homogeniser. Samples were heated to 80 – 100°C in a water bath for 5 minutes or until the NP-40 became cloudy, then were cooled down to room temperature. The heating was repeated to solubilize all triglyceride. Centrifuge for 2 minutes at top speed using a microcentrifuge to remove any insoluble material. Samples were diluted 10-fold with ddH₂O. Standard wells were added 50µL standard dilutions, and 50µL samples. Lipase 2µL was added to all wells (standard and samples) then incubated for 20 minutes at room temperature to convert triglyceride to glycerol, and fatty acid. 50µL of Reaction Mix was prepared, and added for each reaction by using colorimetric reaction mix (Triglyceride Assay buffer 46 µl, Triglyceride Probe* 2µl, Triglyceride Enzyme Mix 2µl). After adding 50µL of Reaction Mix, all samples were incubated at room temperature for 60 minutes. The plate was read on a microplate reader at OD 570 nm.

After applied sample readings to the standard curve Triglyceride concentration was measured as follow: $Concentration = (Ts/Sv) * D$

Where:

Ts = amount of Triglyceride (nmol) from standard curve.

Sv = volume of sample (µL) added in sample wells.

D = sample dilution factor.

2.2.17.2 Measurement of serum triglyceride using colorimetric assay kit

10 µl of triglycerides standard were added (tubes1-8) per well on the 96 well plate in duplicate. 10µl of samples (serum) were added in wells in duplicate. The reaction was initiated by adding 150µl of diluted enzyme buffer solution to each well. The plate was covered, and incubated for 15 minutes at room temperature. The color absorbance was read at 550nm using plate reader. After applying sample readings to the standard curve by using prism pad, triglyceride concentration (mg/dl) was measured.

2.2.18 NEFA Measurement

Extraction methods are widely used for the colorimetric determination of non-esterified fatty acids (NEFA) in serum. NEFA are converted to their copper salts that are extracted into an organic solvent. The salts are then complexed with a dye for the purpose of colorimetric measurement. Alternatively, extracted NEFA are titrated with standard alkali to an acid base indicator endpoint.

The Wako enzymatic method relies upon the acylation of coenzyme A (CoA) by the fatty acids in the presence of added acyl-CoA synthetase (ACS). The acyl-CoA thus produced is oxidized by adding acyl-CoA oxidase (ACOD) with generation of hydrogen peroxide, in the presence of peroxidase (POD) permits the oxidative condensation of 3-methy-N-ethyl-N(β -hydroxyethyl)-aniline (MEFA) with 4-aminoantipyrine, to form a purple coloured adduct which can be measured colorimetrically at 550nm. 7 μ l of serum was used (DAKO instructions). Colour reagent working solutions were prepared according to the package insert instructions. The NEFA standard was preparing provided standard diluted with distilled water. 7 μ l of mice serum, and standards were used in duplicate in to each well. 200 μ l of colour reagent A was added, mixed well, and incubated at 37°C for 5 minutes. The absorbance of each well was measured at 550nm (Abs1) (sample blank). After 100 μ l of colour reagent B solution was added, mixed, and incubated at 37°C for 5 minutes then measured at 550nm (Abs2). The final reading was obtained by subtraction first reading from the second reading. Absorbance versus concentration was plotted to construct the calibration curve.

2.2.19 Measurement of glycated haemoglobin in mouse serum (Ghb A 1C)

The 50 μ l of standard, and sample serum (1:10 dilution) were added to each 96 well plate. 50 μ l HRP-conjugate (1x) was added to each well immediately (not to Blank well). The plate was mixed with the pipette, and shaken gently for 60 seconds. The plate was incubated for 60 minutes at 37°C.

Each well was aspirated, and washed, four times. Each well was washed with wash Buffer. The plate was aspirated, finally inverted, and blotted against clean paper towels. 90 μ l of TMB substrate was added to each well. Incubate for 20

minutes at 37°C. The 50µl of Stop solution was added to each well. A microplate reader 450 nm was used to read the optical density.

2.2.20 Vitamin D serum mice measurement

Vitamin D (CUSABIO. catalog number: CSB-EL006401MO). The 50µl of standard, and sample serum (1:50 dilution) were added to each 96 well plate. 50µl HRP-conjugate (1x) was added to each well immediately (not to Blank well). The plate was mixed with the pipette, and shaken gently for 60 seconds. The plate was incubated for 60 minutes at 37°C.

Each well was aspirated, and washed, four times. Each wells were washed with wash Buffer. The plate was aspirated, finally inverted, and blotted against clean paper towels. 90µl of TMB substrate was added to each well. Incubate for 20 minutes at 37°C. The 50µl of stop solution was added to each well. A microplate reader 450 nm was used to read the optical density.

2.2.21 Complement activation

2.2.21.1 Classical and alternative complement activation pathway

The procedure was performed according to Kotimaa et al., (2015). Human purified IgM (BIORAD) was coated at 1µg/ml in CB buffer (1.5g of Na₂CO₃ + 2.9g of NaHCO₃ to 1 liter of D.W) (diluted 1:1000) for classical (CP) pathway. LPS (Lipopolysaccharide from *Salmonella enteriditis*) S form (HyCult Biotechnology) was coated at 1µg/ml in PBS/10 mM MgCl₂ (diluted 1:1000) for alternative pathway (AP). The final volume was 100µl per well. The Maxisorp plates were incubated for 16h at room temperature. Then, the wells were washed with 200 µl of PT buffer (200 µl of 0.05% Tween 20 to 400 ml of PBS) (3times, 5minutes). The AP was not blocked, while the CP was blocked with 150µl of PB buffer (1g of BSA to 100 ml of PBS) per well for 90 minutes at 37°C. Then, the wells were washed with 200µl of PT buffer per well (3times, 5minutes). Classical pathway serum dilution into BVB++buffer (Veronal buffer, 0.5mM MgCl₂, 2mM CaCl₂) AP in to BVB++/MgEGTA (5mM MgCl₂, 10 mM EGTA).

The concentrations of normal mouse serum (NMS) were added (100µl per well) in triplicates on the Maxisorp plates, and incubated for 1h at 37°C, then the wells were washed with 200µl of PT buffer per well (3times, 5minutes). After washing, 100µl of rabbit anti-complement component 9 polyclonal antibody (MyBioSource) (concentration 0.2mg/ml; diluted 1:200 with D.W.) was added per well, and incubated at 37°C for 1h. Then wells were washed with 200µl of PT buffer per well (3times, 5minutes). After washing, 100µl of polyclonal swine anti-rabbit-IgG HRP antibody (Dako) (concentration 1mg/ml, diluted 1:200 with D.W.) was added per well, and incubated at 37°C for 1h. Then the wells were washed with 200µl of PT buffer per well (3times, 5minutes). Later, 100µl of the coloured substrate (TMB) (Sigma) was added per well, and left at room temperature for 5-10 minutes, and then 50µl of the stop solution was added per well to stop the reaction. Finally, the result was read immediately by using ELISA reader TECAN Magelian for F50. The activation of Classical pathway, and alternative pathway was determined by using normal mouse serum (NMS), and heated normal mouse serum (56°C for 30minutes), to see C59 complement activation levels for both pathways *in vitro*. The percentage was calculated as follow: serum complement activation concentration /normal mouse serum)*100, for each mouse sample.

2.2.21.2 Human Classical, and Alternative complement activation pathway

Following protocol of serum mice CP, and AP complement activation pathway procedure as mentioned previously except antibodies. Mouse monoclonal IgG28 C5b-9 (aE11) Sc-58835 (Santa Cruz Biotechnology) was used as primary antibody (1:100). Poly clonal goat anti mouse Immunoglobulins (HRP) (Darko) was used as secondary Antibody (1:200).

2.2.21.2.1 Set up experiment for human serum complement activation

The concentration was chosen as follow: different serum concentrations were used (1:5, 1:10, 1: 20, 1:50, 1:100, 1:200, 1:400, 0) for both classical, and alternative pathway serum human samples. Serum dilution for human samples: 1:20 for classical pathway, 1:5 for Alternative pathway showed the highest

activity. Based on these normalisation procedures, human serum samples dilutions were performed for CP, and AP complement activation test.

2.2.22 Procedure of Mouse XL cytokine array kit

200 mg mouse thigh muscle was homogenised in 1% (v/v) Triton X-100, (n=2), each sample includes two mice muscles pooled in to one tube. After, the samples were centrifuged then the supernatant was collected in to a new tube. Protein concentration was measured by Nano drop. The concentration was adjusted to 20mg/ml. 2ml of array buffer 6 (block buffer) was added into each well of the 4-Well Multi-dish. Membranes were placed in separated wells, and facing upwards.

After one hour incubation on a rocking platform shaker, samples were prepared by adding up to 1mL of each sample to 0.5mL of Array Buffer 4 in separate tubes, then sample volumes were adjusted to a final volume of 1.5 mL with Array Buffer 6. Array Buffer 6 was aspirated from the wells of the 4-Well Multi-dish, and the prepared samples were added. The lid was placed on the 4-Well Multi-dish, then overnight incubation was performed at 2-8°C on a rocking platform shaker. The membranes were removed, and placed in individual plastic containers with 20 mL of 1X Wash Buffer. The 4-Well Multi-dish was rinsed with distilled water, and dried. Each membrane was washed with 1X Wash Buffer for 10 minutes on a rocking platform shaker (2 times for 3 washes). For each array, 30 µL of Detection Antibody Cocktail was added to 1.5 mL of 1X Array Buffer 4/6 of diluted Detection Antibody Cocktail (1.5mL per well), and was pipetted into the 4-Well Multi-dish. Each array was removed from its wash container. The array was returned to the 4-Well Multi-dish containing the diluted Detection Antibody Cocktail, and it was covered with the lid. After one hour incubation at room temperature on a rocking platform shaker, the arrays were washed as described in previous steps. 2.0 mL of 1X Streptavidin-HRP was pipetted into each well of the 4-Well Multi-dish, then each membrane was removed from its wash container. After the membranes were returned to the 4-Well Multi-dish containing the 1X Streptavidin-HRP, wells were covered with the lid, and incubated for 30 minutes at room temperature on a rocking platform shaker. Membranes were washed as described in previous steps. Each

membrane was removed from its wash container, it was drained by blotting on to paper towel. Afterwards, 1.0 mL of the prepared Chemi Reagent Mix (for 1 minute) was added onto each membrane then covered with the top sheet of the plastic sheet protector. After the excess Chemi Reagent Mix was squeezed out, then membranes were left on the bottom plastic sheet protector. To smooth out any bubbles, the membranes were covered with plastic wrap. Membranes were exposed to X-ray film for 1-10 minutes. Then the film was submerged in Develop solution for 2min until antibody-reactive spots appeared, washed in water, and submerged in solution, then washed in water and left to dry.

2.2.23 Microarray for adipose tissue

The method of extracting proteins from fat tissue was developed by Dr S. Byrne: 400 mg epididymal fat pad were homogenised in 400 µl, Butan-1-ol: Diisopropylether (2:3) with added Oil Red O to colour the organic phase and 200 microl PBS using a glass homogeniser. After centrifugation (1200 xg 5 min), the top, pink phase is discarded, more, Butan-1-ol: Diisopropylether, the tube shaken, centrifuged, the top phase discarded. This procedure is repeated twice, and needs to occur in the fumehood. After a final spin, the aqueous phase was transferred to a fresh tube. Protein concentration was measured by Nano drop (Thermo scientific). After 100µl sample buffer was mixed with 100µl protein sample then the samples were heated in 95°C for 3 minutes. Each well was loaded 20µl sample (4mg /ml of each well). 2ml of array buffer 6 (block buffer) was added into each well of the 4-Well Multi-dish. Membranes were placed in separated wells, and facing upwards, the reset procedure as above 2.2.21. ImageJ2 software was used to analyse the data by measuring the pixel densities on developed X-ray film for each spot that reflects the different protein expression levels. The density of each protein, reference spots (positive control), negative control (PBS) and background signal (clear area of the array (no antibody) spots were measured in duplicate and the mean average was calculated. Then the average of the background density was subtracted from each spot. Finally, each spot was normalised with the reference spot and the graphs were plotted to compare the signal of the proteins in the two samples:

$\frac{\text{The mean of each spot}}{\text{The mean of the reference spots (positive control)}}$
--

2.2.24 Detection of apoptosis by cytochemical method

Using ApopTag[®] *In Situ* Apoptosis Detection Kits (Millipore, Cat no. S7100). Sections were cut by microtome at 4 μ m and heated on to 52°C water, the wax picked up on glass slides. Slides were prepared after being dried then the wax was removed by rinsing in xylene for 5 minutes (2 times). The slides were rinsed in 100% ethanol for 5minutes (2 times) then immersed in 95% ethanol for 5minutes. Slides were rinsed 70% ethanol for 5minutes then washed with water for 5 minutes. Finally, slides were rinsed to PBS for 2 minutes. Specimens were applied Proteinase K (20 μ g/ml) was added for 10 minutes at room temperature to digest away some of the nuclear protein. 3.0% (v/v) freshly prepared hydrogen peroxide (Sigma, Cat no. 216763) in PBS was added to the slides for 10 minutes. Then the specimens were rinsed with PBS for twice, 5 minutes each. Excess water was removed, and equilibrium buffer 30 μ l/2cm² was applied for 15 minutes at 37°C. The equilibrium buffer was discarded, and 55 μ L working strength TdT enzyme was added to each specimen for 1 hour, and incubated at 37°C in the incubator. One of the nucleotides was labelled with digoxigenin. During apoptosis, many 3' OH available; these are the sites where TdT incorporates a new "tail" which contain the DG label. After 1 hour the working strength stop/wash buffer was added to the slides at room temperature. The slides were washed in 3 changes of PBS for 1 minute each, and 65 μ L of anti-digoxigenin peroxidase to 30 μ l/2cm², and incubated in 37°C for 30minutes. The slides were washed with 4 changes of PBS for 2 minutes per wash at room temperature. Then, 75 μ L of 0.05% DAB (3, 3'-diaminobenzidine) (Sigma, Cat no. D-5637) (working strength peroxidase substrate) in PBS (w/v) was added to each 30 μ l/2cm² specimen for 6 mints at room temperature, and washed three times with dH₂O for 1 mint each. The specimens were stained with 0.5% Methyl green (Counterstain) for 10 minutes at room temperature, and washed in 3 brief changes of dH₂O, 100% isopropanol, and Xylene. Finally, mount under a glass

coverslip in D.P.X mountant (BDH, Cat no. 36029), and left to dry. The slides were examined under the light microscope (PRIOR).

2.2.25 HepG2 cells by Oil Red O staining

2.2.25.1 Intracellular lipid content assessment

HepG2 cells were plated in 25cm² flask at 70% confluence, and co incubated with 30Mm FFAs (oleic acid/palmitic acid, 2:1) in serum-free medium containing 1% FFAs-free BSA for 24 hours. Cells were observed under phase contrast. Six well plates were used to seed the HepG2 cells with FFA with and without Vitamin D in different concentration for 48 hours then Oil Red O staining as follow:

2.2.25.2 Oil Red O staining measurement by spectrophotometer

HepG2 cells were grown at an initial density of 105 cells/well in a 24-well plate and treated with 30Mm FFA, and different concentrations of vitamin D (0.4, 2,4µg/ml) for 48 hours. Iced PBS was used to wash the cells which were fixed with 4% formaldehyde for 10 minutes then washed 3 times with PBS. Oil Red O solution was used to stain cells (working solution, 0.5g Oil Red O powder dissolved in 60% ethanol) for 10 minutes at room temperature. To remove unbound staining, cells were washed with PBS. Dimethyl sulfoxide was added to each sample so as to quantify Oil Red O content levels; after shaking at room temperature for 5 minutes, spectrophotometer at 510 was used to read the density of cells that have Oil Red O staining.

2.2.25.3 Generation of Bone marrow derived macrophages

Femurs and tibias from LDLR^{-/-}PWT, and LDLR^{-/-}PKO mice fed high fat diet were used to prepare macrophages, the reason was to investigate lipid loaded in macrophages with and without Vitamin D. The bones are put in 100% IMS for a few minutes, and subsequently washed with PBS. The bones are then cut from both sides, and flushed with PBS in to a 15ml falcon tube using a 1 ml syringe which has a 0.45mm diameter needle. The tube is vigorously shaken to break up cell clusters. After a few minutes the supernatant is transferred to a new tube then centrifuged at 277 g for 5 minutes. The supernatant is discarded,

and the pellet re-suspended in freezing medium (10 % (v/v) dimethylsulfoxide/FCS), and transferred to -80°C. Thawing bone marrow cells were added to RPM1-160 medium, and spun for 5 minutes at 1200 rpm. The supernatant was discarded, and cover slip was added in to each 6 well plate. The pellet was suspended in to the media so as to collect all the cells then the media was added in to each well plate after that (20ng/ml) of GMCSF was added. Incubation at 37°C for 7 days was performed, after 7 days the cells were preconditioned with Vitamin D (2µg/ml) for 1 day. Cells were stimulated by lipopolysaccharide from *E. coli*, serotype O111:B4 100ng/ml for 24 hours. Cells in 6 wells were washed by PBS 3 times then the cells were fixed in neutral buffered formalin for 10 minutes. 10ml 0.2% Oil Red O in propan2-ol stock, and 6.6ml dH₂O were added through a 0.7Nm filter for 5-10 minutes. After staining cells in 6 well plates were washed 3 times by distilled water in order to clean from excess stain. Carazzi's Haematoxylin was added for 3 minutes to stain the nuclei of cells. The cells were washed with tap water 3times to remove the excess stain. The cover slips were mounted by using 50% glycerol in PBS. After cover slips were put on slides, and examined by using light microscope under 40X magnification.

2.2.26 Stimulation of macrophages *in vitro*

2.2.26.1 Using J774 cell line

Fish oil (commercial capsule %10) (3ml/well) was added to J774, and in a 6 well plate in complete medium for 5 days, then cells were stimulated with 1µg/ml LPS *E. coli* O111: B4. The well plate cells were fed with 1 ml medium on day 4, then all media was removed on day 5. 2ml complete RPMI medium (10% FCS) were added with, and without washing with PBS, 2 wells were run in parallel which remained unstimulated with fish oil, one of which received the LPS treatment.

2.2.26.2 Bone marrow derived macrophages

Thawing bone marrow cells were added to RPMI-160 medium, and spun for 5 minutes at 1200 rpm. The supernatant was discarded, and 20ml RPMI-160 media was added in to each falcon tube then 4µl Granulocyte Monocyte Colony Stimulating Factor (GM-CSF) was added for the two falcon tubes (20ml each). The media was suspended in to the pellet so as to collect all the cells. After adding 5ml of media in to each small flask then the flasks were incubated at 37°C for 7 days. After 7 days 5µl DHA (25 mg/760 µl ethanol) was added to each of two small flasks, and 5µl ethanol to the others as a control. After 2 days the cells were stimulated by lipopolysaccharide from *E. coli*, serotype O111:B4 1000ng/ml for 24 hours. Cells were harvested, and RNA extraction, DNase digest, cDNA synthesis, and cyclic amplification for inflammatory mediators were performed.

2.2.27 Data analysis

Unpaired T-test was used to analyse data statistically by Graph Pad Prism 7 programme (Graph Pad, San Diego California, USA). Unpaired-test, parametric was used because we compared between two independent groups assumed that the sampled data follow a Gaussian bell-shaped distribution and both population have same standard deviations. T-test calculates two group means divided by standard error of the difference. The sign of the t shows us which group had a larger mean. The p value is derived from the absolute value of t. Degree of freedom in t-test is equal to total sample size minus 2. Prism calculated p-value from t and degree of freedom. The P-value answered our questions either had effect or not. If the Null hypothesis was not true then only there is 5% chance that p value more than 0.05.

ANOVA one-way was used when the comparison was more than two groups and the data categorized in one way for instance, comparing control with two treated groups. ANOVA, parametric test was used because we compared between three or more groups assumed that the sampled data follow a Gaussian bell-shaped distribution and both population have same standard deviations. Turkey post-test was used to compare pairs of group means, it shows that multiple and interrelated comparisons. Post-tests are working as t-test calculation instead divided by standard error of the difference, they divide by a value calculated from the residual mean square, p –value-represents for multiple comparison. Prism presents a P value for the defence between each pair of mean, but the probability value represents to all family of comparisons, not for each individuals. If the Null hypothesis is true then only there is 5% chance that p value less than 0.05.

Non-reproducible results for replicates of tested sample in the experiment was not accepted, the experiment was excluded and should be repeated. Data were expressed as Means \pm SD for all experiments (n= the total number of mice). The density of protein array was measured by ImageJ software. Non parametric data were evaluated blinded and scored as described. We have decreased the extent of variability between individuals as follows: in vivo, all mice held in the

same unit so exposed to the same stimuli, littermates analysed. Mice of certain ages analysed. "matched"; reduction of stress due to environmental enhancement (towards the end of your studies), especially important for males. In vitro, cultured according to standard procedure so they were used in comparable growth phases throughout the study. Own controls for each stimulation to compare against treatment. Null hypothesis means that there is no difference between groups. P value is the probability of observing a difference larger than is observed if the null hypothesis were true. Prior to starting experiment, a threshold p value (called α) was set to 0.05 and null hypothesis was defined. If the p value was less than threshold, null hypothesis was rejected and the difference was significantly statistical different; whereas, if the p value was greater than threshold, null hypothesis was not rejected and it was not significantly statistical different. When we reached to find that significantly different between groups, which is called Type 1 error, when the populations are identical. Type 1 error in 5% of experiments no significant different ($p < 0.05$). While, we reached to find that there was not significantly different between groups, which is called Type 2 error, when the populations are not identical. Type 2 error in 5% of experiments was significant different ($p < 0.05$) If the p value is greater than 0.05, it means the overall mean differs from the hypothetical value we entered, the 95% confidence intervals will start with negative number, the hypothetical mean is larger than actual mean. If the p value is small (less than 0.05), it means that the difference is not due to coincidence in between sample mean hypothetical mean, the 95% sure they were different.

Chapter 3 Characteristics of common nutrient additives with beneficial dietary effect

3.1 Introduction

The aim of this study was to investigate whether DHA, Vitamin D (D3) and Allicin affect TNF- α response of macrophages after stimulation with LPS.

3.1.1 Anti-inflammatory Role of Allicin

Allicin is also had anti-inflammatory role by the inhibition of P38, and JNK pathways, and the expression of NF- κ B in rats given trinitrobenzenesulfonic acid (Li et al., 2015). In an *in vitro* study Allicin (10-30 μ M 24 hours) killed parasites (Jesus Corral-Caridad et al., 2012). Garlic extracts has contributed to ameliorate obesity, metabolic syndrome, cardiovascular disorders, gastric ulcer, and even cancer (Arreola et al., 2015).

In the study by Lee et al., 2011, male C57BL/6J mice were given a high-fat diet (45% fat) for 8 weeks to establish obesity. In the group receiving high fat diet supplemented with garlic, body weight gain was less as well as the amount of white adipose tissue, and levels of plasma and hepatic triglycerides, total cholesterol compared to control mice (male C57BL/6J fed high fat diet without supplemented garlic). In addition, liver function enzymes such as AST and ALT were normalised in mice fed high fat supplemented with garlic. mRNA levels such as PPAR γ and SREBP-1c, which are involved in adipocyte differentiation, were investigated in white adipose tissue. The result showed that as PPAR γ and SREBP-1c mRNA expression was significantly lower in mice fed high fat supplemented with garlic, pointing to a likely mode of action for allicin. In addition, AMPK activity, which has a role in thermogenesis and downregulation of adiposity, was lower in mice given high fat diet-supplemented with garlic (Lee et al, 2011). The beneficial effect of dietary garlic when on a high fat diet (x% fat) was observed as early as 5 weeks, in terms of reduced body weight gain, epididymal fat accumulation, improved liver histology as well as triglyceride and cholesterol levels (Kim and Kim, 2011).

3.1.2 Anti-inflammatory Role of Omega 3

Omega 3, a polyunsaturated fatty acid, inhibits inflammation (Simopoulos, 2002). It also has an additional beneficial effect on NASH by regulating hepatic lipid metabolism (see below). In fact, NAFLD patients have been treated by omega 3 supplementation, and compared to control (2g EPA combined with diet for 6 months in 42 patients). They were found to have improvement of liver steatosis, and liver enzymes in the treatment group compared to the control group (Capanni et al., 2006). Omega 3 deficiencies are associated with the development of insulin resistance, fatty liver disease, dyslipidemia (Scorletti and Byrne, 2013).

Omega-3 fatty acid has a role in regulation of lipid metabolism including hepatic *de novo* lipogenesis by inhibition of sterol regulatory element-binding protein (SREBP-1) (Capanni et al., 2006), and carbohydrate regulatory element-binding protein (ChREBP) activity (Musso et al., 2009), reduction in VLDL synthesis due to the increase of hepatic fatty acid -oxidation, apoB100 secretion and autophagic degradation (Chan et al., 2003), and activation of PPARs (peroxisome proliferator-activated receptors), they are transcriptional factors that are involved in lipid, protein, and carbohydrate metabolism, and form part of the analysis (Chan et al., 2003)

Omega3-fatty acids also have anti-inflammatory effects by inhibiting TNF- α , and IL-1 β , adipokine secretion, and inhibition of macrophage activation, and recruitment, decreasing release of fatty acids. In addition, omega-3 fatty acid causes increasing bile acid synthesis, and secretion, and up-regulation of cholesterol 7 α -hydroxylase (CYP7A1) (Scorletti and Byrne, 2013).

Fish oils are rich in long chain n-3 polyunsaturated fatty acids (LC n-3PUFA), eicosapentanoic (EPA), and docosahexaenoic (DHA). They play a significant role in the metabolic syndrome, and inflammation treatment (Mullen *et al.*, 2010). The aim of this study was to investigate whether DHA, and Vitamin D (D3) affect TNF- α response of macrophages after stimulation with LPS.

According to previous work, macrophages preconditioned with DHA (50 μ M) for 5 days led to anti-inflammatory effect by inhibition of TNF- α , attenuated LPS-induced nuclear factor (NF) kB activation, resulting in less TNF- α produced (Oliver et al., 2012). In this study, J774 macrophages were pre-treated with

DHA (50 μ M) for 5 days were stimulated with 100ng/ml LPS for 30 min. Cells were washed in PBS and fresh media was added and left to incubate with cells for a further 48 hour. DHA-preconditioned J774 led to the decrease of pro inflammatory cytokines such as IL-6, TNF α , and the increase of IL-10 as measured by ELISA (Oliver et al., 2012).

Adipocytes co cultured with DHA enriched macrophages developed insulin sensitivity, and also enhanced insulin-stimulated 3 H-glucose transport, GLUT4 translocation (Oliver *et al.*, 2012). In their work, J774 macrophages pretreated with DHA (50 μ M) for 5 days and stimulated with 100ng/ml LPS (30 minutes, 24 hours) were washed and placed in transwell inserts above fully differentiated 3T3-L1 adipocytes (48,72 hours). DHA (50 μ M) enriched macrophages for 5 days led to the increase of IL-10 (M2 macrophage) secretion. As a result, no insulin resistance, and adipocyte inflammation appeared when co-cultured with adipocytes, while in the absence of DHA, adipocytes caused the enhancement of M1- macrophage activities (TNF- α , IL-6 production). It can be concluded that DHA, pre-treatment with adipocytes, prevented IL-6 secretion, lower NF κ B activity, and reduced adipocyte p38 phosphorylation, as a result insulin resistance may diminish or the insulin sensitivity may increase (Figure 3.1).

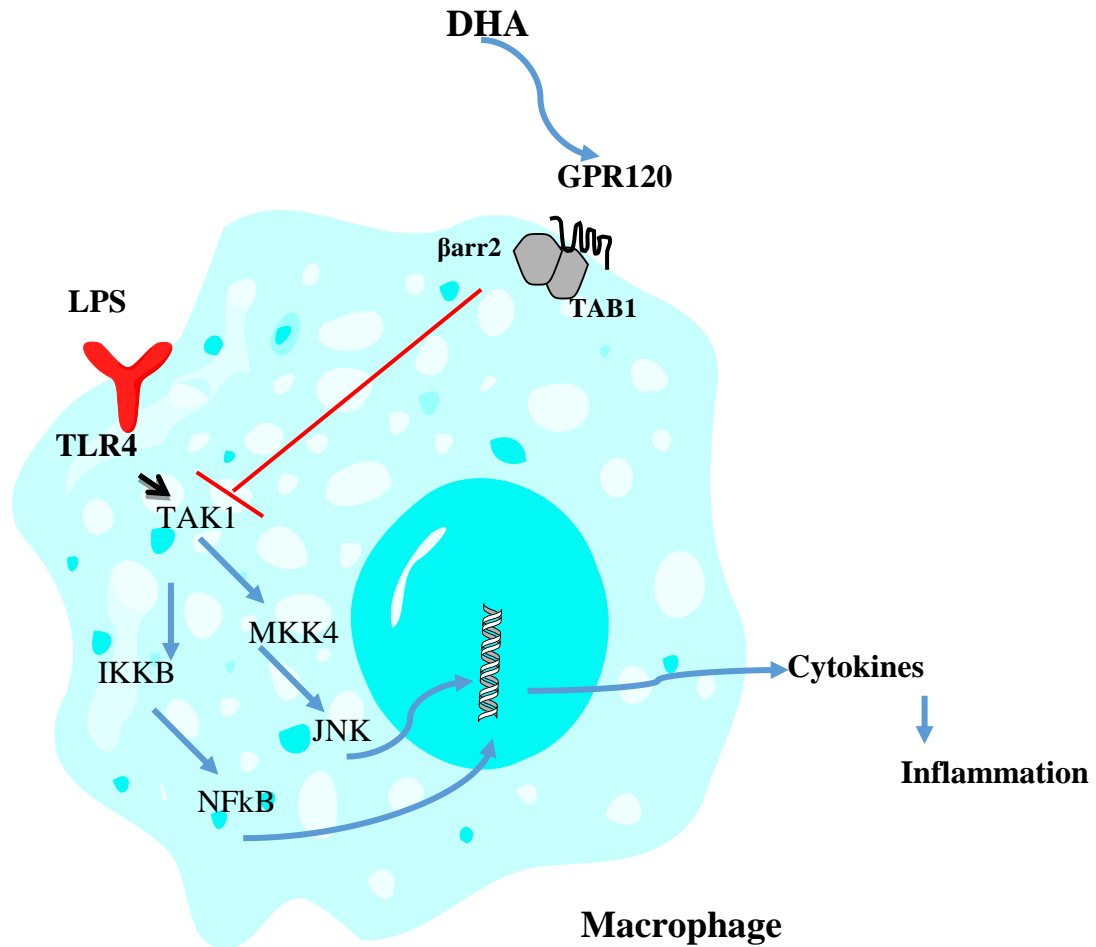


Figure 3-1 Mechanism action of DHA in macrophage, and adipocyte.

DHA leads to the decrease of inflammation in macrophage, and increase of insulin sensitivity in adipocyte. Glucose transporter protein (GLUT4) is the rate-limiting step in glucose utilization. GLUT4 is expressed in adipocytes. DHA is a potent activator of GLUT4, and upregulates GLUT 4 activity via its receptor GPR120; as the result there is no glucose increase in the blood circulation. DHA leads to the blocking of TAK1 process in macrophages so it causes the decrease of phosphorylation, and translocation of NFκB, and p38MAPK into the cell nucleus. This antagonises the activity of LPS, which binds to TLR4, signalling via NFκB, and p38MAPK. Red lines indicate the intracellular inhibitory effect of DHA.

3.1.3 Anti-inflammatory Role of Vitamin D

According to Mutt *et al.*, (2014) $1,25(\text{OH})_2\text{D}_3$ (Vitamin D₃) led to the down regulation of inflammation by NF κ B, and MAPK signaling pathway inhibition in mouse adipocyte cell line, and human adipocytes. According to Gupta and colleagues Vitamin D₃ (2 μ g/ml) led to the inhibition of cholesterol synthesis in J774, and HepG2 cell lines (Gupta *et al.*, 1989). The experimental design, and concentration for Vitamin D were taken from work cited above (Oliver *et al.*, 2012), and increased in my work to include treatment (posthoc stimulation).

3.2 Result

3.2.1 The effect of anti-inflammatory agents (DHA, Vitamin D, Allicin) on LPS-induced TNF- α mRNA expression, and protein *in vitro*

3.2.1.1 DHA, and Vitamin D revert inflammation after stimulation with LPS

While sufficient experimental animals to begin the mouse diet studies were being bred, a series of *in vitro* investigations was started in order to quantify the anti-inflammatory response generated by immune modulators, which were being considered as supplements to the high fat mouse diets. The experimental model drew on experience in the lab: mouse macrophages stimulated with 1000ng/ml LPS for 4hrs produce a significant increase in TNF- α mRNA expression. The mouse macrophage cell line J774 was tested in different stimulation times as follows: 2 hours, 4 hours, 6 hours, 18 hours, and 24 hours: After two hours' stimulation, there was a minor increase in the expression of TNF- α mRNA compared to control condition. Its expression after four hours had five-fold increase over the control. After that, its expression decreased steadily until it reached 2.5-fold at the 24th hour point, which was near to the control sample (2-fold). It was concluded from experience in the lab that 4 hours stimulation with LPS concentration of 1000ng/ml LPS E.coli 0111: B4, had the highest TNF- α mRNA expression, and reached a peak compared to the other time points (Data not shown).

Fish oils are rich in long chain n-3 polyunsaturated fatty acids (LC n-3PUFA), eicosapentanoic (EPA), and docosahexaenoic (DHA). They play a significant

role in the metabolic syndrome, and inflammation treatment (Mullen *et al.*, 2010). Vitamin D3 led to the down regulation of inflammation by NFκB and MAPK signaling pathway inhibition in mouse adipocyte cell line and human adipocytes (Mutt *et al.*, 2014).

The experimental design, and concentration for Vitamin D were taken from work cited above (Oliver *et al.*, 2012).

3.2.1.2 Vitamin D3, and DHA preconditioning for five days prevents inflammation

A pilot study for Omegas 3 was performed by using 10% fish oil (commercial capsule), but it did not mix with the culture medium. Therefore, a commercial, medium soluble, DHA product (Sigma) was used to attempt to modulate the inflammatory reaction of macrophages.

J774 macrophage cells were preconditioned with DHA (16µg/ml) or Vitamin D (VD) (4µg/ml) for 5 days, then stimulated with 100ng/ml LPS *E.coli* 0111:B4 for 24 hours (A), and 4 hours (B). DNA digested, and cDNA synthesised for qPCR analysis. DHA (16µg/ml), and Vitamin D (4µg/ml) were stimulated with 100ng/ml LPS for 24 hours in order to know to what extent DHA and Vitamin D for 5 days causes down regulation of M1 macrophage characteristics after 24 hours stimulation, and to investigate whether a combination of Vitamin D and DHA works together. To compare four separate experiment for 24 hours stimulation (A) to two separate experiment for 4 hours stimulation (B), experiments set up at different times, LPS induced TNF-α expression (normalised to GAPDH housekeeping gene).

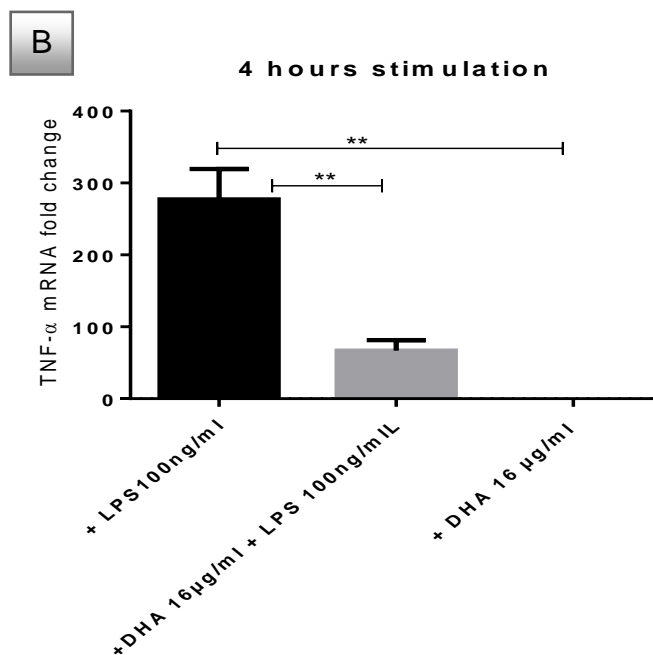
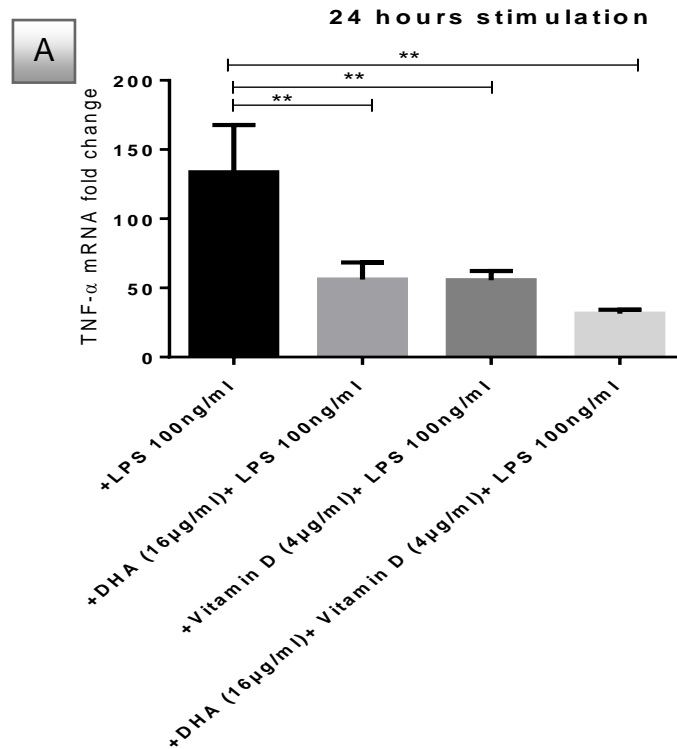


Figure 3-2 DHA (16 μ g/ml), Vitamin D (4 μ g/ml) preconditioning for 5 days.

DHA (16 μ g/ml), Vitamin D (4 μ g/ml) preconditioned to J774 cells for 5 days, and combination of them, then stimulated by 100ng/ml LPS for 24hours, compared to J774 cell line stimulated by 100ng/ml LPS, four separate experiments were performed (panel, A). DHA (16 μ g/ml) preconditioned for 5 days then stimulated with 100ng/ml LPS for 4hours, compared to J774 cell line stimulated with 100ng/ml LPS, two separate experiments were performed (panel B). Results are presented as averages \pm SD from triplicate determinations. ** $p < 0.01$ (adjusted p -values).

All experiments that included a modulator DHA or Vitamin D decreased the LPS-induced TNF- α mRNA significantly. DHA (16 μ g/ml) was significantly efficient in reducing mRNA expression of TNF- α stimulated with 100ng/ml LPS for 24 hours stimulation (Figure 3-2, A). Vitamin D (4 μ g/ml) was significantly efficient in reducing TNF- α expression. The combination of DHA (16 μ g/ml), and Vitamin D (4 μ g/ml) was significantly efficient in reducing TNF- α , also J774 enriched DHA was tested without stimulation with 100ng/ml LPS to investigate whether DHA caused the release of TNF- α . To test whether DHA caused the death of cells or not, the cells were checked under the microscope by using trypan blue stain, the principle was that live cells possessed intact cell membranes which excluded the stain, but dead cells did not. It suggests that Vitamin D (4 μ g/ml), and DHA (16 μ g/ml) both separately, and in combination play a potent role at down regulation of TNF- α mRNA expression. Interestingly, the combination of Vitamin D (4 μ g/ml), and DHA (16 μ g/ml) had a significant greater effect at lowering TNF- α mRNA after stimulation with 100ng/ml LPS. To test the biological effects of DHA, and Vitamin D in different concentrations (5 days preconditioned) after 4 hours stimulation with 100ng/ml LPS, the following experiment was performed. LPS (100ng /ml) stimulation reaches the peak at 4 hours stimulation. DHA (16 μ g/ml) was used (Figure 3-2, B), and stimulated by 100ng/ml LPS for 4 hours in order to investigate to what extent it affects the increase of TNF- α mRNA expression for 4 hours, and the decrease by DHA after 5 days preconditioning.

Insulin receptor mRNA expression was performed for J774, HepG2 cells preconditioned with Vitamin D (0.4, 2, 4, μ g/ml) for 1 day, and stimulated with 100ng/ml LPS for 24 hours. The doses of Vitamin D₃ (0.4, 2, 4 μ g/ml) were chosen based on a pilot experiment that investigated induction of insulin receptor mRNA in target cells (Kheder et al., 2016, Supplementary Figure 1).

PCR was performed for Vitamin D receptor, and toll like receptor 4 (TLR4) so as to know expression of ligand relevant mRNA for Vitamin D receptor, and Toll-receptor of J774, and HepG2. The LPS dose of 1000ng/ml was found to negatively impact TLR, an VDR mRNA expression in J774, which behaved as

acute sensors of the presence of this PAMP in comparison with HepG2 (Kheder et al., 2016, Supplementary Figure 2).

It was found DHA (16µg/ml), Vitamin D (4µg/ml), combination of DHA (16µg/ml) and Vitamin D (4µg/ml) preconditioning for 5 days were efficient in reducing mRNA expression of TNF-α (stimulated with LPS 100ng/ml) for 24 hours, interestingly DHA and Vitamin D combination were greater efficient at lowering TNF-α (Figure 3.2, panel A), and also DHA (16µg/ml) preconditioning for 5 days stimulation by 100ng/ml LPS for 4 hours was efficient in reducing mRNA expression of TNF-α (Figure 3.2, B). In order to investigate whether Vitamin D for 1 day preconditioning with J774 affects TNF-α stimulation at different concentrations (0.4µg/ml, 2µg/ml, and 4µg/ml), the following experiment was used:

3.2.1.3 One day preconditioning with Vitamin D prevents inflammation

This experiment was performed to investigate which concentrations of Vitamin D are biologically most effective at reducing inflammation in J774 cells, during 24 hours' preconditioning, and subsequent stimulation with LPS 100ng/ml for 4 hours.

Concentrations used for Vitamin D were 0.4µg/ml, 2µg/ml, 4µg/ml (Figure 3.3). After preconditioning with Vitamin D (1day), and stimulating with 100ng/ml LPS for 4 hours TNF-α mRNA expression was measured. Vitamin D (4µg/ml, and 2µg/ml) were more efficient in reducing TNF-α compared to Vitamin D (0.4µg/ml) (Figure 3.3).

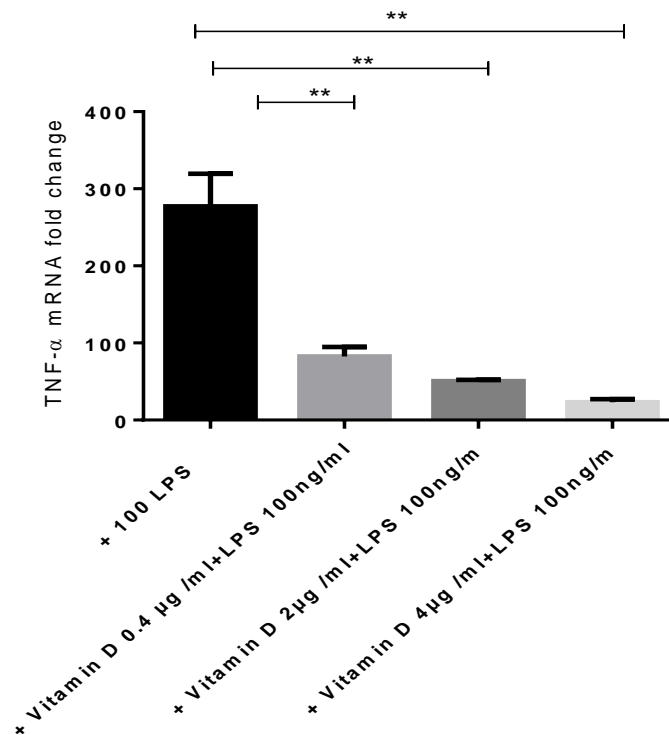


Figure 3-3 Vitamin D preconditioning for 1 day at different concentrations.

Then J774 stimulated by 100ng/ml LPS for 4hours, compared to J774 cell line preconditioned with Vitamin D 0.4 µg /ml, Vitamin D 2µg/ml, Vitamin D 4 µg/ml for one day and stimulated by 100ng/ml LPS for 4 hours, two separate experiments were performed. Results are presented as averages \pm SD from triplicate determinations. ** $p < 0.01$ (adjusted p -values).

To further support the anti-inflammatory role of Vitamin D HepG2, and J774 cell lines were used to study lipid body inclusions. Cells were preconditioned with Vitamin D for 24 hours then stimulated with 100ng/ml LPS for 24 hours. Oil Red O staining was performed, and the result showed cells preconditioned with Vitamin D then stimulated with 100ng/ml LPS for 24 hours had less Oil Red O staining compared to stimulated cells with LPS, but the control (unstimulated HepG2, J774) had some Oil Red O staining. In addition, no differences were seen between cells stimulated with 100ng/ml LPS, and 1000ng/ml LPS. For further investigation, qPCR also was performed for TNF- α mRNA expression in HepG2 after stimulation with LPS 100ng/ml, and to what extent Vitamin D caused the decrease of TNF- α mRNA expression.

3.2.2 Anti-inflammatory effect of Vitamin D on HepG2 cells

HepG2 cells were preconditioned with Vitamin D (VD) (0.4, 2, 4 μ g/ml) for 1 day, then stimulated with 100ng/ml LPS *E.coli* 0111:B4 for 4 hours mRNA was prepared, the DNA digested, and cDNA synthesized for qPCR analysis. The result (Figure 3.4) shows that 1000ng/ml LPS induces higher levels of TNF- α mRNA compared to 100ng/ml LPS. Vitamin D (0.4 μ g/ml) was not effective at lowering TNF- α mRNA compared to HepG2 stimulated with 100ng/ml LPS without Vitamin D. However, Vitamin D (2 μ g/ml and 4 μ g/ml) alone effectively lowered TNF- α mRNA compared with HepG2 stimulated with 100ng/ml LPS (Figure 3).The reason for using high dose of LPS was to know whether LPS (1000ng/ml) caused the increase TNF- α mRNA compared to LPS (100ng/ml) in HepG2 cells.

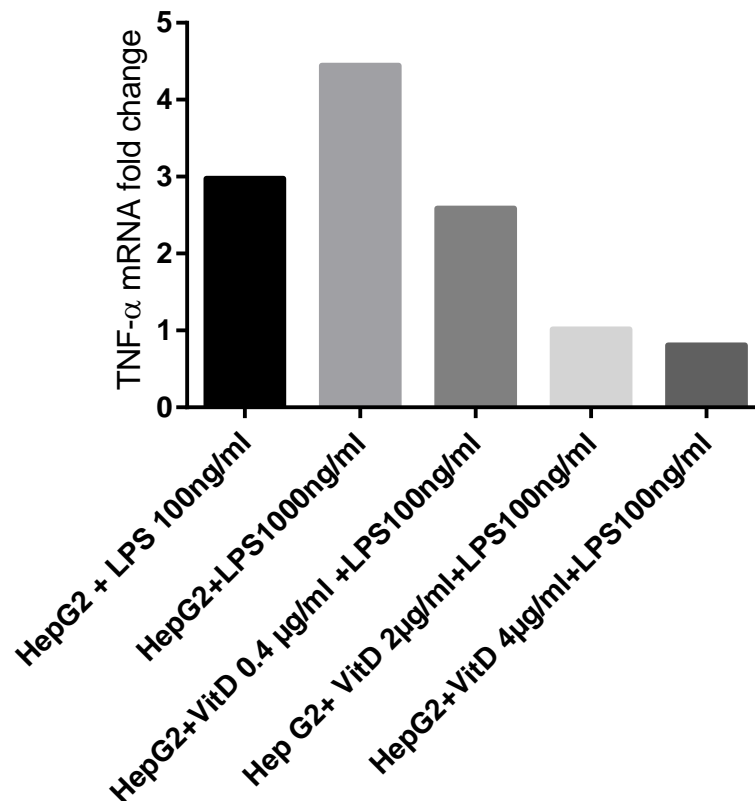


Figure 3-4 TNF- α mRNA expression in HepG2 cell.

Preconditioned HepG2 with Vitamin D (0.4, 2, 4 μ g/ml) for 1 day then stimulated by 100ng/ml LPS for 4hours, compared to HepG2 cell line stimulated by100ng/ml LPS. This experiment was performed once only.

3.2.3 Stimulation of J774 cells with LPS, and Tunicamycin (ER stress marker) by using Oil Red O staining method

In order to investigate the foam cell formation by Tunicamycin, and LPS, Oil Red O staining method was performed. Tunicamycin is an endoplasmic reticulum stress producer (Suganya et al., 2014). Tunicamycin (1 µg/ml, 2 µg/ml) was added to J774 cells for 24 hours with, and without stimulation by 100ng/ml LPS. Also LPS (100ng/ml, and 1000ng/ml) were added to J744 cells separately for 24 hours. The result showed the possibility to foam cell formation in J774 stimulation with Tunicamycin was higher (23 %) compared to J774 LPS stimulation cells (18 %), interestingly, high dose Tunicamycin (2 µg/ml) and high dose LPS (1000ng/ml) combination had the higher foam cell formation (35 %). (Figure 3.5).

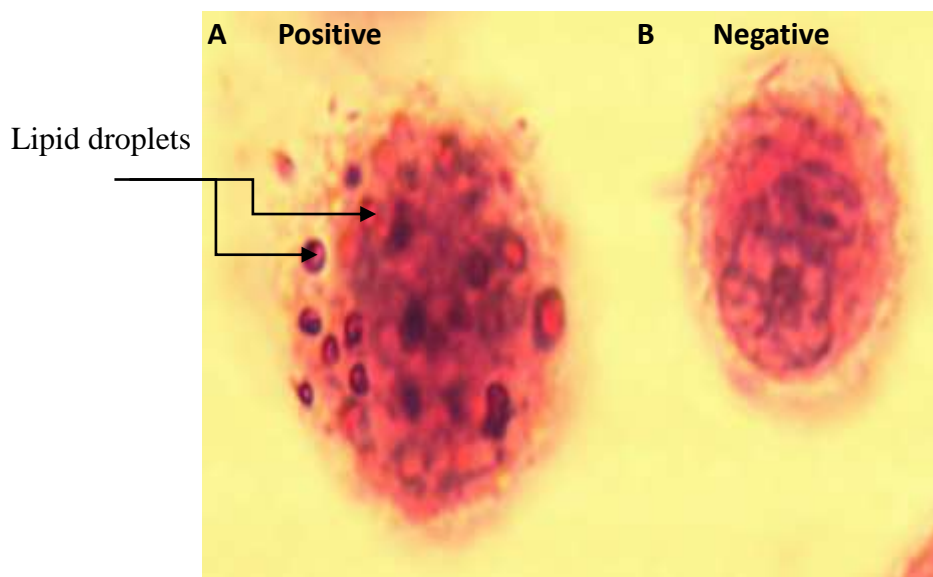


Figure 3-5 Oil Red O staining in J774 stimulation with Tunicamycin and LPS.

Foam cell formation positive, which has lipid droplets (panel A), No form cell formation, no fat droplets J774 cells without stimulation with Tunicamycin, and LPS (panel B).

3.2.4 Allicin has anti-inflammatory role on J774

In order to investigate anti-inflammatory role of Allicin (Sigma) and the dose it is relatively most effective against the literature (10-30 μ M 24 hours) (Corral-Cardad *et al.*, 2012). Different doses of Allicin were used (30 μ M, 15 μ M, and 6 μ M), so as to know the minimum effective dose. Allicin in J774 cells was preconditioned for 1 day, and 5 days (for 30 μ M) (Figure 3.6), then stimulated with 100ng/ml LPS. TNF- α mRNA expression decreased at all Allicin concentrations used (30 μ M, 15 μ M, and 6 μ M). Interestingly, 30 μ M Allicin for 5 days preconditioning had a greater effect compared to 1 day preconditioning. Surprisingly, 30 μ M Allicin, and 6 μ M Allicin preconditioning for 5days had a lower effect compared to 15 μ M 5 days preconditioned.

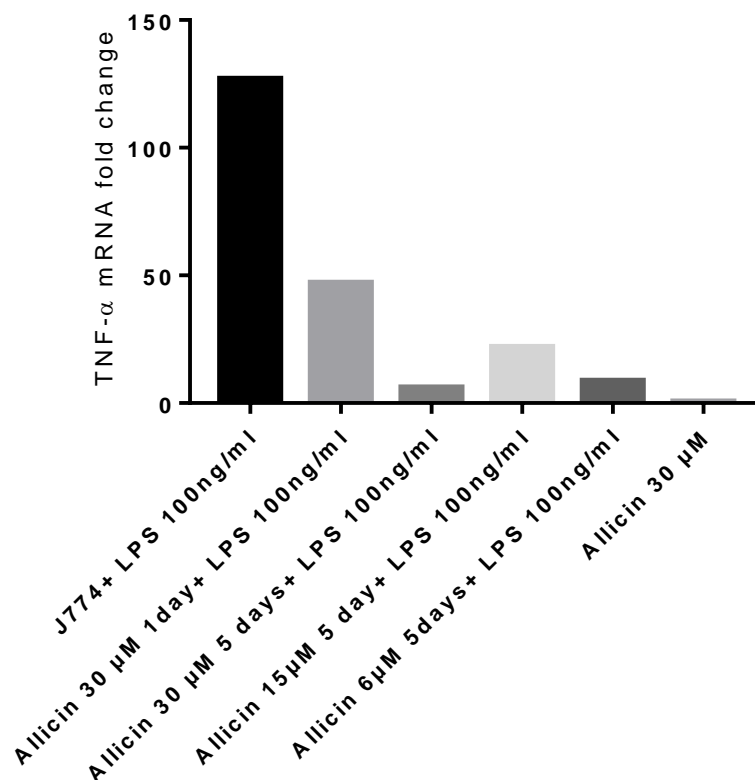


Figure 3-6 Using J774 cells to investigate TNF- α mRNA expression in the presence of Allicin.

QPCR for TNF- α mRNA expression in J774 macrophage cell line, in the presence of Allicin preconditioning for 1 day (30 μ M), and 5days at 30 μ M, 15 μ M, 6 μ M concentration (1 day preconditioned), then stimulated by 100ng/m LPS for 4 hours.

Another experiment was performed to study curative effects of Allicin. J774 cells were exposed to Allicin (30 μ M) for 1 day after stimulation with LPS (100

ng/ml) for four hours J774 cells were exposed to LPS (100ng/ml) for 4 hours (Figure 3.7). As a result, Allicin led to the decrease mRNA expression of TNF- α . Allicin did not release any TNF- α without stimulation by 100ng/ml LPS (Figure 3.7), therefore it means Allicin is not toxic to cells; to investigate viability of cells with Allicin, the viability of cells were checked under the microscope by using trypan blue stain as described previously.

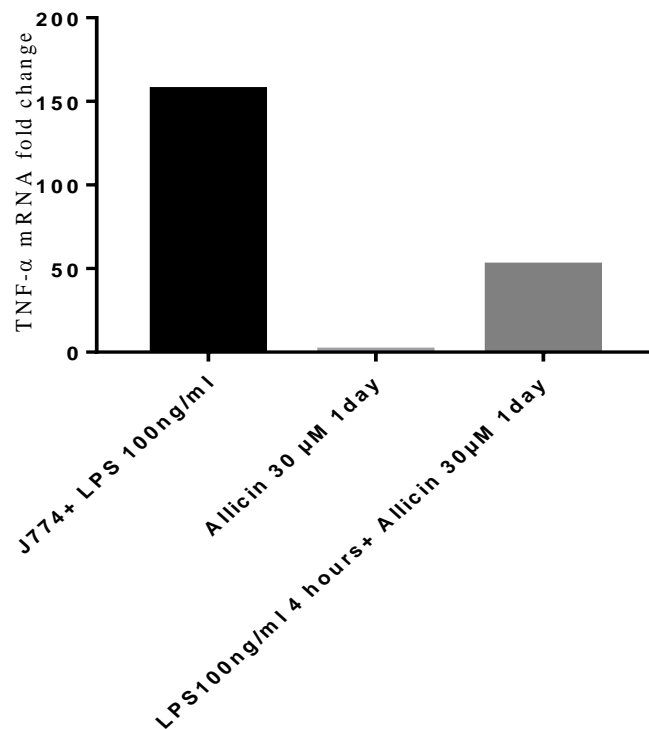


Figure 3-7 Using Allicin as treating J774 cells after stimulation with LPS 100ng/ml.

QPCR for TNF- α in J774 macrophage cell line, J744 stimulated with 100ng/ml LPS for 4 hours then treated with 30 μ M Allicin for 1 day. No TNF- α mRNA expression was induced by 30 μ M Allicin alone.

It can be concluded that Allicin in different doses (30 μ M, 15 μ M, 6 μ M) (5 days preconditioned), and 30 μ M (1 day preconditioned) have an efficient role at lowering mRNA expression of TNF- α following LPS stimulation.

3.2.5 Effect of Allicin, DHA, and Vitamin D on TNF- α secretion

To investigate TNF- α protein expression, ELISA TNF- α was performed. TNF- α mRNA was decreased by using Vitamin D, DHA, and Allicin after stimulation with 100ng/ml LPS. Therefore, the protein level of TNF- α was measured after 24 hours stimulation with 100ng/ml LPS, in the presence, and absence of these modulators, to confirm mRNA expression of TNF- α . The reason for using 24 hours stimulation was that protein translocation is initiated in by 24 hours. In unstimulated J774 cells preconditioned with DHA (16 μ g/ml), J774 preconditioned with Vitamin D (2 μ g/ml), and J774 preconditioned with Vitamin D (4 μ g/ml), TNF- α release was reduced by less than 5 fold compared to J774 stimulated with 100ng/ml LPS. This appears that Vitamin D, DHA, and Allicin did not cause the release of TNF- α . To further investigate their viability cells were checked under microscope, and also by Trypan blue exclusion to check living, and non-living cells. J774 cells stimulated with 100ng/ml LPS for 24 hours showed an increase TNF- α by 5 fold, and half. In J774 cells preconditioned with DHA (16 μ g/ml) stimulated by 100ng/ml LPS for 24 hours, DHA led to the decrease of TNF- α amount reduced by more than half (Figure 3.9). In J774 preconditioned with Vitamin D (2 μ g/ml) then stimulated LPS 100ng/ml for 24 hours, a threefold decrease of TNF- α was found. DHA (16 μ g/ml) led to the decrease of TNF- α by two-third. It appears that there is a tendency for Vitamin D (2 μ g/ml) to be more efficient than DHA (16 μ g/ml) at lowering TNF- α secretion. J774 preconditioned with Vitamin D (4 μ g/ml) for 1 day then stimulated by 100ng/ml LPS for 24 hours, caused the decrease of TNF- α by half compared to J774 preconditioned with Vitamin D (2 μ g/ml). It appears that there is a tendency for Vitamin D (4 μ g/ml) to be more effective than Vitamin D (2 μ g/ml), and DHA (16 μ g/ml) at lowering TNF- α secretion.

In J774 preconditioned with 30 μ M Allicin for 1 day then stimulated with 100ng/ml LPS for 24 hours, Allicin led to the decrease of TNF- α secretion by three fold. It means that there is a tendency for Allicin to be more effective than Vitamin D (2 μ g/ml), Vitamin D (2 μ g/ml), but more efficient than DHA (16 μ g/ml) at lowering TNF- α secretion.

In combination group J774 cells were preconditioned with DHA (16µg/ml), Vitamin D (4µg/ml), and 30 µM Allicin (30 µM), and then stimulated by 100ng/ml LPS. TNF-α resulted in the decrease amount of TNF-α secretion by nearly one-third. While in combination DHA 16µg/ml, Vitamin D 4µg/ml stimulated by 100ng/ml LPS, it resulted in the reduction of TNF-α secretion by one-fourth. There is a tendency for combination of DHA, Vitamin D, and Allicin at the doses chosen are more efficient than the combination of DHA, and Vitamin D together (Figure 3.8).

In conclusion, DHA 16µg/ml, Vitamin D 2µg/ml, Vitamin D 4µg/ml, and 30 µM Allicin play an anti-inflammatory role, because they have as a significant role at lowering TNF-α secretion. Taken together, the most efficient is Vitamin D 4µg/ml, then Vitamin D 2µg/ml, and Allicin is more efficient than DHA (16µg/ml) at lowering TNF-α secretion. Combination of the three compounds together (DHA 16µg/ml, Vitamin D 4µg/ml Vitamin, 30 µM Allicin) there was a tendency for having more efficient than the combination of DHA 16µg/ml, Vitamin D 4µg/ml.

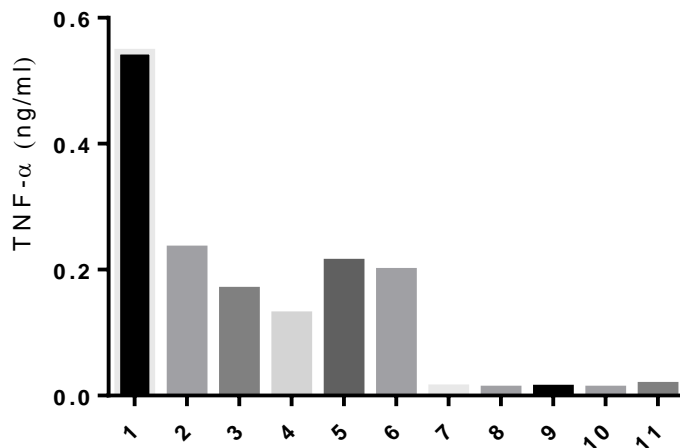


Figure 3-8 ELISA test to investigate TNF-α protein in the presence of, Vitamin D, DHA and Allicin.

J774 cell lines, with 100ng/ml LPS stimulation for 24 hours with, and without DHA (16µg/ml), Vitamin D (4, 2µg/ml), and 30 µM Allicin. Supernatant was collected and TNF-α ELISA test was performed. 1- J774+LPS100ng/ml, 2- J774+DHA16µg/ml+LPS100ng/ml, 3- J774+Vitamin D 2µg/ml+ LPS100ng/ml, 4- J774+Vitamin D 4µg/ml+ LPS100ng/ml, 5- J774+Allicin 30µm +LPS 100ng/ml, 6- J774+ DHA16µg/ml+ Vitamin D 4µg/ml+ +Allicin 30µm LPS100ng/ml. 7- J774, 8- J774+DHA16µg/ml, 9- J774+Vitamin D 2µg/ml, 10- J774+Allicin 30µm, 11- J774+ DHA16µg/ml+ Vitamin D 4µg/ml+ Allicin.

3.3 Discussion

The main purpose of this study was to transfer Vitamin D from *in vitro*, and also investigate the effect of DHA, and Allicin in favour of treating mice with induced inflammation. The reason for 4 hours and 24 hours stimulation is to know the effectiveness of Vitamin D, and DHA at lowering TNF- α in the two different stimulation periods, and also it is established that in 4 hours stimulation TNF- α mRNA reaches a peak. Vitamin D was given to mice via food in order to prevent mice from NAFLD, NASH after given HFD, and high fructose for 10 weeks. DHA was not supplied to mice models because Omega-3 (DHA) has a similar calorific value to other fats on a gram by gram basis. However, the biological effects are very different. When altering diets, it is important we substitute an alternative fat (SFA) with the omega-3. Simply adding omega-3 in one group of mice means they are exposed to a higher amount of fat which may affect results.

DHA had a significant role at reducing mRNA expression of TNF- α in J774 cell line. Our results are supported by a previous study which has shown anti-inflammatory role of DHA (Oliver et al., 2012). According to Mullen *et al.*, 2010, DHA plays a significant role in lowering pro-inflammatory mediators IL-1 β , and IL-6, after stimulation with 0.1ng/ml LPS for 24 hours in monocytic THP-1 cell line (1×10^6 cell). DHA-treated macrophages, during 5 hours activation with 0.1 μ g/ml LPS, led to the reduction of transcription factor NF- κ B p65 expression (Mullen *et al.*, 2010). Nuclear binding of p65 was significantly decreased in DHA-treated cells at 2-h LPS activation.

In *vitro* experiments, Vitamin D3 was used to investigate skewing M1 macrophages to M2 in J774 cell line. Our results showed that Vitamin D3 plays a significant role at lowering TNF- α mRNA expression. Our results are coincidence with previous study which has documented that anti-inflammatory role of Vitamin D (Zhang et al., 2012).

Macrophages elicited from peritoneal cavities of obese mice by intraperitoneal injection of 4% thioglycollate solution, showed foam cell formation, which is formed by acetylated LDL (AcLDL), oxidized LDL (oxLDL); while in the presence Vitamin D less foam cells were formed, because AcLDL- or oxLDL-

induced cholesteryl ester formation was reduced by Vitamin D (1, 25(OH) 2D3) (Oh et al., 2009).

Allicin was used to reduce TNF- α (Lang et al., 2004) (Lang *et al.*, 2004). It has been shown that garlic extracts has contributed to ameliorate obesity, metabolic syndrome disease (Arreola et al., 2015). Our results showed that Allicin, in different doses (30 μ M, 15 μ M, 6 μ M), led to lowering of TNF- α mRNA in J774 cells after stimulation with 100ng/ml LPS. Allicin might be used in favor of treating mice with induced inflammation.

Liver inflammation is triggered by endoplasmic reticulum stress, and Kupffer cells activation that will promote NASH development (Scorletti and Byrne, 2013). The “second hit” of NAFLD is oxidative stress development in hepatocytes, which is followed by steatohepatitis, and liver cirrhosis (Lim et al., 2010). Our result showed that Tunicamycin, which is an endoplasmic reticulum stress producer (Kim et al., 2013), with 100ng/ml LPS, led to the increase of foam cell formation.

To summarise, Vitamin D (4 μ g/ml) and DHA (16 μ g/ml), both separately and in combination, play a potent role at down regulation of TNF- α mRNA expression, and TNF- α protein expression in J774 cells activated with LPS. Interestingly, the combination of Vitamin D (4 μ g/ml), and DHA (16 μ g/ml) had a greater effect at lowering TNF- α mRNA after stimulation with 100ng/ml LPS, but they did not lead to the decrease TNF- α protein expression. Notably, the combination of Vitamin D, DHA, and Allicin had the greatest inhibitory effect on TNF- α protein release. There was a greater tendency to decrease TNF- α mRNA at 5 days preconditioning 30Mm Allicin then stimulated with 100ng/ml LPS compared to 1 day preconditioning; in addition, 30Mm Allicin led to the reduction of TNF- α protein expression. TNF- α mRNA expression also decreased in HepG2 preconditioned with Vitamin D, after stimulation with LPS 100ng/ml. The treatment idea has been established by stimulated J774 with 100ng/ml for 4 hours then treated with Allicin for 1 day which led to the decrease TNF- α mRNA compared to 100ng/ml LPS. Oil Red O staining showed that Vitamin D led to the decrease of lipid in HepG2 cells compared FFA acid group alone. It also showed that LPS led to the increase foam cell formation, which was prevented

by Vitamin D in J774, and HepG2 cells. Based on the significant positive effect of Vitamin D, DHA, Allicin and lipotoxicity of free fatty acids, different doses of Vitamin D (0.4, 2, 4 $\mu\text{g/ml}$), DHA (8, 16, 32 $\mu\text{g/ml}$) were chosen to prevent, and treat J774, and HepG2 cells before and after stimulation with 100ng/ml LPS. In addition, free fatty acids (oleic acid/palmitic acid 2:1, 15 and 30 mM) were used in HepG2 cells to investigate lipid accumulation and prevent it by Vitamin D. The result showed that Vitamin D, and DHA exerted a consistent, dose dependent anti-inflammatory effect, and increased PPAR α relative to Srebp-1c in both cell types. However, addition of free fatty acids (FFA, oleic acid/palmitic acid 2:1) led to the aggravation of LPS-induced inflammatory reaction, and an increase of Srebp-1c relative to PPAR α . Our results argue in favor of dietary supplementation of Vitamin D, DHA (and avoidance of monounsaturated/saturated fatty acids) and Allicin to alleviate development of fatty liver disease. The paper that arose from this, and other related work is included hereafter (appendix) (Kheder et al., 2016). These studies are limited by the use of cell lines from mouse and human, and could be complemented by FACS analysis for macrophage polarization and hepatocyte receptor expression.

Chapter 4 The effects of Vitamin D3 as a nutraceutical during high fat diets

4.1 Introduction

No study has yet investigated the effect of dietary Vitamin D supplements on enzymatic liver function, endotoxin levels, and inflammatory mediators in one single study. Liver steatosis was observed in Vitamin D receptor deficiency mice compared to wild type mice (Geier, 2011). Some studies have shown that NAFLD patients have Vitamin D deficiency. It therefore appears that lower Vitamin D is more likely to increase susceptibility to develop NAFLD. Recently, Vitamin D has been given as treatment to ameliorate NAFLD, and also it was given to patients who received liver transplants in order to prevent rejection by the body (Stein and Shane, 2011). Vitamin D is decreased by 1.3nm/L with each 1kg/m² body mass index (BMI), low vitamin D is associated with insulin resistance that is associated with the development NAFLD. Women with sufficient level of Vitamin D had a lower risk of developing Diabetes mellitus type 2. Vitamin D response element is located on promoter region of insulin gene (Kitson and Roberts, 2012). There was a low level of Vitamin D level in obese people (Daniel et al., 2015). Obesity could be prevented by improving Vitamin D low level (Foss *et al.*, 2009). Vitamin D levels show a correlation with increased risk of type 2 diabetes (von Hurst et al., 2010).

Vitamin D is synthesized, and metabolized as follows: Skin, liver and kidney provide distinct enzyme activities to generate the metabolically active form of Vitamin D (Figure 4.1).

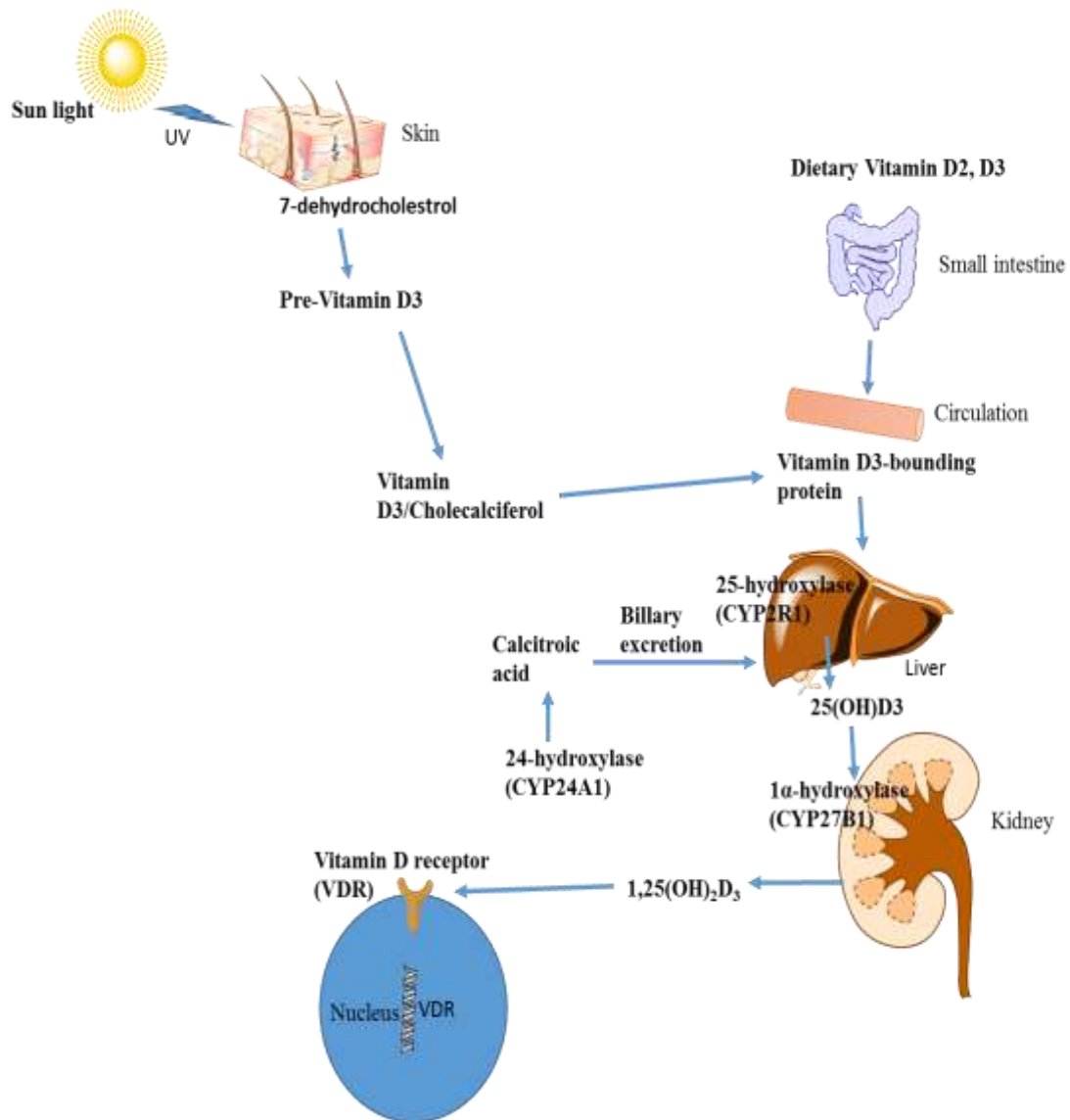


Figure 4-1 Vitamin D3 synthesis and metabolism.

Vitamin D is a fat-soluble Vitamin, when the skin is exposed to certain wavelengths of ultraviolet B (UVB) rays from the sun; the stored 7- dehydrocholesterol is converted to pre-Vitamin D3 or pre-calciferol. Vitamin D3 is formed by pre Vitamin D3 isomerization then cholecalciferol is formed. Dietary Vitamin D2 or D3 is incorporated to chylomicron Vitamin D then it is bound to binding protein (DBP) liver. In the liver both skin and dietary Vitamin D3 is metabolised by 25-hydroxylase (CYP2R1), a so-called calcidiol. It is transported to the kidney where second hydroxylation is happened by 1α-hydroxylase (CYP27B1) to form 1, 25-(OH)₂ D₃ (calcitriol) which the active form. It has receptors on the cell membrane or the nucleus resulting in different genes expression. The main regulators of the active form of these enzymes are the parathyroid hormone, 1, 25(OH)₂D, and fibroblast growth factor 23 (FGF23). Parathyroid hormone is a main stimulus for 1α-hydroxylase transcription, fibroblast growth factor 23, which is produced from osteoblasts, promotes kidney to inhibit 1α-hydroxylase and produce 24-hydroxylase activities a result 1, 25(OH)₂D₃ production can be decreased .

The Vitamin D used in this study corresponds to 1, 25 (OH)₂ D₃. Vitamin D plays an important role in protection liver from NAFLD because it has anti-inflammatory characteristic. A rodent study showed that deficiency in vitamin D

led to the development of NASH while inflammation, fibrosis, and apoptosis were reduced by giving vitamin D via diet. Furthermore, rodents which had been given HFD without vitamin D developed NAFLD, insulin resistance, and liver inflammation was observed (Kitson and Roberts, 2012). In human monocytes, and bone marrow derived macrophages Vitamin D up regulates the expression of MAPK phosphatase-1 (MKP-1). As a result, Vitamin D leads to the decrease LPS-induced p38 activation pro-inflammatory cytokines such as IL-6, and TNF- α (Zhang *et al.*, 2012). Physiological range of 25(OH) D3 (inactive Vitamin D) (15 days half-life), which led to the suppression of IL-6, and TNF- α , is more than 30ng/ml, and it is comparable with 0.04ng/ml of the active form (1, 25(OH) 2D3) (approximately 15 hours half-life) (Zhang *et al.*, 2012). Vitamin D has anti-inflammatory role, it also prevents fatty liver disease (Figure 4.2) and also it leads the increase of insulin sensitivity in adipocytes and muscle cells which caused by diabetes or obesity related disease (Figure 4.3). Therefore the aim of this chapter was to to investigate hepatic and adipose response to high fat high sugar diet and systemic measures of liver function tests, liver steatosis, liver inflammation, insulin resistance, metabolic syndrome, lipid peroxidation, pro-inflammatory mediators, cholesterol metabolism, and endotoxin level. Additionally, to investigate the anti-steatotic, anti-inflammatory role of Vitamin D, and to know whether Vitamin D prevents pre diabetic phenotypes, metabolic syndrome parameters, and LPS translocation from intestine to blood stream.

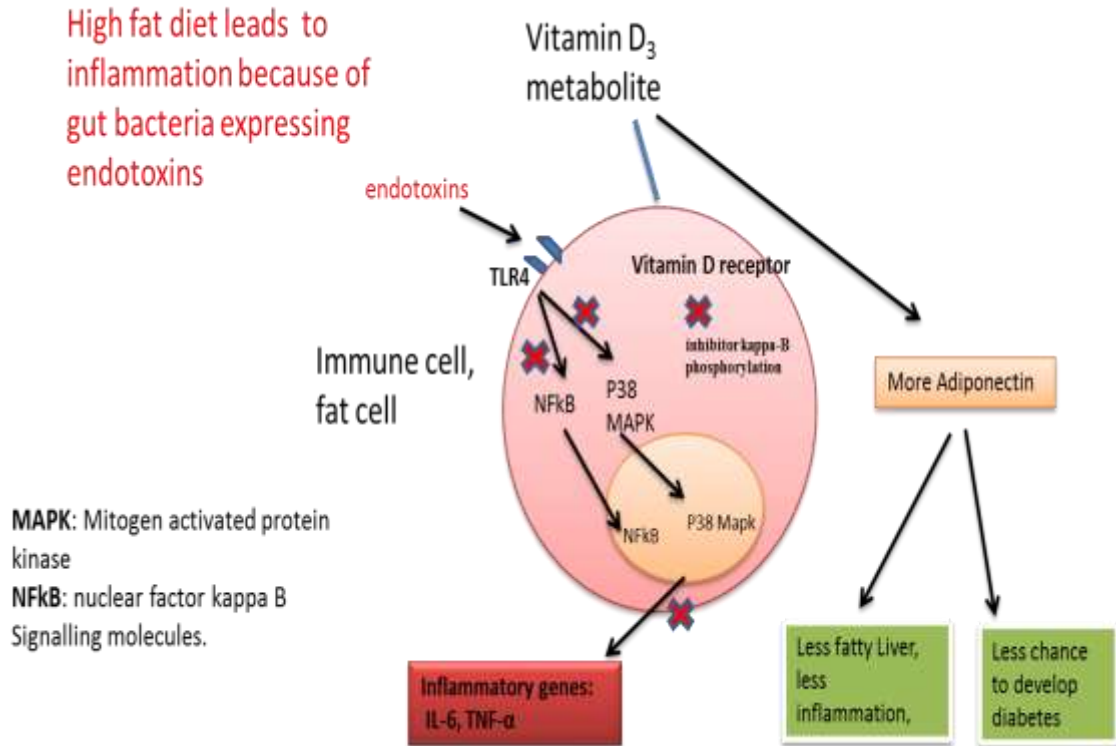


Figure 4-2 Proposed model of action of Vitamin D3 on macrophage or adipocyte.

Vitamin D3 binds to an intracellular receptor, VDR, and inhibits I κ B phosphorylation, and translocation of NF κ B, and p38MAPK into nucleus. This antagonises the activity of endotoxin (lipopolysaccharide) (LPS) which binds to TLR4, signalling via NF κ B, and p38MAPK. Red crosses indicate the intracellular inhibitory effect of Vitamin D3. In addition, Vitamin D3 increases adiponectin production, which is beneficial in decreasing susceptibility to developing liver steatosis, and insulin resistance.

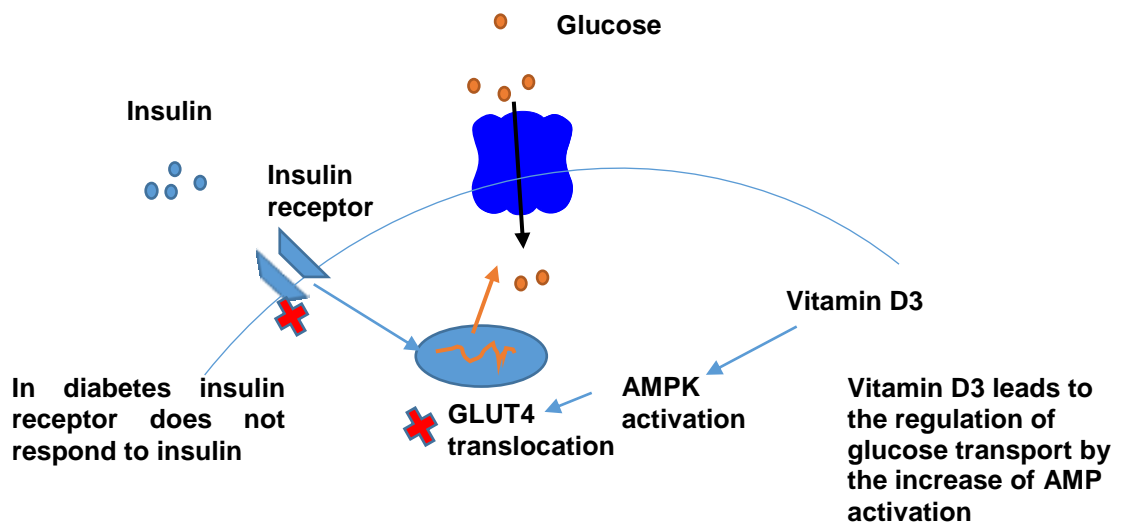


Figure 4-3 Proposed model of action of Vitamin D3 on muscle cells.

GLUT4 is expressed in muscle cells. Insulin, and exercise are most potent activators of GLUT4. High fat–high sugar diet increases the risk of diabetes. In diabetes, GLUT4 translocation is impaired, therefore, GLUT4 is not activated by insulin. Vitamin D is beneficial because it can upregulate GLUT 4 activity by increasing AMPK (activated protein kinase) activation.

Our hypothesized that Vitamin D plays a vital role in the prevention of metabolic syndrome diseases such as fatty liver disease and diabetes caused by high fat–high sugar diet given to mice for 10 weeks or five weeks.

4.2 Results

Ten weeks and five weeks diet were studied

4.2.1 Ten weeks study

Mice were housed in a barrier facility, and were fed a maintenance diet termed 5LF2 (14% protein, 6% fat, 65% carbohydrate) (low fat diet). At 3 months' of age, they were randomized to two groups and fed for 10 weeks a formulated cholesterol free diet 58R3 (high fat -high sugar diet) (Test Diet ® product 20% protein, 36% fat, 35% carbohydrate, rich in sucrose) differing in the content of admixed Vitamin D3 (1 IU/g vs 10 IU/g) (Test Diet ® product). Animal experimentation was performed in accordance with UK Home Office regulations, and institutional ethical guidelines. Mice were weighed weekly by animal technician. Preliminary experiments revealed that 10 weeks duration of altered diet intake was sufficient to generate histological changes consistent with NAFLD. At 12 weeks high fat diet, a decline in food intake was observed; therefore, 10 weeks duration was chosen for reason of lesser severity (refinement). LDLR^{-/-} mice represent a model of familial hypercholesterolemia, LDLR^{+/+} mice were in bred, but not congenic WT control, but reared in the same pathogen free barrier facility.

4.2.2 Effect of Vitamin D on fatty liver disease in ten weeks

15 mice (6 Female LDLR^{-/-}, 6 Female LDLR^{+/+}, and 3 male LDLR^{-/-}) were given high fat -high sugar diet for 10 weeks, and 17 mice (7 Female LDLR^{-/-}, 7 Female LDLR^{+/+}, and 3 male LDLR^{-/-}) were given mice Vitamin D supplemented high fat high sugar diet.

4.2.2.1 Effect of Vitamin D on serum Vitamin D level

Low Vitamin D level was documented in patients who had diabetes (Zoppini et al., 2013) and there was abnormal regulation of serum 1,25(OH)₂D concentrations mice fed high fat diet (Park et al., 2015). The aim of this experiment was to determine whether Vitamin D level was elevated when mice

were given a high fat high sugar diet supplemented with Vitamin D. Our results showed that the high fat diet group mice supplemented with Vitamin D had higher Vitamin D serum levels compared to high fat diet group mice without additional Vitamin D (Figure 4.4, A , B). Interestingly, the level of Vitamin D was lower in LDLR^{-/-} group mice compared to LDLR^{+/+} mice. It can be reported that Vitamin D supplementation caused the increase Vitamin D serum level.

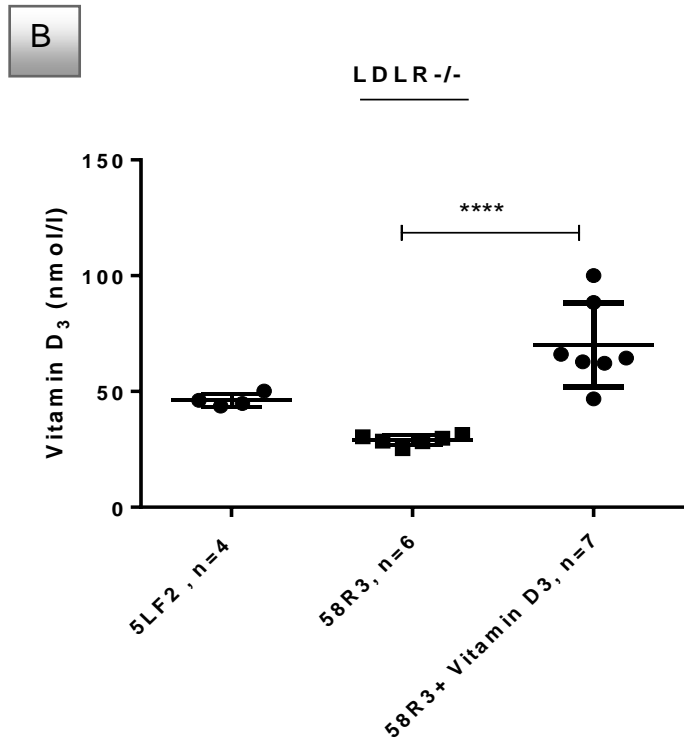
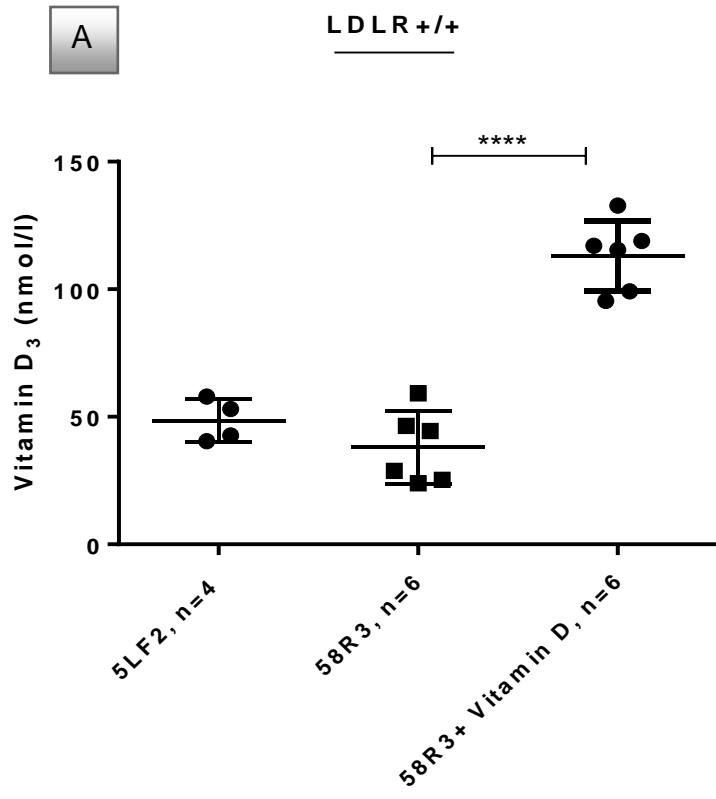


Figure 4-4 The effect of Vitamin D supplemented high fat high sugar diet compared to high fat high sugar diet in mice sera on Vitamin D levels.

LDLR^{+/+} mice fed high fat high sugar diet with and without Vitamin D (panel A), LDLR^{-/-} mice fed high fat high sugar diet with and without Vitamin D (panel B). Results are presented as averages ±SD from duplicate determinations. **** p<0.0001(adjusted *p*-values).

4.2.2.2 Body Weight measurement

The main purpose for weight measurement is to investigate whether body weight increases by giving high fat -high sugar diet, and in relation to Vitamin D supplementation. All mice (age 16 weeks) sex matched, the results were recorded as follows:

Body weight was measured once per week (10 weeks) for all experimental mice, where equal amounts of diet were added. The percentage of body weight increase was calculated as follow:

$(\text{End body weight}/\text{first body weight} * 100) - 100$.

It increased in LDLR^{+/+} mice fed a high fat-high sugar diet compared to LDLR^{+/+} mice fed the maintenance diet. The percentage of body weight gain tendency was higher in LDLR^{-/-} mice fed a high fat -high sugar diet compared to mice fed the maintenance, but as far as Vitamin D group was concerned, mice tended to show less body weight gain or stability so as not to get overweight. However, LDLR^{+/+} mice fed high fat-high sugar diet showed mice that had a tendency to have greater body weight when compared to LDLR^{+/+} mice on maintenance diet. However, the Vitamin D supplemented diet group mice had a tendency to have greater the percentage body weight gain significantly compared to high fat -high sugar diet group mice (Figure 4.5).

Taken together, these results suggest the most striking result is that the two backgrounds behave differently to Vitamin D, and LDLR^{-/-} are heavier on maintenance diet mice group.

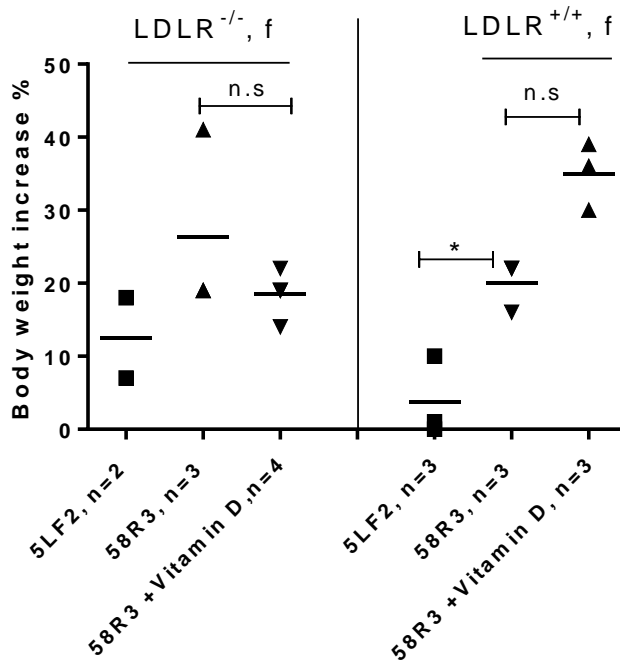


Figure 4-5 The percentage of body weight gain in female mice.

LDLR^{+/+} and LDLR^{-/-} mice fed high fat high sugar diet with and without Vitamin D on different diet. Results are presented as averages \pm SD from duplicate determinations. * $p < 0.05$ (adjusted p -values).

4.2.2.3 Analysis of liver weight in experimental female LDLR^{-/-} , LDLR^{+/+} mice

The main goal was to determine whether high fat-high sugar diet led to increased liver weight compared to maintenance diet, and to assess whether Vitamin D supplemented diet affected liver weight. However, weight possibly does not reflect accurately the development of hepatomegaly. This is because fat has a different density compared to liver parenchyma. The percentage of liver body weight was measured as follow: liver mouse weight/body weight mouse *100. It may represent or more relevant measurement, and was measured in order to know the relative weight. This was done to more accurately express the extent of hepatomegaly in relation to obesity. In LDLR^{-/-} mice, high fat -high sugar diet led to the increase % liver weight gain ($5.067\% \pm 0.18$) compared to maintenance diet ($3.92\% \pm 0.29$) (Figure 4.6). In Vitamin D supplemented LDLR^{+/+} group, liver weights were lighter, but not significantly when expressed as % of body weight. In LDLR^{+/+} mice liver weight (g) was not

significantly different compared to maintenance diet mice group. Liver weight analysis revealed that high fat-high sugar diet led to the increase of liver weight, and the decrease by supplementing Vitamin D. It suggests that Vitamin D supplemented diet plays a significant role in diminishing development of diet-induced hepatomegaly.

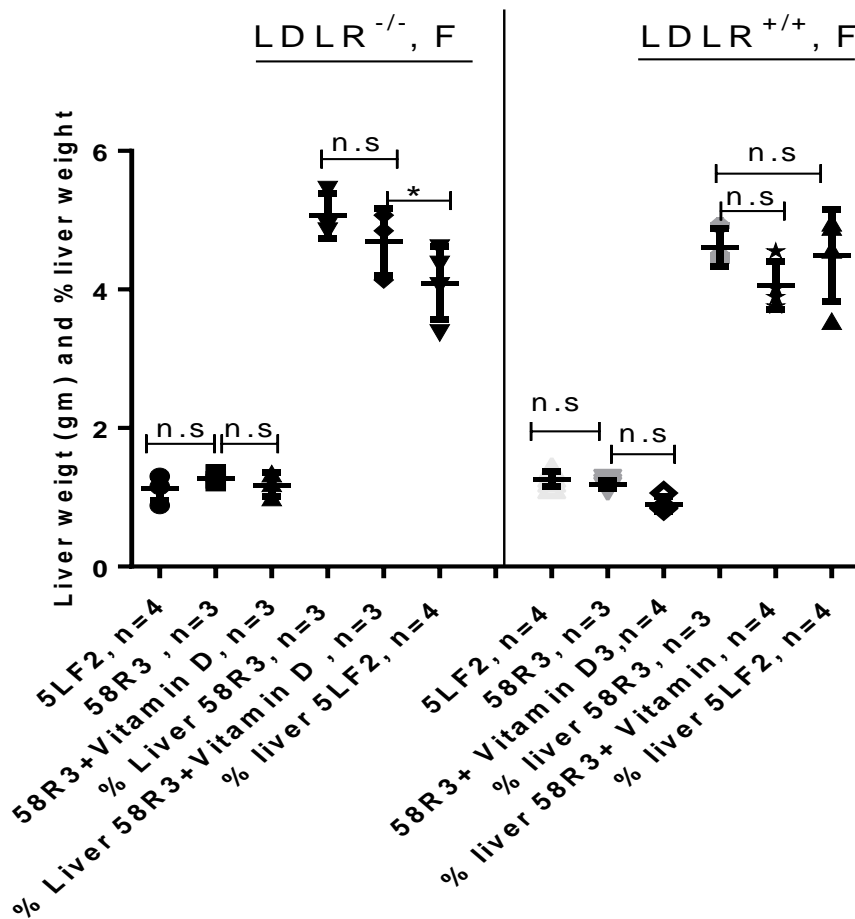


Figure 4-6 Liver weights both in grams (g), and percentage of liver weight (%) in female mice.

LDLR^{+/+} and LDLR^{-/-} mice fed high fat high sugar diet with (58R3 +Vitamin D) and without Vitamin D (58R3), low fat diet (5LF2) . Results are presented as averages \pm SD from duplicate determinations.

4.2.2.4 Analysis of Fat pad weight in experimental male LDLR^{-/-} mice

The aim was to analyse the development of central obesity, following the hypothesis that high fat -high sugar diet leads to the increase epididymal fat pad weight, and Vitamin D plays a role in the decrease of the fat pad weight. Three male LDLR^{-/-} mice fed high fat-high sugar diet had greater fat pad weight (g)

compared to 3 male LDLR^{-/-} mice fed maintenance diet (Figure 4.7). Fat pad weight of LDLR^{-/-} mice with Vitamin D was significantly lower than male LDLR^{-/-} mice without Vitamin D (Figure 4.7). The body weight of high fat -high sugar diet was compared to Vitamin D group mice. The evidence from this study suggests that fat pad weight measurement, a measure of central obesity, was increased by high fat diet-high sugar compared to maintenance diet mice group, and most importantly was less in the supplementary dietary Vitamin D group mice. The current data highlight the importance of supplementary dietary Vitamin D in the decrease of central obesity.

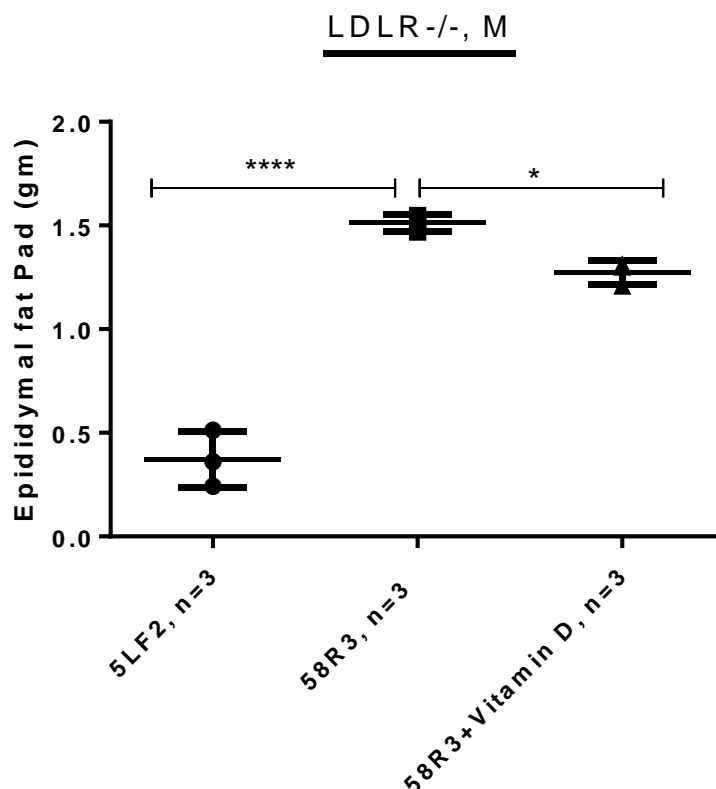


Figure 4-7 The Epididymal fat pad (g) in male LDLR^{-/-} mice.

LDLR^{-/-} mice fed high fat high sugar diet with (58R3 +Vitamin D) and without Vitamin D (58R3), low fat diet (5LF2). Results are presented as averages \pm SD from duplicate determinations. * $p < 0.05$, **** $p < 0.0001$ (adjusted p -values).

4.2.2.5 Histopathology of livers from experimental LDLR^{-/-} , and LDLR^{+/+} mice on high fat high sugar diet with, and without Vitamin D

The aim of the experiment was to investigate the development of fatty liver disease and how Vitamin D influences fatty liver changes in LDLR^{-/-} and LDLR^{+/+} mice. Sections were prepared from liver, stained with haematoxylin/eosin, and analysed microscopically.

Evidence of liver steatosis, and inflammation was seen in mice fed high fat diet high sugar. Vitamin D supplementation led to the amelioration of fatty liver changes, and inflammation. Macro vesicles were detected in mice fed high fat - high sugar diet, while in the presence of Vitamin D there were only micro vesicular changes. Lipid accumulation was observed near the central vein (zone 3) in mice fed high fat -high sugar diet; however, there was no fatty changes near central vein in supplemented Vitamin D mice group and maintenance diet (Figures 4.8, 4.9).

4.2.2.5.1 Haematoxylin and eosin staining

Parts of livers of 16 week old female LDLR^{-/-} mice, were fixed, paraffin embedded, and 4µm slides were prepared, and stained with haematoxylin, and eosin. Fifteen mice (6 LDLR^{-/-}, 6 LDLR^{+/+}, 3 male LDLR^{-/-}) fed high fat diet-high sugar were compared with seventeen mice fed the Vitamin D supplemented high fat high sugar diet (7 Female LDLR^{-/-}, 7 Female LDLR^{+/+}, and 3 male LDLR^{-/-}) and with two controls (LFD mice). Fatty changes were predominately detected in the absence of Vitamin D. Lipid accumulation was observed near the central vein (CV) (zone 3) in high fat –high sugar diet in (LDLR^{-/-}, LDLR^{+/+} high fat -high sugar diet (Figures 4.8, 4.9 Panel B), but was more intensive in LDLR^{-/-} mice. Contrasting with normal liver (Figures 4.8, 4.9 Panels A), there are many microvesicular, and macro-vesicular lipid droplets in high fat -high sugar diet liver mice (Figures 4.8, 4.9 Panels B). Many inflammatory changes were detected; they might be neutrophilic infiltration or mononuclear cells around the portal vein producing portal inflammation, or appearing between cells, where they are called lobular inflammation (Figures 4.8, B). In high fat-high sugar diet group mice supplemented with Vitamin D, there was less evidence of steatosis, and inflammation. Fatty changes were microvesicular.

Macro-and microvesicular fatty changes refer to the size of the observed space that was occupied by fat prior to paraffin processing. Typically, macrovesicular fat accumulation is the size of a hepatocyte, while microvesicular accumulation appear as small droplets in size (Schwen et al., 2016). These are accepted descriptive terms in histopathological evaluation of livers. Hepatocytes are the chief functional cells of the liver, and perform an astonishing number of metabolic, endocrine, and secretory functions. Approximately 80% of the mass of the liver is made up of hepatocytes. In three dimensions, hepatocytes are arranged in plates that anastomose with one another. The cells are polygonal in shape, and their sides can be in contact either with sinusoids (sinusoidal face) or neighboring hepatocytes (lateral faces). A portion of the lateral faces of hepatocytes is modified to form bile canaliculi. Microvilli are present abundantly on the sinusoidal face, and project sparsely into bile canaliculi (Hindley et al., 2014, Schwen et al., 2016).

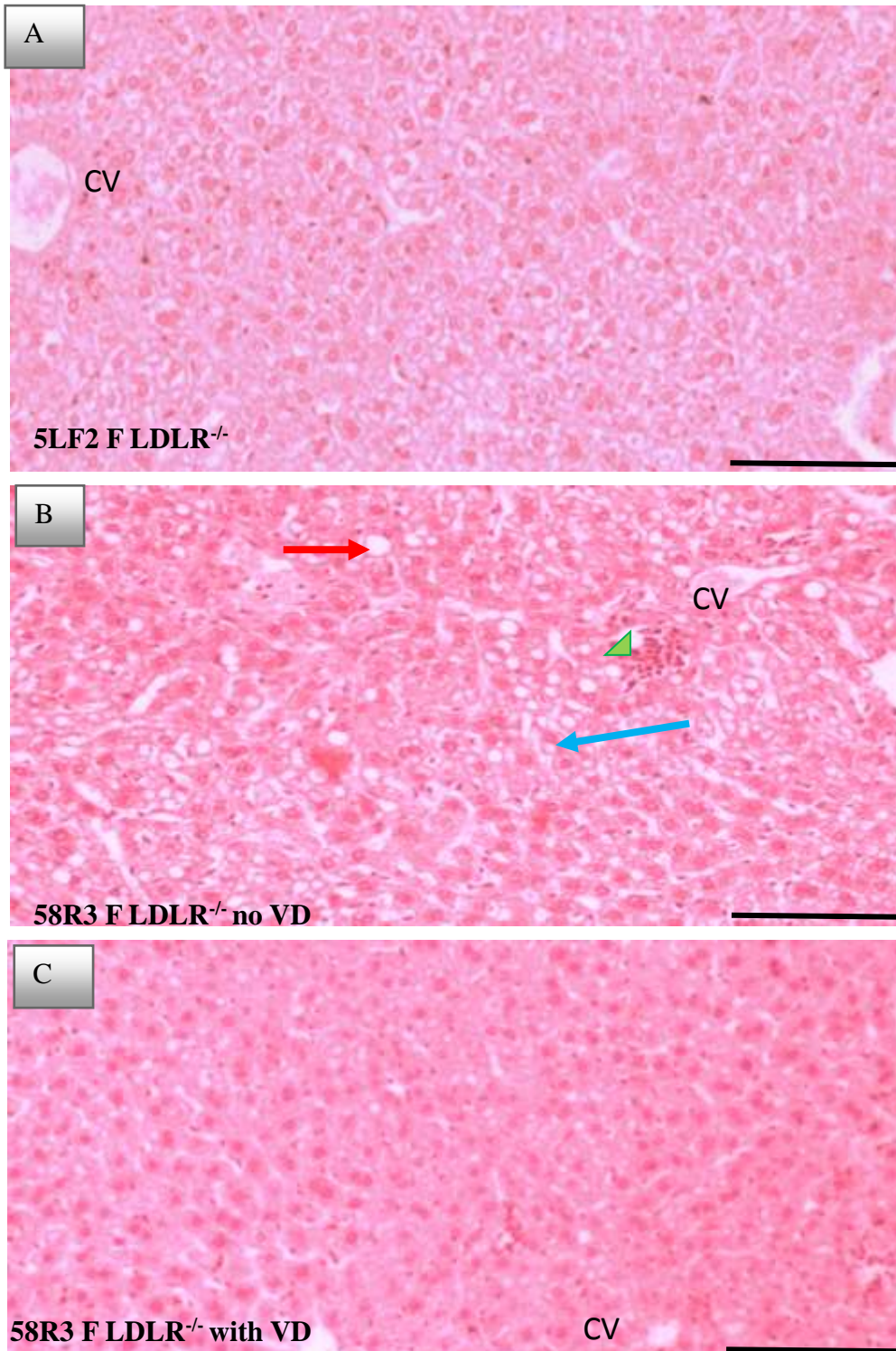


Figure 4-8 Haematoxylin and eosin staining of paraffin embedded liver sections obtained from LDLR^{-/-} mice.

Representative images, no inflammation, and steatosis (panel, A). Fatty changes in great amount, microvesicular (blue arrows), macrovesicular (red arrows) (steatosis) and leukocyte infiltration (lymphocytes) (green- heads) presence of marked fatty changes near CV (zone 3) in middle column (panel B LDLR^{-/-} mice fed high fat-high sugar diet). LDLR^{-/-} supplemented Vitamin D group mice (panel C). CV, central vein. VD, Vitamin D, 100x. Scale bar represents 100 micron.

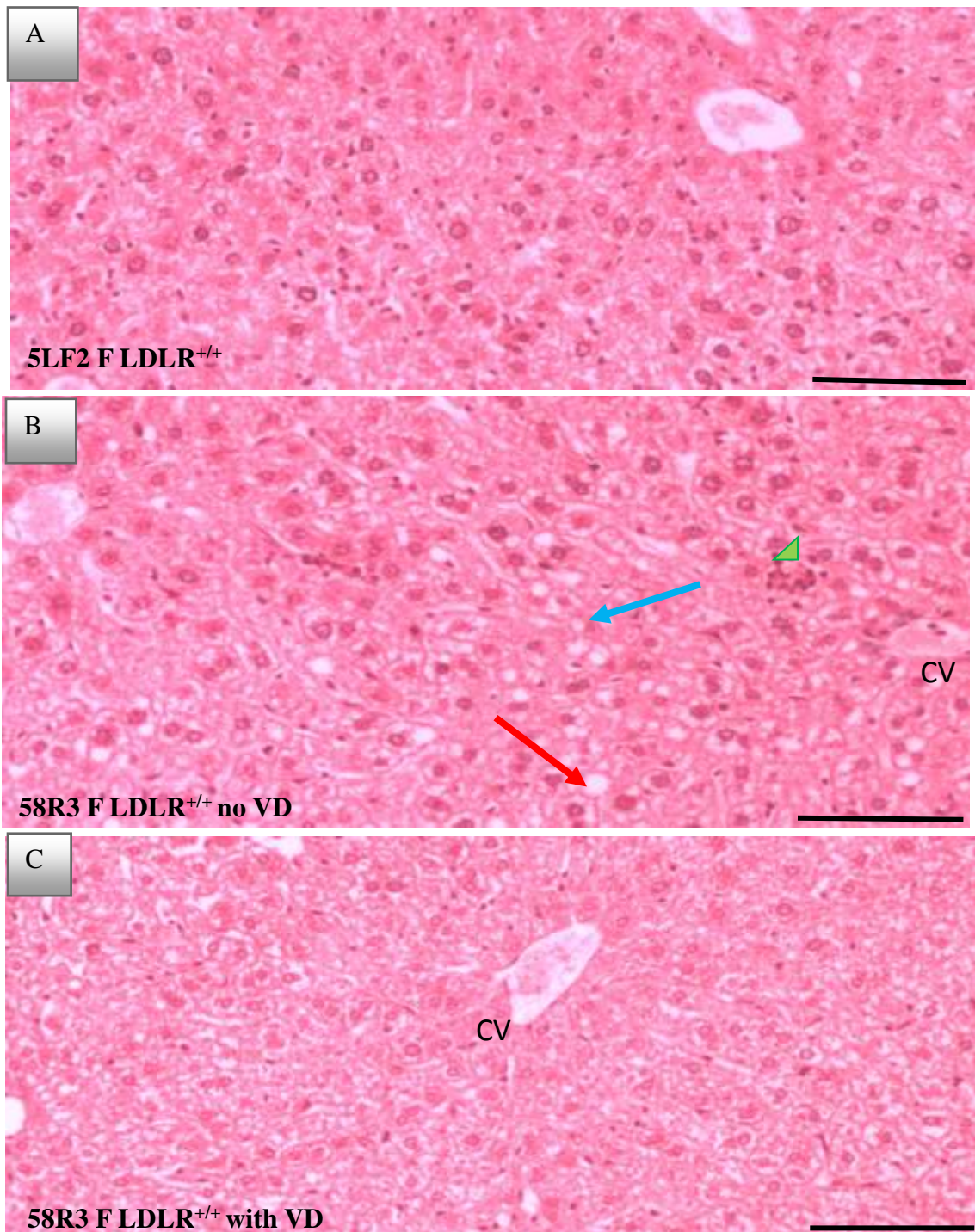


Figure 4-9 Haematoxylin and eosin staining of paraffin embedded liver sections obtained from LDLR^{+/+} mice

Representative images. No inflammation, and steatosis in control (panel, A). Fatty changes in great amount, microvesicular (blue arrows), macrovesicular (red arrows) (steatosis), and inflammation (green- heads) presence of marked fatty changes near CV (zone 3) in middle column in high fat –high sugar diet (panel B LDLR^{+/+} mice fed high fat -high sugar diet). No steatosis, no fatty changes near zone 3 and no inflammation (Panel C). CV, central vein. VD, Vitamin D, 100x. Scale bar represents 100 micron.

Histological scoring system was performed for lobular inflammation and steatosis (Kleiner et al., 2005). Scoring was performed by two observers who were blinded to the identity of the slides. Lobular inflammation (score 2) was seen in high fat diet-high sugar. However, only grade one, and zero was documented of lobular inflammation in Vitamin D supplemented diet group, and maintenance diet (LFD) (Tables 4.1 A, 4.2 A). Steatosis scores (ranges from 0- to 3) shows that in high fat diet high sugar group appear severe fatty change (grade 3), while in Vitamin D supplemented diet group mice and control mice, no grade three was documented (Tables 4.1 B, 4.2 B).

Table 4.1 Lobular inflammation scores, and steatosis scores in LDLR^{-/-} mice.

Lobular inflammation (A) scores, and steatosis scores (B) for LDLR^{-/-} mice fed high fat high sugar diet with Vitamin D (58R3+VD), and without Vitamin D (58R3) and maintenance diet (5LF2).

A

Lobular inflammation score	Meaning (foci per 200X field)	LDLR ^{-/-} 58R3	LDLR ^{-/-} 58R3+VD	LDLR ^{-/-} 5LF2
0	No foci	0/6	0/6	2/4
1	Less than 2	4/6	5/6	2/4
2	2-4	2/6	1/6	0/4
3	More than 4	0/6	0/6	0/4

B

Steatosis score	Meaning (parenchymal involvement by steatosis)	LDLR ^{-/-} 58R3	LDLR ^{-/-} 58R3+VD	LDLR ^{-/-} 5LF2
0	Less than 5%	0/6	0/6	3/4
1	5-33%	0/6	5/6	1/4
2	33-66%	2/6	1/6	0/6
3	More than 66%	4/6	0/6	0/6

Table 4.2 Lobular inflammation scores, and steatosis scores in LDLR+/+ mice.

Lobular inflammation scores (A), and steatosis scores (B) for LDLR+/+ mice fed high fat high sugar diet with Vitamin D (58R3+VD), and without Vitamin D (58R3) and maintenance diet (5LF2).

A

Lobular inflammation score	Meaning (foci per 200X field)	LDLR+/+	LDLR+/+	LDLR+/+
		58R3	58R3+VD	5LF2
0	No foci	2/6	5/7	2/4
1	Less than 2	4/6	2/7	2/4
2	2-4	0/6	0/7	0/4
3	More than 4	0/6	0/7	0/4

B

Steatosis score	Meaning (parenchymal involvement steatosis)	LDLR+/+	LDLR+/+	LDLR+/+
		58R3	58R3+VD	5LF2
0	Less than 5%	0/6	0/7	0/4
1	5-33%	0/6	5/7	4/4
2	33-66%	1/6	2/7	0/4
3	More than 66%	5/6	0/7	0/4

It appears from Haematoxylin, and eosin staining that high fat -high sugar diet caused steatosis, and inflammation in LDLR^{-/-}, and LDLR^{+/+} mice. Steatosis was seen in all mice (10 mice), but there was greater steatosis in high fat diet-high sugar, contrasting with less steatosis, and inflammation in the supplementary dietary Vitamin D group. To investigate liver damage, and influence by Vitamin D, liver function tests were performed.

4.2.2.6 Liver function

Liver histology showed that high fat diet-high sugar diet caused fatty changes, and inflammation, and in the presence of Vitamin D less fatty changes were documented. There are specific enzymes in the liver such as AST (Aspartate aminotransferase; also known as glutamate-oxaloacetate transaminase GOT), and ALT (alanine transaminase; also called glutamate-pyruvate transaminase GPT). AST, and ALT localisation are present as a cytoplasmic, or soluble isoenzyme, and a mitochondrial isoform. ALT activity is located in the cytosol. Both AST, and ALT are present equally in hepatic cell cytoplasm (Botros and Sikaris, 2013). AST, and ALT are measurement markers of hepatocellular damage, and are increased in high fat diet given to mice (Meli et al., 2013). After 10 weeks of high fat diet-high sugar diet with and without Vitamin D, there was significant increase of AST in LDLR^{-/-} mice fed high fat diet-high sugar diet compared to Vitamin D supplemented diet group mice. LDLR^{+/+} mice fed high fat diet-high sugar also showed elevation of AST compared to Vitamin D supplemented diet group though differences were not significant. The enzymatic activity of ALT had a tendency to elevate in high fat diet-high sugar group compared to LDLR^{-/-} mice Vitamin D supplemented diet group (Figure 4.10, A). LDLR^{+/+} mice, ALT has also had a tendency to increase in high fat diet-high sugar group compared to LDLR^{-/-} mice Vitamin D supplemented diet (Figure 4.10, B). This is the first study to demonstrate the effect of high fat diet-high sugar diet on hepatic damage markers, which were normalised by supplemented dietary Vitamin D containing diet in LDLR^{-/-} and LDLR^{+/+} mice. To understand how high fat diet-high sugar diet affects insulin levels as a measure of developing insulin resistance, insulin ELISA was tested.

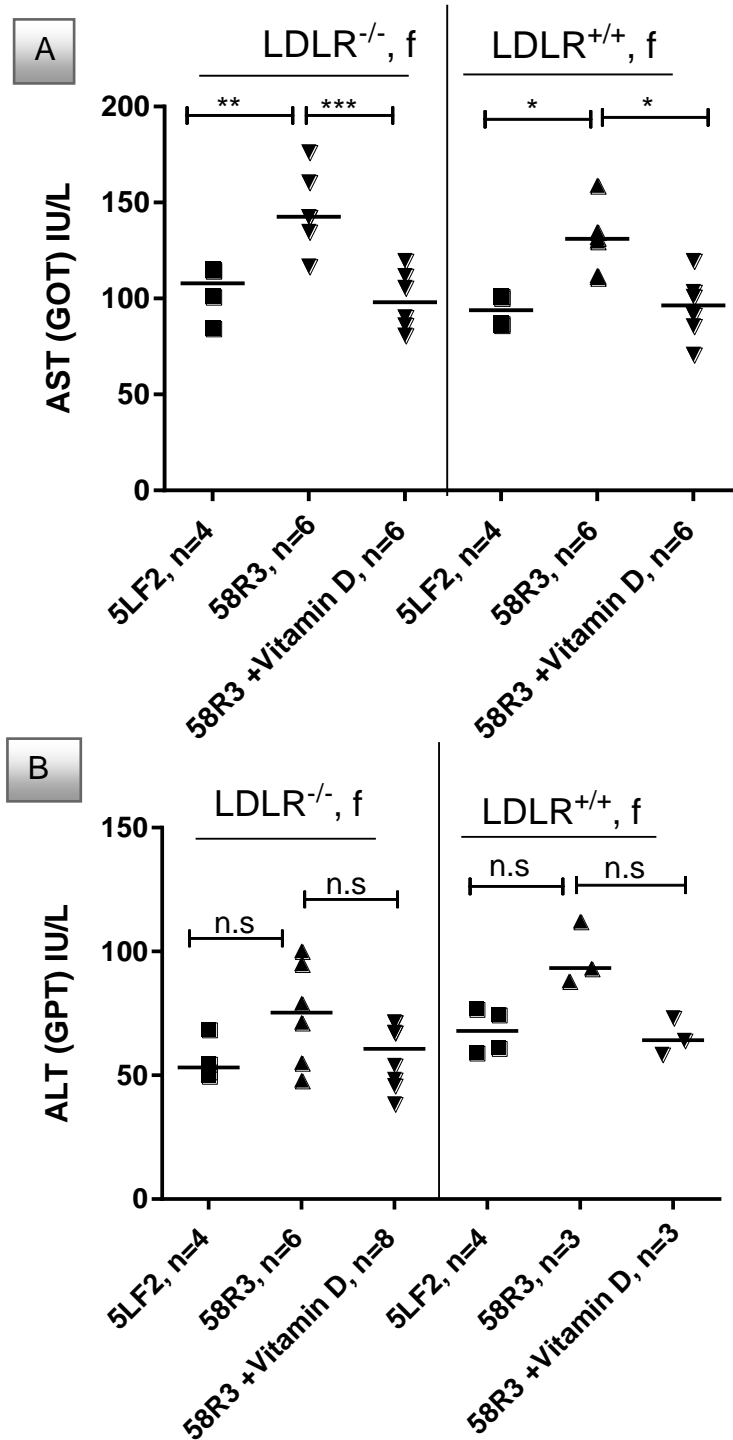


Figure 4-10 The effect of high fat high sugar diet with and without Vitamin D diet on liver function.

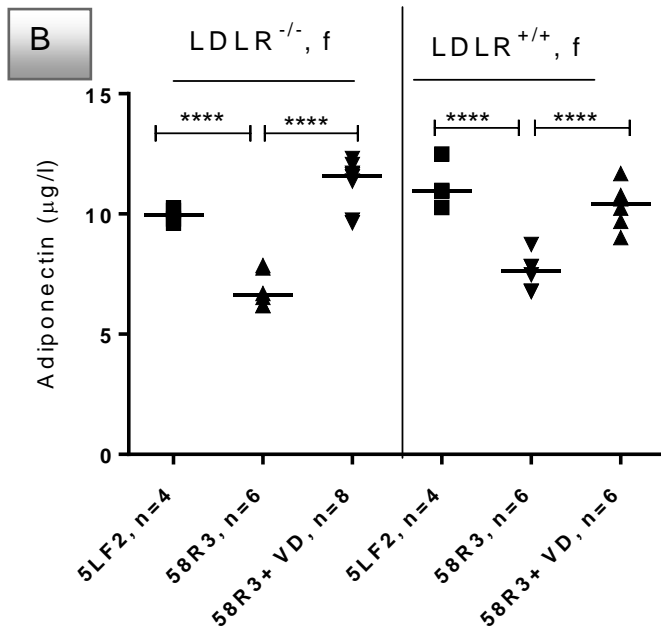
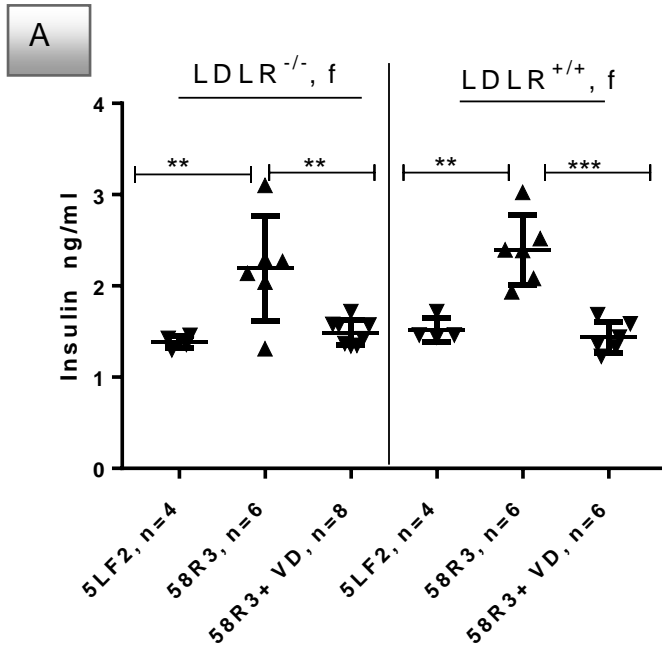
Female LDLR^{-/-} mice fed high fat high sugar diet with Vitamin D (58R3 +VD) and without Vitamin D (58R3), low fat diet (5LF2) (AST, Panel A), (ALT, Panel B). Results are presented as averages \pm SD from triplicate determinations. * $p < 0.05$, ** $p < 0.01$, *** $p < 0.005$ (adjusted p -values), n.s=no significant.

4.2.2.7 Effect of Vitamin D on insulin level, and chronic glycaemia

Because high fat diet- high sugar diet led to increased body weight and fat pad weight, an insulin ELISA test was performed in order to investigate whether high fat diet-high sugar diet affects insulin level, and to know whether Vitamin D supplemented diet (at the dose applied) normalises this level. Insulin levels have been shown to be increased in circulation in mice given high fat diet compared to control mice (Ha and Chae, 2010). Besides the insulin ELISA test, adiponectin protein measurement was performed. This is because adiponectin levels are reciprocal to insulin levels. A study reported that adiponectin deficient mice developed insulin resistance, because circulating adiponectin inhibited both the expression of hepatic gluconeogenic enzymes and the rate of endogenous glucose production (Kadowaki et al., 2006). After 10 weeks, insulin level increased in LDLR^{-/-} mice fed high fat diet-high sugar diet compared to Vitamin D supplemented diet group. In LDLR^{+/+} mice high fat diet-high sugar led to the elevation of insulin compared to Vitamin D group. The adiponectin level decreased in high fat diet-high sugar group, but returned to normal levels in LDLR^{-/-} mice fed Vitamin D (Figure 4.11, A). In LDLR^{+/+} mice, adiponectin was also decreased in high fat diet-high sugar group, but significantly increased in LDLR^{-/-} mice fed Vitamin D supplemented diet (Figure 4.11, B). These findings suggest that in general high fat diet-high sugar caused the increase of insulin level which was normalised by supplementary dietary Vitamin D containing diet in LDLR^{-/-} and LDLR^{+/+} mice.

In order to investigate blood glucose level, serum samples were measured using a clinical glucose meter, but this proved not to be accurate, due to past hemolysis of the samples. The difference in glucose levels between maintenance diet and high fat diet mice obtained in a previous measurement using non hemolysed plasma samples could not be reproduced. Recently, blood glucose measurement was performed in whole blood in tenth week for LDLR^{-/-} and LDLR^{+/+} mice with and without Vitamin D supplemented diet, there were no difference in blood glucose measurement, but there was a big variation between samples (data not shown). A naturally occurring deletion of exons 7-11 in the nicotine amide nucleotide transhydrogenase gene in C57BL/6 mice from the Jackson Laboratories (C57BL/6J) results in impaired glucose-stimulated

insulin secretion (Freeman et al., 2006). This is the reason for not doing glucose tolerance test. To monitor glucose binding to haemoglobin, haemoglobin A1C (HbA1c) was performed (Figure 4.11, C). The result showed that mice given high fat high sugar with Vitamin D supplemented diet led to the reduction of HbA1c compared to mice given high fat high sugar without Vitamin D. Noticeably, in LDLR^{-/-} mice given high fat high sugar HbA1c was higher compared to LDLR^{+/+} mice. It appears that Vitamin D plays a significant role in the decrease HbA1c and the risk to develop diabetes is higher in LDLR^{-/-} mice compared to LDLR^{+/+} mice. To understand how high fat diet-high sugar diet affects inflammation expression of specific genes related inflammation was tested.



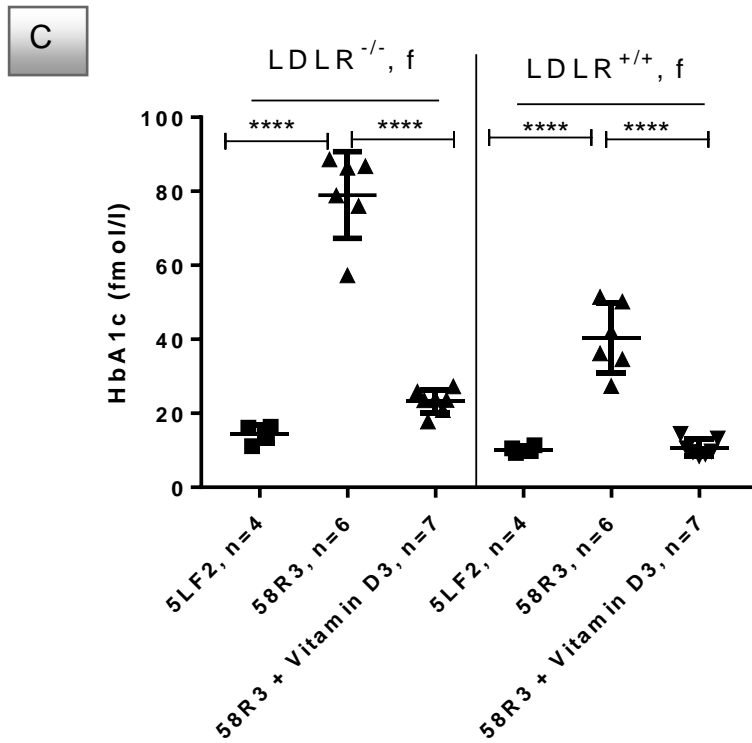


Figure 4-11 The effect of mice fed high fat high sugar diet with, and without Vitamin D diet on insulin, adiponectin, and HbA1c test.

Female LDLR^{-/-} mice fed high fat high sugar diet with Vitamin D (58R3 +VD) and without Vitamin D (58R3), low fat diet (5LF2) (insulin, Panel A), (adiponectin, Panel B), (HbA1c, Panel C). Results are presented as averages \pm SD from triplicate determinations. ** $p < 0.01$, *** $p < 0.005$, **** $p < 0.0001$ (adjusted p -values).

4.2.2.8 Anti-inflammatory effect of Vitamin D

Because of the presence of inflammatory cells in liver histopathology (Figure 4.12, B), qPCR for hepatic TNF- α , and IL-6 was performed, mRNA was prepared from livers of high fat diet mice with, and without Vitamin D and maintenance diet mice in LDLR^{-/-} and LDLR^{+/+} groups, and used for cyclic amplification. Expression of GAPDH (glyceraldehyde 3-phosphate dehydrogenase) was analysed for normalising amplifications of interest. Candidate inflammatory markers are TNF- α , involved in monocyte attraction, and IL-6 (Hursting and Hursting, 2012) involved in monocyte attraction. TNF- α , liver mRNA expression had a tendency to have lower from mice fed the Vitamin D supplemented high fat high sugar diet and higher in high fat -high sugar diet group mice (Figure 4.12, A). IL-6, liver mRNA expression was significantly lower from mice fed the Vitamin D supplemented high fat high sugar diet and higher in high fat -high sugar diet group mice (Figure 4.12, B). To further investigate the anti-inflammatory role of Vitamin D, ELISA test for IL-6 was performed in serum mice. IL-6 protein levels confirmed the hepatic gene expression of IL-6, and showed that the presence of Vitamin D led to the decrease of IL-6 protein in LDLR^{-/-} mice compared to high fat -high sugar diet compared to high fat -high sugar diet (4.12, C). These current data highlight the importance of supplementary dietary Vitamin D in an anti-inflammatory role in the liver. To further understand the role of Vitamin D as anti-inflammation, endotoxin was measured.

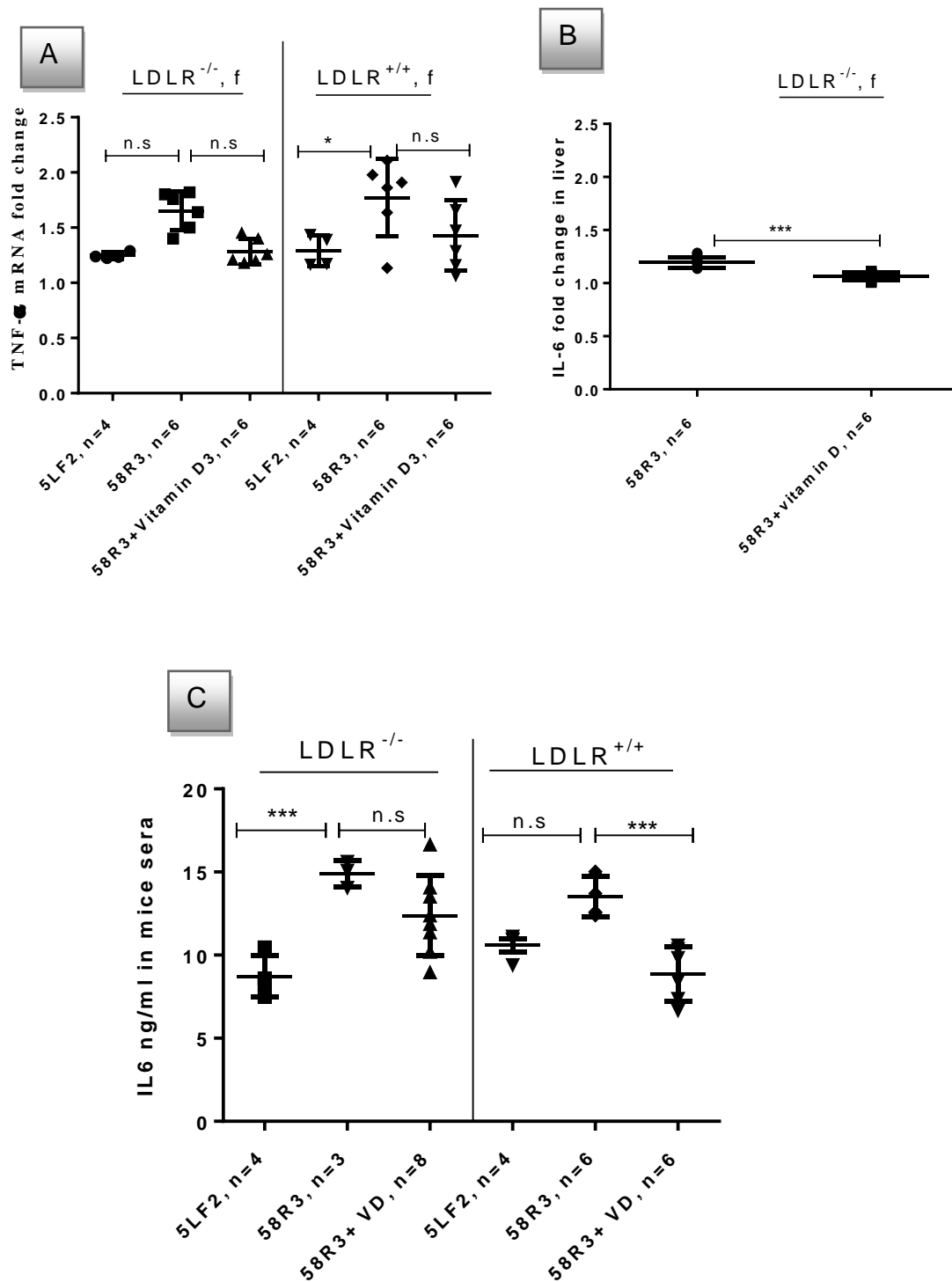


Figure 4-12 The effect of mice fed high fat high sugar diet with, and without Vitamin D diet on hepatic gene expression of TNF- α , IL-6, and ELISA IL-6.

Female LDLR^{-/-} and LDLR^{+/+} mice fed high fat high sugar diet with Vitamin D (58R3 +VD) and without Vitamin D (58R3), low fat diet (5LF2) (hepatic gene expression of TNF- α , Panel A), (hepatic gene expression of IL-6, female LDLR^{-/-} only, Panel B), (ELISA IL-6, Panel C). Results are presented as averages \pm SD from triplicate determinations. * $p < 0.05$, *** $p < 0.005$, (adjusted p -values), n.s=no significant.

4.2.2.9 Effect of Vitamin D on serum endotoxin

High fat diet-high sugar diet may affect intestinal permeability, therefore TLR4 mRNA expression and endotoxin were measured. A high fat diet increased translocation of LPS into the blood and this led to higher endotoxin level in NAFLD patients compared to controls (Harte et al., 2010). For this reason, TLR4, and endotoxin were measured in parallel. Vitamin D may modulate gut permeability (Garg et al., 2012). Hepatic mRNA was prepared from livers of high fat-high sugar diet mice, with, and without Vitamin D, and from mice on the maintenance diet. Our results showed that TLR4 mRNA was significantly higher in LDLR^{-/-} and LDLR^{+/+} mice fed high fat -high sugar diet compared to the Vitamin D₃ supplemented group (Figure 4.13, A). Endotoxins were also significantly higher in high fat -high sugar diet compared to Vitamin D group in both LDLR^{-/-} and LDLR^{+/+} mice (Figure 4.13, B). This result suggests that supplementary dietary Vitamin D prevents intestinal leakage. To understand the anti-steatosis effect of Vitamin D, srebp-1c as steatosis marker was performed.

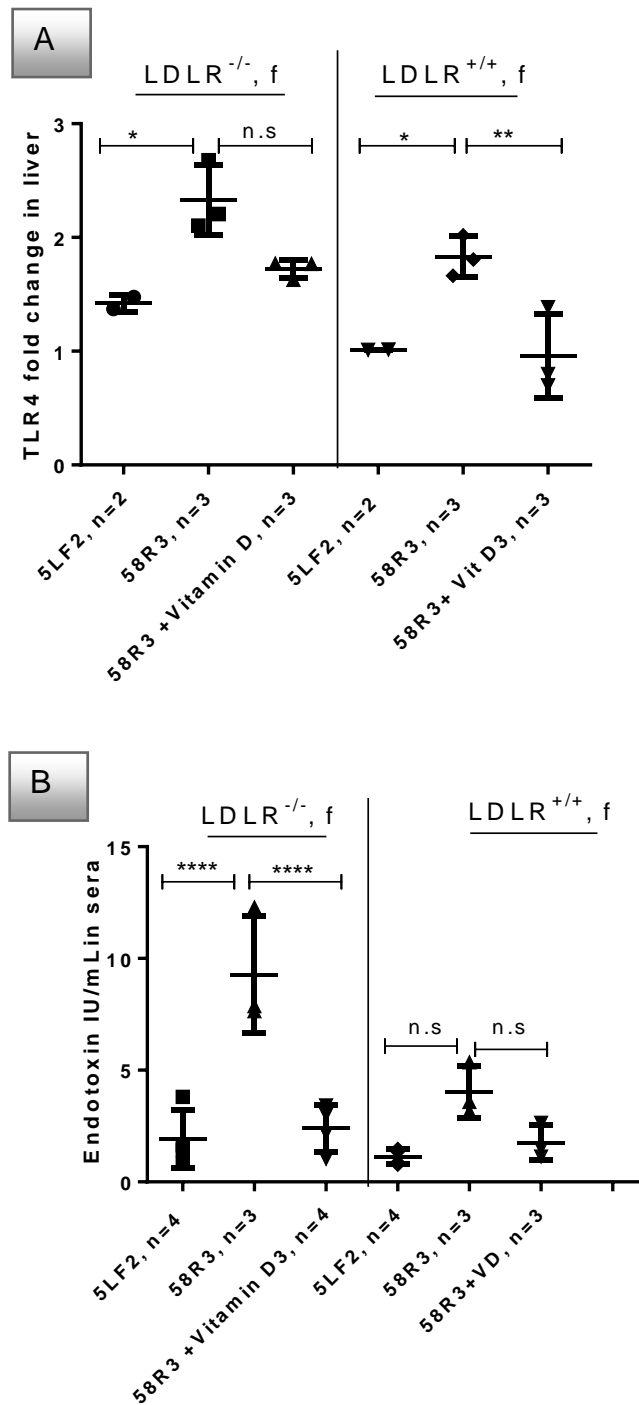


Figure 4-13 The effect of mice fed high fat high sugar diet with, and without Vitamin D diet on hepatic gene expression of TLR4 and serum endotoxin level.

Female LDLR^{-/-} and LDLR^{+/+} mice fed high fat high sugar diet with Vitamin D (58R3 +VD) and without Vitamin D (58R3), low fat diet (5LF2) (hepatic gene expression of TLR4, Panel A), (Endotoxin level, Panel B). Results are presented as averages \pm SD from triplicate determinations. * $p < 0.05$, ** $p < 0.01$, $p < 0.0001$ (adjusted p -values), n.s=no significant.

4.2.2.10 Anti-steatosis effect of Vitamin D

Elevated sterol regulatory element binding protein (SREBP), a lipogenic transcription factor, contributes to the development of fatty liver, and insulin resistance in animals (Cui and Jia, 2013). In this study, mRNA for this transcription factor was analysed. Hepatic gene expression of Srebp-1c increased significantly in high fat-high sugar diet compared to mice fed the Vitamin D supplemented high fat high sugar diet in both LDLR^{-/-} and LDLR^{+/+} mice (Figure 4.14). The empirical findings in this study provide a new understanding of supplementary dietary Vitamin D plays a significant role in the prevention of steatosis.

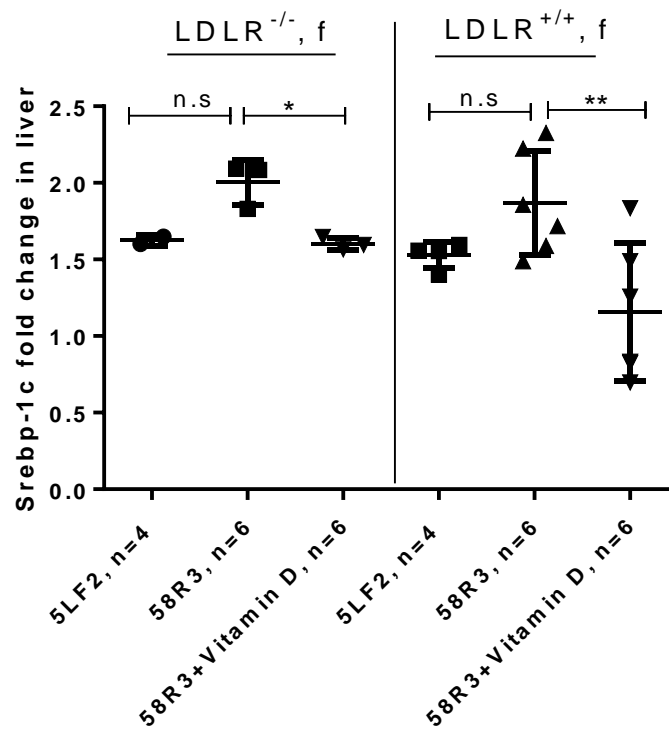


Figure 4-14 The effect of mice fed high fat high sugar diet with, and without Vitamin D diet on hepatic gene expression of Srebp-1c.

Female LDLR^{-/-} and LDLR^{+/+} mice fed high fat high sugar diet with Vitamin D (58R3 +VD) and without Vitamin D (58R3), low fat diet (5LF2) on hepatic gene expression of Srebp-1c. Results are presented as averages \pm SD from triplicate determinations. * $p < 0.05$, ** $p < 0.01$ (adjusted p -values), n.s.=no significant.

In order to investigate how mice fed high fat high sugar diet with, and without Vitamin D affect features of metabolic syndrome, triglyceride, and NEFA were measured.

4.2.2.11 The effect of mice fed high fat high sugar diet with, and without Vitamin D on manifestation of metabolic syndrome

The increase of non-esterified fatty acids (NEFAs) in obese situation was documented to contribute to the development of various disturbances related to the metabolic syndrome, such as hepatic and peripheral insulin resistance, and dyslipidaemia (Sarafidis and Bakris, 2007). Because liver histology showed in high fat diet -high sugar diet signs of steatosis, and no steatosis, and less strep-1c in the Vitamin D treated group, NEFA, and triglyceride were tested in serum samples. Our result showed that triglycerides were significantly higher in LDLR^{-/-} and LDLR^{+/+} mice fed high fat-high sugar diet compared to Vitamin D supplemented group (4.15, A). NEFA levels were significantly higher in high fat-high sugar diet compared to Vitamin D group in both LDLR^{-/-} and LDLR^{+/+} mice (4.15, B). These results highlight that supplementary dietary Vitamin D prevents metabolic syndrome disease by reducing of triglyceride, and NEFA serum level.

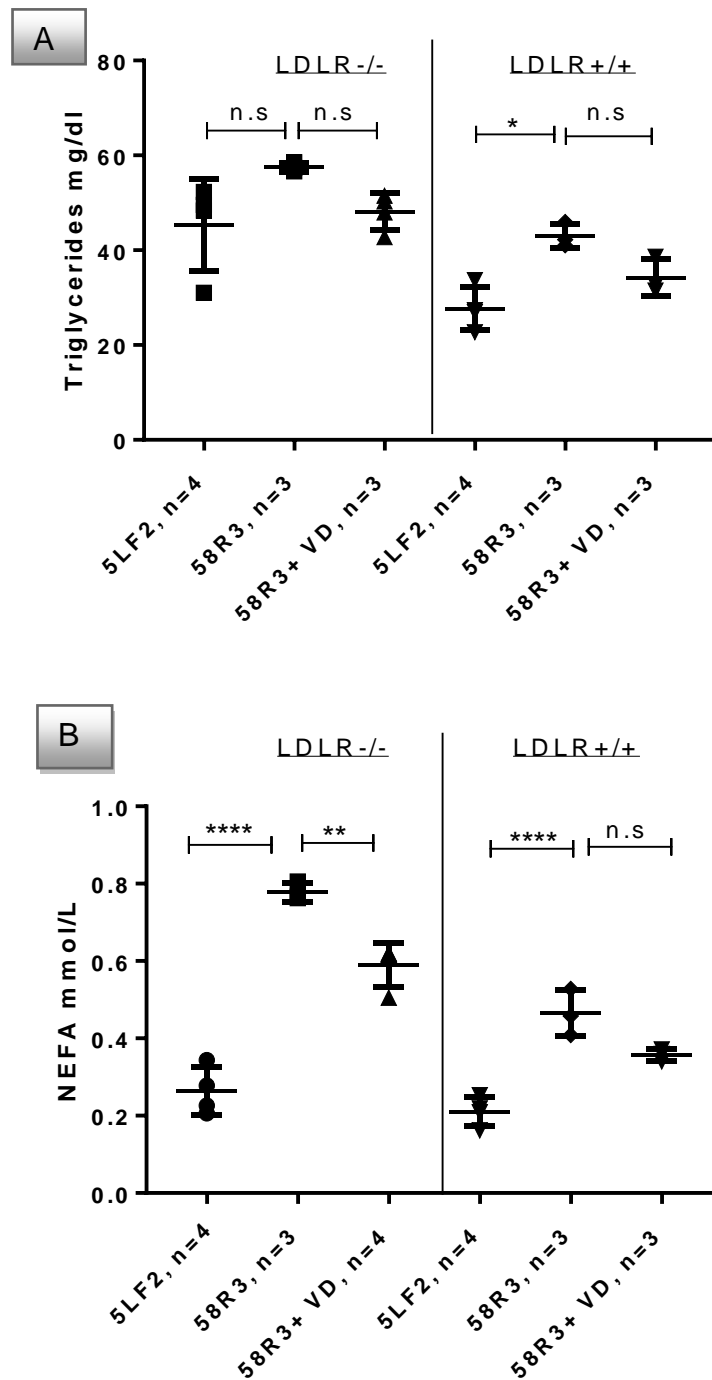


Figure 4-15 The effect of mice fed high fat high sugar diet with, and without Vitamin D diet on triglyceride (TG) and NEFA serum level. Female LDLR^{-/-} and LDLR^{+/+} mice fed high fat high sugar diet with Vitamin D (58R3 +VD) and without Vitamin D (58R3), low fat diet (5LF2) on triglyceride (TG) (Panel A) and NEFA (Panel B) serum level. Results are presented as averages ±SD from triplicate determinations. **p* < 0.05, ***p* < 0.01, ****p* < 0.005 (adjusted *p*-values), n.s=no significant.

4.2.2.12 Effect of Vitamin D on lipid peroxidation product levels, and vascular adhesion molecular mRNA expression

The enhancement of oxidative stress combined with endothelial dysfunction as indicated by reduced activity of endothelial nitric oxide pathway, and enhanced expression of sVCAM-1 play an important intermediary role in the pathogenesis of macrovascular complications in type 2 diabetes mellitus (Singhania et al., 2008).

We hypothesised that high fat-high sugar diet influences formation of malondialdehyde (MDA), and that Vitamin D prevents MDA initiation. Thiobarbituric acid (TBA) detects MDA, an end product of nonenzymatic polyunsaturated fatty acid (PUFA) oxidative degradation, which has therefore been used for decades as a marker of lipid peroxidation (Gutteridge et al., 1982). Lipid peroxidation is tightly linked to high fat diet and obesity (Johnson et al., 2007). Diet-induced obesity is associated with an increase in the formation of lipid peroxidation-derived aldehydes (Baba et al., 2011).

MDA increased significantly in mice on high fat -high sugar diet compared to mice fed the Vitamin D supplemented high fat high sugar diet in both LDLR^{-/-} and LDLR^{+/+} mice (Figure 4.16, A). It can be concluded that that Vitamin D plays a significant role in preventing MDA production. The present study confirms previous findings, and contributes additional evidence that MDA increases in high fat diet. To investigate the effect of aortic endothelium and to see the relationship of adhesion molecule expression to initiation factors and the sites of lesion formation, VCAM-1 (vascular cell adhesion molecule-1) gene expression was measured in aorta and atria of mouse hearts of mice fed the vitamin D supplemented high fat high sugar diet. The result showed that supplementary dietary Vitamin D may play a role in the decrease of VCAM-1 gene expression (Figure 4.16, B). The findings of this experiment could be applied to understand how Vitamin D might prevent atherosclerosis.

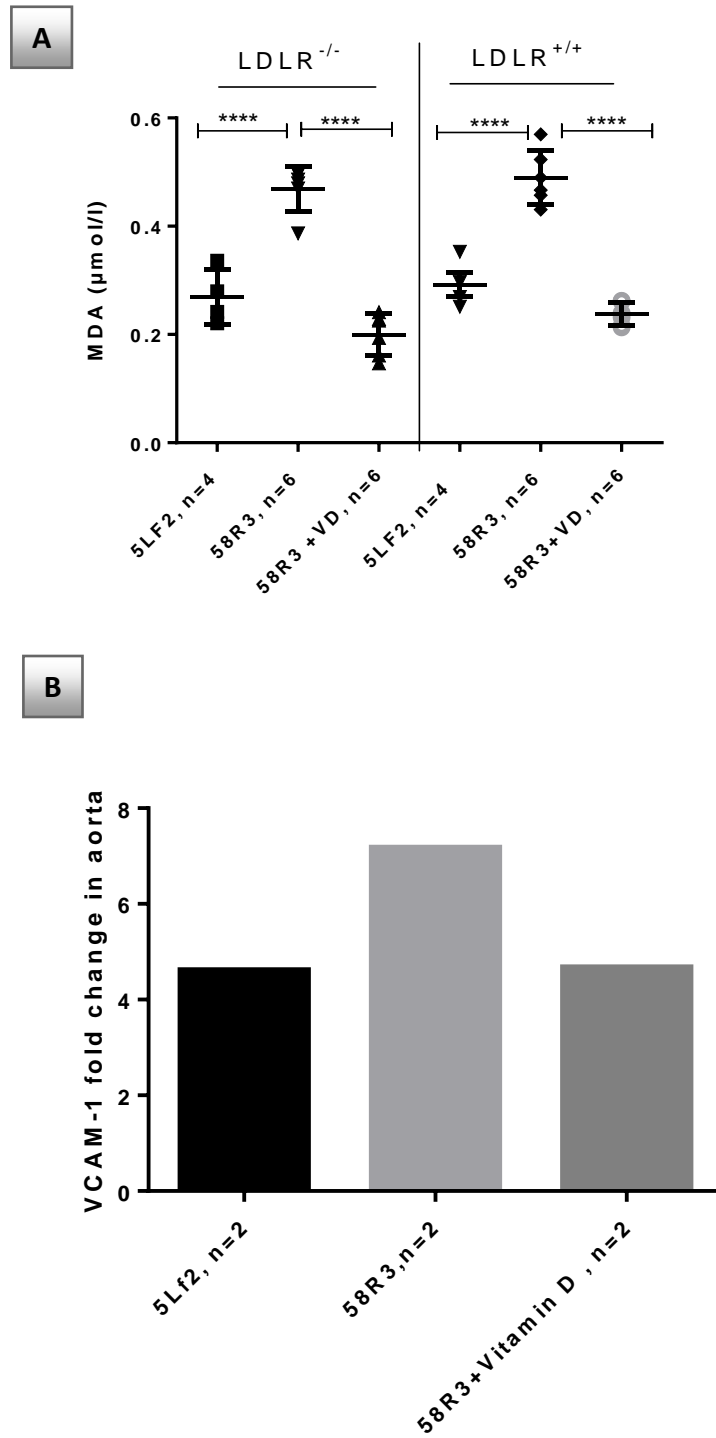


Figure 4-16 The effect of mice fed high fat high sugar diet with, and without Vitamin D diet on serum MDA level and aortic Vcam-1 mRNA expression.

Female LDLR^{-/-} and LDLR^{+/+} mice fed high fat high sugar diet with Vitamin D (58R3 +VD) and without Vitamin D (58R3), low fat diet (5LF2) on MDA serum level (Panel A) and Vcam-1 mRNA expression (Panel B). Results are presented as averages ±SD from triplicate determinations. ****p* < 0.005, *****p* < 0.0001 (adjusted *p*-values).

4.2.2.13 Vitamin D influences macrophage phenotypes in vivo (M2)

4.2.2.13.1 Immunohistochemistry for F4/80 (pan macrophage marker)

The main aim of performing immunohistochemistry for F4/80, as a macrophage marker was to detect macrophages in liver (Kurokawa et al., 2011), in mice fed high fat high sugar diet with and without Vitamin D, and to generate a working protocol that could be applied for M2 characteristic receptor expression such as CD206. Positive cells were detected (Figure 4.17, B) in both high fat-high sugar diet and the Vitamin D supplemented high fat high sugar diet group mice, and then positive cells were counted independently by two persons. To evaluate possible infiltration, the number of positive cells was expressed as means from the evaluated grids. The observation from this measurement was that in high fat-high sugar diet fed mice there were more F4/80 positive cells compared to Vitamin D supplemented group although not significantly different (Figure 14.17, C). To further investigate Vitamin D role as M1 activity, and M2 macrophage activity, mRNA gene expression of iNOS (M1 macrophage activity), and Arginase-1 (M2 macrophage activity) was performed.

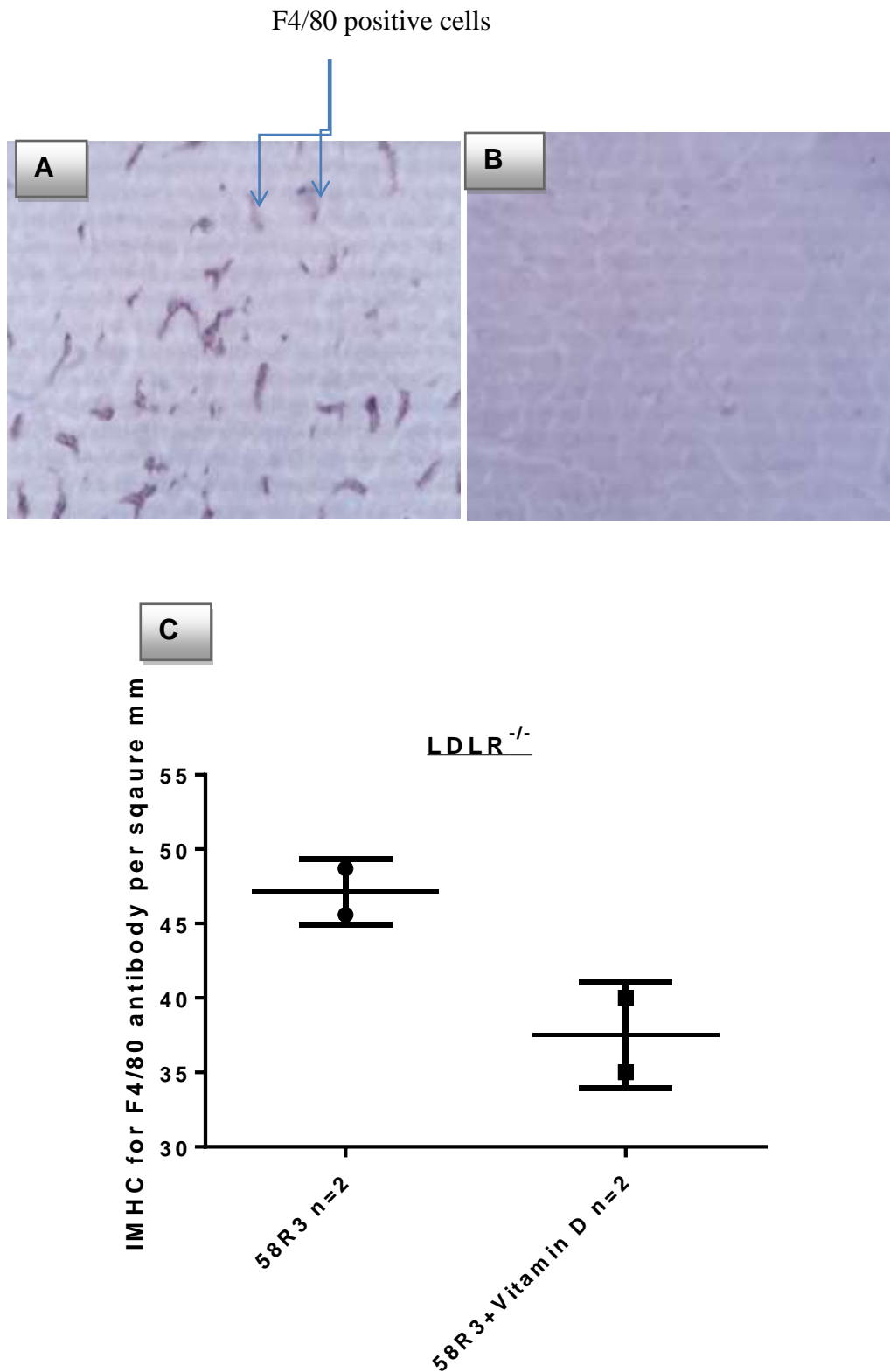


Figure 4-17 Immunohistochemistry of liver paraffin sections of mice fed high fat high sugar diet with, and without Vitamin D.

Female LDLR^{-/-} mice fed high fat high sugar diet with Vitamin D (58R3 +VD) and without Vitamin D (58R3) on immunohistochemistry F4/80 macrophage marker. F4/80 positive cells (Panel A), Negative control (Panel B), number of F4/80 positive cells per five square mm, approximately 500 cells (Panel, C), blue arrows indicate F4/80 positive macrophage, x40.

4.2.2.13.2 Effect of Vitamin D on gene expressions characteristic of M1, and M2 activity

To investigate the effect of Vitamin D on macrophage activity so gene expression of iNOS (marker of M1 macrophage activity), and Arginase-1 (marker of M2 macrophage activity) of spleen, and liver were performed (Sharda et al., 2011). Mice fed high fat diet showed a significant increase of iNOS (Liu et al., 2015). My results showed the increase of iNOS mRNA expression, and the decrease of Arginase-1 mRNA expression in spleens from high fat -high sugar diet mice group; however, in mice fed the Vitamin D supplemented high fat high sugar diet group, a lower level of iNOS mRNA, and inversely, a higher level of Arginase-1 mRNA were found (Figure 4.18, A, B). In order to further investigate the effect of Vitamin D on the presence of M2 type macrophages, hepatic mRNA expression was performed for both candidate genes. The result showed also in liver, mRNA expression of iNOS in high fat high sugar diet was significantly higher compared to the Vitamin D supplemented high fat high sugar diet (Figure 4.19, A). Interestingly, arginase-1 in livers from the Vitamin D supplemented high fat high sugar diet was significantly higher compared to high fat -high sugar diet (Figure 4.19, B). Prussian blue staining was performed as an alternative measure of M1 activity, and splenocytes were stained to compare Vitamin D supplemented high fat high sugar diet, and high fat -high sugar diet.

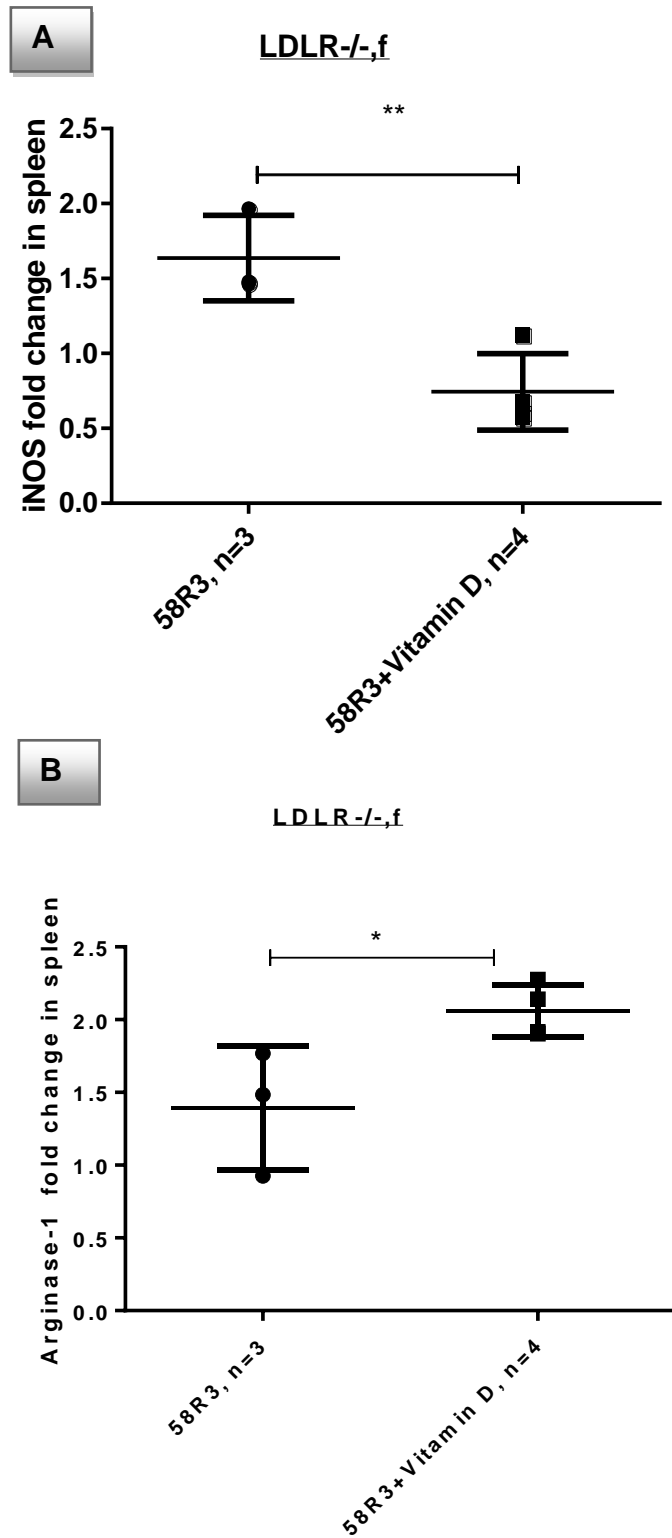


Figure 4-18 The effect of mice fed high fat high sugar diet with, and without Vitamin D diet on splenic gene expression of iNOS and Arginase -1.

Female LDLR^{-/-} mice fed high fat high sugar diet with Vitamin D (58R3 +VD) and without Vitamin D (58R3), low fat diet (5LF2) on hepatic gene expression of iNOS (Panel A), Arginase-1 (Panel B). The data are represented as means \pm SD (*p<0.05, **p<0.01).

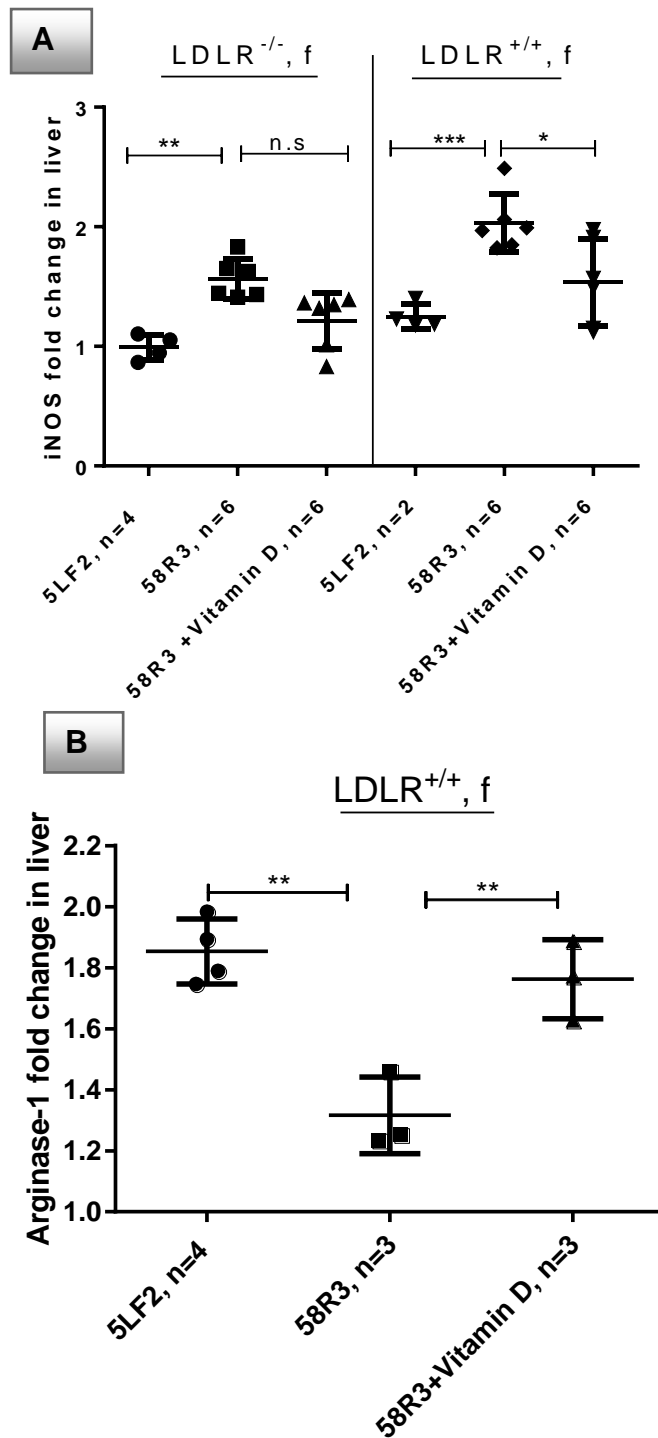


Figure 4-19 The effect of mice fed high fat high sugar diet with, and without Vitamin D diet on hepatic gene expression of iNOS and Arginase -1.

Female LDLR^{-/-} and LDLR^{+/+} mice fed high fat high sugar diet with Vitamin D (58R3 +VD) and without Vitamin D (58R3), low fat diet (5LF2) on hepatic gene expression of iNOS (Panel A), Arginase-1, only LDLR^{+/+} mice (Panel B). Results are presented as averages \pm SD from triplicate determinations. * $p < 0.05$, ** $p < 0.01$, *** $p < 0.005$ (adjusted p -values), n.s=no significant.

4.2.2.13.3 Prussian blue staining

Prussian blue staining represents a surrogate marker of macrophage activity (intracellular iron storage = antimicrobial, M1 feature). Tissue sections are treated with hydrochloric acid to denature the binding proteins of the haemosiderin molecule, and thereby release ferric (3+) ions. Potassium ferrocyanide was then introduced. The ferric ions combine with this solution, resulting in the formation of ferric ferrocyanide, an insoluble bright blue pigment. Splenocytes were prepared *in vitro* and reviewed under the microscope (40x). On average, 300 cells were counted per group, and % calculated. The result showed a highly significant amount of positive cells in high fat-high sugar diet compared to mice fed the Vitamin D supplemented high fat-high sugar diet group mice (Figure 4.20, B). It can be concluded that functional Prussian blue staining matches iNOS/arginase ratio in liver. This finding shows that Vitamin D plays an important role in the decrease of M1 activity, and the increase of M2 activity.

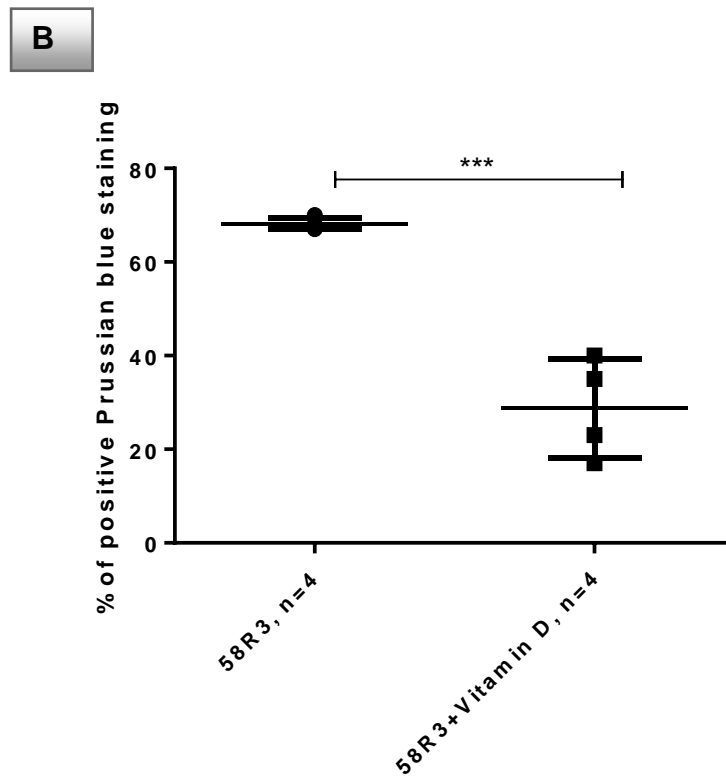
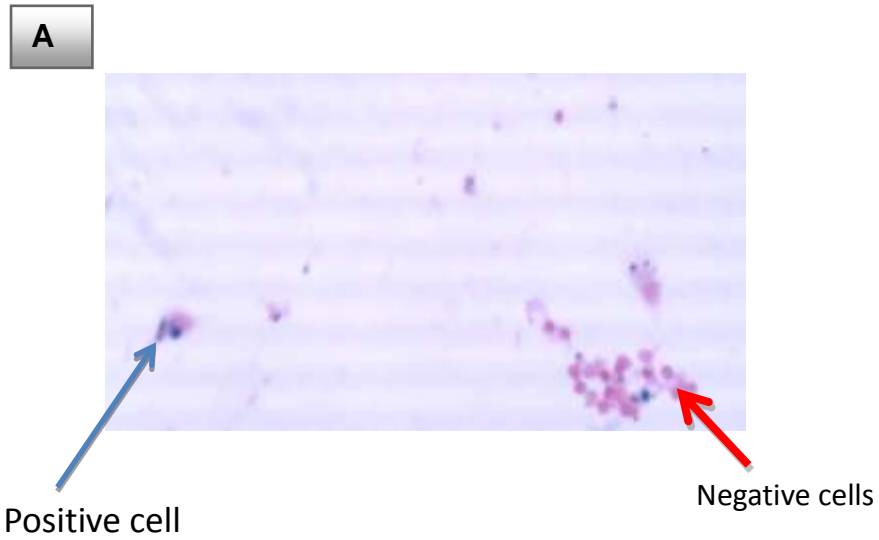


Figure 4-20 Prussian blue staining of splenocytes of mice fed high fat high sugar diet with, and without Vitamin D.

LDLR^{-/-} mice splenocytes on average 300 cells were counted per genotype, and % calculated (x40). Blue arrow indicates positive cells, and red arrow indicates negative cell (Panel A). Positive Prussian blue staining in high fat -high sugar diet compared to mice fed high fat high sugar diet with Vitamin D group (Panel B). The data are represented as means \pm SD (Unpaired t test *** $p < 0.005$).

4.2.2.14 Effect of Vitamin D on candidate genes involved in cholesterol metabolism (SR-B1, HMGCR, PPAR- γ)

Next, the influence of high fat–high sugar diet on the expression of genes involved in cholesterol metabolism was tested. Scavenger receptor-1 (SR-B1) (cholesterol uptake) upregulation is associated with development of NAFLD (Qiu et al., 2013). HMGCR (3-hydroxy-3-methylglutaryl-co-enzyme a reductase) (cholesterol synthesis) expression is increased by free cholesterol, and dysregulation is related to NAFLD, and atherosclerosis (Min et al., 2012). Our results showed that hepatic mRNA expression of SR-B1 increased in high fat diet-high sugar compared to Vitamin D group mice in LDLR^{+/+} mice, although in LDLR^{-/-} mice the increase was not significantly different (Figure 4.21, A). The results showed that hepatic mRNA expression of HMGCR increased in high fat diet-high sugar compared to Vitamin D group mice in LDLR^{-/-} mice and LDLR^{+/+} mice (Figure 4.21, B).

PPAR- γ (cholesterol regulation) increased due to oxidized LDL, and it has anti-inflammatory role (Shalhoub et al., 2011), consistent with M2 property in the presence of Vitamin D (Vitamin D R-PPAR gamma pathway) (Yin et al., 2015). Hepatic mRNA expression of PPAR γ was significantly lower in LDLR^{-/-} mice fed high fat –high sugar diet supplemented with Vitamin D (Figure 4.21, C). These results concluded that high fat–high sugar caused the increase of mRNA expression of genes involved in cholesterol synthesis, and dysregulation of cholesterol, and it was prevented by supplement Vitamin D to mice group. In order to see the Vitamin D effect on adipocyte protein expression, therefore, protein array was performed.

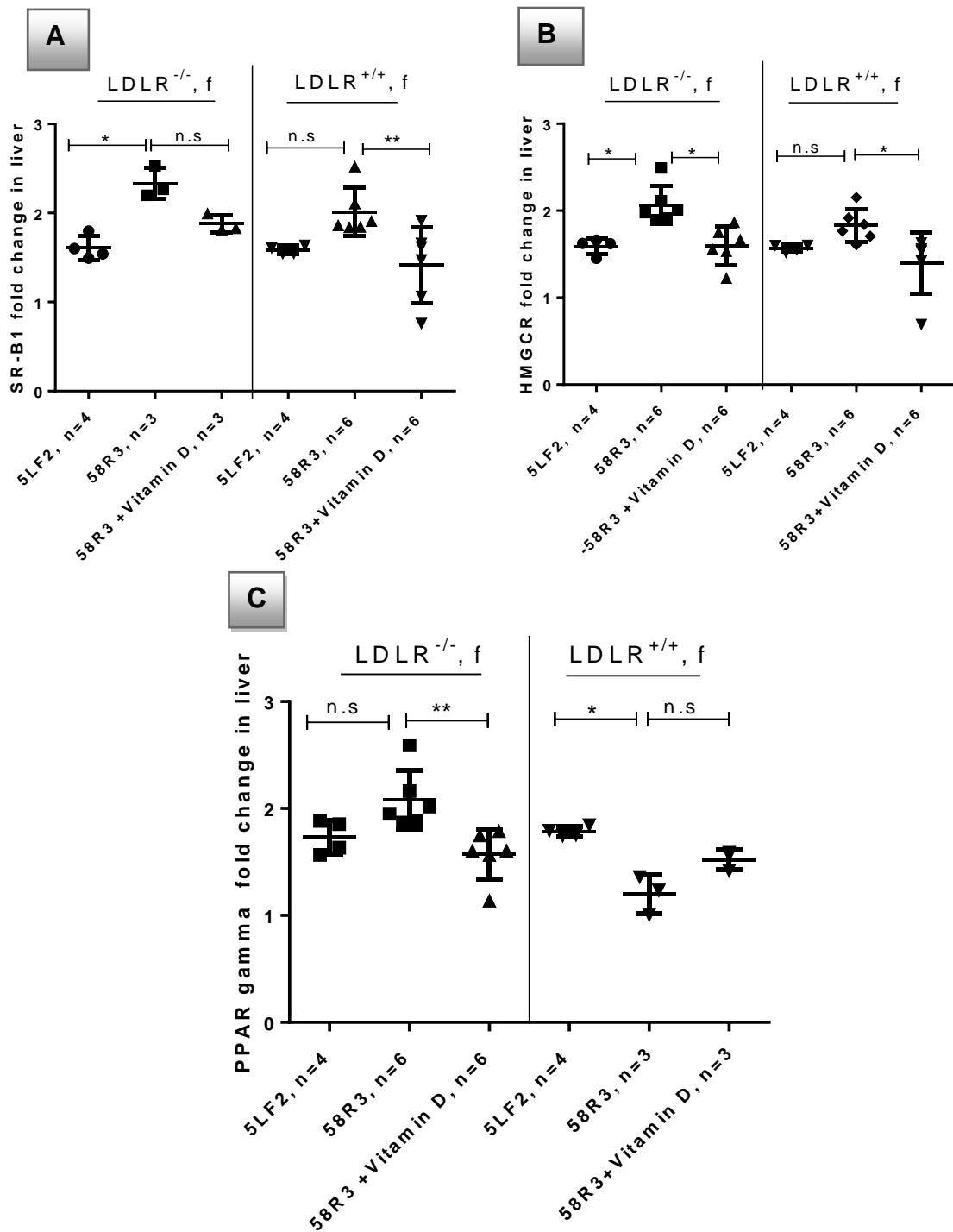
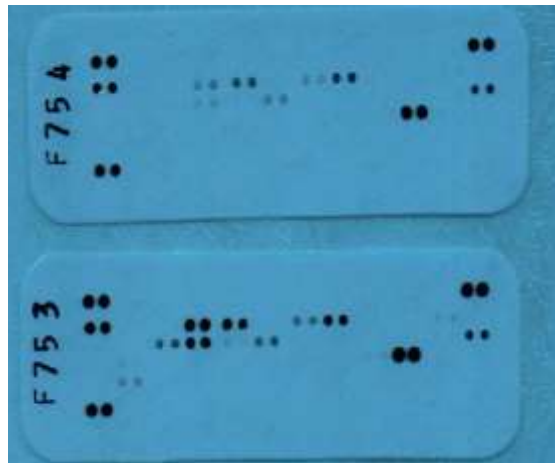


Figure 4-21 The effect of mice fed high fat high sugar diet with, and without Vitamin D diet on hepatic gene expression of genes involved in cholesterol metabolism. Female LDLR^{-/-} and LDLR^{+/+} mice fed high fat-high sugar diet with Vitamin D (58R3 +VD) and without Vitamin D (58R3), low fat diet (5LF2) on hepatic gene expression of SR-B1 (scavenger receptor class b1) (Panel A), HMGCR (3-hydroxy-3-methylglutaryl-co-enzyme A reductase), (Panel B), PPAR- γ (Panel C). Results are presented as averages \pm SD from triplicate determinations. * $p < 0.05$, ** $p < 0.01$ (adjusted p -values), n.s=no significant.

4.2.2.15 Effect of Vitamin D on abundance of adipokinins in epididymal fat pads

The main purpose to perform microarray was to see the effect of high fat diet–high sugar in the presence, and absence of Vitamin D. Vascular endothelial growth factor (VEGF), which is also act as proinflammatory cytokines by increasing endothelial permeability, stimulated expression of intercellular adhesion molecule-1 (ICAM-1), vascular cell adhesion molecule-1 (VCAM-1), ICAM-1 (intracellular adhesion molecular -1) (Kim et al., 2001). The increase of endothelial adhesion molecules (VCAM-1, ICAM-1) may develop Atherosclerosis, diabetes, and hypertension in obese people (Ferri et al., 1999). Our result showed that VEGF, VCAM-1, ICAM-1 had a tendency to have higher in mice fed high fat diet group compared to supplemented Vitamin D high fat–high sugar diet group. Serum RBP4 (Retinol binding protein 4) correlated positively with presence of insulin resistance in individuals with obesity (Graham et al., 2006). My result showed that RBP4 protein had a tendency to increase in mice fed high fat diet group compared to supplemented Vitamin D high fat–high sugar diet group.

DPPIV (Dipeptidyl peptidase I V), inhibition caused the prevention diabetes and insulin resistance in mice fed high fat diet (Conarello et al., 2003). Our result showed that mice fed high fat-high sugar diet supplemented with Vitamin D had a tendency to have less DPPIV protein presence compared to no-Vitamin D diet group mice. Fetuin A is increased in obesity, and diabetes (Trepanowski et al., 2015), IGFBP-3, 5, 6 (Insulin like growth factor binding protein-3, 5, 6) (Shimasaki and Ling, 1991) and C-reactive protein (Fronczyk et al., 2014) are elevated during obesity and diabetes. In conclusion it can be said that proteins involved in fibrosis, steatosis and inflammation are increased in adipose tissue of mice given high fat diet (Figures 4.22). There was a marked decrease of these proteins in adipose tissue of mice given high fat diet plus Vitamin D. Adiponectin, resistin, and lipocalin remained the same between the pooled samples (n=2).

A

58R3+VD

58R3

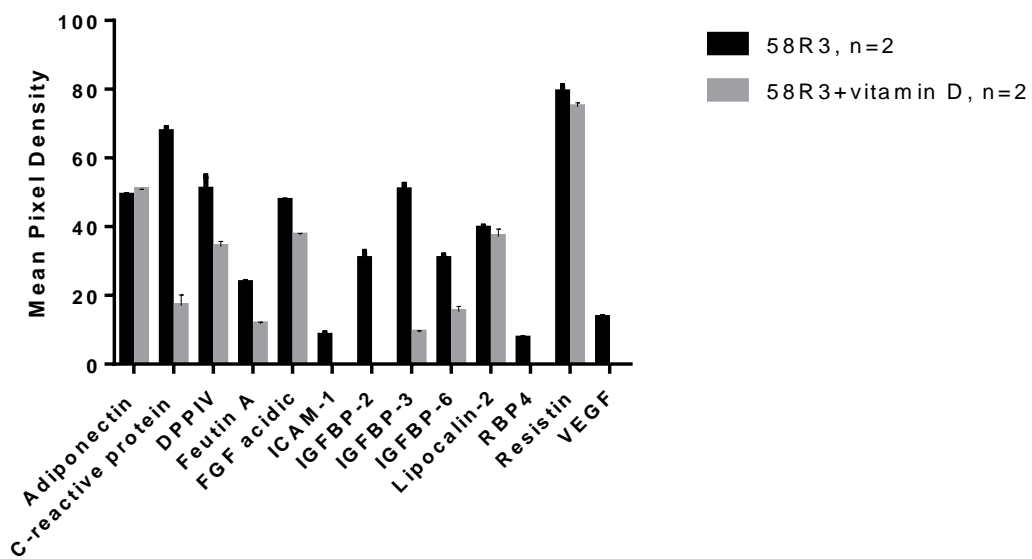
B

Figure 4-22 Mouse adipokine array detects multiple protein analyses in adipose tissue of mice.

Proteome profile mouse adipokine array in mice fed high fat-high sugar diet with supplanted Vitamin D (58R3+VD), mice fed high fat high sugar diet without Vitamin D (Panel A), mice fed high fat high sugar diet without Vitamin D vs with Vitamin D (Panel B). Adipose tissues were excised and prepared as described in the adipose tissue array preparation.

4.2.2.16 Effect of Vitamin D on functional complement activation ELISAs (classical, and alternative pathway activation)

The aim was to study whether Vitamin D plays a significant role in the decrease of classical, and alternative pathway activation *in vivo*. Because oxidized LDL caused classical complement activation in human serum (Saad et al., 2006), we tested classical pathway activation in serum of mice at the level of C9.

Our results showed that LDLR^{+/+} mice fed the Vitamin D supplemented high fat-high sugar diet had higher residual activity of the classical pathway compared to high fat high sugar diet without Vitamin D (Figure 4.23, A). The elevation of residual activity in mice given high fat high sugar diet supplementary Vitamin D is the result of preserving activity *in vivo*. LDLR^{-/-} mice had lower classical residual activity compared to LDLR^{+/+} mice.

In a study comparing obese versus lean people, chylomicrons were higher and more enriched with LPS in obese people when compared with lean people (Vors et al., 2015). Chylomicron accelerates C3 tick-over by regulating the role of factor H, leading to the overproduction of ASP resulting in acceleration of alternative pathway activation (Fujita et al., 2007). Our previous results showed more triglycerides (TGs), endotoxins in high fat-high sugar and low TGs in mice treated with Vitamin D. LDLR^{-/-} mice had lower residual activity of the alternative pathway of complement compared to LDLR^{+/+} mice

Our results showed that mice fed the Vitamin D supplemented high fat-high sugar diet had higher residual complement activities of the alternative pathway compared to the high fat high sugar diet without Vitamin D (Figure 4.23, B). The Vitamin D intervention is likely to exert its effect on classical, and alternative pathway indirectly (via increase of residual activity in Vitamin D group compared to high fat- high sugar diet).

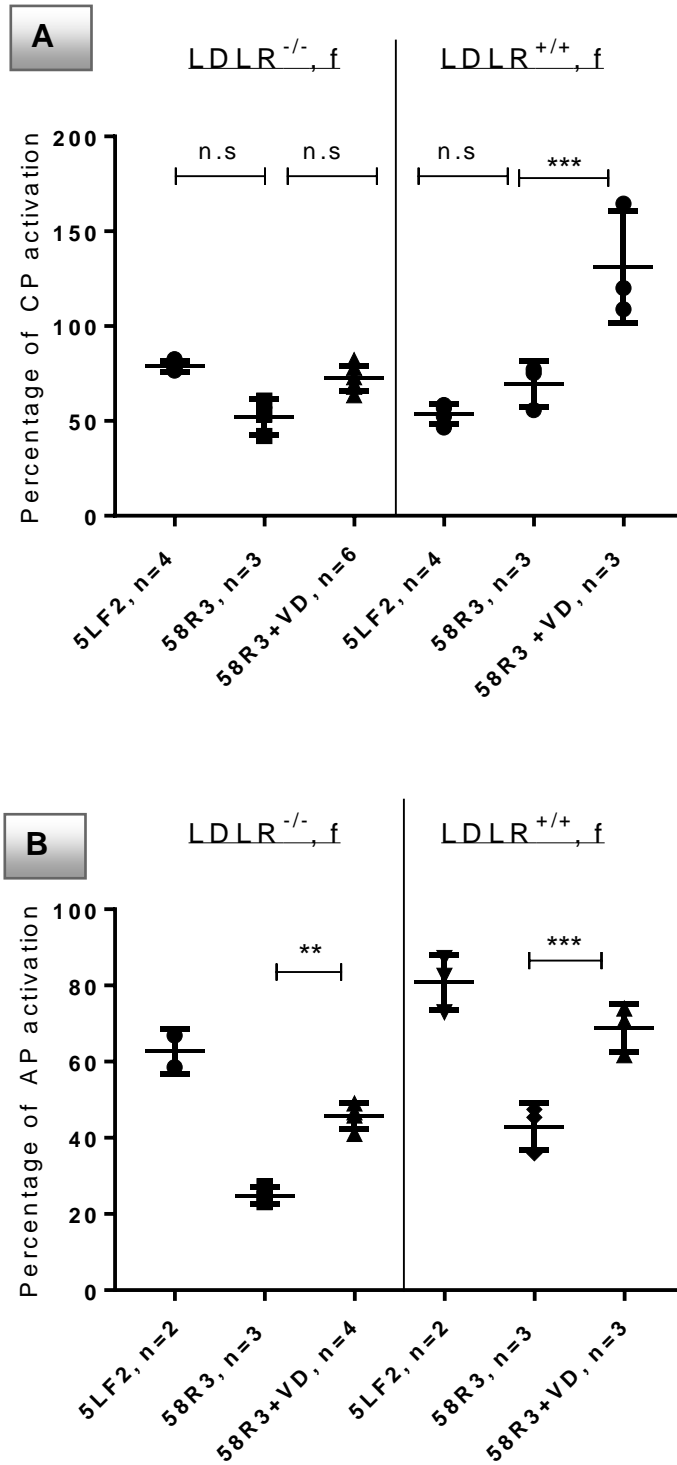


Figure 4-23 The effect of mice fed high fat high sugar diet with, and without Vitamin D diet on functional complement residual activities.

Female LDLR^{-/-} and LDLR^{+/+} mice fed high fat high sugar diet with Vitamin D (58R3 +VD) and without Vitamin D (58R3), low fat diet (5LF2) (percentage of complement classical pathway activation (Panel A), percentage of alternative pathway activation (Panel B)). Results are presented as averages \pm SD from triplicate determinations. ** $p < 0.01$, *** $p < 0.005$ (adjusted p -values).. CP=classical pathway, AP=complement alternative pathway, n.s=no significant.

To summarise this section, body weight increased significantly in LDLR^{-/-} mice fed high fat -high sugar diet compared to LDLR^{-/-} fed LFD stable weight, but as far as Vitamin D group was concerned mice tended to show less body weight gain or stability so as not to get overweight. However, LDLR^{+/+} mice fed high fat-high sugar diet had significantly greater body weight when compared to LDLR^{+/+} mice, and Vitamin D supplemented diet group mice increased the percentage body weight gain significantly compared to high fat -high sugar diet group mice. Taken together, the most striking result is that the two backgrounds behave differently to Vitamin D, and LDLR^{-/-} are heavier on maintenance diet. Liver weight analysis revealed that high fat -high sugar diet led to the increase of liver weight which was reduced by supplementary Vitamin D. These suggest that in LDLR^{+/+} mice fed high fat high sugar diet, supplementary Vitamin D played a significant role in diminishing development of diet-induced hepatomegaly.

The evidence from this study suggests that fat pad weight measurement was increased by high fat diet-high sugar compared to maintenance diet mice group, and most importantly was less in the supplementary dietary Vitamin D group mice. These data highlight the importance of supplementary dietary Vitamin D in the decrease of central obesity. Haematoxylin eosin staining showed that high fat -high sugar diet caused steatosis, and inflammation in LDLR^{-/-}, and LDLR^{+/+} mice. Steatosis was seen in high fat-high sugar diet mice, and in the supplementary dietary Vitamin D there was less steatosis, inflammation, and systemically also less pronounced measures of metabolic syndrome were detected. The empirical findings in this study provide a new understanding of the role that supplementary dietary Vitamin D plays in the role in the prevention of steatosis, and lipid peroxidation. To investigate liver damage, and the influence on it of Vitamin D, liver function tests were performed. The effect of high fat -high sugar diet caused the increase of hepatic damage markers (raised liver enzymes), and this was normalised by supplementary dietary Vitamin D containing diet in LDLR^{-/-} and LDLR^{+/+} mice. In mice, high fat -high sugar diet caused the increase of insulin resistance. This was shown by high insulin level, and low Adiponectin level, and was normalised by supplementary dietary Vitamin D containing diet in LDLR^{-/-} and LDLR^{+/+} mice. The current data highlight the importance of supplementary dietary Vitamin D in an anti-

inflammatory role, and also supplementary dietary Vitamin D may prevent intestinal leakage by decreasing endotoxin level. The result showed that supplementary dietary Vitamin D plays a major role in the decrease of Vcam-1 gene expression. It was shown that in high fat -high sugar diet mice, there were more F4/80 positive cells compared to Vitamin D supplemented group although not significantly different, Arginase-1 in hepatic mice fed the Vitamin D supplemented high fat high sugar diet was significantly higher compared to LDLR^{+/+} mice fed high fat -high sugar diet, and also iNOS mRNA hepatic expression mice fed the Vitamin D supplemented high fat high sugar diet was significantly lower compared to LDLR^{+/+} mice fed high fat -high sugar diet. This finding suggests that Vitamin D plays an important role in the decrease pro inflammatory activity (M1-macrophages), and the increase anti-inflammatory macrophages (M2 Microphages). Vitamin D supplemented group mice diet led to the decrease of mRNA expression of genes involved in cholesterol synthesis, and dysregulation of cholesterol. Vitamin D supplementation also resulted in the decrease of functional complement activation classical, and alternative pathway activation. It also can be concluded that adipocyte protein presence which are involved in fibrosis, steatosis, and inflammation are decreased in adipose tissue of mice given high fat diet supplemented with Vitamin D compared to mice given high fat diet without Vitamin D supplementation.

4.2.3 The effects of Vitamin D3 as a nutraceutical during high fat diets on Five weeks' diets

The main reason for performing the diet study in only five weeks was to investigate whether mice get fatty liver disease by this time. This would deliver a study of refinement, following best practice which could be adopted by others. Mice were given high fat high sugar diet for 5 weeks with, and without Vitamin D (58R3+ Vitamin D). Age matched female LDLR^{-/-}, female LDLR^{+/+}, and male LDLR^{-/-} were analysed.

4.2.4 Effect of Vitamin D on Fatty liver disease in male mice

Eight mice (four male LDLR^{-/-}) were given high fat-high sugar diet (58R3) for 5 weeks, and (four male LDLR^{-/-}) were given Vitamin D supplemented high fat high sugar diet (58R3+Vitamin D).

4.2.4.1 Histopathology of livers from male LDLR^{-/-} mice in relation to Vitamin D

4.2.4.1.1 Electron microscopic analysis

This analysis was qualitative in nature, but individual lipid droplets were measured as part of the documentation of findings. Large lipid droplets were seen in mice fed high fat-high sugar diet (Figure 4.25, A), but in mice given high fat-high sugar diet with Vitamin D no large, only small, droplets were seen (Figure 4.25, B).

Megamitochondria are features of fatty liver disease (Ahishali et al., 2010). Megamitochondria are present mostly in hepatocytes with microvesicular steatosis. The reason for this is still poorly understood, but the enlarged organelles may be the result of injury from lipid peroxidation, or may represent an adaptive change (Takahashi and Fukusato, 2014). Our result showed that mega mitochondria were observed in mice fed high fat-high sugar diet (Figure 4.26, (A), Figure 4.27), while in mice fed high fat high sugar diet with Vitamin D only small mitochondria were observed (Figure 4.26, B). According to Schonthal and colleagues, dilated, blebby, and more prominent distribution of rough

endoplasmic reticulum appeared due to endoplasmic reticulum stress (Schonthal, 2012). These were seen in mice fed high fat high sugar diet group (Figure 4.27). In obese-state, chronic enrichment of mitochondria –contacted endoplasmic membranes leads to mitochondrial dysfunction (Arruda et al., 2014). Mice fed high fat-high sugar appeared deformed nucleus (Figure 4.28, A), and lobular inflammation with sinusoids (Figure 4.28, B).

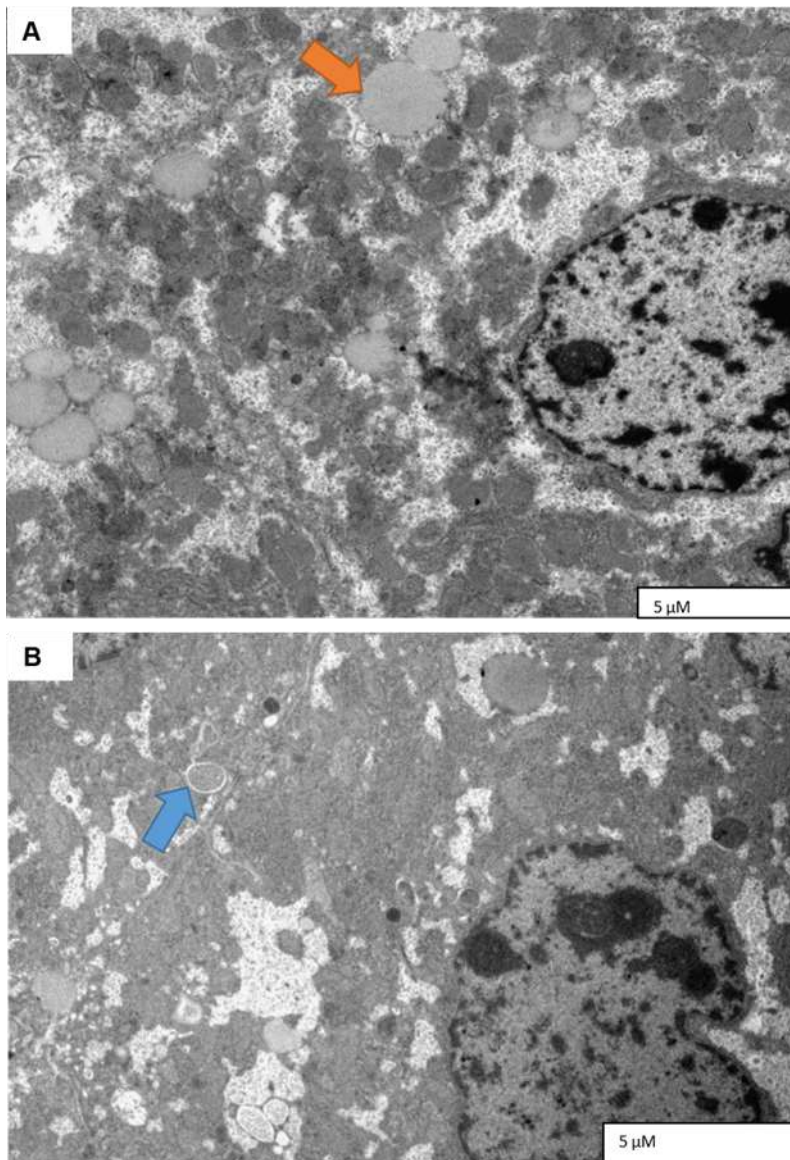


Figure 4-24 Electron micrograph showing lipid droplets from livers of mice fed high fat diet with, and without Vitamin D.

Mice given high fat-high sugar diet without supplemented Vitamin D for five weeks (panel A). In a mouse fed high fat high sugar diet with Vitamin D for 5 weeks (panel B). Large fat droplets (orange arrows), a smaller fat droplet (blue arrow). N=nucleus. X8000. Representative images are shown.

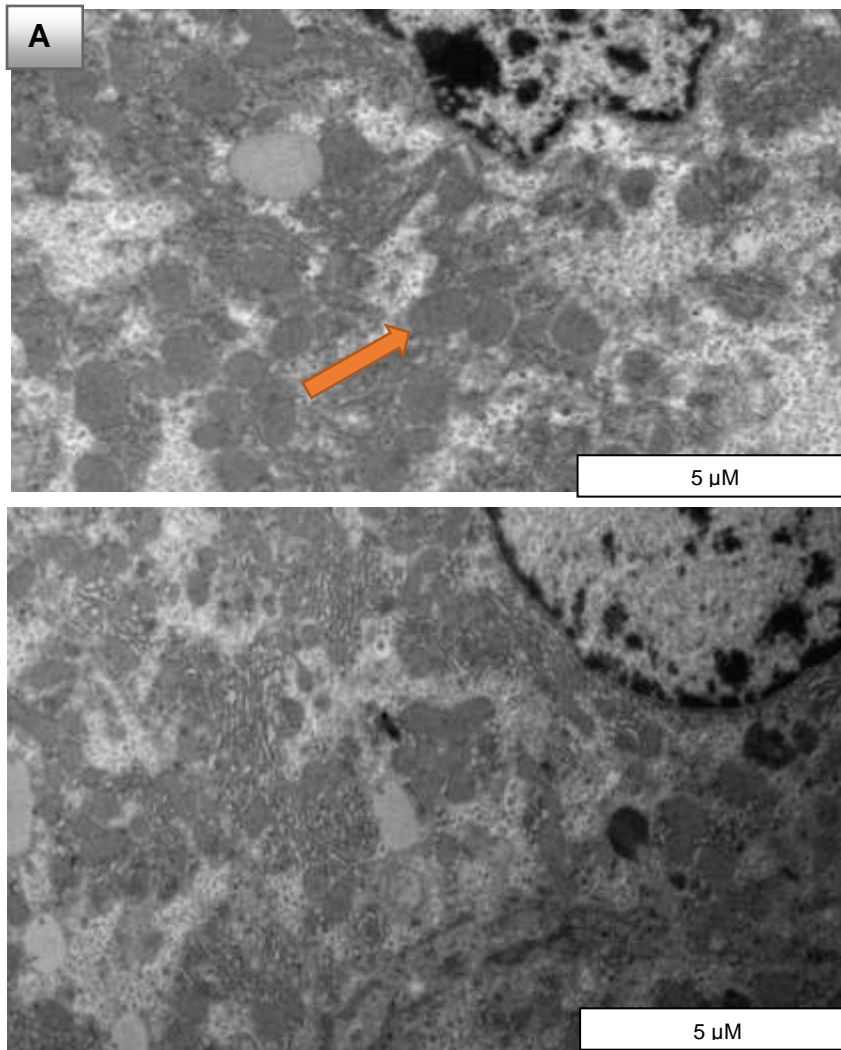


Figure 4-25 Electron micrograph showing mitochondria from livers from mice fed high fat-high sugar diet with, and without Vitamin D.

Mice given high fat –high sugar diet without supplemented Vitamin D for five weeks (panel A). Mice given high fat –high sugar diet supplemented with Vitamin D for five weeks (panel B). Megamitochondrion in the cytoplasm of a hepatocyte (orange arrows), normal mitochondria (black arrow), X8000, Representative images are shown.

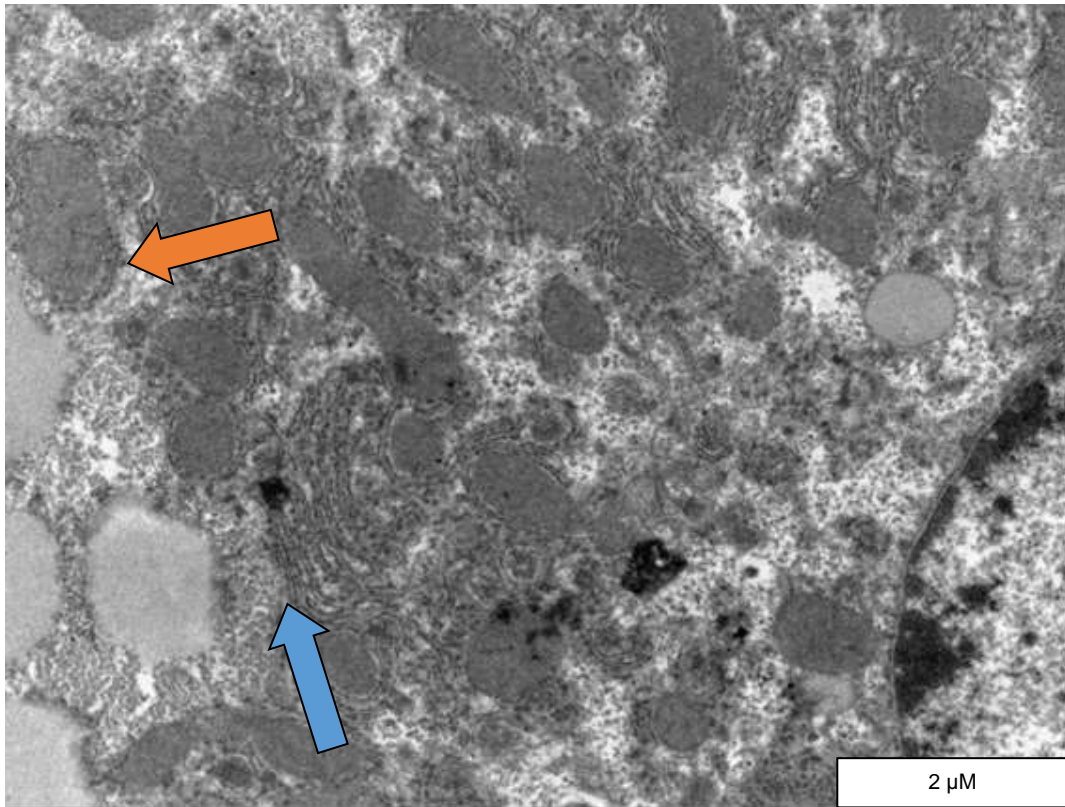


Figure 4-26 Electron micrograph showing mega mitochondria from livers of mice fed high fat -high sugar diet without Vitamin D.
Megamitochondrion (orange arrows), rough endoplasmic reticulum (blue arrow). X8000

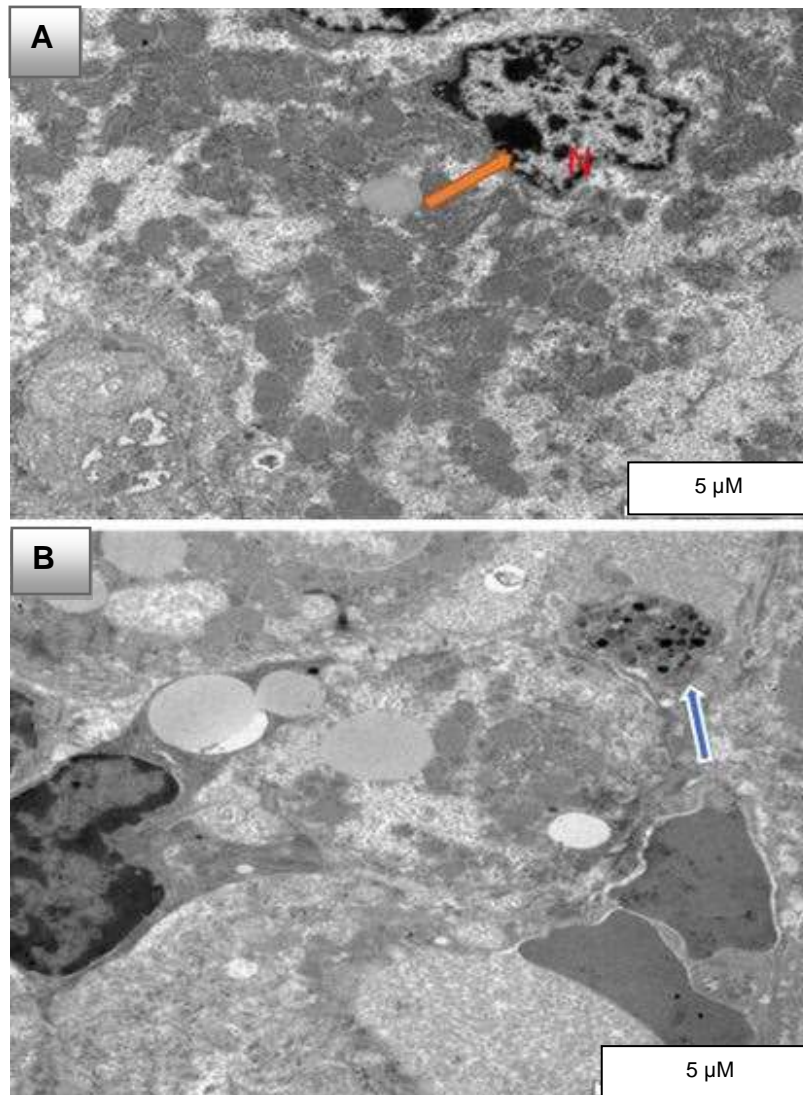


Figure 4-27 Electron micrograph showing nuclei from livers of mice fed high fat-high sugar without Vitamin D.

A deformed nucleus appeared, N=nucleus (A) (orange arrow), lobular inflammation within sinusoid (B) (blue arrow). X8000.

4.2.4.1.2 Haematoxylin eosin staining of livers

Parts of livers from all mice were fixed, paraffin embedded, and 4 μ m slides were prepared, and stained with haematoxylin and eosin. Fatty changes were predominately detected in the absence of Vitamin D. Lipid accumulation was observed near central vein (zone 3) in middle column in high fat –high sugar diet in (LDLR^{-/-}, LDLR^{+/+} 58R3, Figure 4.29, A), but more intensive in LDLR^{-/-} mice. Contrasting with vitamin D group (Figure 4.29, B), there were many microvesicular, and macro-vesicular lipid droplets in mice fed high fat high sugar diet (Figure 4.29, A). It can be said that in high fat-high sugar diet supplemented with vitamin D, there was less evidence of steatosis, and inflammation except some microvesicular fatty changes. Macro-and microvesicular fatty changes refer to the size of the observed space that was occupied by fat prior to paraffin processing. Typically, macrovesicular fat accumulation is the size of a hepatocyte, while microvesicular accumulation appear as small droplets in size. These are accepted descriptive terms in histopathological evaluation of hepatocytes (Schwen et al., 2016).

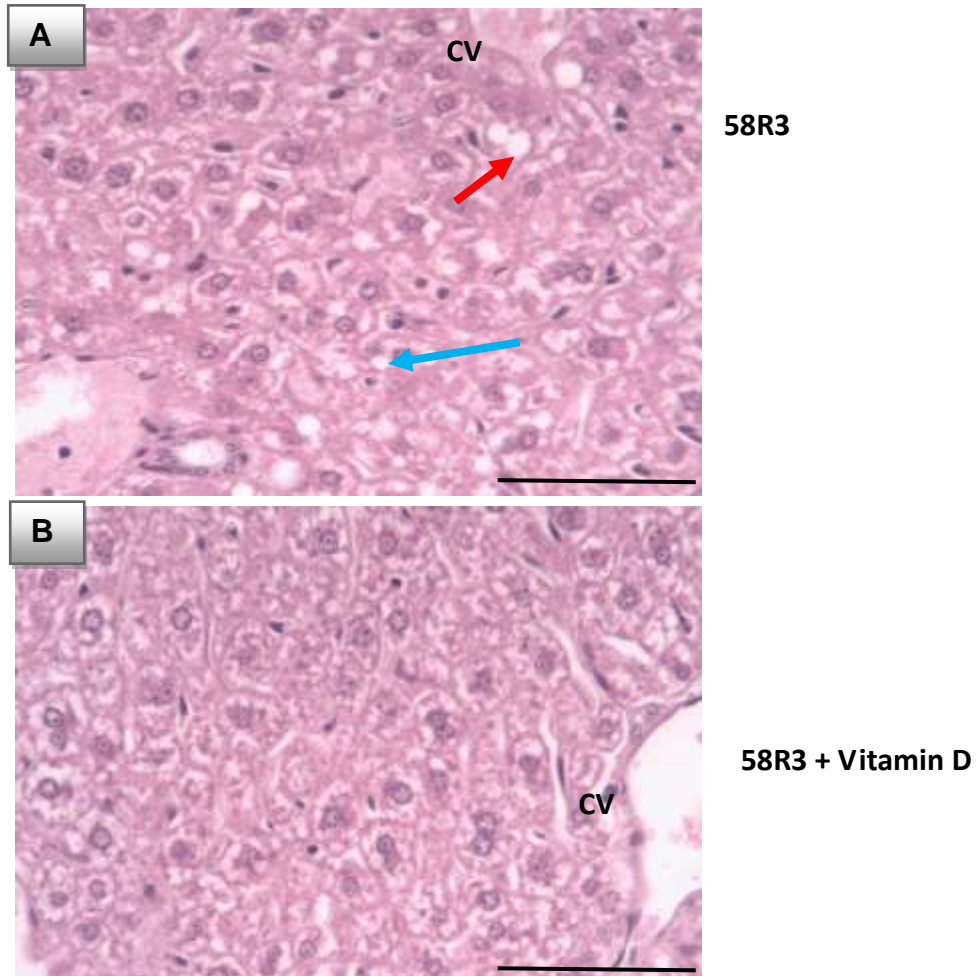


Figure 4-28 Haematoxylin and eosin staining of paraffin embedded liver sections obtained from mice.

Mice given high fat-high sugar diet without supplemented Vitamin D for five weeks (panel A) mice given high fat-high sugar diet without supplemented Vitamin D for five weeks (panel B). Representative images of male mice, microvesicular (blue arrows), macrovesicular (red arrows) (steatosis). CV, central vein 200x. Scale bar represents 100 micron.

The current data from Haematoxylin eosin staining highlight that male, LDLR^{-/-} mice given high fat high sugar diet for five weeks developed steatosis.

4.2.4.2 Body weight, and fat pad weight percentage

In fat pad % body weight (g) which was measured as follow: fat pad mouse weight/body weight mouse *100. There were no significant differences between high fat diet with and without Vitamin D group mice in male and female mice, but the tendency of fat pad weight was lower in male LDLR^{-/-} mice given Vitamin D compared to high fat-high sugar diet (Table 4.3). The low fat diet (control group) had significantly lower percentage body weight gain in female mice compared to high fat high sugar diet (Table 4.4).

4.2.4.3 Effect of Vitamin D on Liver function

The previous ten-week diet study revealed that Vitamin D prevented liver damage based on ALT, and AST levels. To investigate liver damage, and influence of Vitamin D in five weeks diet, liver function tests were performed. This is the first study to be performed over five weeks to establish a model of metabolic syndrome by giving high fat-high sugar diet, and to investigate the prevention of liver damage by Vitamin D supplemented diet. Male mice LDLR^{-/-} given high fat-high sugar for five weeks showed an increase of liver transaminases compared to mice given high fat-high sugar diet supplemented with Vitamin D for five weeks. Therefore, the effect of high fat-high sugar diet caused the increase of hepatic damage markers, and this was normalised by supplementary Vitamin D containing diet for five weeks in male LDLR^{-/-} mice (Table 4.3).

4.2.4.4 Effect of Vitamin D on endotoxin level, and inflammation

Lower level of endotoxin and Il-6 were detected in male LDLR^{-/-} and female LDLR^{-/-}, LDLR^{+/+} mice given high fat-high sugar diet supplemented with Vitamin D compared to mice given high fat-high sugar diet. The current data highlight the importance of supplementary dietary Vitamin D in an anti-inflammatory role, and supplementary dietary Vitamin D prevents endotoxin formation in five weeks (Table 4.3). Vitamin D might prevent intestinal leakage in five weeks mice given high fat-high sugar diet.

4.2.4.5 Effect of Vitamin D on Metabolic syndrome

At ten weeks, mice given high fat-high sugar diet developed metabolic syndrome, based on increased weight, elevated insulin levels, deranged liver transaminases and hypertriglyceridemia. High fat–high sugar diet supplemented with Vitamin D was significantly less of a strain on overall metabolism.

Five weeks' duration was chosen based on the refinement idea to make a model in five weeks instead of ten weeks. Thereby, reaching the same scientific conclusion in less time, mice were on a regulated procedure for a shorter period, and thereby suffered less. In five weeks, mice fed high fat-high sugar diet developed the increase of insulin resistance. This is demonstrated by high insulin level, high glycated haemoglobin, and low Adiponectin level, and was normalised by supplementary dietary Vitamin D containing diet in male LDLR^{-/-} mice (Table 4.3). Mice given high fat-high sugar had features of developing metabolic syndrome (NEFA, TG, and lipid peroxidation) compared to mice given Vitamin D as early as five weeks (Table 4.3).

Our results showed that five weeks high fat-high sugar diet also developed central obesity, fatty liver, and metabolic syndrome disease in male mice. Consistent with the ten-week-study, high fat diet supplemented with Vitamin D caused the prevention of fatty liver disease, and metabolic syndrome. It can be concluded that supplementary dietary consumption of Vitamin D for only five weeks plays a significant role in the prevention of steatosis inflammation, insulin resistance, and metabolic syndrome disease in male LDLR^{-/-} mice.

Table 4.3 Male mice given high fat-high sugar diet with and without supplemented Vitamin D (58R3± Vitamin D) for five weeks.

Measurements	M LDLR ^{-/-} , 58R3, n=4	M LDLR ^{-/-} , 58R3+VD, n=4
Percentage of body weight gain	19.34 +/- 10.24 (control was 9.70 +/- 3.52, n=3)	24.92 +/- 14.05
Percentage of fat pad weight	3.215 +/- 0.69 (control was 1.92 +/- 0.85, n=3)	2.698 +/- 0.93
AST Mean +/- SD	124.3 +/- 13.07 (control was 78.27 +/- 6.99, n=2)	94.47 +/- 5.52**
ALT (IU/L) Mean +/- SD	68.54 +/- 5.11 (control was 45.77 +/- 9.65, n=2)	54.12 +/- 3.78 n.s
Insulin (ng/ml) Mean +/- SD	1.95 +/- 0.51 (control was 0.59 +/- 0.04, n=2)	0.75 +/- 0.32*
Adiponectin (µg/l) Mean +/- SD	2.09 +/- 0.11 (control was 2.69 +/- 0.10, n=2)	3.00 +/- 0.07****
HbA1c (fm/l) Mean +/- SD	61.19 +/- 8.85 (control was 6.97 +/- 2.32, n=2)	31.3 +/- 6.06**
Triglyceride (mg/dl) Mean +/- SD	65.85 +/- 11.64 (control was 39.42 +/- 7.27, n=2)	45.66 +/- 2.75*
NEFA (mmol/l) Mean +/- SD	0.59 +/- 0.01 (control was 0.33 +/- 0.03, n=2)	0.39 +/- 0.04****
Endotoxin (IU/ml) Mean +/- SD	5.57 +/- 0.58 (control was 2.105 +/- 0.92, n=2)	3.54 +/- 0.32 n.s
IL-6 (ng/ml) Mean +/- SD	13.68 +/- 3.05 (control was 6.80 ± 0.07, n=2)	8.86 +/- 1.12 n.s
MDA (µmol/l) Mean +/- SD	0.30 +/- 0.01 (control was 0.18 +/- 0.00, n=2)	0.20 +/- 0.01***

Male LDLR^{-/-} fed high fat high sugar diet with Vitamin D (58R3 +VD) and without Vitamin D (58R3), low fat diet (58R1) on measurements. Results are presented as averages ±SD from triplicate determinations (**** p<0.0001, *** p<0.0005, **p<0.005, *p<0.05), (adjusted p-values), n.s=no significant. Comparisons were between: 58R3+VD vs 58R3, vs=versus, n.s=no significant.

For further investigation, female mice were used. Seventeen mice were LDLR^{+/+}, LDLR^{-/-} with, and without supplement Vitamin D for five weeks (Table, 4.4). The result showed that female given high fat high sugar diet for 5 weeks developed fatty liver disease, and metabolic syndrome. This was prevented by diet supplemented Vitamin D. Inflammation marker (IL-6), prediabetic (insulin) and metabolic syndrome such as NEFA were increased in mice given high fat-high sugar diet, and were higher compared to mice given high fat-high sugar supplemented with Vitamin D. LDLR^{-/-} background had higher IL-6, insulin compared LDLR^{+/+} background mice (Table 4.4).

Table 4.4 Female mice given high fat-high sugar diet with and without supplemented Vitamin D (58R3± Vitamin D) for five weeks.

Genotypes	IL-6 (ng/ml) +/- SD	Insulin (ng/ml) +/- SD	NEFA (mmol/l) +/- SD	Percentage of body weight gain
LDLR^{+/+} 58R3	1.86 +/- 0.10 (n=7)	1.94 +/- 0.27 (n=7)	0.28 +/- 0.06 (n=4)	20.37 +/- 0.90, (n=4)
LDLR^{+/+} 58R3+VD	0.79 +/- 0.11**** (n=10)	1.21 +/- 0.33*** (n=10)	0.08 +/- 0.02 (n=5)****	19.96 +/- 9.38, (n=5) n.s.
LDLR^{-/-} 58R3	2.3 +/- 0.21 (n=4)	2.19 +/- 0.06 (n=4)	0.24 +/- 0.03 (n=4)	10.45 +/- 3.60 (n=2)
LDLR^{-/-} 58R3+VD	0.75 +/- 0.09**** (n=5)	0.99 +/- 0.41** (n=4)	0.15 +/- 0.01* (n=4)	11.37 +/- 1.88 (n=2) ^{n.s}

LDLR^{-/-}, LDLR^{+/+} female mice fed high fat high sugar diet with Vitamin D (58R3 +VD) and without Vitamin D (58R3), low fat diet (58R1) on measurements. The data are represented as means ± SD (Unpaired t test **** p<0.0001, *** p<0.0005, **p<0.005, *p<0.05). Comparisons were between: 58R3+VD vs 58R3, vs=versus, n.s=no significant.

To summarise, mice given high fat-high sugar diet for five weeks developed fatty liver disease, increased insulin level, and NEFA level, while in Vitamin D supplemented diet groups lower levels were detected in female LDLR^{-/-} and LDLR^{+/+} mice. All measurements were higher in mice after ten weeks given high fat-high sugar diet compared to five weeks' given high fat-high sugar diet. The tendency to express inflammation in the development of metabolic syndrome disease was higher in male compared to female LDLR^{-/-} at five weeks' given high fat high sugar, based on NEFA, and IL-6 levels.

4.3 Discussion

LDLR^{-/-} and LDLR^{+/+} mice were in parallel fed a high fat -high sugar diet for five and ten weeks to develop steatosis and body weight gain, and additionally, in both LDLR^{-/-} and LDLR^{+/+} mice fed high fat high sugar diet the effect of additional Vitamin D was analysed. The main reason for performing the diet study in only five weeks was to investigate whether mice get fatty liver disease by this time. This would deliver a study of refinement, following best practice, which could be adopted by others.

Body weight and food intake were measured once per week. Interestingly, high fat -high sugar diet mice had significantly greater body weight, fat pad weight, IL-6 and insulin level compared to mice fed high fat high sugar diet supplemented with Vitamin D 10 weeks and five weeks. Our results coincide with Lira and colleagues who showed that circulating IL-6 concentrations are highly correlated with percentage of body fat and insulin resistance (Lira et al., 2011). There is a relationship between hepatocyte ballooning, high serum cholesterol, and insulin resistance (Yeh and Brunt, 2007). This means there is a possibility to have steatosis in the case of having hepatocytes ballooning. There are many features related to NASH, such as steatosis, ballooning degeneration, lobular inflammation, and giant mitochondria (Yeh and Brunt, 2007). Liver histology showed that high fat-high sugar diet mice group developed steatosis, and inflammation in LDLR^{-/-} and LDLR^{+/+} mice given high fat high sugar diet for ten weeks and five weeks. Steatosis was seen in all mice, but greater steatosis (more macrovesicles) were seen in high fat diet-high sugar diet mice, while in the supplementary dietary Vitamin D group less steatosis (microvesicles) and inflammation was detected. Electron microscope result showed that megamitochondria were observed in liver of mice fed high fat-high sugar diet for five weeks, while in mice fed high fat high sugar diet with Vitamin D supplementation only small mitochondria were observed. The reason for this is still poorly understood, but the enlarged organelles may be the result of injury from lipid peroxidation, or may represent an adaptive change (Takahashi and Fukusato, 2014). Megamitochondria, larger than usual mitochondria, are features of fatty liver disease (Ahishali et al., 2010).

In addition, hepatic Strepb-1c, which is regulated by insulin, is increased in high fat-high sugar diet mice compared to the supplementary diet with Vitamin D. The result is supported support by Yin and colleagues who showed Vitamin D inhibits lipogenesis (Yin et al., 2012). In an *in vitro* experiment, Vitamin D was used to investigate the role as anti-steatotic molecule. Our results showed that Vitamin D plays a significant role at lowering Oil Red O staining. This is supported by a previous study which documented that macrophages derived from peritoneal cavity of obese mice (elicited by intraperitoneal injection of 4% thioglycollate) developed into foam cells, while in the presence Vitamin D less foam cells were found. This is because oxLDL-induced cholesteryl ester formation was reduced by Vitamin D (1, 25(OH)₂D₃) (Oh et al., 2009). This is the first study to investigate the effect of high fat-high sugar diet on the increase of hepatic damage markers in mice given high fat-high sugar diet for ten and five weeks, and this was normalised by supplementary dietary Vitamin D containing diet in LDLR^{-/-} and LDLR^{+/+} mice. This may be how Vitamin D prevents liver damage. In general high fat-high sugar diet for ten weeks and five weeks caused the increase of insulin resistance, this was associated with high insulin level, and low adiponectin level, and was normalised by supplementary dietary Vitamin D containing diet in LDLR^{-/-} and LDLR^{+/+} mice. This is consistent with findings by Forouhi and colleagues who showed that low serum Vitamin D may associate with glycaemia and insulin resistance in non- diabetic subjects (Forouhi et al., 2008). To investigate the effect of Vitamin D on aortic endothelium, and to see the relationship of adhesion molecule expression to initiation factors, and the sites of lesion formation, VCAM-1 (vascular cell adhesion molecule-1) gene expression was performed for aorta of mice fed the Vitamin D supplemented high fat high sugar diet for ten weeks. The result showed that supplementary dietary Vitamin D may plays a role in the decrease of VCAM-1 gene expression. The findings of this experiment could be used to suggest that Vitamin D prevents atherosclerosis. Hepatic mRNA expression of iNOS in high fat -high sugar diet was significantly higher compared to Vitamin D supplemented high fat high sugar diet for ten weeks, and hepatic Arginase-1 mRNA in Vitamin D supplemented high fat high sugar diet was significantly higher compared to LDLR^{+/+} mice fed high fat-high sugar diet for ten weeks without supplementary Vitamin D. Prussian blue staining shows that Vitamin D

plays an important role in the decrease of M1 activity, and the increase of M2 activity, as measured by intracellular iron content. Vitamin D plays an anti-inflammatory role (Ogura et al., 2009), that coincides with our results, which showed Vitamin D led to the decrease of inflammatory mediators such as TNF- α , and IL-6. Hepatic mRNA expression of both SR-B1, and HMGCR increased in high fat diet (Qiu et al., 2013, Thacker et al., 2015), compared to Vitamin D supplemented diet group in LDLR^{-/-} mice, although in LDLR^{+/+} mice the increase was not significantly different. These results concluded that high fat-high sugar diet for ten weeks caused the increase of genes involved in cholesterol synthesis, and dysregulation of cholesterol, and it was prevented by supplementation with Vitamin D. Our results showed significantly less triglyceride and NEFA level in mice sera fed high fat diet supplemented with Vitamin D for ten weeks and five weeks studies. There are association between elevation of NEFA, obesity, dyslipidaemia, and insulin resistance state. It is thought that insulin inhibit FFA mobilisation process from adipose tissue. Therefore, lipolysis in adipose tissue is increased in the insulin resistance situation (Karpe et al., 2011).

Based on the proteome array, it can be said that proteins involved in fibrosis, steatosis and inflammation are increased in adipose tissue of mice given high fat diet for ten weeks. There was a marked decrease of these proteins in adipose tissue of mice given high fat diet plus Vitamin D. In obese, and diabetes conditions, Vitamin D level decreased compared to lean, and non-diabetic humans (Zoppini et al., 2013, Park et al., 2015). This coincides with our results, that showed high fat high sugar diet without supplementary Vitamin D had lower Vitamin D levels compared to mice supplemented with Vitamin D in their high fat-high sugar diet. Oxidized LDL caused classical complement activation in human serum (Saad et al., 2006). Our result showed that the Vitamin D supplemented diet group had increased residual activity of the classical pathway (less classical pathway activation in vivo) compared with mice given high fat-high sugar diet for ten weeks. This is likely to be due to Vitamin D leading to a decrease of oxLDL (Oh et al., 2009). Our result showed less alternative pathway residual activity (higher alternative pathway activation in vivo) in mice fed high fat-high sugar diet for ten weeks. Chylomicron accelerates C3 tick-over by regulating the role of factor H, leading to the

overproduction of ASP; as a result it leads to the increase of alternative pathway residual activity (Fujita et al., 2007). In keeping with this, mice fed Vitamin D supplemented high fat high sugar diet had higher alternative pathway residual activity (lower alternative pathway activation in vivo) compared to mice high fat high sugar diet mice group. One limitation of this part of the study might appear to be the small numbers. However, it has to be borne in mind that these mice had to be bred in house. It was essential in the design of the study to probe mice from the same litters for their reaction to the diet and treatments. It was found that the body weight gain was unequal between litters, so littermates were analysed in this study to ensure a similar reaction of diet induced metabolic reaction. All mice were kept in the same barrier unit and exposed to the same handling and procedures. The Vitamin D dose tested which was tenfold higher than normal was found to be nontoxic from the current literature. It would be interesting to study a concentration-dependent effect of Vitamin D, and also, determine whether which dose is effective in studies in animals treated for longer than ten weeks. This is of particular interest as significant NASH develops later in the disease process.

Chapter 5 The role of properdin in fatty liver disease

5.1 Introduction

The study investigating side by side properdin deficient, and wildtype mice concluded that Properdin limited the diet induced increase of body weight, fat pad weight, and the increase of NEFA. In murine 3T3-L1 adipocytes, addition of properdin inhibited the insulin-mediated stimulation of fatty acid uptake, and incorporation into triglyceride, but this experiment lacked a control (Gauvreau et al., 2012). In NASH patient's liver (n=12), neutrophilic marker peroxidase was performed to detect neutrophils around steatotic hepatocytes, and also extracellular properdin by immunofluorescent staining. While in healthy liver not or less amount of properdin was seen. Immunofluorescent staining for MPO (Myeloperoxidase), which is expressed in neutrophils, and also double positives (MPO/properdin) were documented in NASH patients compared to healthy livers (n=10). In NASH patients, there was colocalization of properdin, and C3c in steatotic hepatocytes (Segers et al., 2014).

According to Rensen and colleagues, NAFLD patient's liver (n=43) compared to healthy liver (control) (n=10), immunohistochemistry was performed to detect neo-epitopes on C3c, and iC3 (cleavage fragments of C3) as a result deposition of act-C3 was seen around hepatic steatosis in 74% patients of the most obese patients; whereas, deposition of act-C3 deposition was not detected in liver control. Plasma levels of NAFLD patients also had higher act-C3 compared to control. Complement activation was detected in relation to apoptosis; TUNEL assay detection was performed to detect apoptosis. As a result, apoptosis was highly seen in act-C3 deposition patients (Rensen et al., 2009a). Insulin, and lipid are increased in obesity. Adipocytes led to the production of C3, factor B, properdin, and factor D. As a result, it leads to local alternative pathway turnover, and generation of C3a. C3a is transformed by a carboxypeptidase to C3a^{desArg} which is called acetylation stimulating protein (ASP). Lipid clearance, glucose uptake, and triglyceride (TG) are performed by ASP through C5L2 receptor (Ricklin et al., 2010). Therefore the aim of this chapter was to investigate the role of properdin in diet induced obesity, and liver disease by

comparing properdin deficient, and wild type mice on a LDLR^{-/-} / LDLR^{+/+} background.

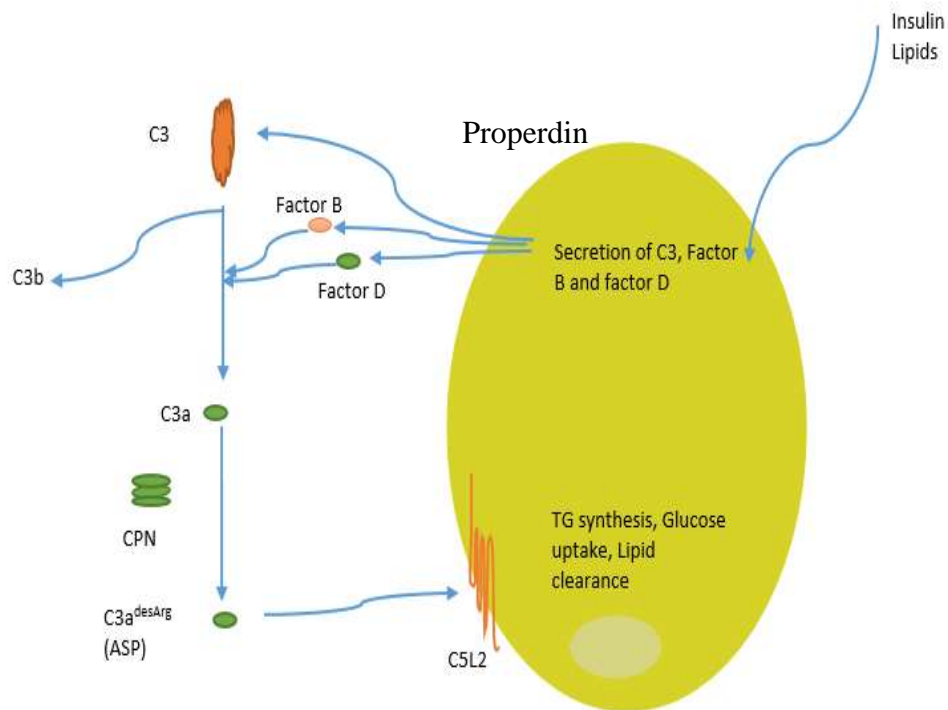


Figure 5-1 Roles of complement in lipid metabolism. Properdin leads to the increase of C5L2 expression, as a result, it leads to triglyceride, lipid clearance and glucose uptake increase.

Our hypothesized that properdin plays a vital role in the development of metabolic syndrome diseases such as fatty liver disease and diabetes caused by high fat–high sugar diet given to mice for 10 weeks or five weeks.

5.2 Results

Two durations were studied, ten and five weeks

5.2.1 Effect of properdin on fatty liver disease in 10 weeks given diet

Fifteen female mice (3 LDLR^{-/-} PWT ,and 3 LDLR^{-/-} PKO, 4 LDLR^{+/+} PWT, and 5 LDLR^{-/-} PKO), twelve male mice (2 male LDLR^{-/-} PWT, and 2 LDLR^{-/-} PKO, 4 LDLR^{+/+} PWT, and 4 LDLR^{-/-} PWT) were given high fat-high sugar diet (58R3) for 10 weeks, and nine female mice (4 LDLR^{+/+} PWT, 5 LDLR^{+/+} PKO), fourteen mice male mice (3 LDLR^{+/+} PWT, 3 LDLR^{+/+} PKO), (4 LDLR^{-/-} PWT, 4 LDLR^{-/-} PKO) were given Western diet (high fat diet) (5TJN) for ten weeks. In parallel, maintenance diet low in fat (LFD) (5LF2) was given to mice in both LDLR^{+/+}PWT/PKO and LDLR^{-/-}PWT/PKO groups. The aim of using high fat-high sugar diet, and Western diet was to initiate steatosis (NAFLD) and inflammation in LDLR^{-/-}, LDLR^{+/+} background, in order to investigate the role of properdin in NAFLD.

5.2.1.1 Body weight and fat pad weight measurement

The main purpose for weight measurement was to compare properdin deficient to properdin wild type mice in LDLR^{-/-} and LDLR^{+/+} background, in mice high fat-high sugar diet, Western diet or low fat diet. All mice were age (16 weeks at the start of diet) and sex matched, the results were as follows:

Body weight was measured once per week (10 weeks) for mice fed high fat-high sugar diet, Western diet or low fat diet. The percentage of body weight was significantly higher in properdin wild type mice fed Western diet compared to properdin deficient mice but there were not significant differences in fat pad weight (Tables 5.1, and 5.2). However, Female LDLR^{+/+} PWT mice fed high fat-high sugar diet significantly had less body weight gain (Figure 5.2, A) and less percentage of body weight in mice fed Western diet (Table 5.2) compared to LDLR^{+/+} PKO mice. Furthermore, in male LDLR^{+/+} PWT mice fed Western diet had significantly less body weight, and fat pad weight compared to male

LDLR^{+/+} PKO (Table 5.3). There was a variation between body weight percentage in female LDLR^{-/-} mice. Therefore, there was not significant different between properdin wild type, and properdin deficient in mice fed high sugar-high fat diet (Figure 5.2, B).

Taken together, these results shows that properdin deficient mice on LDLR^{+/+} background had greater body weight gain, and central obesity. This is consistent with the study by (Gauvreau et al., 2012) where body weight, fat pad weight were analysed in a model of obesity. This effect is lost in properdin deficient mice on LDLR^{-/-} background.

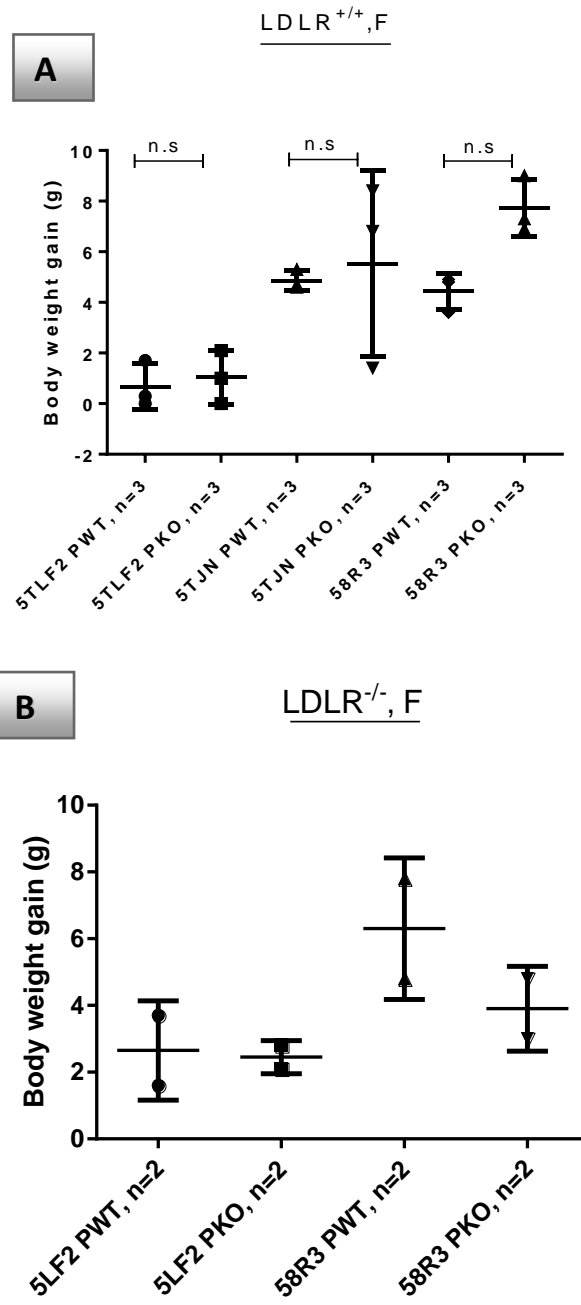


Figure 5-2 The effect of properdin on body weight gain in female mice.

Mice fed low fat diet (5LF2), Western diet (5TJN), and high fat-high sugar diet (58R3) for 10 weeks. LDLR^{+/+} properdin wild type and deficient mice (LDLR^{+/+}PWT/PKO) (panel A), LDLR^{-/-} properdin wild type and deficient mice (LDLR^{-/-}PWT/PKO) (panel B). Results are presented as averages ±SD from triplicate determinations. (adjusted *p*-values), ns=no significant.

Table 5.1 The effect of properdin on body weight, fat pad (weight gain and the percentage) in female and male mice.

Diet/	sex	Body weight gain %, (LDLR ^{+/+} PWT)	Fat pad weight (g) (LDLR ^{+/+} PWT)	Body weight gain %, mean (LDLR ^{+/+} PKO)	Fat pad weight (g) (LDLR ^{+/+} PKO)
5TJN	f	20.4 +/- 5.6 (n=5)*	n.d.	23.6 +/- 12.6 (n=5)	n.d.
5LF2	f	3.3 +/-0.7 (n=3)	n.d.	5.4 +/- 0.8 (n=3)	n.d.
5TJN	m	46.3 +/- 8.1 (n=3)*	2.15 +/- 0.4 (n=3)	34.5 +/- 24.8 (n=3)	2 +/- 1 (n=3)

Mice fed low fat diet (5LF2), Western diet (5TJN), and high fat-high sugar diet (58R3) for 10 weeks. LDLR^{+/+} properdin wild type (LDLR^{+/+}PWT) and deficient mice (LDLR^{+/+}PKO). The data are represented as means ± SD (Unpaired t test *p<0.05), f=female, m=male, n.d=not done.

Table 5.2 The effect of properdin on body weight, fat pad (weight gain and the percentage) in female and male mice.

Diet	sex	Body weight gain %, mean (LDLR ^{-/-} PWT)	Fat pad weight (g) (LDLR ^{-/-} PWT)	Body weight gain %, (LDLR ^{-/-} PKO)	Fat pad weight (g) (LDLR ^{-/-} PKO)
5TJN	f	28.6 +/- 7.3 (n=5)	n.d.	35.6 +/- 8.6 (n=4)	n.d.
5LF2	f	12.3 +/- 7.4 (n=2)	n.d.	12.7± 0.1 (n=2)	n.d.
5TJN	m	55.9 +/- 32.9 (n=8)*	1.8 +/- 1 (n=8)	47.6 +/- 13.7 (n=8)	1.2 +/- 0.7 (n=8)
5LF2	m	15.3 +/- 12.5 (n=3)	0.52±0.36 (n=2)	20 +/- 23.5 (n=2)	0.36±0.09 (n=2)

Mice fed low fat diet (5LF2), Western diet (5TJN) for 10 weeks. LDLR^{-/-} properdin wild type (LDLR^{-/-}PWT) and deficient mice (LDLR^{-/-}PKO). The data are represented as means ± SD (Unpaired t test *p<0.05), f=female, m=male, n.d=not done.

Table 5.3 The effect of properdin on percentage body weight and fat pad weight (g) in female and male mice.

Diet	sex	Body weight gain %, (LDLR ^{+/+} PWT)	Fat pad weight (g) (LDLR ^{+/+} PWT)	Body weight gain %, (LDLR ^{+/+} PKO)	Fat pad weight (g) (LDLR ^{+/+} PKO)
58R3	M	36.08 +/- 11.26 (n=4)*	1.42 +/- 0.18 (n=4)*	40.85 +/- 7.36 (n=4)	1.92 +/- 0.25 (n=4)
58R3	F	19.33 +/- 7.56 (n=4)	n.d	15.60 +/- 2.68 (n=2)	n.d
5LF2	F	18.20 (n=4)	n.d	10.03 +/- 6.50 (n=4)	n.d

Mice fed low fat diet (5LF2), Western diet (5TJN) for 10 weeks. LDLR^{+/+} properdin wild type (LDLR^{+/+}PWT) and deficient mice (LDLR^{+/+}PKO). The data are represented as means ± SD (Unpaired t test *p<0.05), f=female, m=male, n.d=not done.

5.2.1.2 Liver weight (g), and end liver % body weight (in female LDLR^{-/-}, LDLR^{+/+} mice)

To investigate whether mice developed hepatomegaly, livers were weighed, weights recorded, and expressed as % body weight. There was a wide variation in liver weight. The percentage of liver weight was lower in female LDLR^{+/+} properdin deficient mice compared to properdin wild type mice (Figure 5.3, A). Liver weight analysis revealed that high fat-high sugar diet led to the increase of liver weight, but was not significantly different between properdin deficient mice, and wild type male mice (Figure 5.4, A, B). High fat diet-high sugar and a high fat diet developed hepatomegaly in this model.

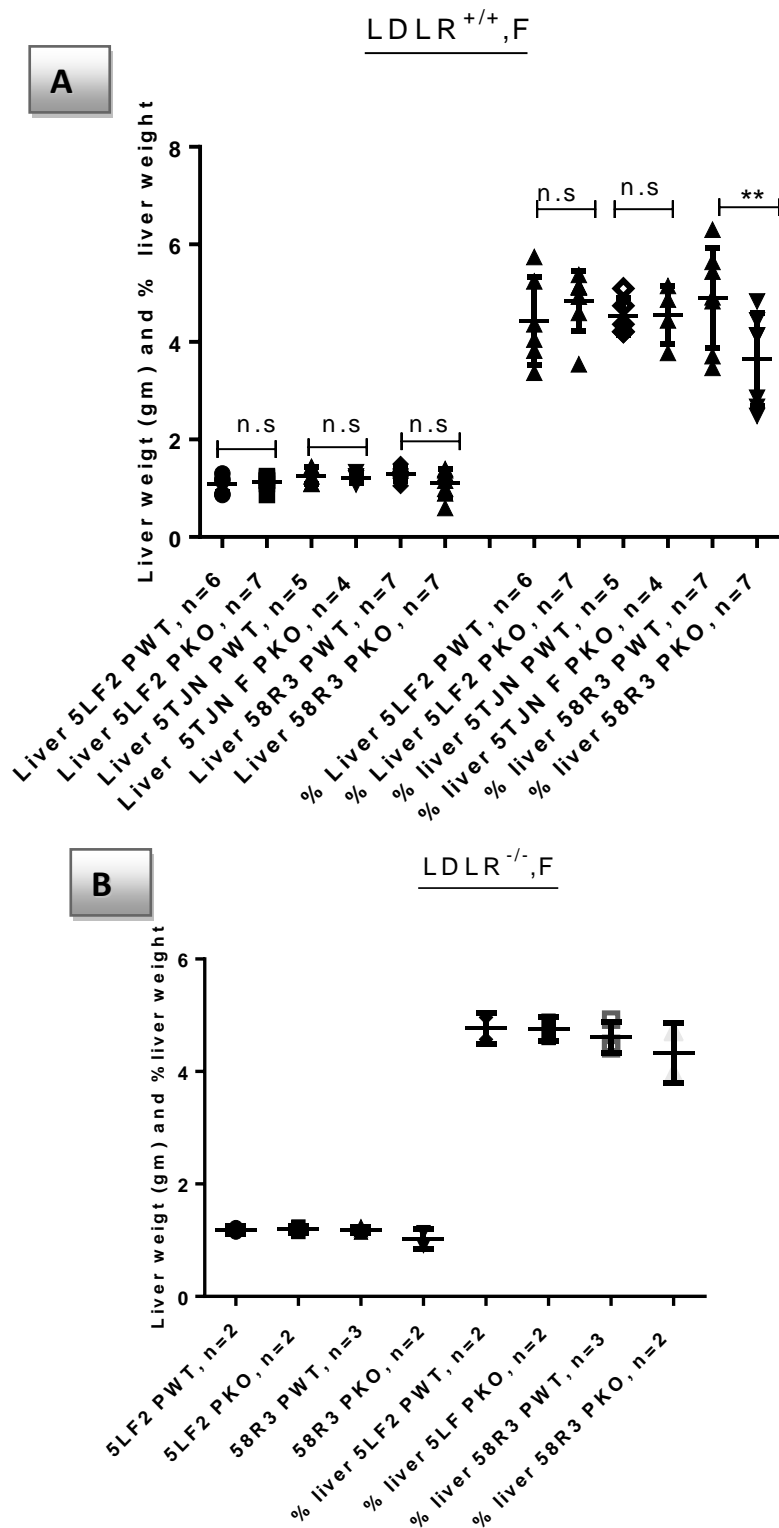


Figure 5-3 The effect of properdin on liver weight and the percentage of liver weight in female mice.

Mice fed low fat diet (5LF2), Western diet (5TJN), and high fat-high sugar diet (58R3) for 10 weeks. LDLR^{+/+} properdin wild type and deficient mice (LDLR^{+/+}PWT/PKO) (panel A), LDLR^{-/-} properdin wild type and deficient mice (LDLR^{-/-}PWT/PKO) (panel B). Results are presented as averages \pm SD from triplicate determinations. ** $p < 0.01$ (adjusted p -values), ns=no significant.

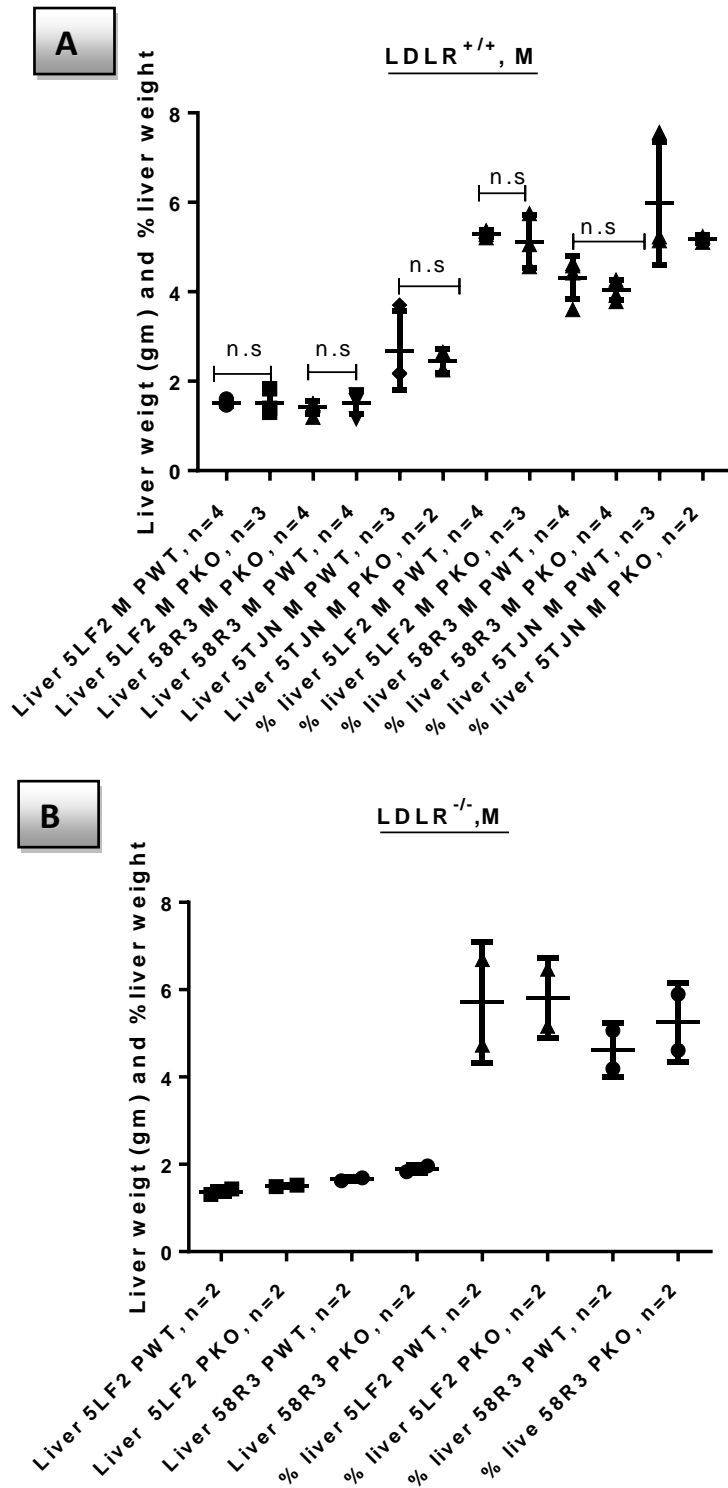


Figure 5-4 The effect of properdin on liver weight and the percentage of liver weight in female mice.

Mice fed low fat diet (5LF2), Western diet (5TJN), and high fat-high sugar diet (58R3) for 10 weeks. LDLR^{+/+} properdin wild type and deficient mice (LDLR^{+/+}PWT/PKO) (Panel A), LDLR^{-/-} properdin wild type and deficient mice (LDLR^{-/-}PWT/PKO) (Panel B). Results are presented as averages \pm SD from triplicate determinations (adjusted *p*-values), ns=no significant.

5.2.1.3 Histopathology of liver high in fat-high sugar diet LDLR^{-/-} PWT/PKO mice, and high fat-high sugar diet, Western diet LDLR^{+/+}PWT/PKO mice

The main purpose was to investigate the properdin role in the development of fatty liver changes. LDLR^{-/-} PWT/PKO mice fed high fat-high sugar diet (58R3), and LDLR^{+/+}PWT/PKO fed high fat-high sugar diet, and Western diet (5TJN). Sections were prepared from liver, stained with haematoxylin/eosin, and analysed microscopically. LDLR^{-/-}PWT mice fed high fat-high sugar diet had less steatosis compared to LDLR^{-/-}PKO mice fed high fat-high sugar diet. In addition, LDLR^{-/-}PWT mice fed high fat-high sugar, and Western diet had lower steatosis, and inflammation compared to LDLR^{-/-}PKO mice. The presence of marked fatty changes were seen near central vein (zone 3) in high fat-high sugar diet, and Western diet; However, in mice fed low fat diet (maintenance diet) (5LF2) there was little evidence of steatosis and inflammation.

5.2.1.3.1 Haematoxylin, and eosin staining

Parts of livers of 16 weeks' female and male LDLR^{-/-} PWT/PKO mice, LDLR^{+/+}PWT/PKO mice were fixed, paraffin embedded, and 4µm slides were prepared, and stained with haematoxylin, and eosin. Fifteen mice (3 LDLR^{-/-} PWT, and 3 LDLR^{-/-} PKO, 4 LDLR^{+/+} PWT, and 5 LDLR^{-/-} PKO) and eight male mice (4 LDLR^{+/+} PWT, and 4 LDLR^{+/+}PKO) were given high fat-high sugar diet for 10 weeks, and nine female mice (4 LDLR^{+/+} PWT, 5 LDLR^{+/+} PKO), and 6 male mice (3 LDLR^{+/+} PWT, 3 LDLR^{+/+} PKO) were given Western diet. Results were documented, and compared between properdin wild type, and deficient mice. Lipid accumulation was observed near CV (zone 3) in middle column in LDLR^{-/-}PWT mice fed high fat-high sugar diet (Figures 5.5, 5.6, 5.7, 5.8 Panels C), but was more intensive in LDLR^{-/-}PKO mice fed high fat-high sugar diet (Figures 5.5, 5.6, 5.7, 5.8 Panels D). Contrasting with normal liver (Figures 5.5, 5.6, 5.7, 5.8 Panels A, and B), there were many microvesicular, and macro-vesicular lipid droplets in livers of mice fed high fat-high sugar diet, and Western diet in both backgrounds. Many inflammatory changes were detected; they included neutrophilic infiltration or mononuclear cells around the portal vein, called portal inflammation, or appearing between cells where they are called

lobular inflammation (Figure 5.5, D). In livers from mice fed a low fat diet there were minor microvesicular fatty changes only.

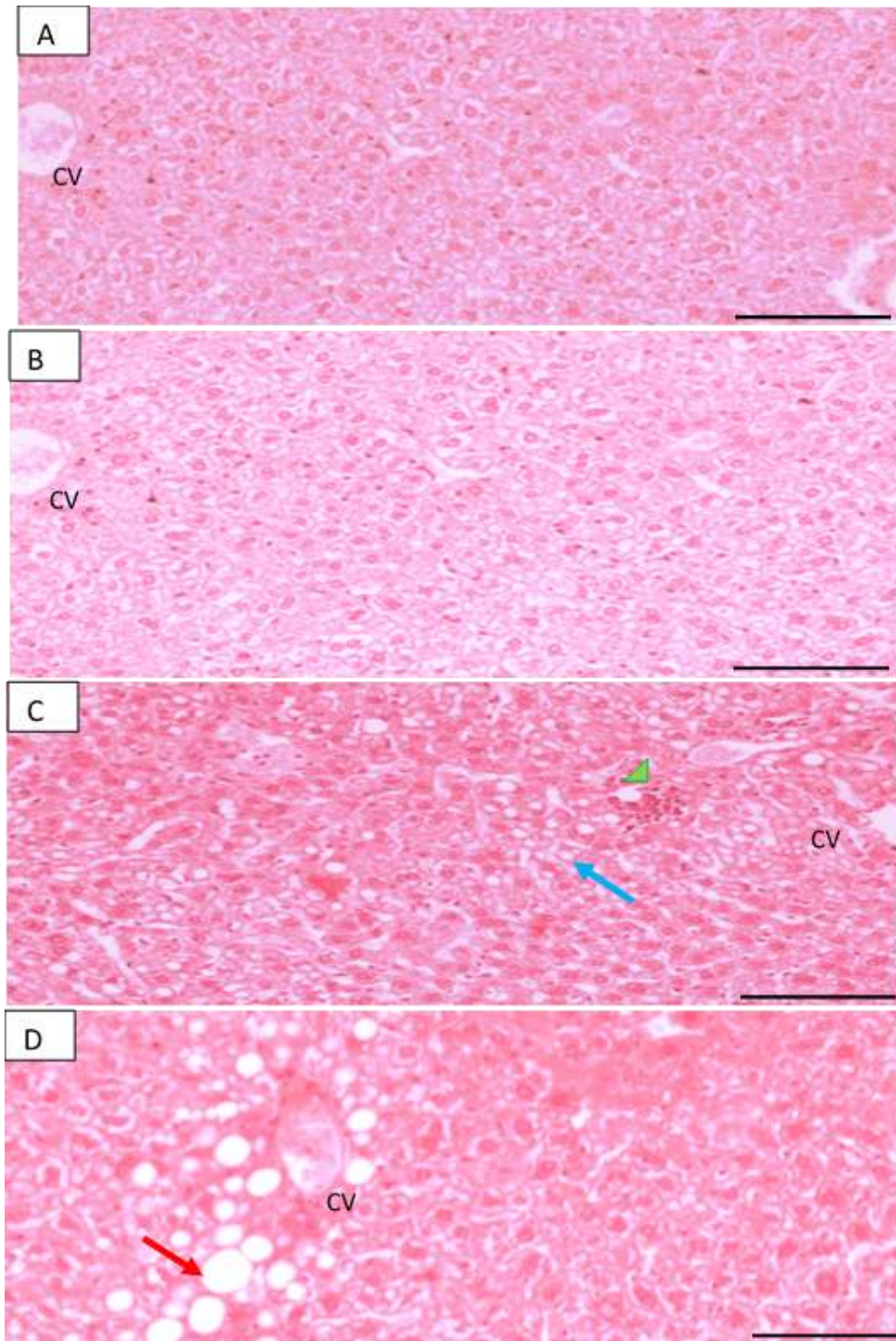


Figure 5-5 Haematoxylin, and eosin staining of paraffin embedded liver sections obtained from female LDLR^{-/-} mice.

Representative images. No inflammation, and steatosis in LDLR^{-/-}PWT mice 5LF2 (Panel A), LDLR^{-/-}PWT mice fed 5LF2 (Panel B). Fatty changes in great amount, microvesicular (blue arrows), macrovesicular (red arrows) (steatosis), and inflammation (green- heads) presence of marked fatty changes near CV (zone 3) in middle column in LDLR^{-/-}PKO mice fed 5TJN (Panel D), and less steatosis in LDLR^{-/-}PWT fed 5TJN (Panel C), CV, central vein, 200x. Scale bar represents 100 micron.

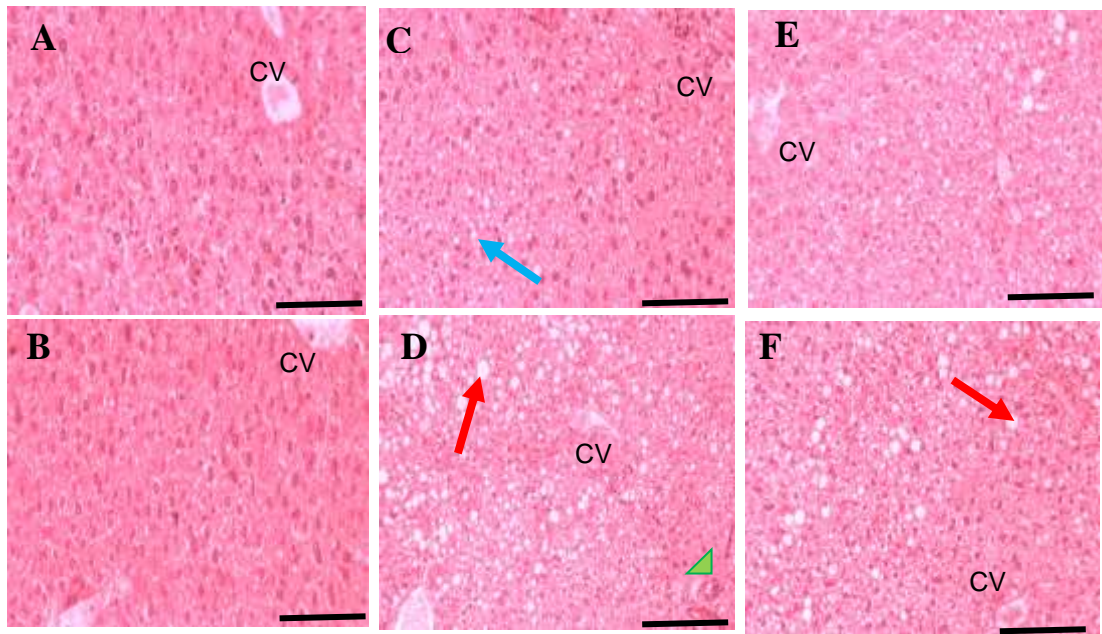


Figure 5-6 Haematoxylin, and eosin staining of paraffin embedded liver sections obtained from female LDLR^{+/+}mice.

Representative images. No inflammation, and steatosis in LDLR^{+/+}PWT mice 5LF2 (Panel A), LDLR^{+/+}PWT mice fed 5LF2 (Panel B). Fatty changes in great amount, microvesicular (blue arrows), macrovesicular (red arrows) (steatosis), and inflammation (green- heads) presence of marked fatty changes near CV (zone 3) in middle column in LDLR^{+/+}PKO mice fed 5TJN (Panel D), and less steatosis in LDLR^{+/+}PWT fed 5TJN (Panel C), CV, central vein, 200x. Scale bar represents 100 micron.

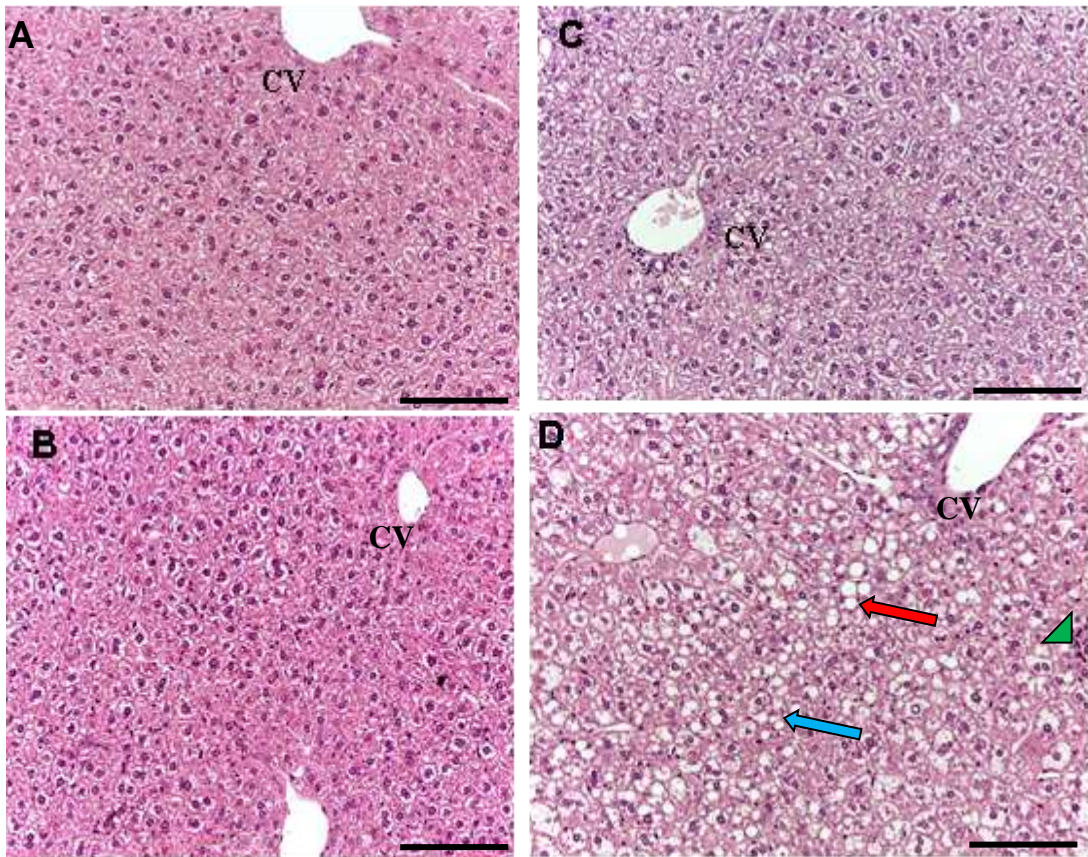


Figure 5-7 Haematoxylin, and eosin staining of paraffin embedded liver sections obtained from male LDLR^{-/-} mice

Representative images. No inflammation, and steatosis in LDLR^{-/-}PWT mice 5LF2 (Panel A), LDLR^{-/-}PWT mice fed 5LF2 (Panel B). Fatty changes in great amount, microvesicular (blue arrows), macrovesicular (red arrows) (steatosis), and inflammation (green- heads) presence of marked fatty changes near CV (zone 3) in middle column in LDLR^{-/-}PKO mice fed 5TJN (Panel D), and less steatosis in LDLR^{-/-}PWT fed 5TJN (Panel C), CV, central vein, 200x. Scale bar represents 100 Micron.

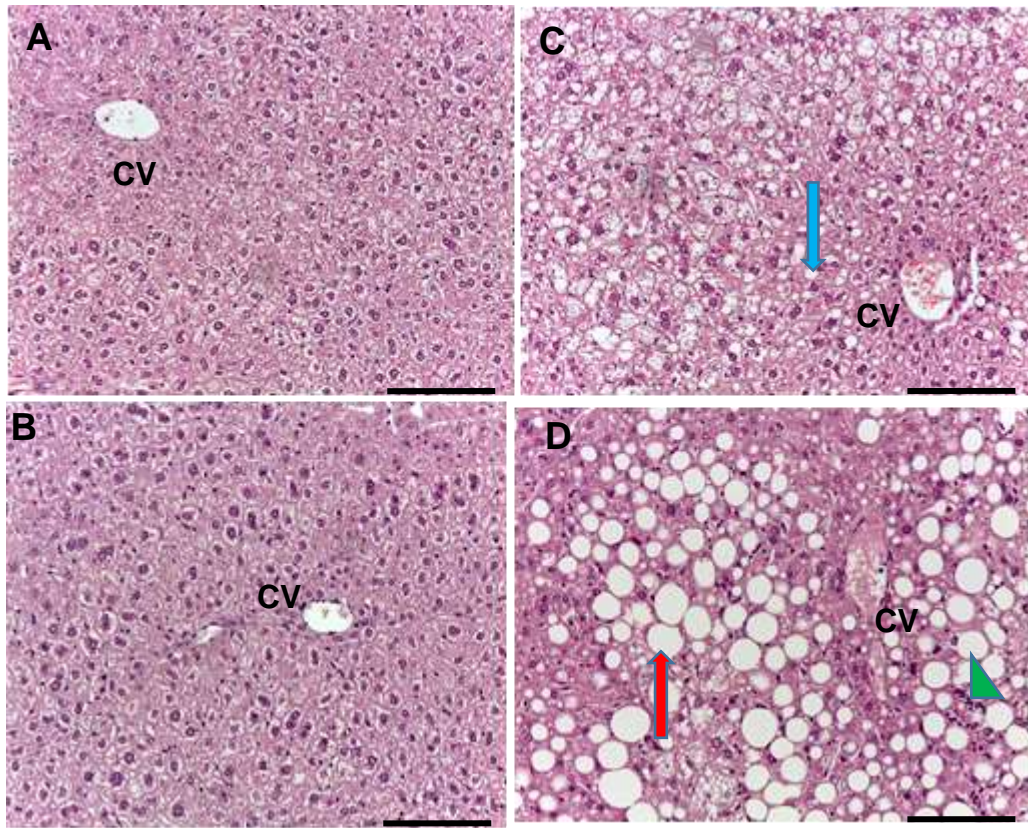


Figure 5-8 Haematoxylin, and eosin staining of paraffin embedded liver sections obtained from male LDLR^{+/+}mice.

Representative images. No inflammation, and steatosis in LDLR^{+/+}PWT mice 5LF2 (Panel A), LDLR^{+/+}PWT mice fed 5LF2 (Panel B). Fatty changes in great amount, microvesicular (blue arrows), macrovesicular (red arrows) (steatosis), and inflammation (green- heads) presence of marked fatty changes near CV (zone 3) in middle column in LDLR^{+/+}PKO mice fed 5TJN (Panel D), and less steatosis in LDLR^{+/+}PWT fed 5TJN (Panel C), CV, central vein, 200x. Sale bar represents 100 Micron.

Histological scoring system was performed for lobular inflammation, and steatosis (Kleiner *et al.* 2005). Scoring was performed by two observers, blinded to the identity of the slides. High score (score 3) for steatosis, and lobular inflammation (score 2) was seen in livers from mice on high fat diet-high sugar. However, only grade one, and zero was documented in mice fed low fat diet. Lobular inflammation was higher in high fat-high sugar diet, Western diet compared to low fat diet. Female LDLR^{-/-} PKO fed high fat-high sugar diet had higher lobular inflammation (higher score 2) compared to female LDLR^{-/-} PWT fed high fat-high sugar diet (Table 5.4, A). In addition, in male LDLR^{+/+}PKO mice fed Western diet, and high fat-high sugar diet had greater lobular

inflammation compared to LDLR^{+/+}PWT mice (Tables 5.5, A and 5.6, A). Steatosis scores (ranges from 0-to 3) shows that in high fat-high sugar, and Western diet mice have severe fatty changes, (grade 3) while in control mice, this extent was documented (Tables 5.4, 5.5, 5.6). Steatosis scores (ranges from 0 to 3) shows that score 3 in female LDLR^{-/-}PKO mice fed high fat-high sugar diet was higher compared to female LDLR^{-/-}PWT mice (Table 5.4, B), and also female LDLR^{+/+}PWT fed Western diet was higher score 3 compared to female LDLR^{+/+}PKO mice. In female LDLR^{+/+}PKO mice fed high fat-high sugar diet was higher steatosis compared to female LDLR^{+/+}PWT, and also female LDLR^{+/+}PKO fed Western diet was higher steatosis compared to LDLR^{+/+}PWT (Table 5.5, B), In addition, male LDLR^{+/+}PWT fed Western diet an high fat-high sugar diet had higher score 3 compared to male LDLR^{+/+}PKO mice (Table 5.6, B). This result appears that properdin may play role in the prevention of steatosis, and inflammation.

Table 5.4 Lobular inflammation (A) scores and steatosis scores (B) for male LDLR^{-/-} PWT/PKO mice.

(A)

Lobular inflammation score	Meaning (foci per 200X field)	LDLR ^{-/-} PWT 58R3	LDLR ^{-/-} PKO 58R3	LDLR ^{-/-} PWT 5LF2	LDLR ^{-/-} PKO 5LF2
0	No foci	0/8	0/8	2/3	1/2
1	Less than 2	4/8	5/8	1/3	1/2
2	2-4	2/8	3/8	0/3	0/2
3	More than 4	0/8	0/8	0/3	0/2

(B)

Steatosis	Meaning (parenchymal involvement by steatosis)	PWT 58R3	PKO 58R3	PWT 5LF2	PKO 5LF2
0	Less than 5%	0/8	0/8	2/3	1/2
1	5-33%	0/8	1/8	1/3	1/2
2	33-66%	4/8	2/8	0/3	0/2
3	More than 66%	4/8	5/8	0/3	0/2

Mice fed high fat high sugar died (high fat-high sugar diet) and maintenance diet (low fat diet).

Table 5.5 Lobular inflammation (A) scores, and steatosis scores (B) for female LDLR^{+/+}PWT/PKO mice.

A)

Lobular inflammation score	Meaning (foci per 200X field)	PWT 58R3	PKO 58R3	PWT 5TJN	PKO 5TJN	PWT 5LF2	PKO 5LF2
0	No foci	3/5	2/5	3/5	1/4	2/4	1/3
1	Less than 2	2/5	1/5	2/5	3/4	2/4	2/3
2	2-4	0/5	2/5	0/5	0/4	0/4	0/3
3	More than 4	0/5	0/5	0/5	0/4	0/4	0/3

B)

Steatosis	Meaning (parenchymal involvement by steatosis)	PWT 58R3	PKO 58R3	PWT 5TJN	PKO 5TJN	PWT 5LF2	PKO 5LF2
0	Less than 5%	0/5	0/5	0/5	0/4	0/4	0/3
1	5-33%	0/5	0/5	0/5	0/4	4/4	2/3
2	33-66%	2/5	0/5	3/5	1/4	0/4	1/3
3	More than 66%	3/5	5/5	2/5	3/4	0/4	0/3

Mice fed high fat high sugar died (58R3), Western diet (5TJN) and maintenance diet (low fat diet) (5LF2) for ten weeks.

Table 5.6 Lobular inflammation (A) scores, and steatosis scores (B) for male LDLR^{+/+}PWT/PKO mice.

(A)

Lobular inflammation score	Meaning (foci per 200X field)	PWT 58R3	PWT 58R3	PWT 5TJN	PKO 5TJN	PWT 5LF2	PKO 5LF2
0	No foci	0/4	0/4	0/3	0/3	4/4	3/3
1	Less than 2	4/4	4/4	3/3	2/3	0/4	0/3
2	2-4	0/4	0/4	0/3	1/3	0/4	0/3
3	More than 4	0/4	0/4	0/3	0/3	0/4	0/3

(B)

Steatosis	Meaning (parenchymal involvement by steatosis)	PWT 58R3	PKO 58R3	PWT 5TJN	PKO 5TJN	PWT 5LF2	PKO 5LF2
0	Less than 5%	0/4	0/4	0/3	0/3	4/4	3/3
1	5-33%	0/4	0/4	0/3	0/3	0/4	0/3
2	33-66%	3/4	1/4	2/3	1/3	0/4	0/3
3	More than 66%	1/4	3/4	1/3	2/3	0/4	0/3

Mice fed high fat high sugar died high fat-high sugar diet (58R3), Western diet (5TJN), and maintenance diet (low fat diet) (5LF2) for ten weeks.

Table 5.7 Lobular inflammation (A) scores, and steatosis scores (B) for male LDLR^{-/-} PWT/PKO mice.

(A)

lobular inflammation score	Meaning (foci per 200X field)	PWT 58R3	PKO 58R3	PWT 5LF2	PKO 5LF2
0	No foci	0/2	0/2	2/3	1/2
1	Less than 2	2/2	2/2	1/3	1/2
2	2-4	0/2	0/2	0/3	0/1
3	More than 4	0/2	0/2	0/3	0/1

(B)

Steatosis	Meaning (parenchymal involvement by steatosis)	PWT 58R3	PKO 58R3	PWT 5LF2	PKO 5LF2
0	Less than 5%	0/2	0/2	2/3	1/2
1	5-33%	0/2	0/2	1/3	1/2
2	33-66%	2/2	0/2	0/3	0/2
3	More than 66%	0/2	2/2	0/3	0/2

Mice fed high fat high sugar diet and Western diet and maintenance diet (low fat diet) for ten weeks.

5.2.1.3.2 Detection of hepatic lipids by Olive green stain

In order to see lipid droplets, a part of livers were sectioned on an ultramicrotome at 400nm then stained with 1% Toluidine blue in 1% borax for 30 seconds at the same temperature (92 °C). The result showed that livers from properdin deficient mice had larger fat droplets (Figure 5.9, D) compared to properdin wild type mice (Figure 5.9, C). In order to further investigate the difference between properdin wild type and properdin deficient mice ultrastructurally, electron microscopic analysis was performed for livers of mice fed high fat diet.

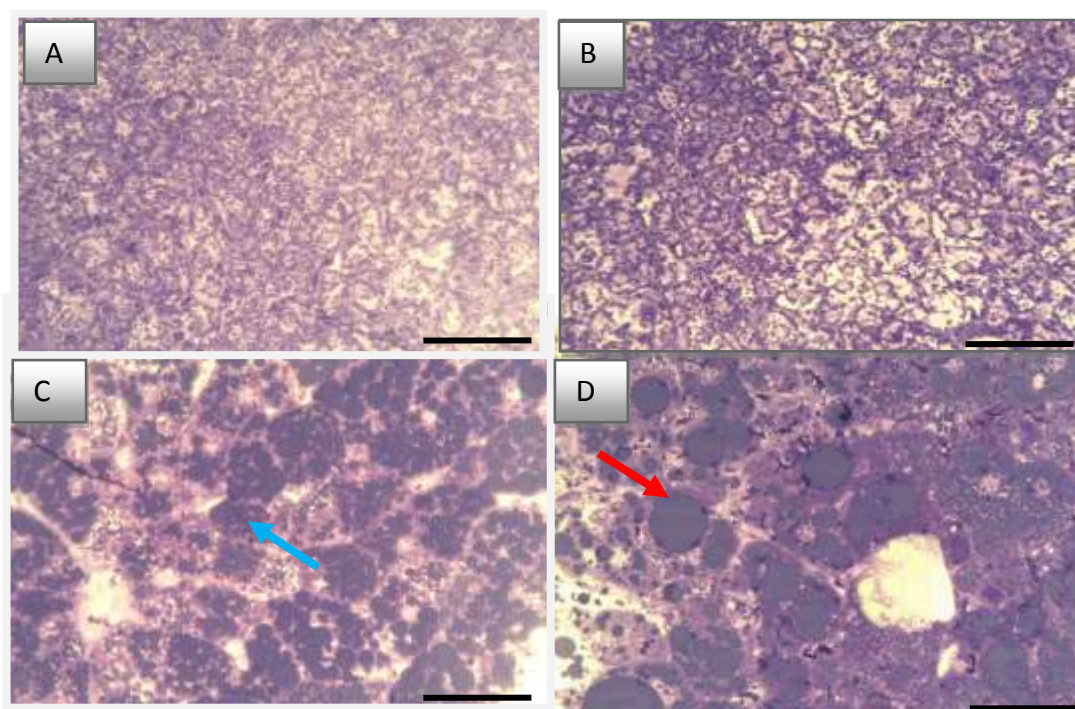


Figure 5-9 Olive green stain in LDLR^{+/±} mice.

Mice fed Western diet, and low fat diet. Representative images (A-D). No fat droplets (panels A, and B). Microvesicular (blue arrows), macrovesicular (red arrows), 5LF2 LDLR^{-/-}PWT (Panel A), 5LF2 LDLR^{-/-}PKO (Panel B), 5TJN LDLR^{-/-}PWT (panel C), 5TJN LDLR^{-/-}PKO (panel D), 100x. Scale bar represents 100 Micron.

5.2.1.3.3 Electron microscopic analysis

As previously mentioned, mice fed a high fat diet developed fatty liver disease. Because haematoxylin and eosin, and olive green stains showed that properdin deficient mice developed higher fatty liver compared to properdin wild type mice, electron microscope was performed. Livers from mice on low fat diet showed normal features: mitochondria rich hepatocytes, euchromatin rich nuclei, few lipid vesicles (Figure 5.10, A, B). Mice given Western diet for ten weeks developed many large lipid droplets inside the hepatocytes. This was more pronounced in properdin deficient mice (Figures 5.11 A and 5.12 A) compared to properdin wild type mice (Figures 5.11, B and 5.12, B). Properdin deficient mice given high fat diet developed more megamitochondria, and swelling of endoplasmic reticulum (Figure 5.13, A) compared to properdin wild type mice (Figure 5.13, B).

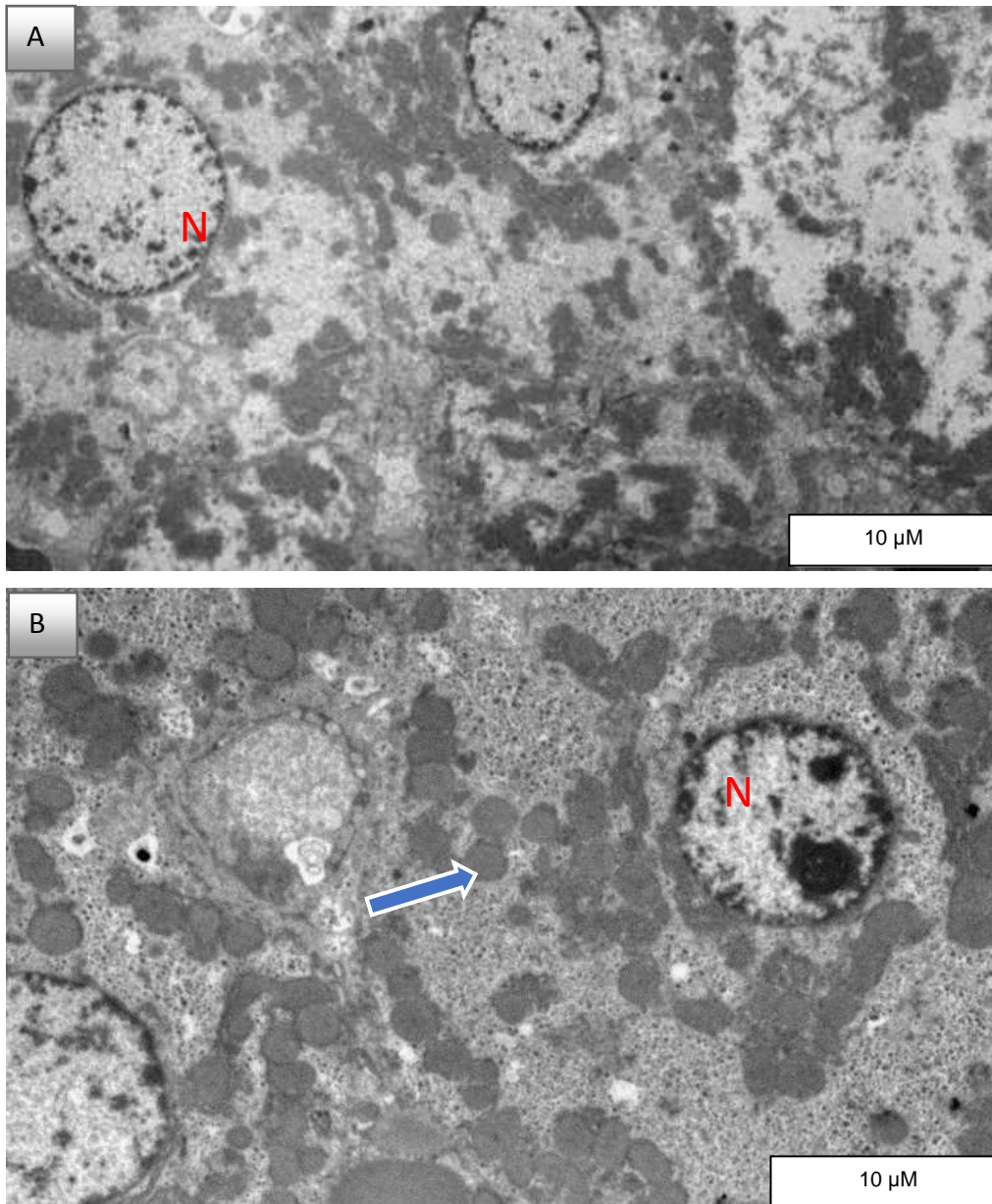


Figure 5-10 Electron micrograph from liver LDLR^{+/+} mice fed low fat diet. Properdin deficient mice (Panel A), properdin wild type (Panel B). N=nucleus, mitochondria (blue arrow), X8000.

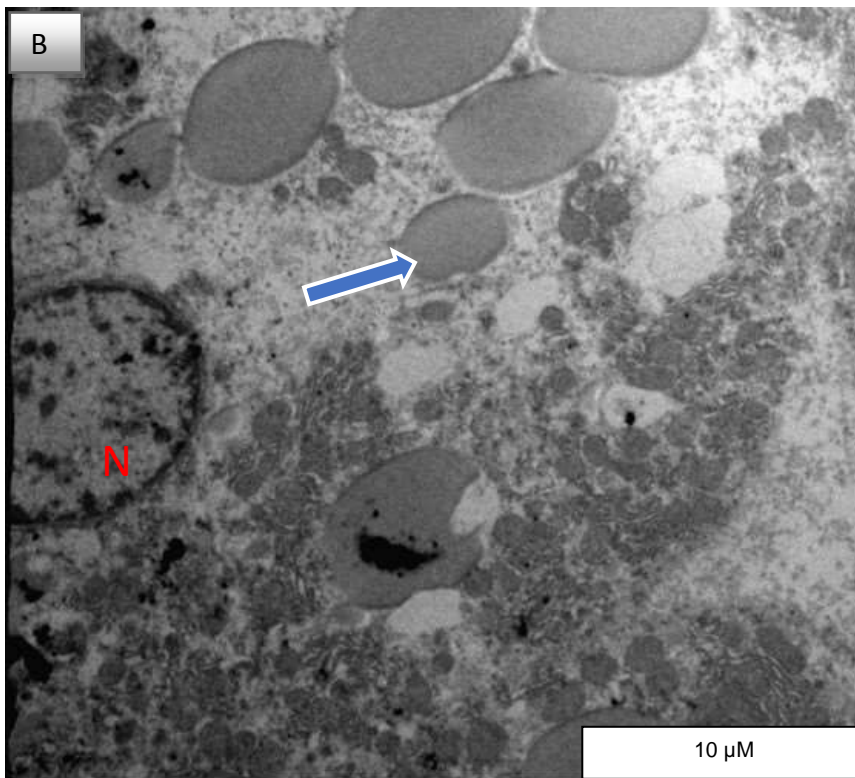
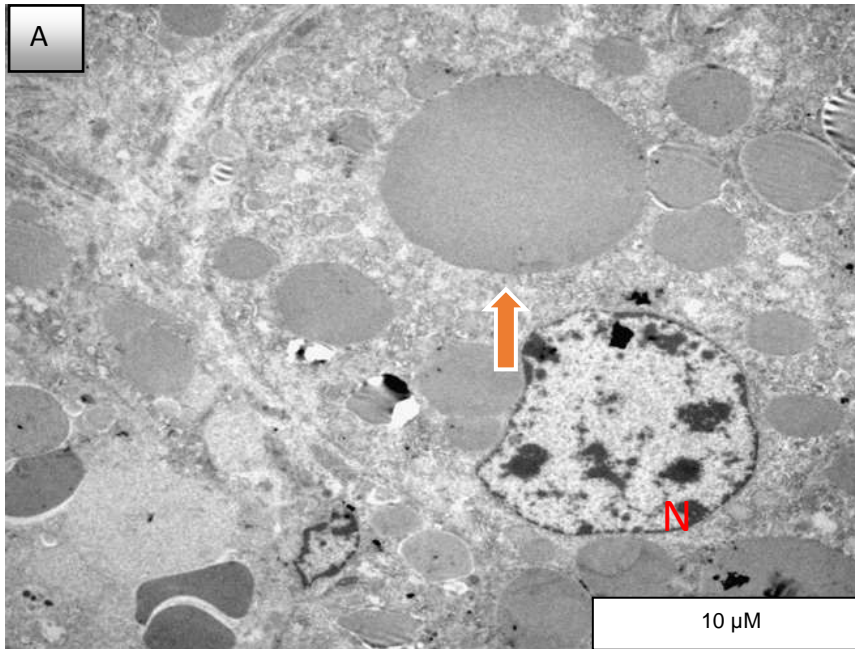


Figure 5-11 Electron micrograph from liver LDLR^{+/+} mice fed Western diet. Properdin deficient mice (panel A), and properdin wild type mice (panel B). Huge fat droplets (orange arrows), smaller fat droplets (blue arrow) (panel B). N=nucleus. X8000.

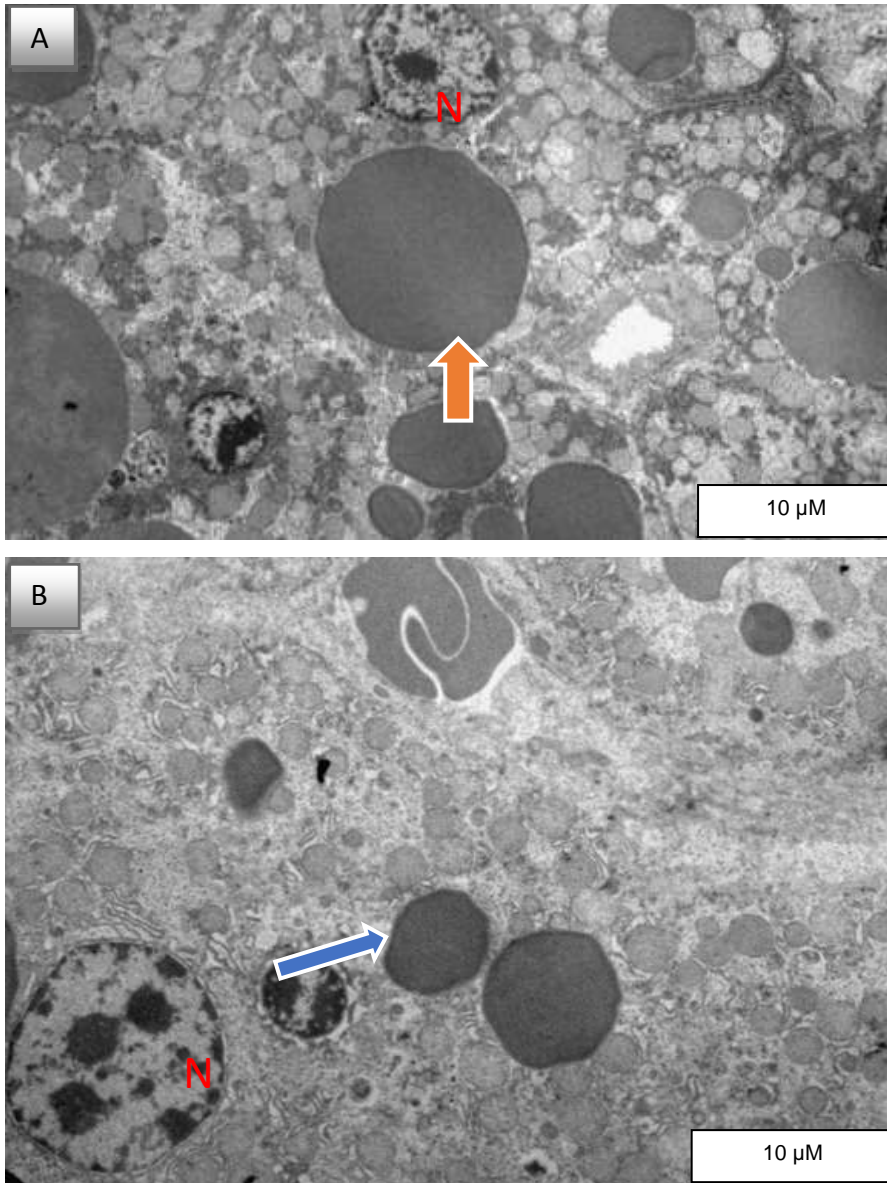


Figure 5-12 Electron micrograph showing lipid droplets from liver LDLR+/+ mice fed Western diet.

Properdin deficient mice (panel A), and properdin wild type (panel B). Huge fat droplets (orange arrows) (panel A), a smaller fat detected (blue arrow) (panel B). N=nucleus. X8000.

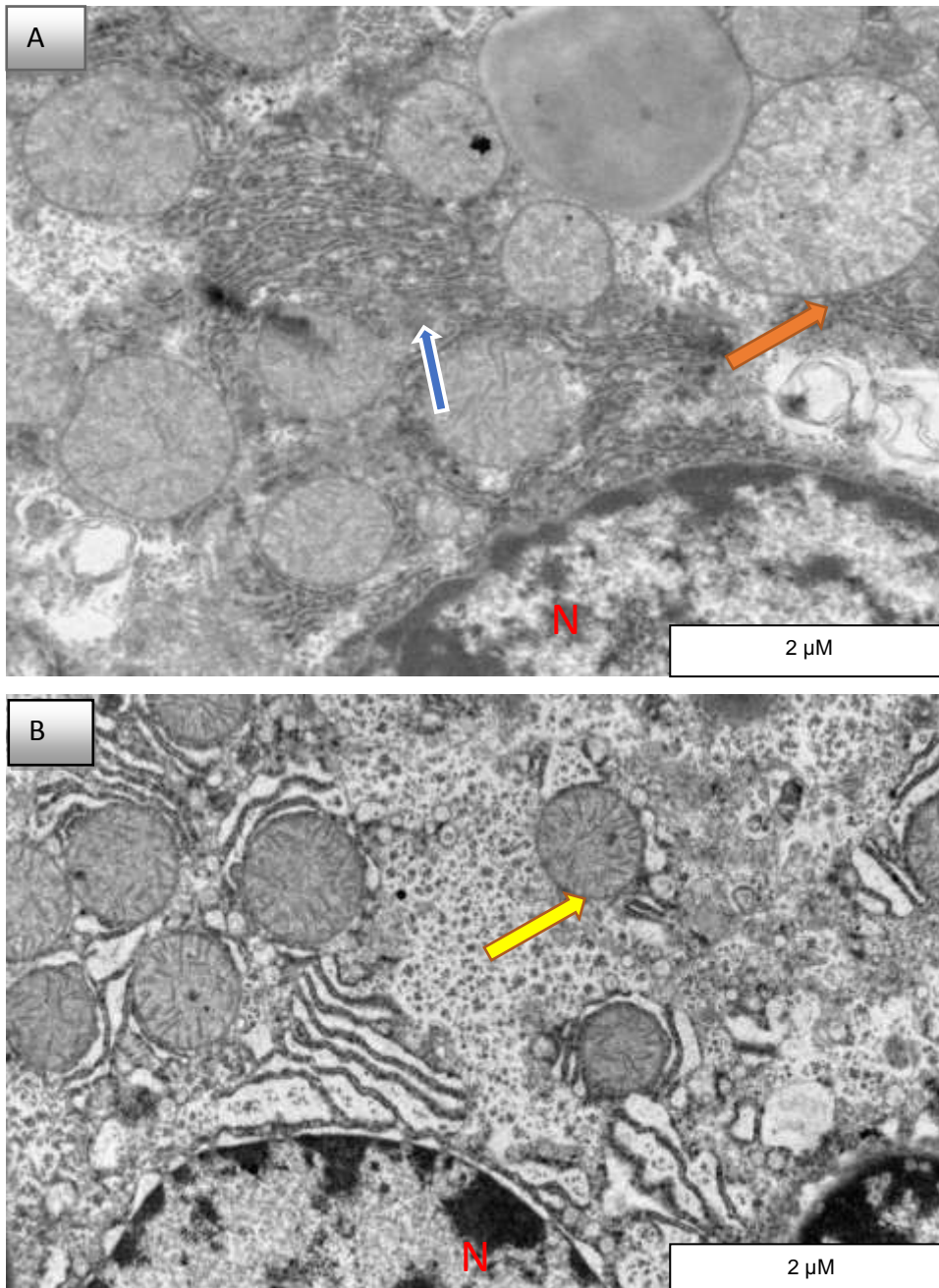


Figure 5-13 Electron micrograph showing mitochondria from liver LDLR^{+/+} mice fed Western diet.

Properdin deficient mice (panel A), and properdin wild type (panel B). A mega-mitochondrion (orange arrows) and smaller mitochondria (yellow arrow), and also rough endoplasmic reticulum (blue arrow) (panel A). N=nucleus. X8000

It can be concluded that properdin deficient mice fed Western diet for 10 weeks developed more severe liver steatosis than properdin wild type mice, based on histopathology, olive green stain, and electron microscopic analysis. Properdin deficient mice had developed more megamitochondria, and swelling of

endoplasmic reticulum. Due to the ultrastructural changes in cells, it can be implied that the metabolic strain is greater on properdin deficient mice given a high fat diet.

5.2.1.4 The effect of properdin on steatosis

Hepatic gene expression of Srebp-1c in LDLR^{+/+} PWT fed Western diet was significantly lower than LDLR^{+/+}PKO fed Western diet (Figure 5.14). This was confirmed the histological result that showed LDLR^{+/+} properdin wild type mice fed high fat-high sugar diet mice group had less steatosis compared to properdin deficient mice. There was not significant differences in LDLR^{-/-}PWT mice fed high fat-high sugar diet compared to LDLR^{-/-}PKO mice. The empirical findings in this study provide a new understanding of properdin, which plays a significant role in the prevention of steatosis. To quantify the extent of liver damage induced by high fat-high sugar diet, Western diet, and to seek the role of properdin, liver function tests were performed.

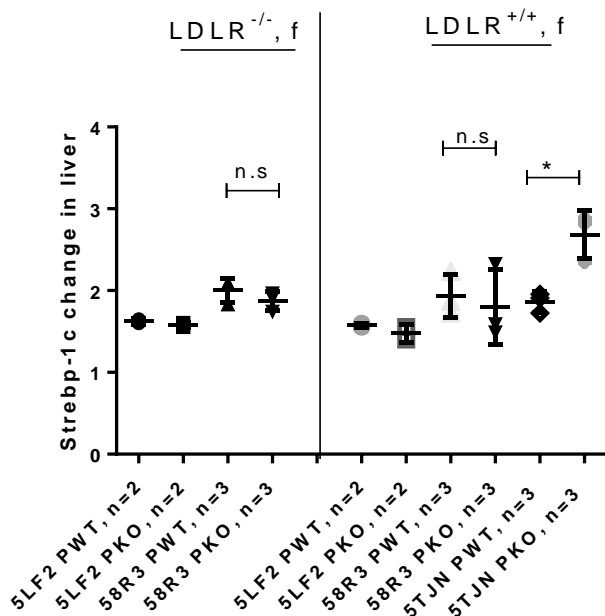


Figure 5-14 The effect of properdin on hepatic gene expression of Srebp-1c.

Female LDLR^{-/-} and LDLR^{+/+} mice fed high fat high sugar diet), low fat diet (5LF2) on hepatic gene expression of Srebp-1c. Results are presented as averages \pm SD from triplicate determinations. (adjusted *p*-values), ns=no significant.

5.2.1.5 Analysis of measurements of Liver function

In non-alcoholic steatohepatitis there is a correlation between increased deposition of C3, lobular inflammation, and an increase of properdin expression (Segers et al., 2014). The complement system activation in NAFLD has resulted the increase of severity, complement system is a part of innate immunity; and its activation has led to the progression of inflammation (Rensen et al., 2009a). AST, and ALT levels were measured as a correlate of liver function. There was not significant different between properdin wild type and properdin deficient mice in AST level of female LDLR^{-/-} mice fed high fat-high sugar diet and LDLR^{+/+} mice fed high fat-high sugar diet and Western diet (Figure 5.15, A, B). Female LDLR^{+/+} mice fed Western diet, properdin deficient mice had a tendency to have lower ALT (60.21±1.30 IU/L) compared to properdin wild type mice (75.84±1.6 IU/L) (Figure 5.16, A). Female LDLR^{-/-} mice fed high fat-high sugar diet, properdin deficient mice had lower ALT (58.22±11.97 IU/L) compared to properdin wild type mice (91.52±10.98 IU/L) (Figure 5.16, B). However, male LDLR^{+/+} mice fed high fat-high sugar diet, properdin deficient mice had higher AST (109.1±2.97 IU/L) compared to properdin wild type mice (93.2±6.62 IU/L) (Figure 5.16, C). In addition, male LDLR^{+/+} mice fed Western diet, properdin deficient mice had a tendency to have higher ALT (109.1±12.88 IU/L) compared to properdin wild type mice (65.8±9.44 IU/L) (Figure 5.16, E). This is the first study to demonstrate the effect of properdin on hepatic damage markers in both LDLR^{-/-} and LDLR^{+/+} back grounds. The result showed that properdin in female LDLR^{-/-} enhances further increase of ALT compared to properdin deficient mice while male LDLR^{+/+} mice properdin deficient mice led to the increase of AST and ALT levels. To investigate the role of properdin in developing metabolic syndrome disease, insulin, adiponectin, HbA1-c were tested.

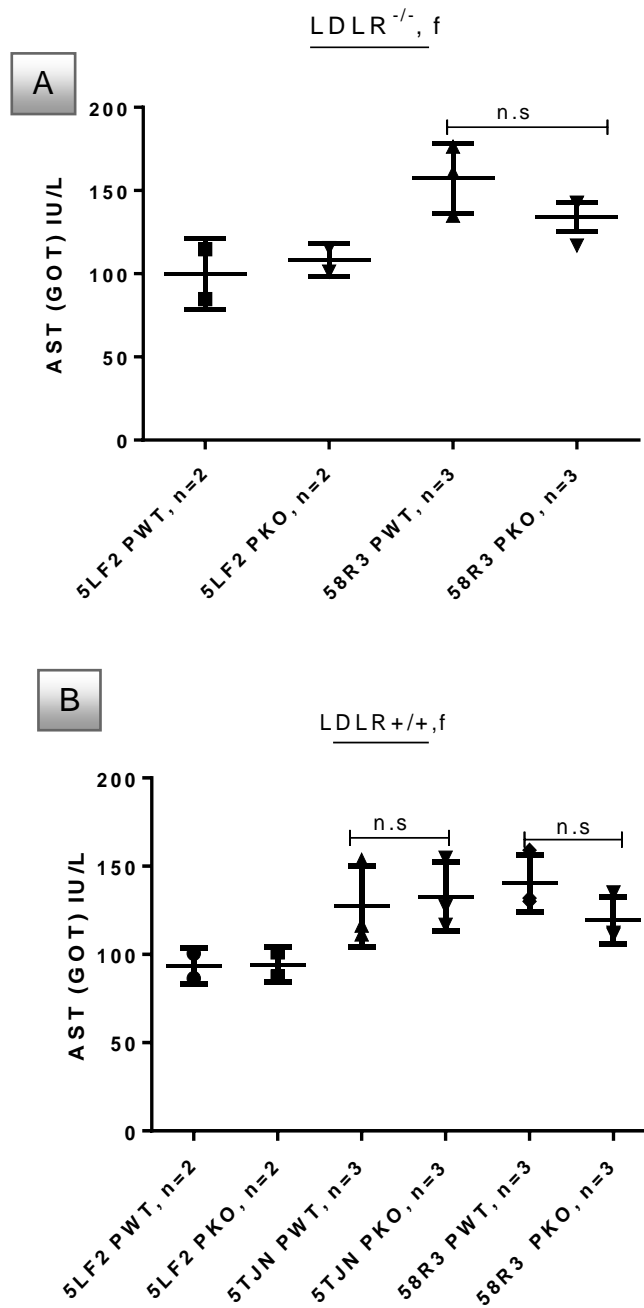


Figure 5-15 The effect of properdin on AST activity in female mice.

Mice fed low fat diet (5LF2), Western diet (5TJN), and high fat-high sugar diet (58R3) for 10 weeks. LDLR^{-/-} properdin wild type and deficient mice (LDLR^{-/-} PWT/PKO) (panel A), LDLR^{+/+} properdin wild type and deficient mice (LDLR^{+/+} PWT/PKO) (panel B). Results are presented as averages \pm SD from triplicate determinations (adjusted *p*-values), ns=no significant.

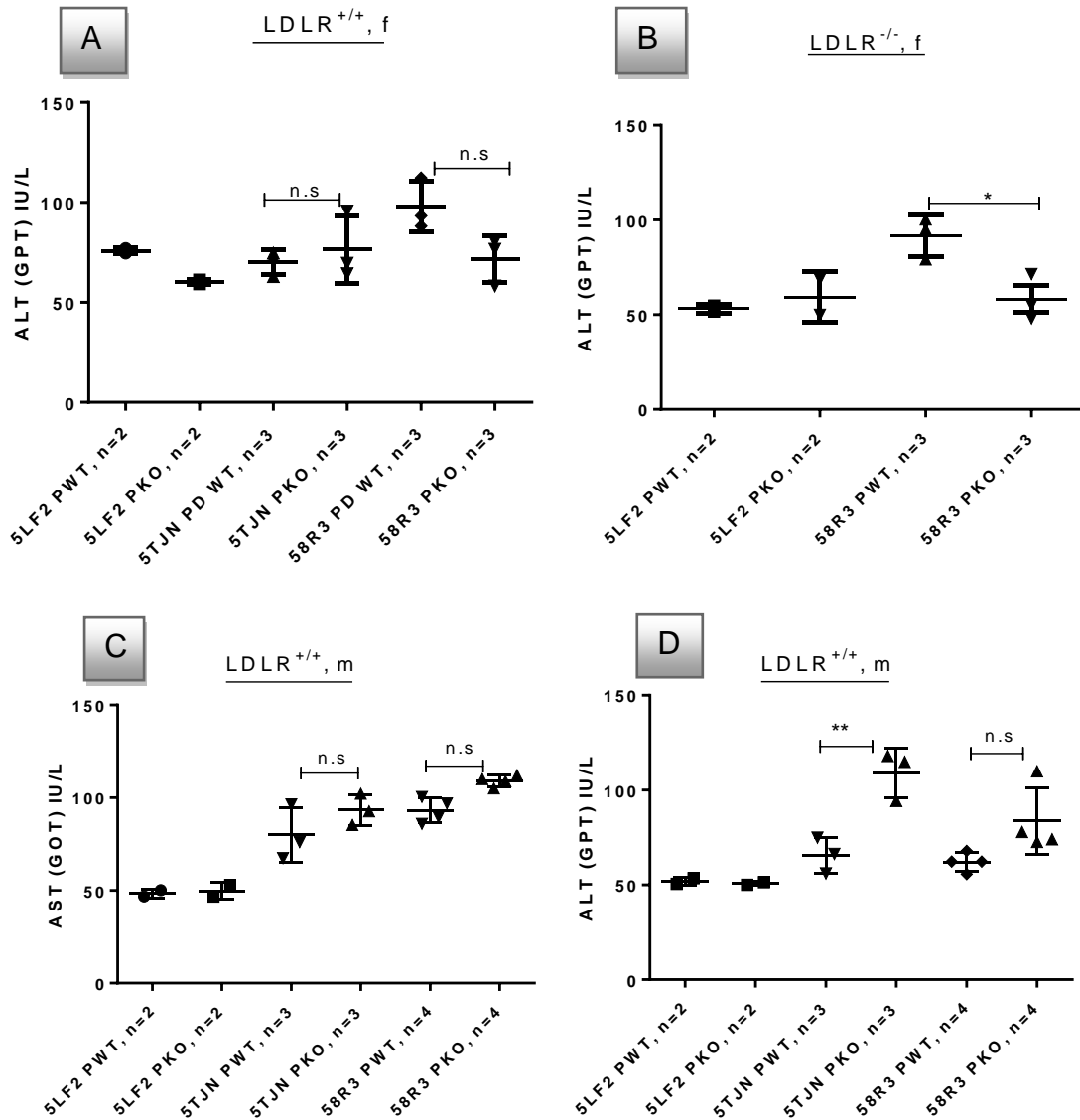


Figure 5-16 The effect of properdin on AST and ALT activity in female and male mice.

The effect of properdin on AST, and ALT activity in mice fed high fat-high sugar diet (58R3), Western diet (5TJN), and low fat diet (5LF2) (A-D). Effect of properdin on ALT in female LDLR^{+/+} mice (panel A), female LDLR^{-/-} mice (panel B) and on AST in male LDLR^{+/+} mice (panel C). Effect of properdin on ALT in male LDLR^{+/+} mice (panel D). Results are presented as averages \pm SD from triplicate determinations. * $p < 0.05$ (adjusted p -values), ns=no significant.

5.2.1.6 Role of properdin on insulin level and chronic glycaemia

Mice were given high fat diet-high sugar diet for 10 weeks (sexes and age matched) in both LDLR^{-/-} and LDLR^{+/+} backgrounds. Female LDLR^{-/-}PWT fed high fat-high sugar diet had a tendency to have lower adiponectin compared to female LDLR^{-/-}PKO mice (Figure 5.17, B). Male LDLR^{+/+} mice fed high fat-high sugar diet and Western diet, properdin deficient mice had a tendency to have higher insulin level (2.07 ±0.62 ng/ml), (3.47±0.63 ng/ml) compared to properdin wild type mice (1.01 ±0.24 ng/ml), (2.073±0.34 ng/ml) respectively (Figure 5.18, A), and a tendency to have lower adiponectin levels (1.70±0.25 µg/l), (1.53±0.10 µg/l) compared to properdin wild type mice (2.08±0.15 µg/l), (1.90 ±0.13 µg/l) respectively (Figure 15.18, B). There was a possibility higher HbA1c in female properdin deficient mice of LDLR^{+/+} fed Western diet compared to properdin wild type mice, but no significant differences between them (Figure 15.18, C). In addition, HbA1c was higher significantly in male LDLR^{+/+} properdin deficient mice fed high fat-high sugar diet (63.85±7.50 fmol/l), and Western diet (76.6±4.58 fmol/l) compared to properdin wild type mice (50.86±750 fmol/l), (42.95±1.03 fmol/l) respectively (Figure 15.18, D). These findings suggest that properdin deficiency in mice may play a role in the initiation of diabetes. To see the role of properdin, candidate genes related to inflammation were tested.

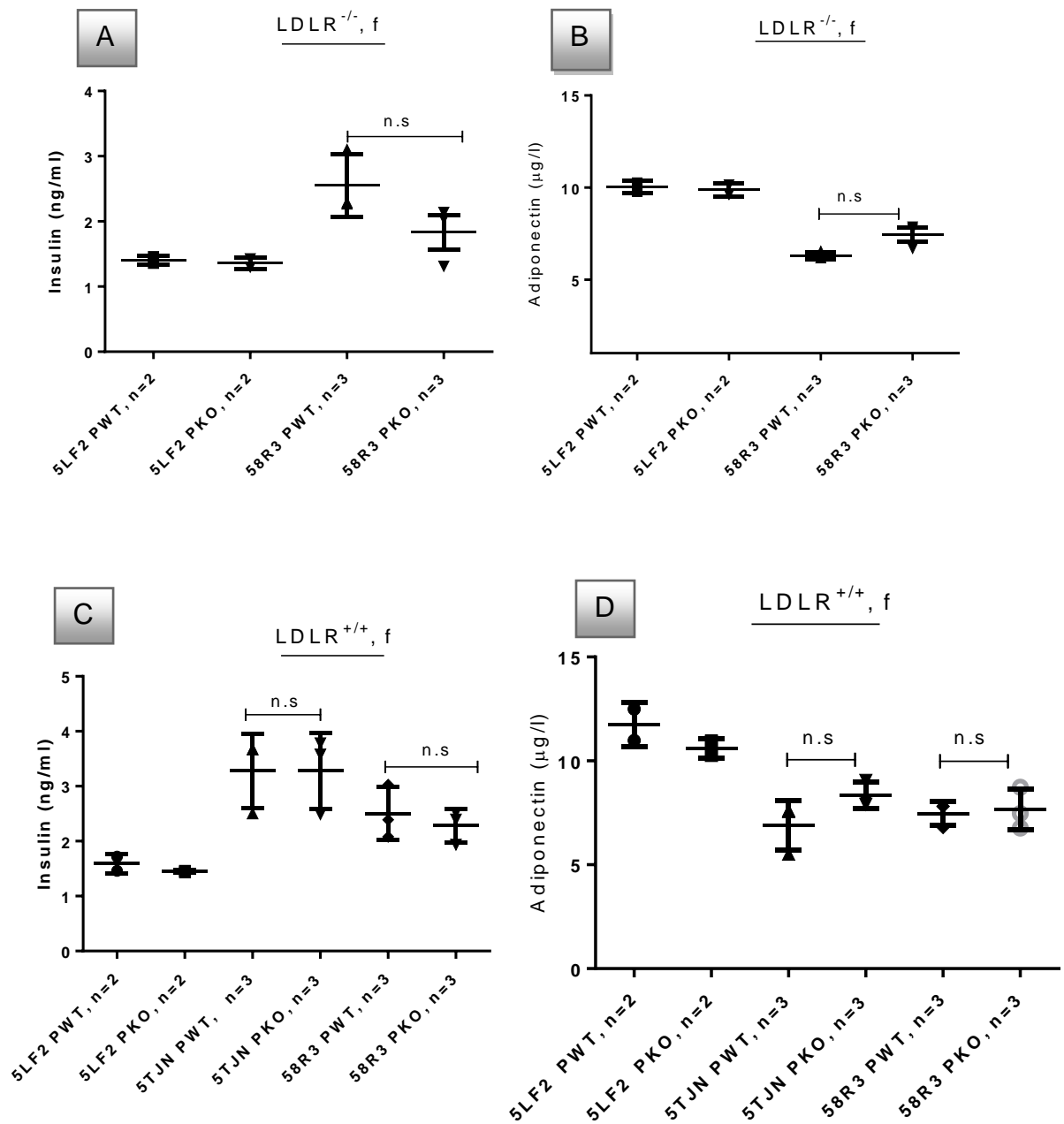


Figure 5-17 The effect of properdin on insulin and adiponectin protein in female mice sera.

Mice fed high fat-high sugar diet (58R3), Western diet (5TJN), and low fat diet (5LF2) (A-D). Effect of properdin on insulin in female LDLR^{-/-} mice (panel A), on adiponectin in female LDLR^{-/-} mice (panel B) and on insulin in female LDLR^{+/+} mice (panel C) on adiponectin in female LDLR^{+/+} mice (panel D). Results are presented as averages \pm SD from triplicate determinations. (adjusted *p*-values), n.s=no significant.

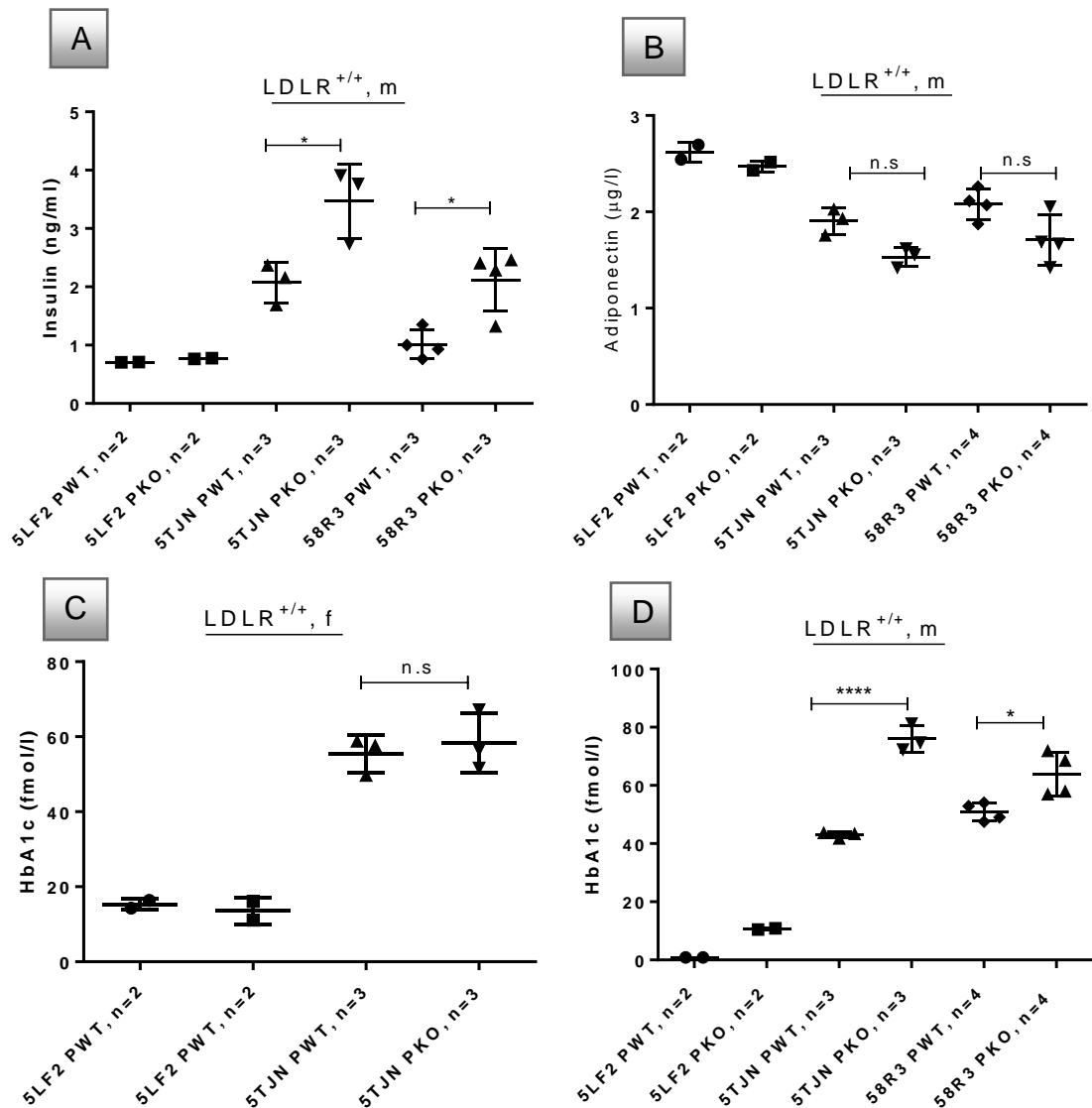


Figure 5-18 The effect of properdin on insulin, adiponectin, HbA1 activity in female and male mice sera.

Mice fed high fat-high sugar diet (58R3), Western diet (5TJN), and low fat diet (5LF2) (A-D). Effect of properdin on insulin in male LDLR^{+/+} mice (panel A), on adiponectin in male LDLR^{+/+} mice (panel B) and on HbA1c in female LDLR^{+/+} mice (panel C) on HbA1c in male LDLR^{+/+} mice (panel D). Results are presented as averages \pm SD from triplicate determinations. * $p < 0.05$, ** $p < 0.01$, *** $p < 0.005$, **** $p < 0.0001$ (adjusted p -values), n.s=no significant.

5.2.1.7 The role of properdin in the IL-6 response

Complement activation in fatty liver disease led to the increase of IL-6 (Rensen et al., 2009a), therefore levels of IL-6 mRNA and protein were studied from properdin wild type and properdin knockout mice on high fat-high sugar diet and Western diet. There were no differences from hepatic TNF- α mRNA expression between properdin wild type, and properdin deficient mice groups in both LDLR^{-/-} and LDLR^{+/+} group female mice (Figure 5.19, A). Hepatic gene expression for IL-6 of LDLR^{-/-}PWT/PKO fed high fat-high sugar diet was performed to see the differences between properdin wild type, and properdin deficient mice, and the result showed that in properdin deficient mice, there was a tendency to be higher IL-6 mRNA in properdin deficient mice compared to wild type mice (Figure 5.19, B). To further investigate the differences, IL-6 ELISA was performed. IL-6 ELISA test confirmed the gene expression of IL-6, showing an increase of IL-6 protein level in LDLR^{+/+}PKO compared to LDLR^{+/+}PWT in mice fed Western diet (Figure 5.19, C). In male LDLR^{+/+} mice fed high fat-high sugar diet, and Western diet, IL-6 protein level was higher significantly in properdin deficient mice (16.45 \pm 0.84 ng/ml), (14.67 \pm 1.33 ng/ml) compared to properdin wild type mice (12.38 \pm 1.55 ng/ml), (8.12 \pm 1.70 ng/ml) respectively (Figure 5.19, D). The current data highlight that male LDLR^{+/+} and female LDLR^{-/-} properdin deficient mice had increased IL-6 compared to properdin wild type mice. To further understand the role of properdin role in inflammation, endotoxin was measured.

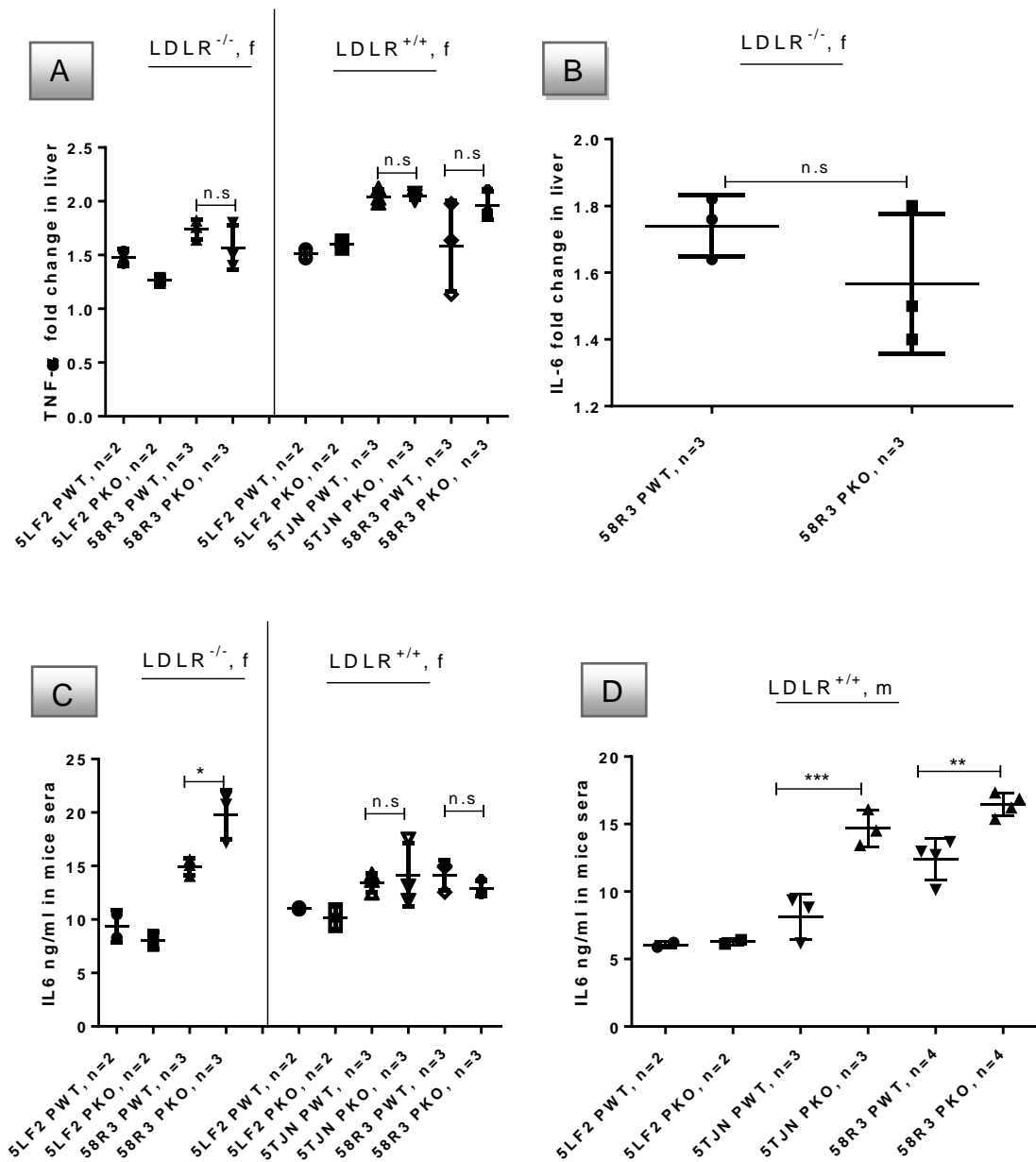


Figure 5-19 The effect of properdin on hepatic TNF- α IL-6 mRNA expression, IL-6 protein in female and male mice sera.

Mice fed high fat-high sugar diet (58R3), Western diet (5TJN), and low fat diet (5LF2) (A-D). Effect of properdin on TNF- α in female LDLR^{+/+}, LDLR^{-/-} mice (panel A), on IL-6 in female LDLR^{-/-} mice (panel B) and on IL-6 protein in female LDLR^{+/+}, LDLR^{-/-} mice (panel C) on IL-6 protein in male LDLR^{-/-} mice (panel D). Results are presented as averages \pm SD from triplicate determinations. * $p < 0.05$, ** $p < 0.01$, *** $p < 0.005$, **** $p < 0.0001$ (adjusted p -values), n.s=no significant.

5.2.1.8 Measurement of endotoxin levels

A high fat diet plays a role in the increased translocation of LPS into the blood, and this led to higher endotoxin level in NAFLD patients compared to control (Harte et al., 2010). For this reason, TLR4, and endotoxin were measured in parallel. Hepatic TLR4 mRNA expression in LDLR^{-/-}PWT/PKO and LDLR^{+/+}PWT/PKO fed high fat-high sugar diet, Western diet, and low fat diet was performed. Our results showed that TLR4 mRNA expression of liver in female LDLR^{+/+}PKO mice fed high fat-high sugar diet significantly higher (1.87 ± 0.05) compared to LDLR^{+/+}PWT mice fed high fat-high sugar diet (0.96 ± 0.21) (Figure 5.20, A), while in LDLR^{-/-} mice fed high fat-high sugar diet, and LDLR^{+/+} mice fed Western diet there were no significant differences between properdin wild type, and properdin deficient mice (Figure 5.20, A). Interestingly, endotoxin level in LDLR^{+/+}PWT fed Western diet (2.78 ± 1.03 IU/ml) was significantly lower than LDLR^{+/+}PKO fed Western diet (6.68 ± 1.7 IU/ml) (Figure 5.20, B). In addition, endotoxin level in female LDLR^{+/+}PWT fed Western diet (2.78 ± 0.59 IU/ml) was significantly lower than LDLR^{+/+}PKO fed Western diet (6.68 ± 0.98 IU/ml) (Figure 5.20, B). However, endotoxin level in female LDLR^{-/-}PWT fed high fat-high sugar diet (9.27 ± 2.62 IU/ml) was significantly higher than LDLR^{+/+}PKO fed Western diet (4.91 ± 0.55 IU/ml) (Figure 5.20, B). In contrast, endotoxin level was significantly higher in male LDLR^{+/+} properdin deficient mice fed high fat-high sugar diet, and Western diet (3.20 ± 0.89 IU/ml), (13.92 ± 4.12 IU/ml) compared to male LDLR^{+/+} properdin wild type mice (1.51 ± 0.37 IU/ml), (4.52 ± 0.78 IU/ml) respectively (Figure 5.20, C). These result concluded that properdin prevents intestinal leakage, and plays a significant role in the prevention of NAFLD, and NASH development, and also showed that Western diet, and high fat-high sugar diet affect the increase of endotoxin in circulation. To understand the effect of properdin on metabolic syndrome, measurements of TGs, and NEFA were performed.

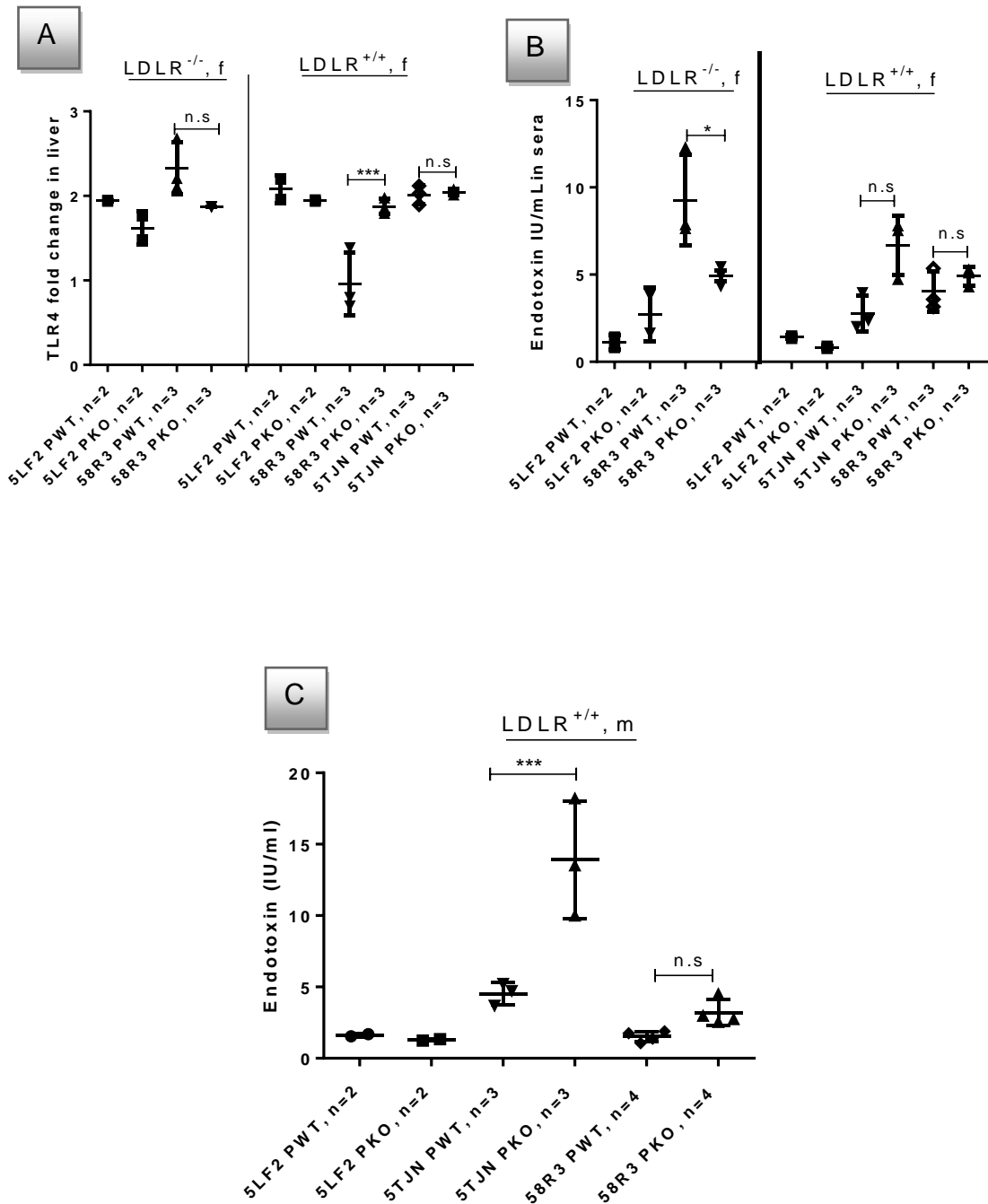


Figure 5-20 The effect of properdin on hepatic TLR4 mRNA expression, endotoxin in female and male mice sera.

Mice fed high fat-high sugar diet (58R3), Western diet (5TJN), and low fat diet (5LF2) (A-C). Effect of properdin on hepatic TLR4 mRNA expression in female LDLR^{+/+}, LDLR^{-/-} mice (Panel A), on endotoxin in female LDLR^{-/-} mice (Panel B) and on endotoxin in male LDLR^{+/+} mice (Panel C). Results are presented as averages \pm SD from triplicate determinations. * $p < 0.05$, ** $p < 0.01$, *** $p < 0.005$, **** $p < 0.0001$ (adjusted p -values), n.s.=no significant.

5.2.1.9 The role of properdin in developing metabolic syndrome

Complement activation during fatty liver disease caused the increase of C3 deposition, and plasma C3, and ASP levels that correlated with insulin resistance, and excessive fat accumulation (Rensen *et al.*, 2009).

Our result showed that triglyceride was significantly higher in properdin deficient mice of female LDLR^{+/+} mice fed high fat -high sugar diet (45.89±7.77 mg/dl), compared to properdin wild type group (30.59±8.84 mg/dl) (Figure 5.21, A). In female LDLR^{-/-} mice fed high fat -high sugar diet triglyceride was significantly higher in properdin deficient mice (87.26±14.82 mg/dl) compared to properdin wild type mice (57.52±0.96 mg/dl) (Figure 5.21, B). Male LDLR^{+/+} mice fed Western diet led to the increase of triglyceride in properdin deficient mice (41.55±4.92 mg/dl) compared to properdin wild type mice group (23.11±0.98 mg/dl) respectively (Figure 521, C). NEFA measurement was significantly higher in properdin deficient of female LDLR^{+/+} mice fed high fat-high sugar diet (0.74±0.11 mmol/L) compared to properdin wild type mice group (0.46±0.05 mmol/L) (Figure 5.22, A) and also there was a tendency to be higher between properdin deficient and properdin wild type mice, but not significant different (Figure 5.22, panel B). Male LDLR^{+/+} mice fed high fat high sugar diet, and Western diet led to the increase of NEFA in properdin deficient mice (0.89±0.07 mmol/), (0.59±0.01 mmol/) compared to properdin wild type mice group (0.59±0.06 mmol/), (0.39±0.09 mmol/) respectively (Figure 5.22, C).

In female LDLR^{+/+}, LDLR^{-/-} mice, and male mice LDLR^{+/+} fed high fat –high sugar diet, and Western diet led to the increase of triglycerides in properdin deficient mice compared to properdin wild type mice. In male LDLR^{+/+} mice fed high fat–high sugar diet, and Western diet resulted in the increase of NEFA in properdin deficient mice compared to properdin wild type mice. This result highlights that properdin prevents metabolic syndrome disease by the decrease of Triglyceride, and NEFA serum level.

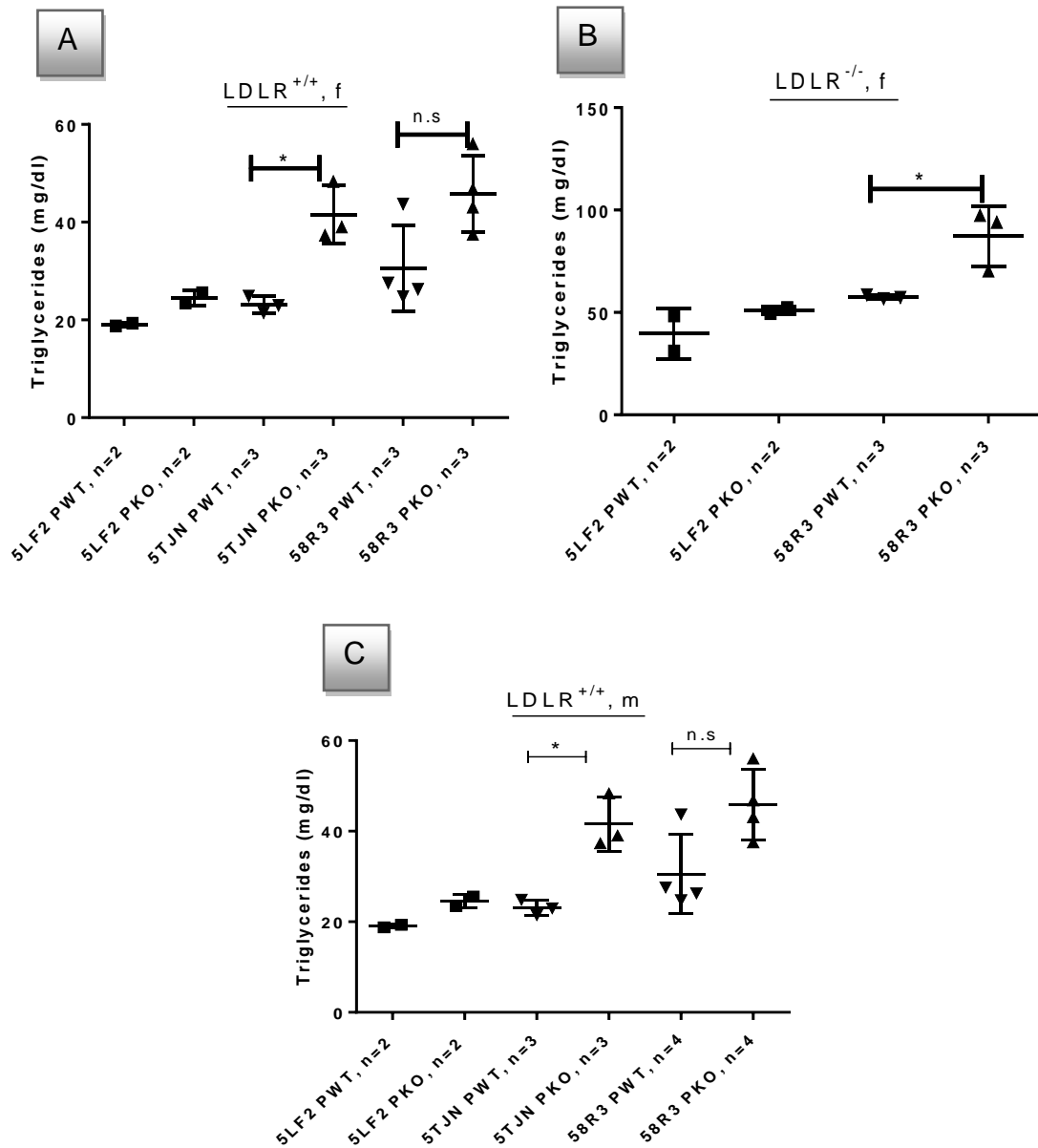


Figure 5-21 The effect of properdin on triglyceride in female and male mice sera.

Mice fed high fat-high sugar diet (58R3), Western diet (5TJN), and low fat diet (5LF2) (A-C). Effect of properdin on triglyceride in female LDLR^{+/+} mice (Panel A), on triglyceride in female LDLR^{-/-} mice (Panel B) on triglyceride in male LDLR^{+/+} mice (Panel C). Results are presented as averages \pm SD from triplicate determinations. * $p < 0.05$, ** $p < 0.01$, *** $p < 0.005$, **** $p < 0.0001$ (adjusted p -values), n.s.=no significant.

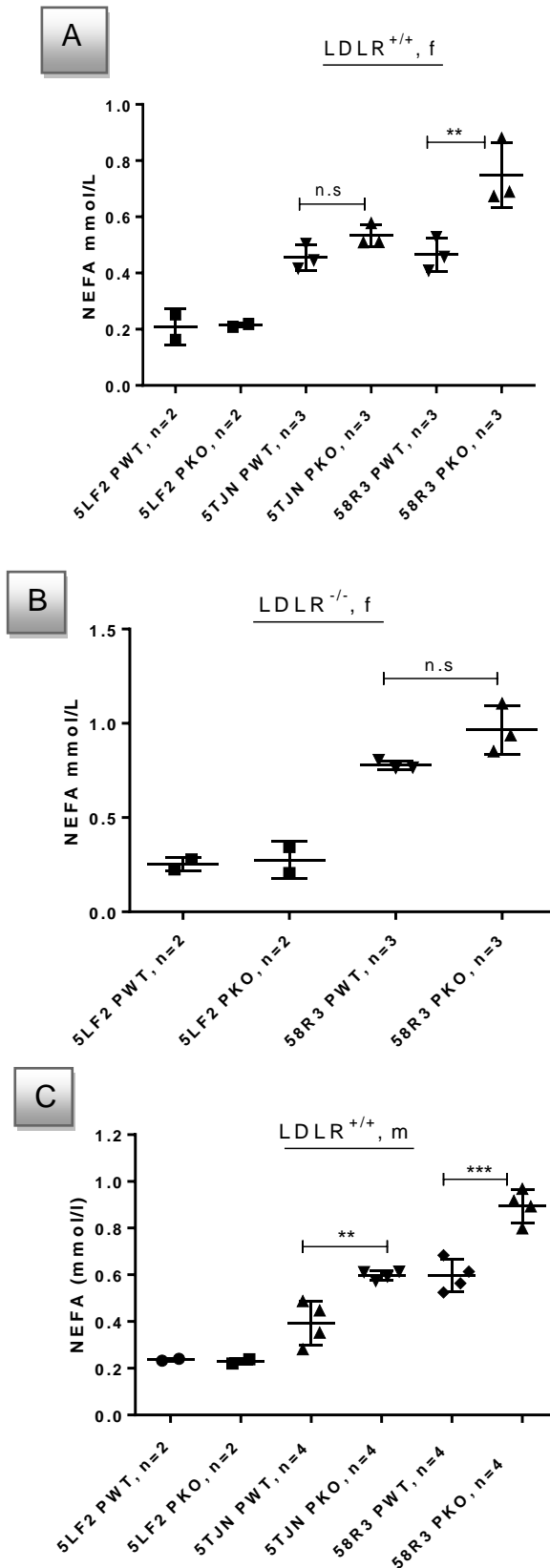


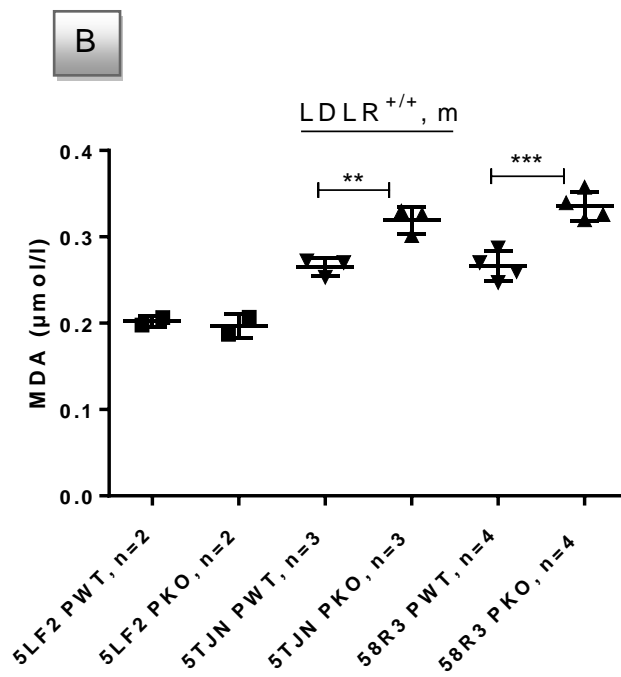
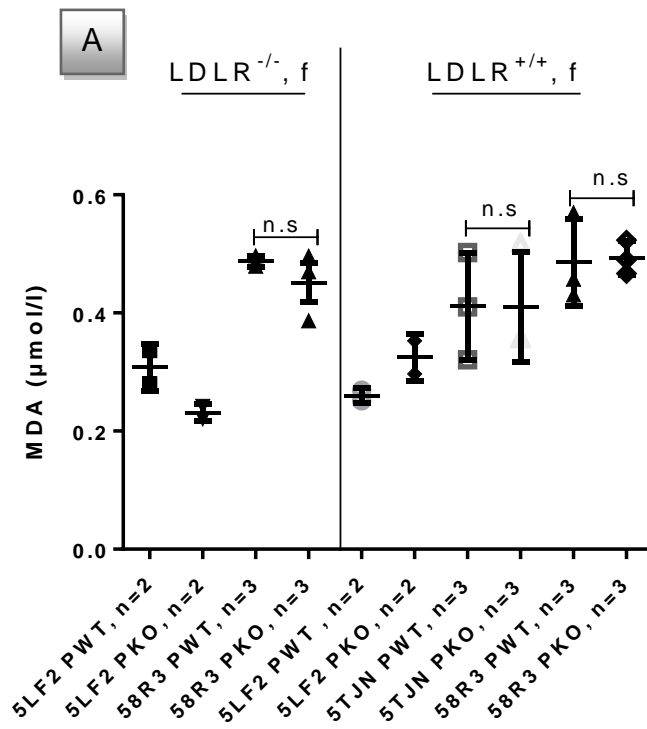
Figure 5-22 The effect of properdin on NEFA in female and male mice sera.

Mice fed high fat-high sugar diet (58R3), Western diet (5TJN), and low fat diet (5LF2) (A-C). Effect of properdin on NEFA in female LDLR^{+/+} mice (Panel A), on NEFA in female LDLR^{-/-} mice (Panel B) on NEFA in male LDLR^{+/+} mice (Panel C). Results are presented as averages \pm SD from triplicate determinations. * $p < 0.05$, ** $p < 0.01$, *** $p < 0.005$, **** $p < 0.0001$ (adjusted p -values), ns=no significant.

5.2.1.10 Lipid peroxidation product, and Vcam-1 mRNA as indicators of inflammatory endothelial damage

Lipid peroxidation is tightly linked to high fat diet, and obesity (Johnson et al., 2007). Diet-induced obesity is associated with an increase in the formation of lipid peroxidation-derived aldehydes (Baba et al., 2011). Therefore, MDA (Malondialdehyde) was performed to investigate properdin wild type and properdin deficient mice fed Western diet and high fat–high sugar diet. As in the previous chapter was mentioned the relation between Vcam-1 and MDA level.

The result showed that MDA had a tendency to be higher in female mice fed high fat -high sugar diet, but there was not the significant different between properdin deficient, and properdin wild type mice (Figure 5.23, A). Interestingly, MDA level was higher in properdin deficient of male LDLR^{+/+} mice fed high fat - high sugar diet (0.33 ± 0.01 $\mu\text{mol/l}$), and Western diet (0.31 ± 0.01 $\mu\text{mol/l}$) compared to properdin wild type group (0.26 ± 0.01 $\mu\text{mol/l}$), (0.26 ± 0.01 $\mu\text{mol/l}$) respectively (Figure 5.23, B). Male LDLR^{+/+} mice fed Western diet had a tendency to be higher aortic Vcam-1 expression in properdin deficient mice compared to properdin wild mice (Figure 5.23, C). It can be concluded that properdin may play a significant role in the decrease of MDA in male LDLR^{+/+} mice groups, and there was a tendency to be higher Vcam-1 in properdin deficient mice compared to properdin wild type mice; however, no significant role of properdin in the initiation of MDA was detected in female mice and also Vcam-1.



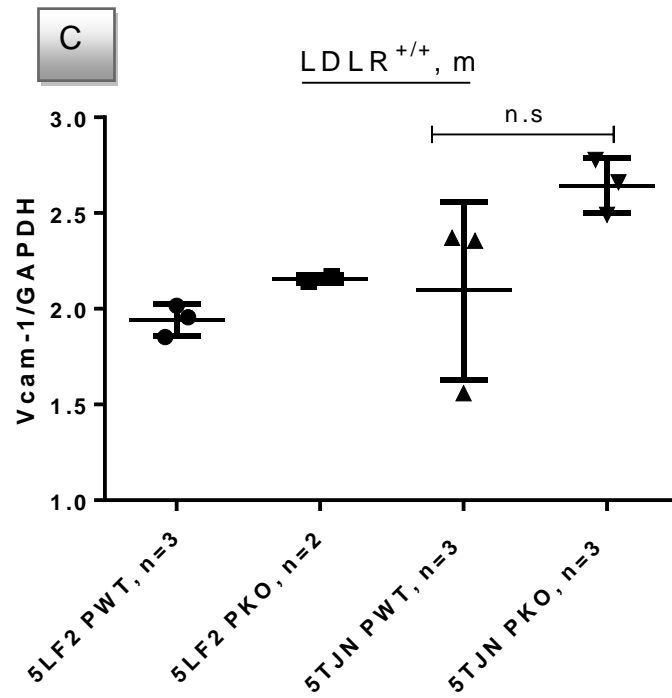


Figure 5-23 The effect of properdin on MDA assay test, and Vcam-1 in aorta.

Mice fed high fat-high sugar diet (58R3), Western diet (5TJN), and low fat diet (5LF2). MDA in female LDLR^{+/+} mice, female LDLR^{-/-} (panel A) male LDLR^{+/+}, LDLR^{-/-} (panel B). Aorta mRNA expression of Vcam-1 in male LDLR^{+/+} mice fed Western diet and low fat diet (panel C). Results are presented as averages ±SD from triplicate determinations. * $p < 0.05$, ** $p < 0.01$, *** $p < 0.005$, (adjusted p -values), ns=no significant.

5.2.1.11 Analysis of gene expressions as markers of M1 and M2 activity

M1 and M2 macrophage markers including Arginase-1 and iNOS were measured previously. The aim was to investigate the effect of properdin on macrophage activity. The result showed there was a tendency to be increased of mRNA expression iNOS (Figure 5.24, A and B), and the decreased of Arginase-1 (Figure 5.25, A) in spleen and liver of properdin wild type mice fed high fat-high sugar diet mice group compared to properdin deficient mice, although the differences between them were not significant. Female LDLR^{+/+} properdin deficient mice fed high fat-high sugar diet had significantly higher Arginase -1 in liver mice compared to properdin wild type mice (Figure 5.25, B). Our results showed that properdin deficient mice may have M2-Macrophage activity; it appears that properdin might play a role as M1-macrophage activity.

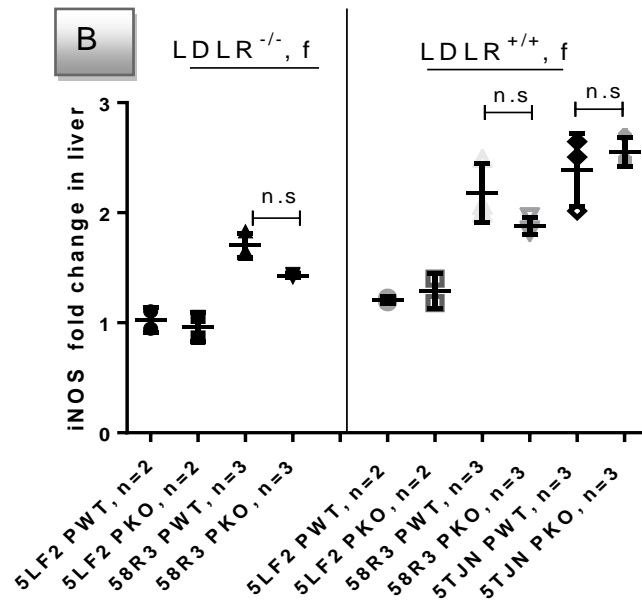
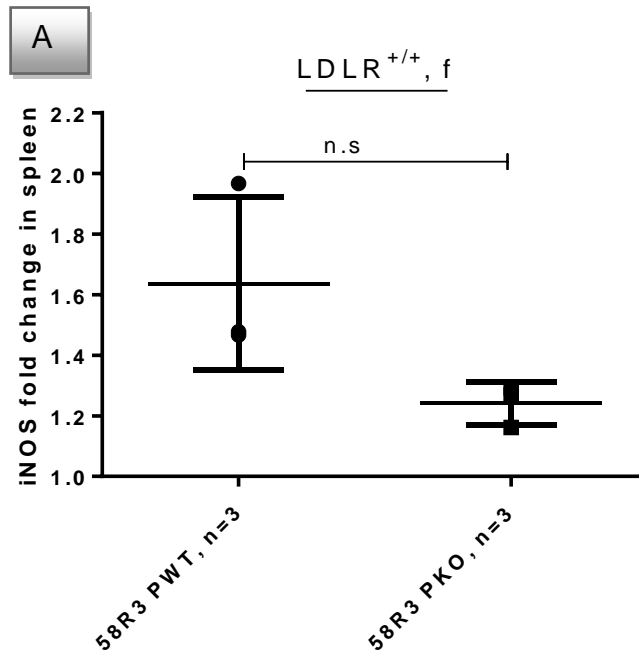


Figure 5-24 The effect of properdin on hepatic and splenic gene expression of iNOS.

Female LDLR^{-/-}, LDLR^{+/+} mice fed high fat high sugar diet (58R3), Western diet (5TJN), low fat diet (5LF2) on splenic gene expression of iNOS (Panel A). Female LDLR^{-/-} and LDLR^{+/+} mice fed high fat high sugar diet (58R3) on hepatic gene expression of iNOS (Panel B). Results are presented as averages ±SD from triplicate determinations. **p* < 0.05 (adjusted *p*-values), ns=no significant.

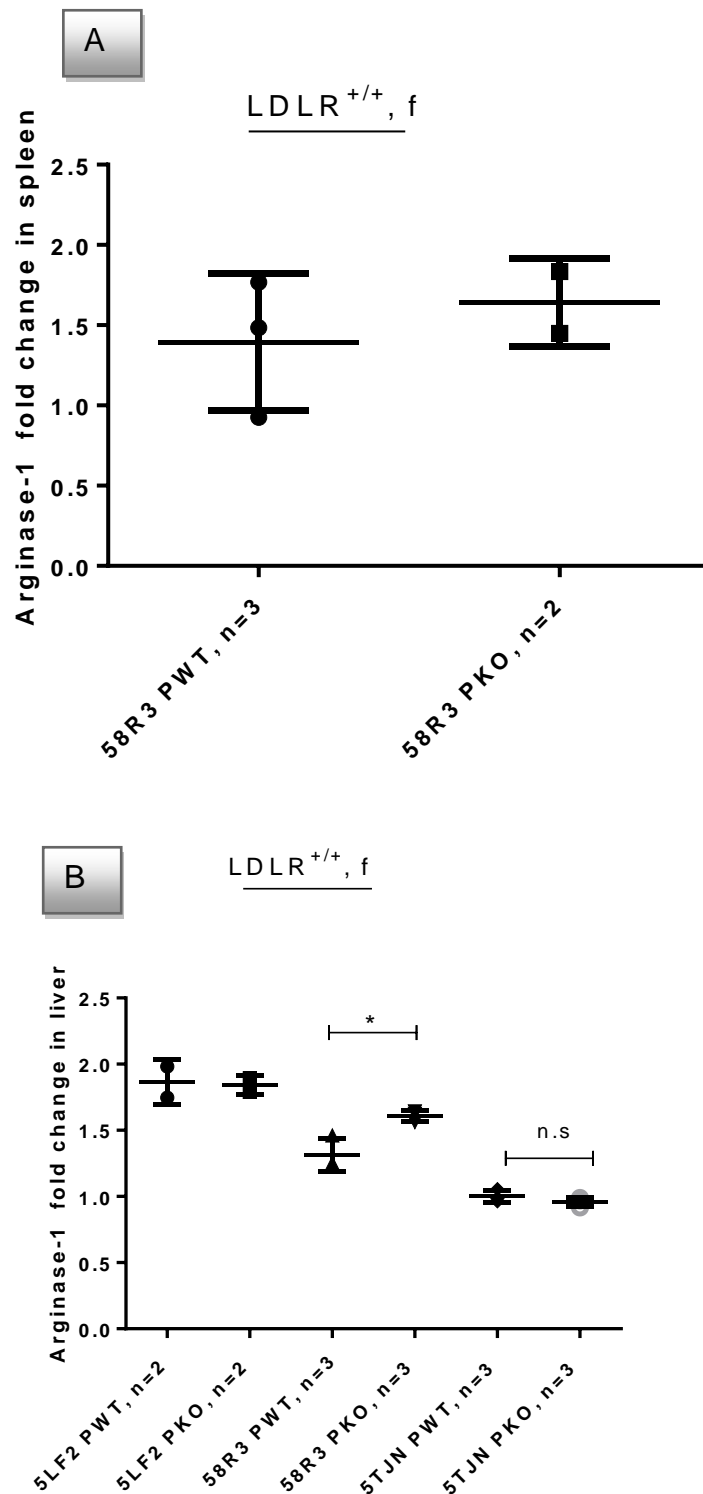
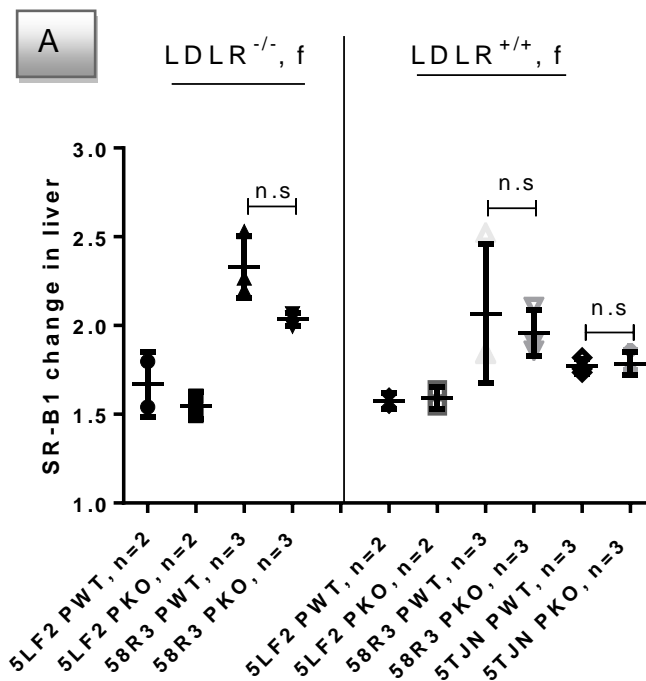


Figure 5-25 The effect of properdin on hepatic and splenic gene expression of Arginase-1.

Mice fed high fat-high sugar diet (58R3), Western diet (5TJN), and low fat diet (5LF2). Splenic mRNA expression of Arginase-1 in female LDLR^{+/+} mice (panel A), spleen mRNA expression of Arginase-1 in female LDLR^{+/+} mice (panel B). Results are presented as averages \pm SD from triplicate determinations. * $p < 0.05$, (adjusted p -values), n.s.=no significant.

5.2.1.12 Candidate genes involved in cholesterol metabolism (SR-B1, HMGCR and PPAR- γ)

In order to investigate whether properdin plays a role in cholesterol regulation, and prevention free cholesterol consequences, therefore candidate genes including SR-B1 (scavenger receptor class b1) (cholesterol uptake), HMGCR (3-hydroxy-3-methylglutaryl-co-enzyme A reductase) cholesterol synthesis and PPAR- γ (Peroxisome proliferator-activated receptor gamma) (Cholesterol regulation) were analysed. Interestingly, SR-B1 mRNA expression of LDLR^{-/-} PWT fed high fat-high sugar diet had a tendency to have higher compared to LDLR^{-/-}PKO fed high fat-high sugar diet (Figure 5.26, A). Interestingly, PPAR- γ mRNA expression in LDLR^{+/+}PWT fed high fat-high sugar diet had a tendency to have lower compared to LDLR^{-/-}PKO fed high fat-high sugar diet (Figure 5.26, C). These results suggested that properdin deficiency may lead to the increase of cholesterol synthesis, and dysregulation of cholesterol metabolism, and this was observed mainly in the groups receiving a high fat-high sugar diet. It is possible that the added sugar aggravates the metabolic compromise found in the absence of properdin.



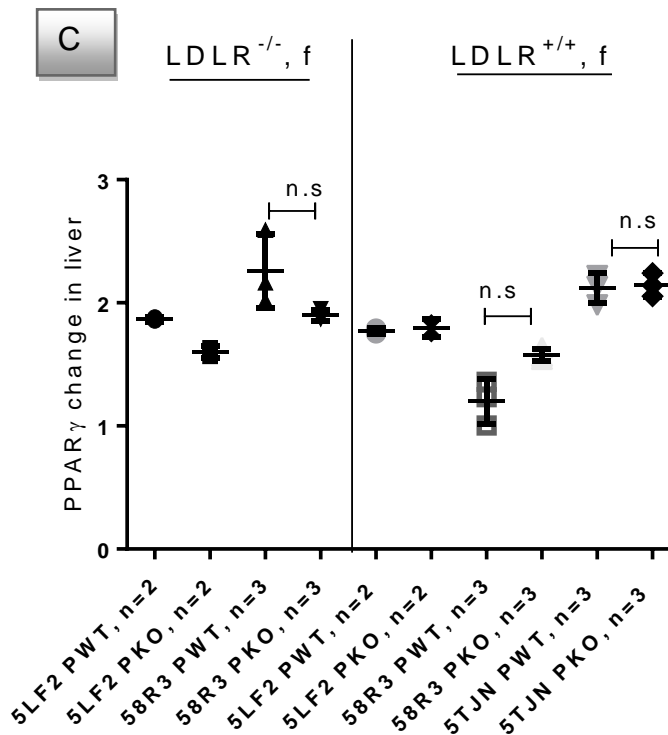
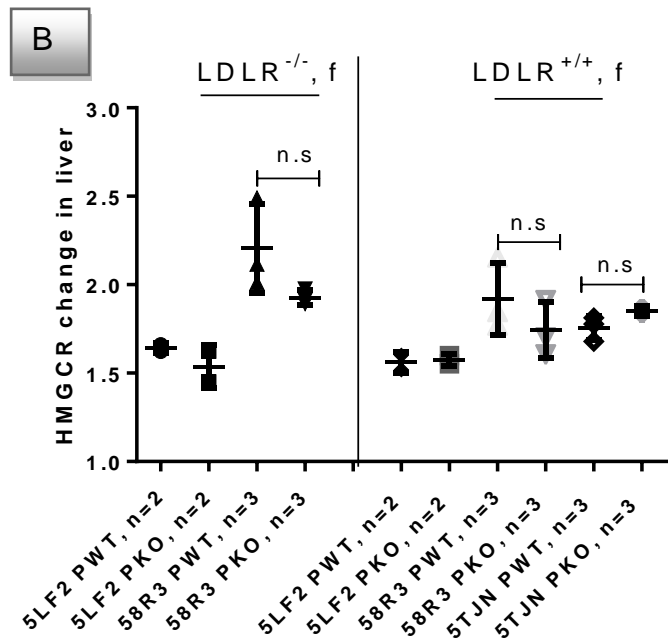


Figure 5-26 The effect of properdin on hepatic gene expression of SR-B1, HMGCR and PPAR γ .

Mice fed high fat-high sugar diet (58R3), Western diet (5TJN), and low fat diet (5LF2). Liver mRNA expression of SR-B1 in female LDLR^{-/-}, LDLR^{+/+} mice (Panel A), liver mRNA expression of HMGCR in female LDLR^{-/-}, LDLR^{+/+} mice (panel B), liver mRNA expression of PPAR γ in female LDLR^{-/-}, LDLR^{+/+} mice (Panel C). Results are presented as averages \pm SD from triplicate determinations. * $p < 0.05$ (adjusted p -values), n.s=no significant.

5.2.1.13 Analysis of adipokinins in epididymal fat pads

The main purpose of performing microarray was to see the effect of Western diet in the presence and absence of properdin on mice adipose tissue. IGFBP-2, 3, 5, 6 (Insulin like growth factor binding protein-2, 3, 5, 6) had a tendency to have lower in properdin wild type mice compared to properdin deficient mice (Figures 5.27, Panels A and B). Adiponectin had a tendency to have lower in properdin wild type compared to properdin deficient mice (Figures 5.27, Panels A and B). Feutin- A, MCP-1, and lipocalin-2 had a tendency to have higher in properdin deficient mice compared to properdin wild type mice (Figures 5.27, Panels A and B). In conclusion, it can be observed that protein involved in fibrosis, steatosis, inflammation, metabolic syndrome disease were higher in properdin deficient mice compared to properdin wild type mice (Figure 5.27, Panels A and B). VEGF, FGFacidic, C-reactive protein, and DPPIV proteins were not changed. To see how properdin affects apoptosis, apoptosis was measured.

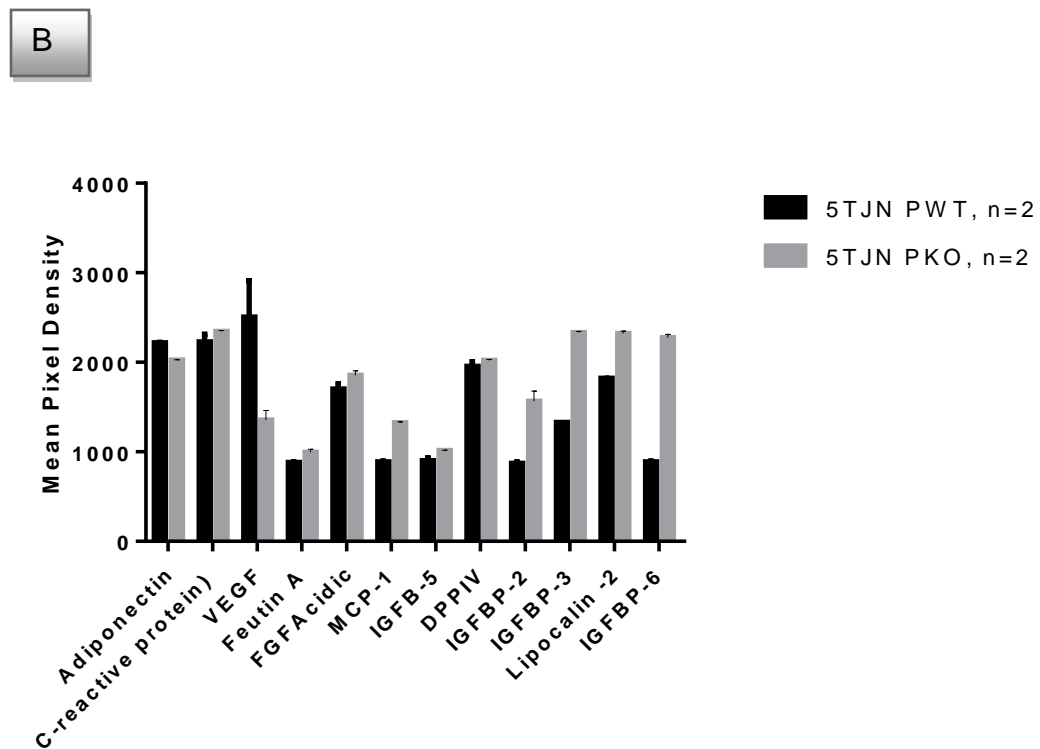


Figure 5-27 The Mouse adipokine array detects multiple protein analyses in adipose tissue of wildtype and deficient mice.

Proteome profile mouse adipokine array in mice fed Western diet with (5TJN PWT), and without properdin (5TJN PKO) (Panel A), mice fed high fat high sugar diet with, and without properdin PKO vs PWT (Panel B). Adipose tissues were excised and prepared as described in the adipose tissue array preparation.

5.2.1.14 Apoptosis in liver

Apoptosis is a key mechanism in the progression and the development of fatty liver disease (Rensen et al., 2009a). Properdin can bind to late apoptotic or necrotic cells, it plays as a focal point for local amplification of alternative pathway complement activation (Xu et al., 2008). In order to investigate the properdin effect on the liver cell damage, apoptosis was measured by cytochemical stain using ApopTag[®] *In Situ* Apoptosis Detection Kits (Millipore, Cat no. S7100). The result showed that the tendency to have more apoptosis was higher in properdin wildtype mice compared to properdin deficient mice fed high fat diet (Figure 5.28, B). In order to know whether properdin plays a role in complement activation and C5a activity, classical, alternative pathways, and C5a ELISA was measured.

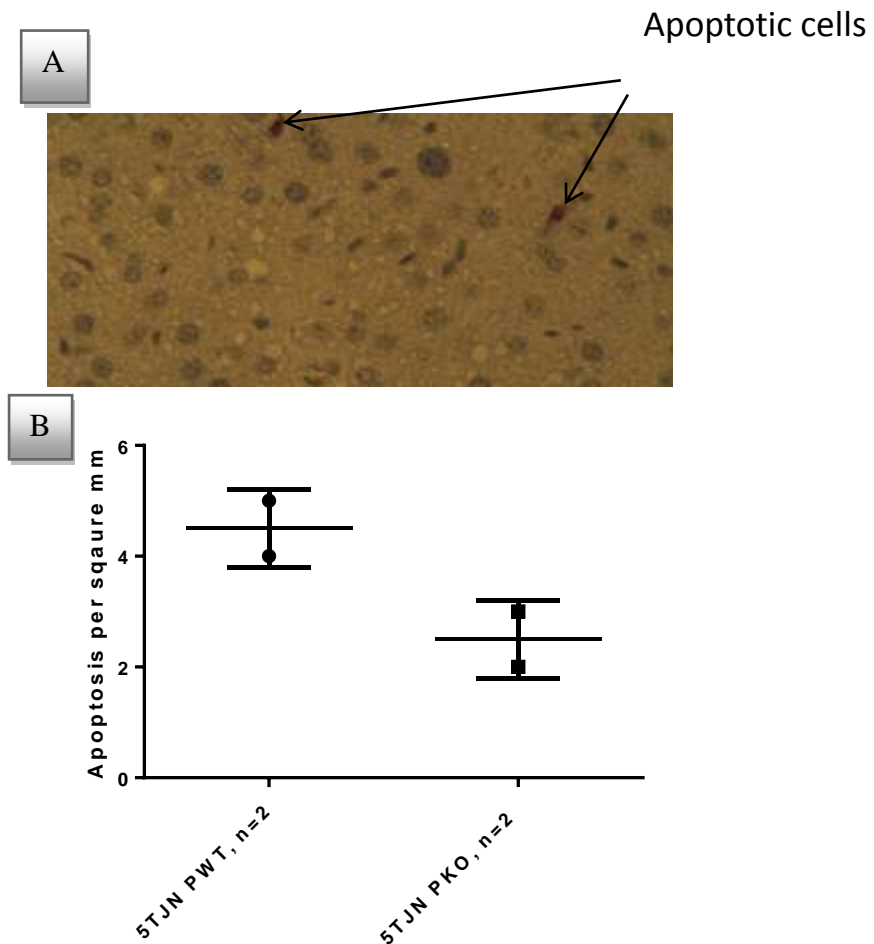
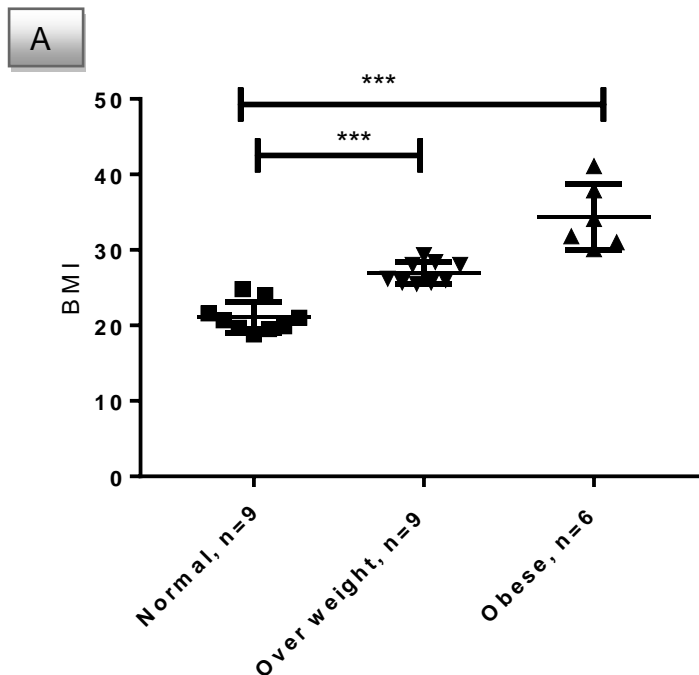


Figure 5-28 Apoptosis test for liver sections of western diet.

A positive liver apoptosis example (panel A), positive cells were counted over five mm² grids (B).

5.2.1.15 Human serum alternative, and classical pathway

Alternative, and classical pathway activation tests were performed for normal, overweight, and obese people. The cohort analysed was taken from a published study while ethical approval was valid (investigation of inflammatory markers in sepsis, PI Prof Jonathan Thompson, (Stover, 2015). Serum samples were stored at -80°C, and heat lability of appropriately diluted samples was verified (56°C, 30 min, data not shown). The aim was to study whether obesity plays a significant role in the increase of classical, and alternative pathway activation in vivo. Because oxidized LDL caused classical complement activation in human serum (Saad et al., 2006), we tested classical pathway activation in serum at the level of C9. Chylomicron accelerates C3 tick-over by regulating the role of factor H, leading to the overproduction of ASP resulting in acceleration of alternative pathway activation (Fujita et al., 2007). The assay captures residual activities of the serum prepared from blood which is activated in vivo. BMI is plotted in Figure 1. Our results showed that normal people had higher residual activity of the classical pathway, and alternative pathway compared to obese people (Figure 2, Figure 3). The elevation of residual activity in normal people was the result of preserving activity in vivo.



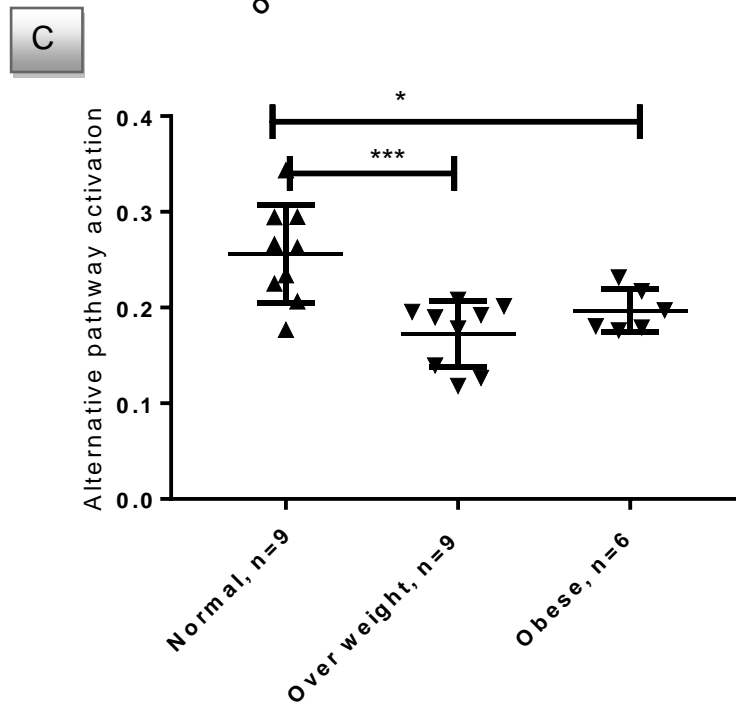
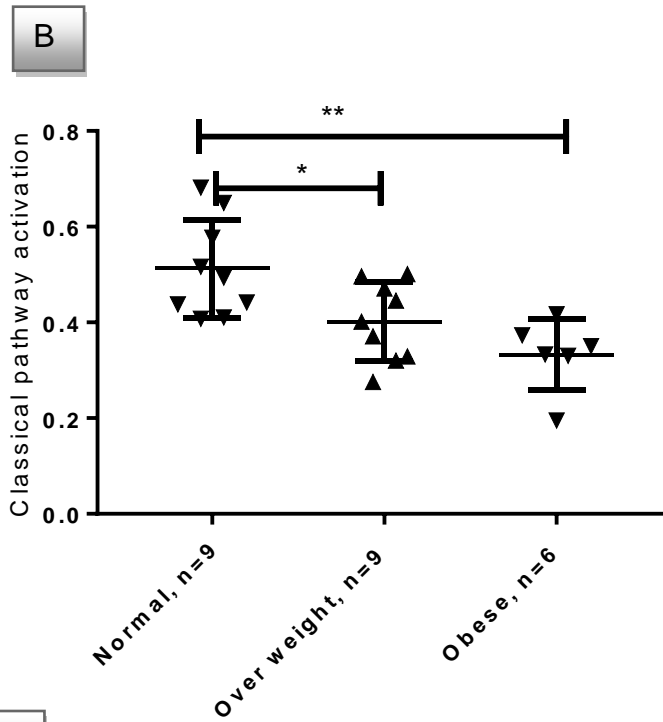


Figure 5-29 Body mass index (BMI), functional complement residual activities of human serum.

Classical pathway complement (CP), and alternative pathway complement (AP) at the level of formation of C9 (A-B). BMI (panel A), classical pathway activation (panel B), alternative pathway activation (panel C). Results are presented as averages \pm SD from triplicate determinations. * $p < 0.05$, ** $p < 0.01$, *** $p < 0.005$, **** $p < 0.0001$ (adjusted p -values), ns=no significant.

5.2.1.16 Effect of properdin on functional complement activation ELISAs (classical, and alternative pathway activation, and C5a level

The purpose was to study whether properdin plays a significant role in the decrease or increase of classical, and alternative pathway activation *in vivo*. Because oxidized LDL caused classical complement activation in human serum (Saad et al., 2006), therefore we tested classical pathway activation in serum of mice at the level of C9. The effect of high fat diet on complement activity has not yet been investigated in mice.

Our results showed that properdin deficient mice fed high fat high sugar diet had lower residual activity of the classical pathway compared to properdin wild type mice (Figure 5.30, panels A, B). In addition, properdin wild type mice in mice fed Western diet had higher classical residual activity compared to properdin deficient mice (Figure 5.30, panels A, B). The elevation of residual activity in properdin wild type mice is the result of preserving activity *in vivo*. Our results showed that properdin wild type mice fed high fat-high sugar diet had higher alternative residual complement activities compared to properdin deficient mice, and lower than low fat diet (Figure 5.31, A). In properdin wild type mice group fed Western diet, C5a protein level was significantly higher compared to properdin deficient mice group (Figure 5.31, B). It can be concludes that the increase of residual activity in properdin wild type mice given high fat- high sugar diet as the result of preserving activity *in vivo*. Properdin is likely to exert its effect on classical, and alternative pathway indirectly (via increase of residual activity in properdin wild type group compared to properdin deficient mice group), and also caused the increase C5a levels. It appears that consumption of high fat diet leads to complement activation in serum (compare 5LF2 with 58R3 for WT), and that there is a requirement for alternative pathway amplification in this process (compare KO 5TJN with WT 5TJN, KO 58R3 with WT 58R3, and lack of difference for 5LF2).

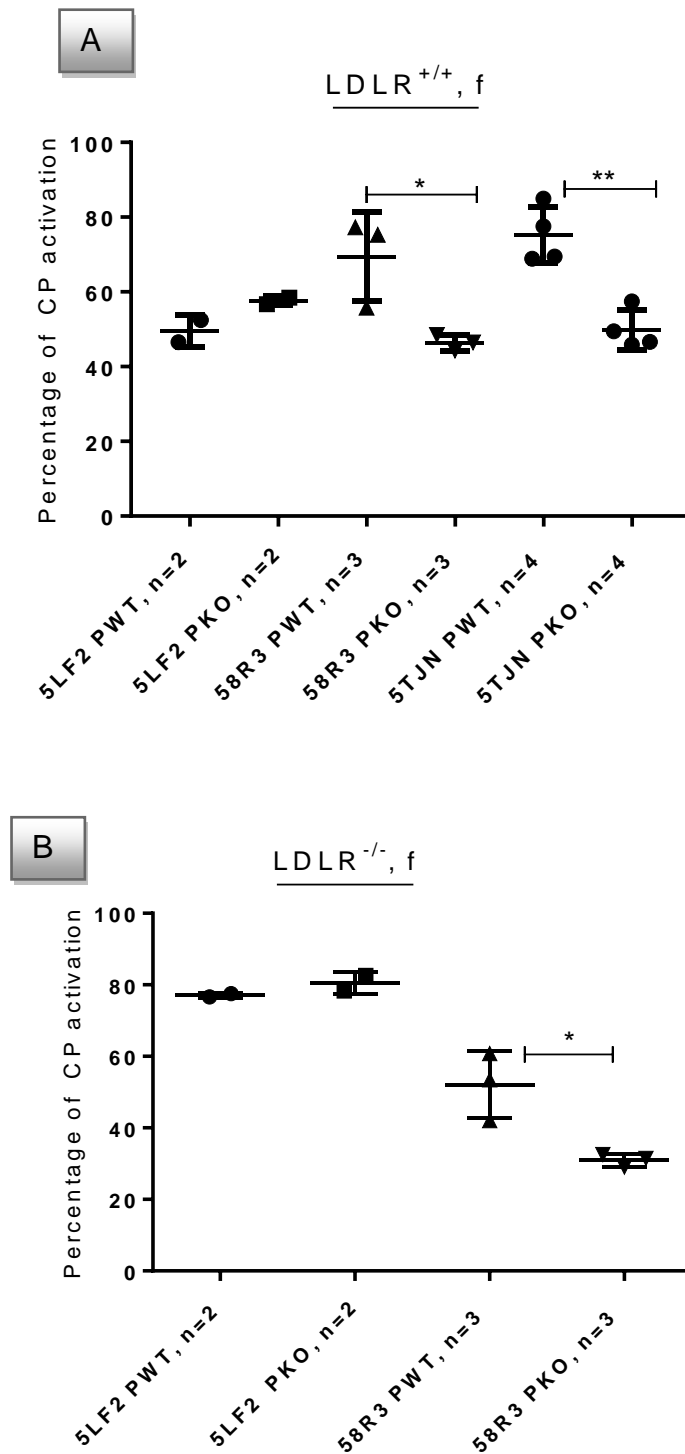


Figure 5-30 The effect of properdin on complement classical pathway activation in female mice sera.

Mice fed high fat-high sugar diet (58R3), Western diet (5TJN), and low fat diet (5LF2) (A-B). Effect of properdin on complement classical pathway activation in female LDLR^{+/+} mice (Panel A), on complement classical pathway activation in female LDLR^{-/-} mice (Panel B). Results are presented as averages \pm SD from triplicate determinations. * $p < 0.05$, ** $p < 0.01$ (adjusted p -values), ns=no significant.

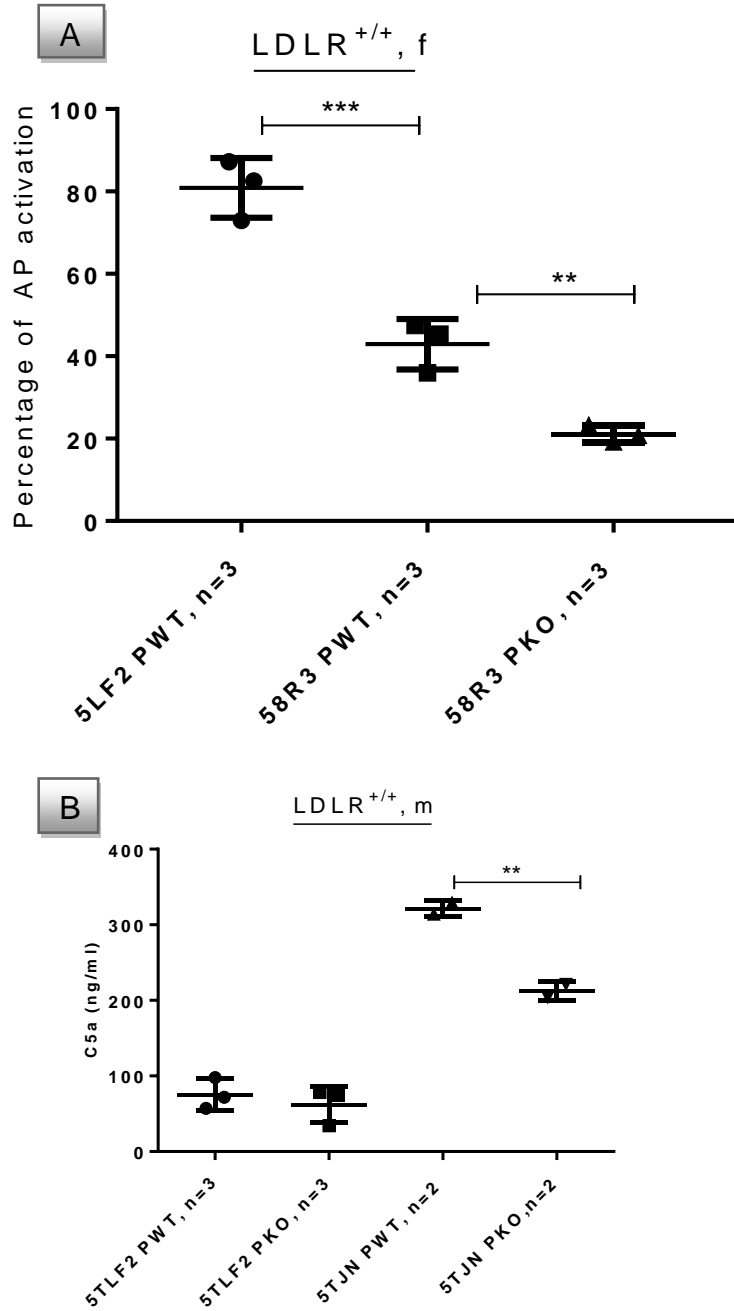


Figure 5-31 The effect of properdin on complement alternative pathway activation and C5a in mice sera.

Mice fed high fat-high sugar diet (58R3), Western diet (5TJN), and low fat diet (5LF2) (A-B). Effect of properdin on complement alternative pathway activation in female $LDLR^{+/+}$ mice (Panel A), effect of properdin on C5a level in male $LDLR^{+/+}$ mice (Panel B). Results are presented as averages \pm SD from triplicate determinations. * $p < 0.05$, ** $p < 0.01$, *** $p < 0.005$, **** $p < 0.0001$ (adjusted p -values), ns=no significant.

5.2.1.17 Serum Vitamin D level

The aim was to determine whether Vitamin D is increased in properdin deficient mice and properdin wild type of mice given high fat-high sugar diet. Our result showed that properdin deficient mice had a tendency of lower Vitamin D in properdin deficient mice of LDLR^{-/-} mice fed high fat-high sugar diet compared to properdin wild type mice, but no significant different between them (Figure 5.32, A). Interestingly, lower Vitamin D serum level (25.99±2.50) of LDLR^{+/+} PKO mice fed high fat-high sugar diet compared to properdin wild type mice (46.7±5.55) (Figure 5.32, B). It can be reported that in properdin deficient mice fed high fat-high sugar diet developed low serum Vitamin D in LDLR^{+/+} background.

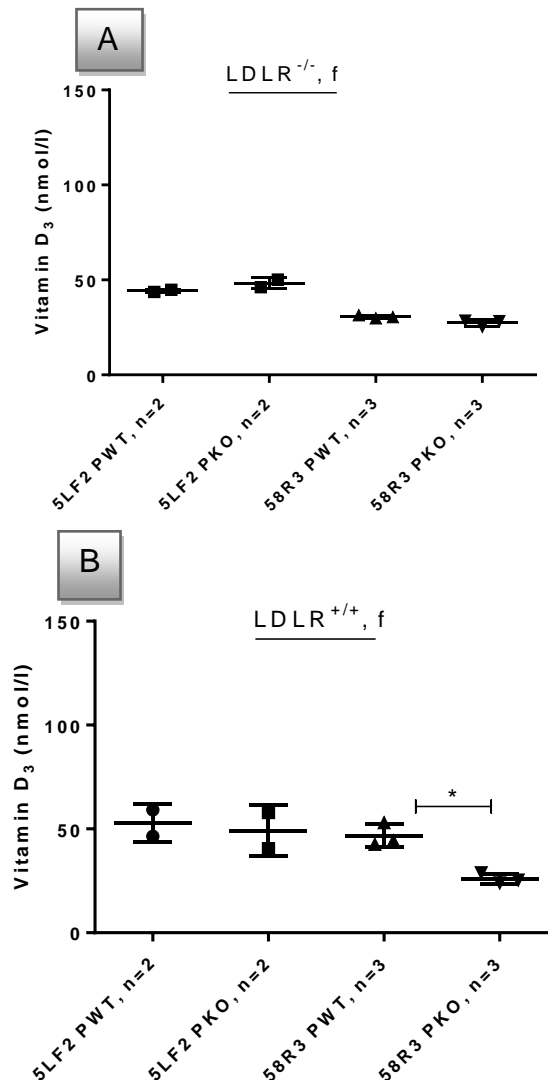


Figure 5-32 The effect of properdin on Vitamin D level of mice sera.

Mice fed high fat-high sugar diet (58R3), Western diet (5TJN), and low fat diet (5LF2) (A-B). Effect of properdin on Vitamin D level in female LDLR^{-/-} mice (Panel A), effect of properdin on Vitamin D level in female LDLR^{+/+} mice (Panel B). Results are presented as averages ±SD from triplicate determinations. **p* < 0.05 (adjusted *p*-values), ns=no significant.

Vitamin D is a lipophilic hormone, hypovitamin D and metabolic syndrome disease are associated with obesity (Barchetta et al., 2013). Because Triglyceride were higher in properdin deficient mice fed high fat-high sugar diet, and Western diet compared to wild type mice, the possibility of VD being less measurable because it is compartmentalised differently, needs to be considered.

5.2.1.18 Relationship of properdin, and C5L2 protein expression, and protein presence

Because ASP (Acylation stimulating protein) plays a role in TG synthesis so any impairment of ASP will lead to the increase of FFA influx to liver. ASP Impairment may lead to TG reduction, FFA influx to liver, VLDL secretion (HyperapoB), and LDL increase with at the result that insulin resistance will be developed (Kildsgaard et al., 1999, Paglialunga et al., 2008))

In C5L2 deficient mice fed a diabetogenic diet, mice developed insulin resistance after 12 weeks (elevated insulin, and glucose levels). The increase of triglyceride storage, and glucose transport in adipocytes has been linked with Acylation stimulating protein (ASP), which is a hormone secreted by the adipose tissue. These effects are mediated by C5L2 receptor, which has also been associated with inflammatory effects. C5L2 deficient mice on a low-fat diet are hyperphagic yet lean, due to increased energy expenditure. Previous study assessed insulin sensitivity, and metabolic, and inflammatory changes in C5L2KO mice vs WT in diet-induced obesity (Fisette et al., 2013). The aim was to see the effect of properdin on C5L2 mRNA expression and C5L2 protein presence. Our result showed that properdin wild type mice had a greater C5L2 mRNA expression in mice fed Western diet (Figure 5.33, A) and high fat high sugar diet (Figure 5.33, B) compared to properdin deficient mice.

Because mRNA expression was performed for adipose tissue therefore adipose tissue was homogenised then the protein was measured by Nano drop, and adjusted to same amount of protein. The aim was to investigate the difference between properdin wild type, and properdin deficient mice effect on C5L2 protein presence by Western blotting method. The Western blot result of

homogenised adipose tissue showed that C5L2 protein presence in properdin deficient mice fed Western diet, and high fat high sugar diet compared to properdin deficient mice (Figure 5.34).

For further investigation of C5L2 protein presence in properdin wild type, and properdin deficient mice, Western blotting was performed for homogenised liver. Interestingly, C5L2 protein presence in homogenised liver in properdin deficient mice of mice fed Western diet, and high fat high sugar diet was greater protein presence compared to properdin deficient mice (Figure 5.35). For further investigation of C5L2 protein presence in properdin wild type, and properdin deficient mice, immunohistochemistry was performed for liver, and adipose tissue.

Because C5L2 Western blot of homogenised adipose tissue and livers were higher in properdin wild type compared to properdin deficient mice, therefore immunohistochemistry for C5L2 was performed in adipose tissue and liver mice. Parts of adipose tissues, livers of 16 weeks' male LDLR^{+/+} mice, were fixed, paraffin embedded and 4µm slides were prepared. The aim was to further investigate the difference between properdin wild type, and properdin deficient mice. Our immunohistochemistry for C5L2 adipose tissue showed that properdin wild type mice had a greater C5L2 protein presence in adipose tissue in mice fed high fat-high sugar diet, and Western diet compared to properdin deficient mice (Figure 5.36). In addition, immunohistochemistry of liver mice showed that properdin wild type had more C5L2 protein presence in liver of mice fed western diet compared to properdin deficient mice (Figure 5.37). For further investigation of C5L2 protein presence in properdin wild type, and properdin deficient mice, immunofluorescent for adipose, and liver homogenised was performed. Because C5L2 Western blot of homogenised liver, and immunohistochemistry of C5L2 in liver parts was higher in properdin wild type compared to properdin deficient mice; therefore immunofluorescent staining of livers and adipose tissue were performed. The aim was to further investigate the difference between properdin wild type, and properdin deficient mice. Our immunofluorescent for C5L2 adipose tissue showed that properdin wild type had more C5L2 protein presence in liver of mice fed Western diet compared to properdin deficient mice (Figure 5.38). In addition,

immunofluorescent staining of livers for C5L2 protein showed that properdin wild type had more C5L2 protein presence compared to properdin deficient mice (Figure 5.39). It appears from our result that properdin deficient mice may have less lipid clearance therefore properdin deficient mice enhances metabolic syndrome disease. It was concluded that properdin deficient mice may have less lipid clearance therefore properdin deficient mice enhances metabolic syndrome disease.

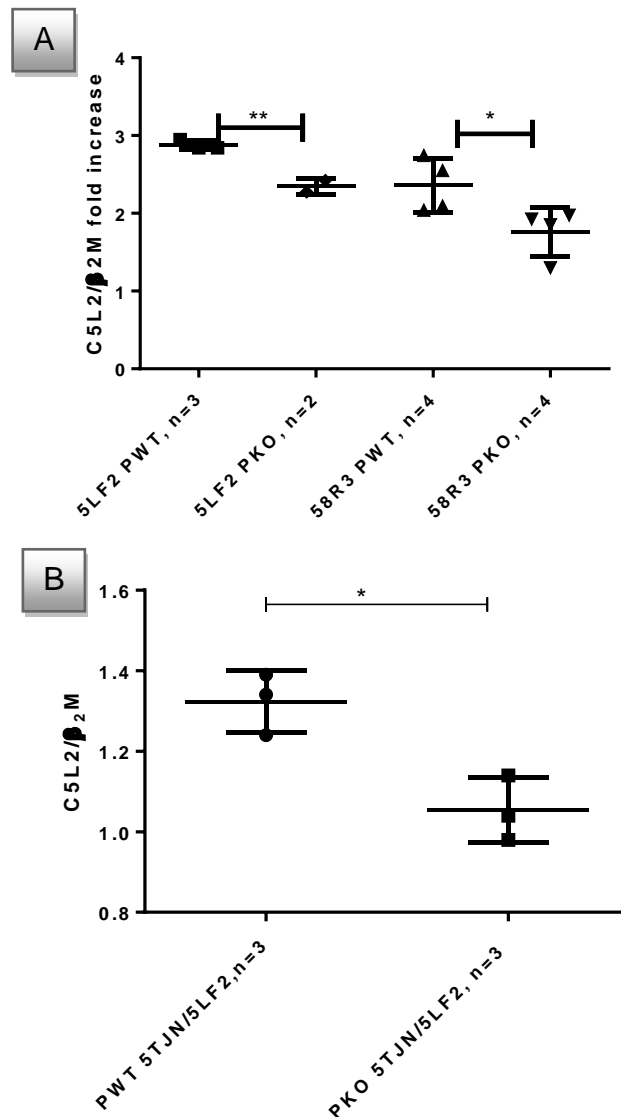


Figure 5-33 mRNA expression of C5L2 in adipose tissue.

The effect of properdin on adipose tissue gene expression of C5L2. Mice fed high fat-high sugar diet (58R3), Western diet (5TJN), and low fat diet (5LF2). Adipose tissue mRNA expression of C5L2 in male LDLR^{+/+} mice fed Western diet and low fat diet (Panel A), adipose tissue mRNA expression of C5L2 in male LDLR^{+/+} mice fed high fat-high sugar diet and low fat diet (panel B). Results are presented as averages ±SD from triplicate determinations. **p* < 0.05, ***p* < 0.01, (adjusted *p*-values), ns=no significant.

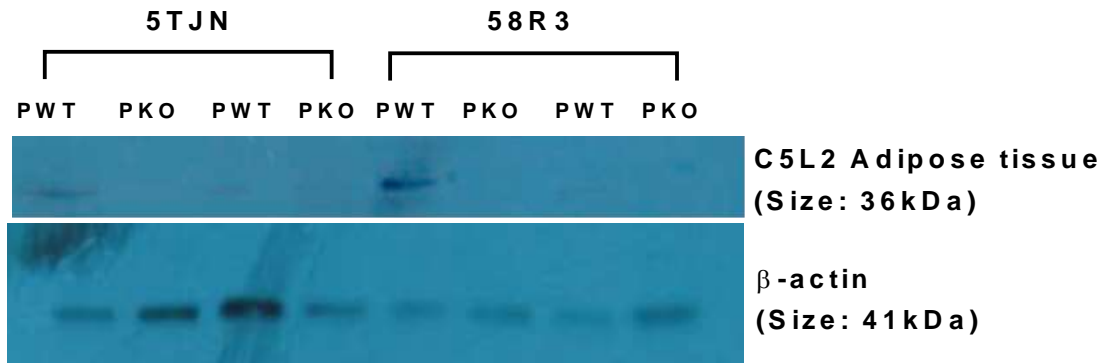


Figure 5-34 Western blot of C5L2 protein presence in adipose tissue. Properdin wild (PWT), and properdin deficient (PKO) of mice fed high fat-high sugar diet (58R3), and Western diet (5TJN) for 10 weeks.

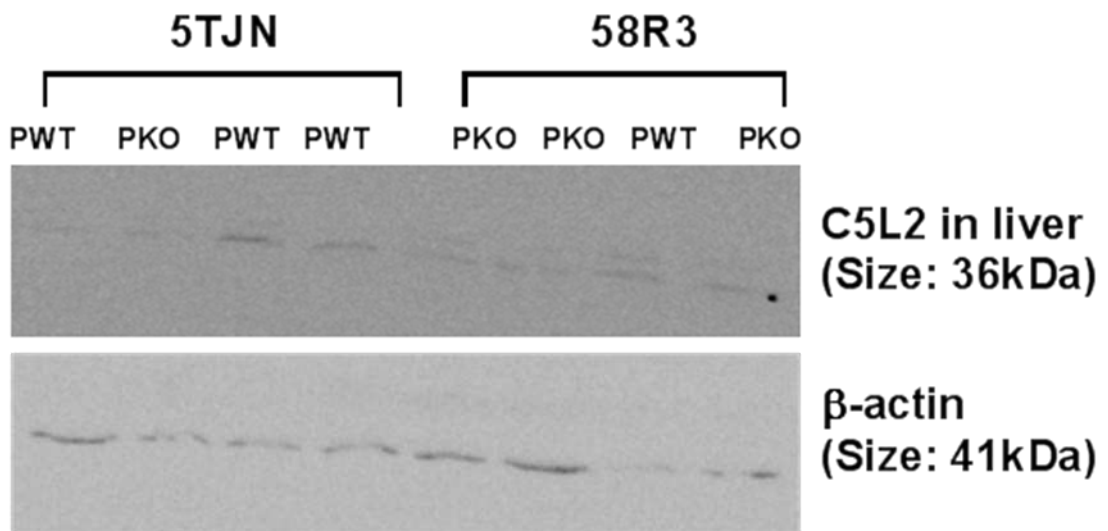


Figure 5-35 Western blot of C5L2 protein presence in livers. Properdin wild (PWT), and properdin deficient (PKO) of mice fed high fat-high sugar diet (58R3), and Western diet (5TJN) for 10 weeks.

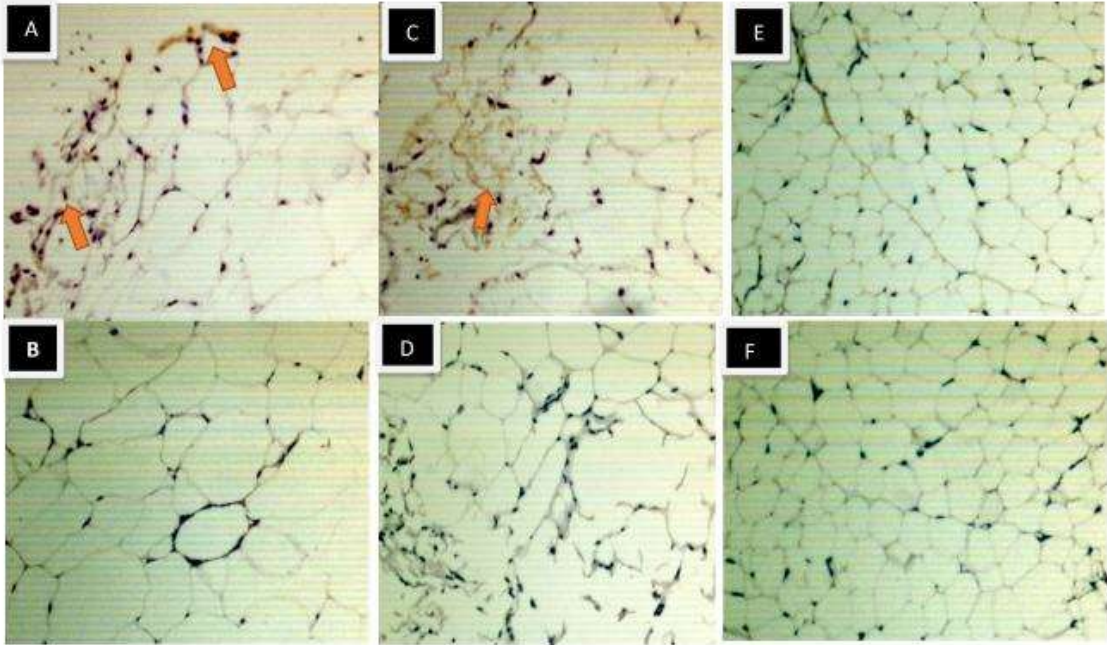


Figure 5-36 Immunohistochemistry of C5L2 adipose tissue of mice fed high sugar-high fat diet, and western diet.

C5L2 protein presence in adipose tissue of 10 weeks of properdin wild type, and properdin deficient of mice fed high fat-high sugar diet, and western diet.

Properdin wild type mice fed Western diet (panel A), properdin deficient mice fed Western diet (Panel B), Properdin wild type mice fed mice fed high fat high sugar diet (panel C), properdin deficient mice fed high fat high sugar diet (Panel D), mice fed low fat diet (Panel E), negative control (panel F)



Figure 5-37 Immunohistochemistry staining of livers of mice fed Western diet.

C5L2 protein presence in liver of 10 weeks of properdin wild type ,and properdin deficient mice fed high fat-high sugar diet ,and Western diet (A-C). Properdin wild type mice (panel A) properdin deficient mice (Panel B), negative control (panel C).

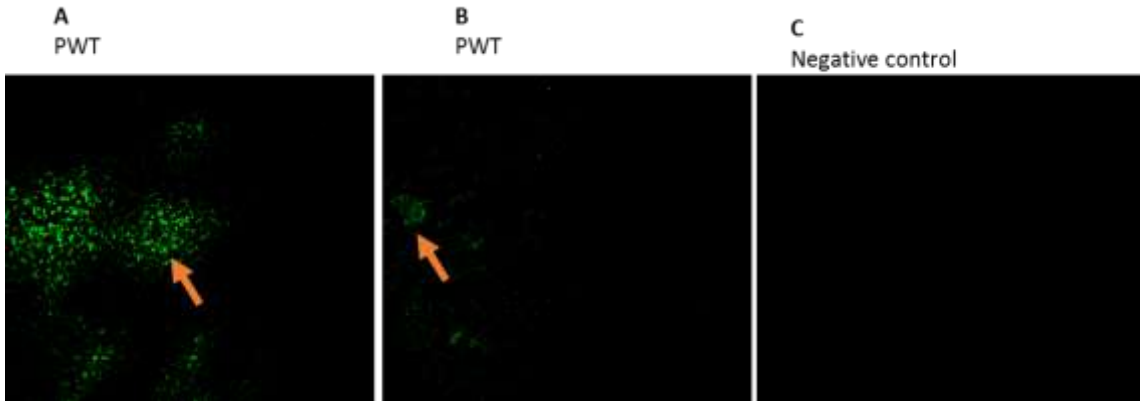


Figure 5-38 Immunofluorescent for adipose tissue of mice fed Western diet.

C5L2 protein presence in adipose tissue sample of 10 weeks of properdin wild type ,and properdin deficient mice fed Western diet (A-B). Properdin wild type mice (panel A) properdin deficient mice (Panel B), negative control (panel C).

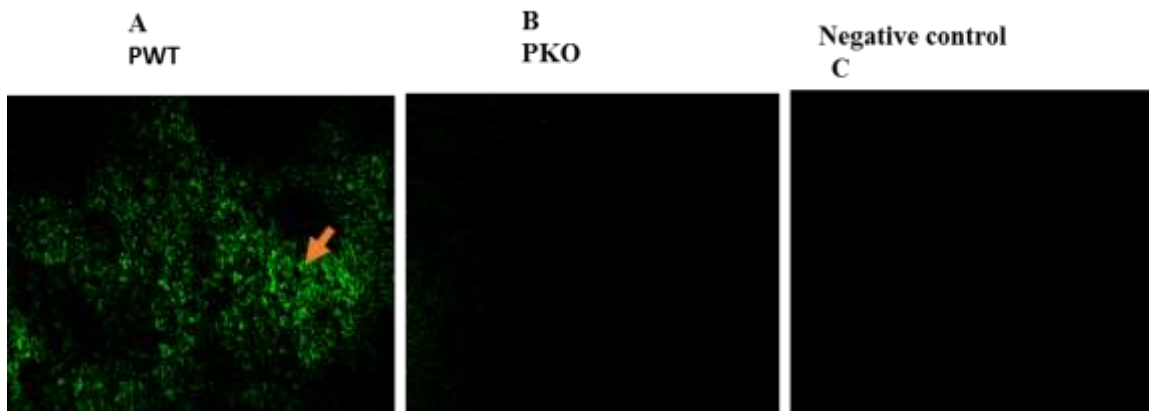


Figure 5-39 Immunofluorescent for livers of mice fed Western diet.

C5L2 protein presence in liver of 10 weeks of properdin wild type, and properdin deficient mice Western diet (A-B). Properdin wild type mice (panel A) properdin deficient mice (Panel B), negative control (panel C).

5.2.2 Effect of properdin on Fatty liver disease in five weeks diet

Effect of properdin on NAFLD in 5 weeks given diet on Five weeks'

To investigate the role of properdin in a dietary model, properdin wild type, and properdin deficient mice were given high fat high sugar diet or western diet for 5 weeks. Age matched Female LDLR^{-/-}, Female LDLR^{+/+}, and male LDLR^{-/-}, LDLR^{+/+} were analysed.

20 male mice (4 LDLR^{-/-}PWT, and 7 LDLR^{-/-}PKO) (3 LDLR^{+/+}PWT, and 6 LDLR^{-/-}PKO), 14 female mice (4 LDLR^{+/+}PWT, 3 LDLR^{+/+}PKO, 3 LDLR^{-/-}PWT, 4 LDLR^{-/-}PKO) were given high fat-high sugar diet for 5 weeks, and also eighteen male mice were given western diet (9 LDLR^{+/+}PWT, 9 LDLR^{+/+}PKO).

5.2.2.1 Histopathology of livers from male LDLR^{-/-} mice in relation to properdin

5.2.2.1.1 Electron microscopic analysis

Mice had electron microscopic analysis of their livers performed. This analysis was qualitative in nature, but individual lipid droplets were measured as part of the documentation of findings. Properdin wild type mice given high fat-high sugar diet no large, only small, droplets were seen (Figure 5.40, A) representative image in a mouse, but large lipid droplets were seen (measuring up to 13.08 Micron) in properdin deficient mice fed high fat-high sugar diet (Figure 5.40, panel B). The results also showed that in properdin wild type mice fed high fat high sugar diet smaller mitochondria were observed (Figure 5.41, A), while mega mitochondria were observed in properdin deficient mice fed high fat-high sugar diet (Figure 5.41, B).

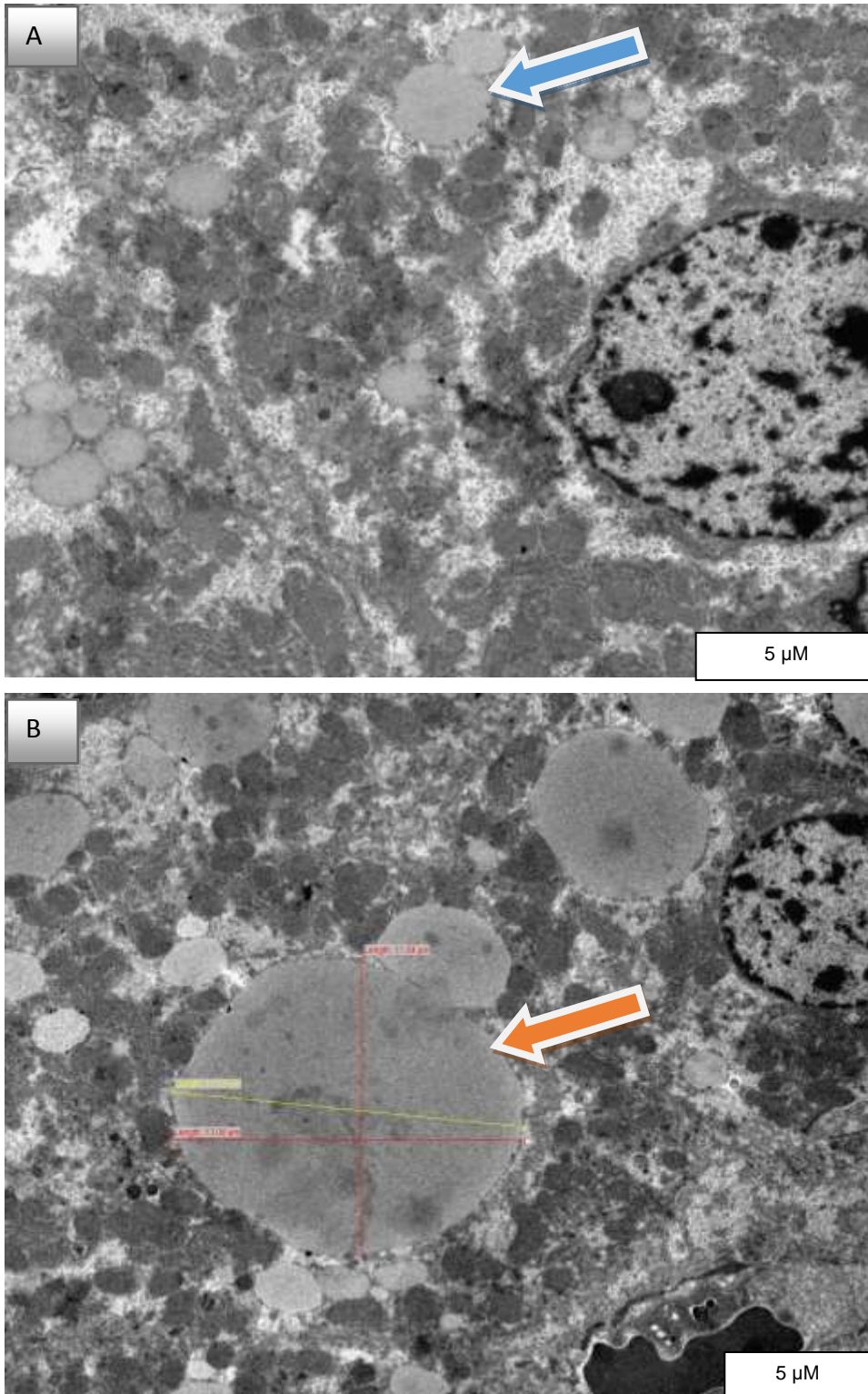


Figure 5-40 Electron micrograph showing fat droplets from livers of mice fed high fat diet for five weeks.

In properdin wild type (panel A), and properdin deficient mice (panel B). Small fat droplet (blue arrow) (panel A). Large fat droplets (orange arrows) (panel B). Five micron, N=nucleus. X8000.

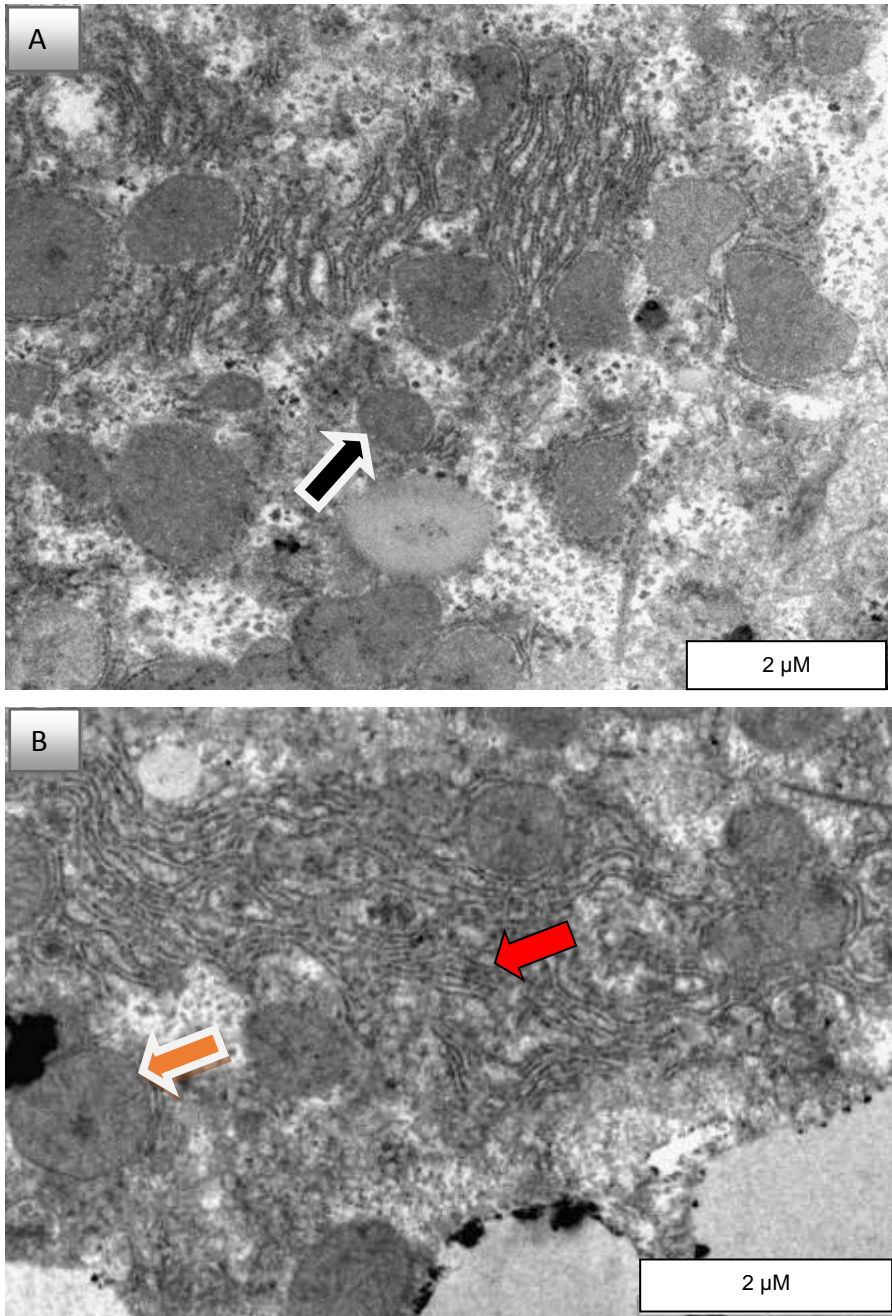


Figure 5-41 Electron micrograph showing mitochondria from livers of mice fed high fat diet for five weeks.

In properdin wild type (panel A) and properdin deficient mice (panel B). Normal mitochondria (black arrow) (panel B). A mega mitochondrion in the cytoplasm of a hepatocyte (orange arrows) (panel B), dilated, blebby, and more prominent distribution of rough endoplasmic reticulum (red arrow) (panel B), X8000.

According to Schonthal and colleagues dilated, blebby, and more prominent distribution of rough endoplasmic reticulum appeared due to endoplasmic reticulum stress (Schonthal, 2012). These were seen in properdin deficient mice (Figure 541, B).

5.2.2.1.2 Haematoxylin eosin staining of livers:

Parts of all livers mice were fixed, paraffin embedded, and 4 μ m slides were prepared. Fatty changes were predominately detected in properdin wild type mice. In properdin wild type mice, there were many microvesicular were seen (Figure 5.42, A). Macrovesicular (red arrows) (steatosis) presence of marked fatty changes near CV (zone 3) in middle column in high fat –high sugar diet in properdin deficient mice (Figure 5.42, B). It can be said that in properdin wild type mice, there was less evidence of steatosis, and inflammation, except some microvesicular, and a few macrovesicular fatty changes. Macro and microvesicular fatty changes refer to the size of the observed space that was occupied by fat prior to paraffin processing. Typically, macrovesicular fat accumulation is the size of a hepatocyte, while microvesicular accumulation appear as small droplets in size. These are accepted descriptive terms in histopathological evaluation of livers (Schwen et al., 2016).

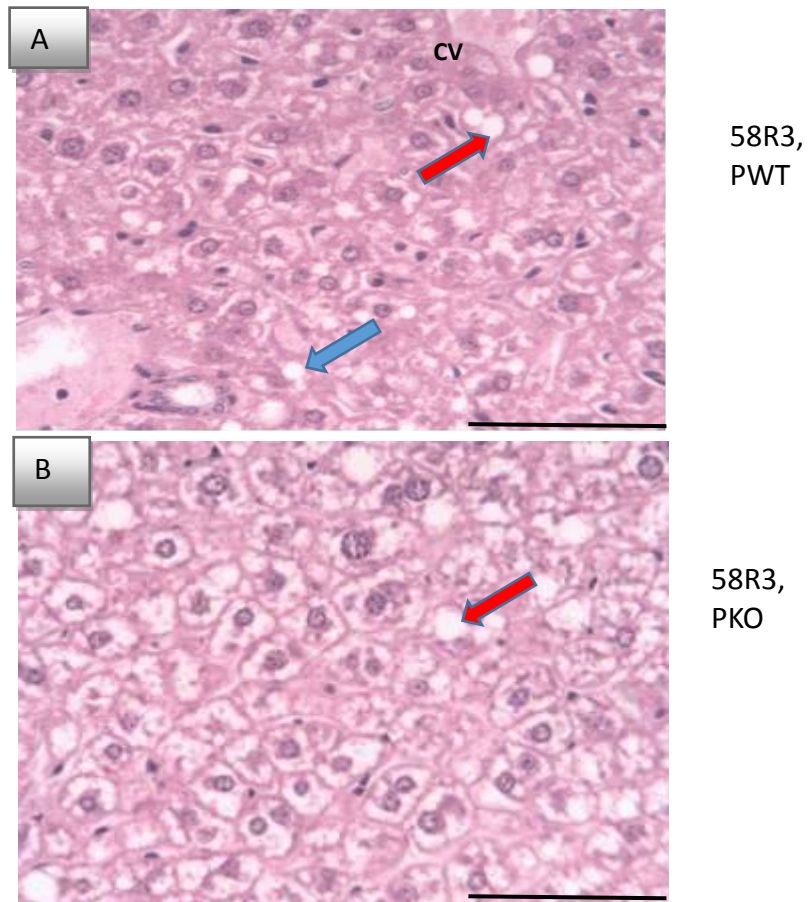


Figure 5-42 Haematoxylin and eosin staining of paraffin embedded liver sections obtained from mice.

Representative images of male mice. Mice fed high fat-high sugar diet for five weeks, properdin wild type mice (panel, A), properdin wild type mice (panel, B). Microvesicular (blue arrows), macrovesicular (red arrows) (steatosis) CV, central vein 100x. Scale bars represents 100 Micron.

The data from Haematoxylin eosin staining highlighted that, properdin deficient male $LDLR^{-/-}$ background mice given high fat high sugar diet for five weeks developed steatosis.

Fatty liver changes are difficult to quantify based on the regional differences within the liver (Schwen *et al.*, 2016). Therefore, a state of the art analysis using magnetic resonance imaging (MRI) was applied to determine a numerical difference in NAFLD for properdin wild type and properdin deficient.

5.2.2.1.3 Magnetic resonance imaging (MRI) from PKO, and PWT liver mice

The main reason for understanding MRI on mouse livers was to accurately measure the amount of lipids present in livers of properdin deficient mice compared to properdin wild type. Previous haematoxylin, eosin, and electron microscopy of livers showed that larger fat droplets were seen in properdin deficient mice compared to properdin wild type. Our MRI results showed that fat fraction % was significantly higher in properdin deficient mice compared to properdin wild type mice (Figure 5.43) (regardless diet), it was higher in in both male and female properdin deficient mice (Table 5.8).

Table 5.8 MRI of mouse livers from female, and male mice.

Diet	Fat fraction % In Male Genotypes		Fat fraction % In Female Genotypes	
	PWT	PKO	PWT	PKO
5TJN	8%	15.6%	Nil	Nil
58R1	6.8%	13.3%	Nil	Nil
58R3	7.4%	12.8%	8.6%	12.9%

Five weeks mice given a Western diet (5TJN), high fat high sugar diet (58R3) or low fat diet (58R1).

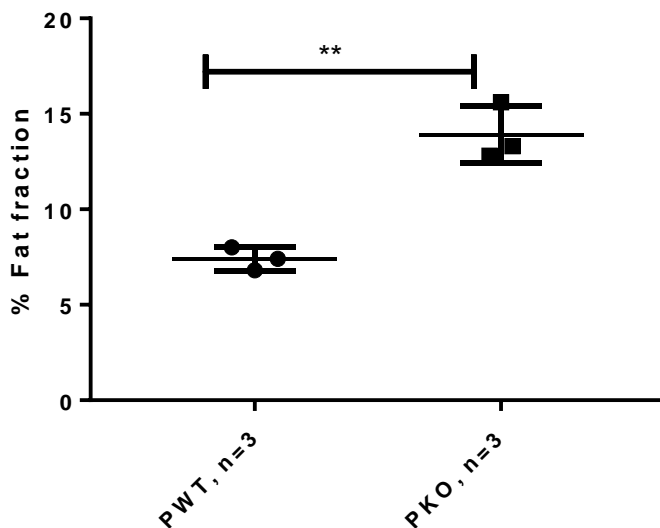


Figure 5-43 Percentage fat fraction using MRI of mouse livers from male mice (regardless diet).

Properdin wild type mice (PWT), properdin deficient mice (PKO).The data are represented as means \pm SD (** $p < 0.01$).

5.2.2.2 Body weight, and fat pad weight percentage

There was a tendency to be higher percentage fat pad weight, and body weight percentage in male LDLR^{-/-}properdin deficient mice fed high fat-high sugar diet compared to wild type mice (Table 5.10). This agrees with Gauvreau *et al.*, (2012) who showed that properdin deficient mice had higher body weight, and fat pad weight compared to properdin wild type mice. In addition, male LDLR^{+/+}properdin deficient mice fed Western diet had higher fat pad weight, and body weight in properdin deficient mice compared to wild type mice (Table 5.12). There were no significant differences in body weight, and fat pad percentage between properdin deficient mice and properdin wild type mice fed Western diet and high fat-high sugar diet (Tables 5.11).

5.2.2.3 Effect of properdin on Liver function

The previous ten-week study revealed that properdin deficient mice developed liver damage. To investigate liver damage mice fed high fat-high sugar diet for five weeks, liver function tests were performed. In male LDLR^{-/-}properdin deficient mice given high fat-high sugar for five weeks, an increase of liver transaminases was detected compared to properdin wild type mice group (Table 5.9). In the absence of properdin, hepatic damage markers, such as AST, and ALT, were increased compared to properdin wild type mice group (Table, 5.9).

5.2.2.4 Effect of properdin on endotoxin level and inflammation

A lower level of endotoxin was detected in properdin wild type compared to properdin deficient mice. Properdin wild type mice had lower IL-6, but was not significantly different compared to properdin deficient mice. The current data highlight the importance of properdin in an anti-inflammatory role, and prevents intestinal leakage (decreased endotoxin level) in five weeks (Table 5.9). Interestingly properdin has been reported to aid in LPS clearance (Kemper and Hourcade, 2008).

5.2.2.5 Effect of properdin on metabolic syndrome

In five weeks, in male LDLR^{-/-} properdin deficient mice, fed high fat-high sugar diet, led to the increase of insulin resistance possibilities, this was due to high insulin level, high glycated haemoglobin, and low adiponectin level compared to

properdin wild type mice (Table 5.9). In properdin deficient mice given high fat-high sugar diet had higher metabolic syndrome such as NEFA, TG, and lipid peroxidation compared to properdin wild type (Table 5.9).

Our results showed in male properdin deficient mice given high fat-high sugar diet for five weeks developed NAFLD, and metabolic syndrome disease, interestingly, properdin wild type mice resulted in the less NAFLD, and metabolic syndrome.

It can be concluded that properdin plays a significant role in the prevention of steatosis inflammation, insulin resistance, and metabolic syndrome disease in male LDLR^{-/-} mice, and female LDLR^{+/+} mice fed high fat –high sugar diet. In addition, male LDLR^{+/+} mice fed western diet may lead to the possibility of metabolic syndrome disease in properdin deficient mice compared to properdin wild mice.

Table 5.9 Male mice, mice given high fat-high sugar diet for five weeks.

Measurements	M LDLR ^{-/-} PWT, 58R3, n=4	M LDLR ^{-/-} , PKO, n=7
Percentage of body weight gain	19.34 +/- 10.24 (control was 9.70 3.52)	21.8 +/- 6.35 ^{n.s} (control was 16.05 +/- 0.91)
Percentage of fat pad weight	3.215 +/- 0.69 (control was 1.92 +/- 0.85)	4.357 +/- 0.60* (control was 2.33 +/- 0.66)
AST Mean +/- SD	124.3 +/- 13.07 (control was 78.27 +/- 6.99)	135.9 +/- 11.85 (control was 96.98 +/- 6.97**)
ALT (IU/L) Mean +/- SD	68.54 +/- 5.11 (control was 45.77 +/- 9.65)	91.09 +/- 11.08* (control was 79.99 +/- 1.32)
Insulin (ng/ml) Mean +/- SD	1.95 +/- 0.51 (control was 0.59 +/- 0.04)	4.43 +/- 1.37* (control was 0.76 +/- 0.14)
Adiponectin (µg/l) Mean +/- SD	2.09 +/- 0.11 (control was 2.69 +/- 0.10)	1.61 +/- 0.24* (control was 2.36 +/- 0.28**)
HbA1c (fm/l) Mean +/- SD	61.19 +/- 8.85 (control was 6.97 +/- 2.32)	70.92 +/- 10.07 ^{n.s} (control was 29.83 +/- 23.6)
Triglyceride (mg/dl) Mean +/- SD	65.85 +/- 11.64 (control was 39.42 +/- 7.27*)	125.3 +/- 40.83* (control was 43.2 +/- 8.67)
NEFA (mmol/l) Mean +/- SD	0.59 +/- 0.01 (control was 0.33 0.03)	0.82 +/- 0.01*** (control was 0.06 0.03)
Endotoxin (IU/ml) Mean +/- SD	5.57 +/- 0.58 (control was 2.105 0.92**)	12.98 +/- 2.97*** (control was 3.22 0.51)
IL-6 (ng/ml) Mean +/- SD	13.68 +/- 3.05 (control was 6.80 ± 0.07)	17.4 +/- 2.77 ^{n.s} (control was 9.32 ± 0.73)
MDA (µmol/l) Mean +/- SD	0.30 +/- 0.01 (control was 0.18 +/- 0.00)	0.32 +/- 0.01* (control was 0.20 +/- 0.01)

Male LDLR^{-/-}PWT/PKO mice fed high fat high sugar diet (58R3) for five weeks. Comparisons were between: control values vs 58R3, and LDLR^{-/-}PWT vs LDLR^{-/-}PKO. Results are presented as averages ±SD from triplicate determinations. **p* < 0.05, ***p* < 0.01, ****p* < 0.005, *****p* < 0.0001 (adjusted *p*-values), vs=versus, n.s=no significant.

For further investigation of the properdin role in mice given high fat-high sugar diet for five weeks, female mice were used. Fourteen mice were fed high fat-high sugar diet (seven LDLR^{+/+} PWT/PKO, and seven LDLR^{-/-} PWT/PKO) for five weeks (Table, 5.10). The result showed that female properdin deficient mice developed NAFLD, and metabolic syndrome disease, which were less developed in wild type mice. Inflammation marker (IL-6), prediabetic (insulin), and metabolic syndrome such as NEFA were increased in properdin

deficient mice compared to properdin wild type mice in LDLR^{+/+} back ground mice . LDLR^{-/-}PKO mice had higher IL-6 compared to properdin wild type mice (Table 5.10).

Table 5.10 Female mice given high fat-high sugar diet for five weeks.

Genotypes	IL-6 (ng/ml) +/- SD	Insulin (ng/ml) +/- SD	NEFA (mmol/l) +/- SD	Percentage of body weight gain
LDLR^{+/+} PWT	1.78 +/- 0.06 (n=4)	1.76 +/- 0.16 (n=4)	0.27 +/- 0.05 (n=4)	20.37 +/- 0.90, (n=4) (control was 1.1 +/- 1.55 ^{***})
LDLR^{+/+} PKO	1.95 +/- 0.05* (n=3)	2.16 +/- 0.22*(n=3)	0.44 +/- 0.03 (n=3) **	18.67 +/- 7.55, (n=3).
LDLR^{-/-} PWT	2.15 +/- 0.09 (n=4)	2.13 +/- 0.01 (n=2)	0.23 +/- 0.02 (n=2)	10.45 +/- 3.60 (n=2) (control was 3.97 +/- 1.50, n=3)
LDLR^{-/-} PKO	2.44 +/- 0.18 (n=3)	2.24 +/- 0.006* (n=2)	0.37 +/- 0.04 (n=2)	0.7 +/- 0.98 (n=2)

Female LDLR^{-/-}PWT/PKO, LDLR^{+/+} PWT/PKO mice fed high fat high sugar diet (58R3) for five weeks). Comparisons were between LDLR^{+/+}PWT vs LDLR^{+/+}PKO, and LDLR^{-/-}PWT vs LDLR^{-/-}PKO. The data are represented as means ± SD (*p<0.05, **p < 0.01, ***p < 0.005), vs=versus

Table 5.11 Male mice given high fat-high sugar diet, and Western diet for five weeks.

Genotypes	Percentage of fat pad weight	Percentage of body weight gain
5TJN LDLR^{+/+} PWT	4.74 +/- 1.08 (n=4) (control was 2.07 +/- 0.88 *)	34.39 +/- 7.76 (n=4) (control was 2.75 +/- 2.70*)
5TJN LDLR^{+/+} PKO	4.01 +/- 1.62 (n=4) control was 2.65 +/- 0.02)	16.02 +/- 16.78 (n=4) (control was 6.56 +/- 2.46)
58R3 LDLR^{+/+} PWT	4.41 +/- 1.48 (n=3)	29.58 +/- 9.16 (n=3) (control was 3.97 +/- 1.50, n=3)
58R3 LDLR^{+/+} PKO	2.26 +/- 0.89* (n=6)	18 +/- 5.83 (n=6)

Comparisons were between 5TJN LDLR^{+/+}PWT vs 5TJN LDLR^{+/+}PKO, and 58R3 LDLR^{+/+}PWT vs 58R3LDLR^{+/+}PKO. The data are represented as means ± SD (*p<0.05), vs=versus

Table 5.12 Male mice given Western diet for five weeks.

Genotypes	Percentage of fat pad weight	Body weight
5TJN LDLR^{+/+} PWT	1.543 ± 0.18* (n=3)	37.17 ± 0.72*, P value=0.02 (n=3)
5TJN LDLR^{+/+} PKO	4.067 ± 0.54 (n=3)	30.33 ± 1.89 P value=0.02 (n=3)

Comparisons were between 5TJN LDLR^{+/+}PWT vs 5TJN LDLR^{+/+}PKO, and 58R3 LDLR^{+/+}PWT vs 58R3LDLR^{+/+}PKO. The data are represented as means ± SD (*p<0.05), vs=versus.

In conclusion, male and female properdin deficient mice given high fat-high sugar diet for five weeks developed NAFLD, the increase of insulin level, NEFA level compared to properdin wild type mice. All measurements were higher in mice given high fat-high sugar diet for ten weeks compared to mice given high fat-high sugar diet for five weeks. The tendency to get metabolic syndrome disease was higher in male mice given high fat-high sugar diet for five weeks compared to female mice given high fat-high sugar diet for five weeks, based on elevated NEFA, and IL-6 levels.

5.3 Discussion

Properdin deficient female, and male LDLR^{+/+} mice fed high sugar-high fat diet had greater body weight gain, and central obesity (in male mice) compared to properdin wild type mice. This is coincidence with Gauvreau and colleagues who showed that properdin limited the diet induced increase of body weight, fat pad weight (Gauvreau et al., 2012). There is a correlation between complement activation and insulin resistance, severe obesity and diabetes mellitus type 2 (Kolev and Kemper, 2017). C1q deficient mice lead to the decrease of insulin resistance. In addition, CD55 (decay acceleration factor, DAF)-deficient animals, which is the key negative complement regulator, led to the increase of complement C3 and C5 activation. As a result, it developed the possibility to be appeared insulin resistance and the increase lipid adiposity (Lewis et al., 2011). Furthermore, the increase of classical pathway activation caused the elevation of triglyceride dysregulation, because adiponectin binding to C1q complement system leads to more C3a-desArg processing from C3a (Peake et al., 2008). There is an association between alternative pathway and the C3a-deArg metabolism because compared to mice control, C3-deficient and factor B deficient mice developed delayed triglyceride, NEFA and glucose tolerance (Paglialunga et al., 2008). Properdin deficient mice led to the increase of fat storage in mice given a high-fat diet and this is associated with decreased energy expenditure and delayed triglyceride clearance (Gauvreau et al., 2012). Liver histology showed that that female, and male LDLR^{+/+}PKO mice fed Western diet, and high fat-high sugar diet had greater liver steatosis, and lobular inflammation compared to LDLR^{+/+}PWT mice. Olive green stain, and electron microscopy showed that properdin deficient mice fed Western diet for 10 weeks developed severe steatosis, and all features of NAFLD, while in properdin wild type mice less steatosis was observed. To understand the further effect of properdin on steatosis, strebp-1c mRNA expression as a steatosis marker was performed. Complement components could enhance triglyceride (TG) formation by lipolysis inhibition, enhanced glucose, and FFA uptake, and the decrease of FFA release indirectly (Phieler et al., 2013). The result showed higher strebp-1c mRNA expression in properdin deficient mice compared to wild type mice fed high fat-high sugar diet. For further investigation of inflammation,

IL-6, and TNF- α in serum were measured. The current data highlight that male LDLR^{+/+} and female LDLR^{-/-} properdin deficiency mice led to the increase of IL-6 compared to properdin wild type mice in mice fed Western diet and high fat-high sugar diet. IL-6 level increased during expansion of adipose tissue which was more obvious in properdin deficient mice. Adipose tissue expansion which is associated with obesity the result it leads to the increase of FFA, inflammatory cytokines adipose tissue which impact insulin sensitivity and lipid metabolism disorders (Gutierrez et al., 2009). The current data highlight the importance of properdin in an anti-inflammatory role, and prevents intestinal leakage (decreased endotoxin level). Interestingly, properdin has been reported to aid in LPS clearance (Kemper and Hourcade, 2008). This coincidence with our result which showed that endotoxin level was higher in properdin deficient mice compared to properdin wild type mice. The empirical findings in this study provide a new understanding of properdin, and suggest that it plays a significant role in the prevention of steatosis. This is the first study to analyse liver function tests, to detect properdin effect in mice fed Western diet and high fat-high sugar diet in both LDLR^{-/-} ,and LDLR^{+/+} back grounds. The results showed that male properdin deficient mice fed Western diet had higher AST, and ALT levels compared to properdin wild type mice. However, ALT level was normal in female LDLR^{-/-} properdin deficient mice fed high fat-high sugar diet, so there might be a sex dependent effect for this observation. Insulin, adiponectin, and glycosylated haemoglobin were performed to investigate prediabetic features. My result showed that properdin deficiency in mice fed high fat-high sugar diet, and Western diet may play a role in the initiation of diabetes. To further understand the role of properdin in inflammation, endotoxin was measured. Relatively lower levels of endotoxin were seen in wild type mice which may mean increased properdin dependent clearance of LPS or decreased intestinal permeability, neither of which this study addressed mechanistically. This result concludes that properdin plays a significant role in the prevention of NAFLD, and NASH development, and also showed that Western diet, and high fat-high sugar diet affected the increase of endotoxin in circulation. Delayed postprandial TG clearance, and reduced adipocyte size were shown in C5L2-deficient mice fed a diabetogenic diet, and also some insulin resistance features, and inflammation were detected including higher glucose uptake, and

lipid deposition in the liver (Paglialunga et al., 2007). Properdin plays a significant role in complement activation which leads to the development more ASP initiates as a result triglyceride synthesis is increased, lipid storage in adipocytes and liver through C3a, C5a and C5L2 (Phieler et al., 2013). Our result showed that C5L2 mRNA expression was higher in in adipose tissue of properdin wild type mice compared to properdin deficient mice fed Western diet, high fat-high sugar diet and low fat diet. For further investigation of C5L2 protein presence in properdin wild type, and properdin deficient mice, Western blotting was performed for homogenised liver and adipose tissue. The result showed higher C5L2 expression in adipose tissue and liver of properdin wild type mice compared to properdin deficient mice. In addition, C5L2 protein presence in liver, and adipose tissue was higher in properdin wild type mice compared to properdin deficient mice by immunohistochemistry and immunofluorescent staining. It appears from our results that properdin deficient mice may have less lipid clearance, therefore properdin deficient mice have enhanced metabolic syndrome disease. Properdin increases NEFA level, in murine 3T3-L1 adipocytes, addition of properdin inhibited the insulin-mediated stimulation of fatty acid uptake, and incorporation into TG, but this experiment lacked a control (Gauvreau et al., 2012). However, our result showed that properdin prevented metabolic syndrome disease by the decrease of triglyceride, and NEFA serum level compared to properdin deficient mice. The differences were detected between our study and Gauvreau and colleagues study was in the high fat diet content used for establish the model. The differences were detected between our study was the high fat diet content given to mice. The fat percentage in our Western diet and high fat-high sugar diet study was 39.1 % and 59.4 % consequently, while the percentage of fat in Gauvreau and his collages study was 45 %. The elevation of lipopolysaccharide and NEFA, which are bound to TLR4, associated with insulin resistance (Gray et al., 2011). Adiponectin binds to C1q (Peake et al., 2008) which leads to classical pathway activation (Cui et al., 2009). As a result, more C5a, C3a and C5L2 are expressed. The high level of C5L2 leads to more lipid clearance, so our properdin wild type had less NEFA and NAFLD. Because our result showed that properdin deficient mice fed Western diet and high fat-high sugar diet had higher NEFA, TLR4, and endotoxin levels, and low adiponectin. Therefore, our

properdin deficient mice caused the obesity and insulin resistance. Properdin may also play a significant role in the decrease of MDA in male LDLR^{-/-} mice groups, and there was a tendency to higher Vcam-1 expression in aorta in properdin deficient mice compared to properdin wild type mice. However, no significant role of properdin in the initiation of MDA or vcam-1 was detected in female mice. The results showed that properdin deficient mice had higher M2-Macrophage activity; and it appears that properdin might play a role as maintaining M1-macrophage activity. Properdin deficiency may lead to the increase of cholesterol synthesis, and dysregulation of cholesterol. It can be observed that protein involved in fibrosis, steatosis, inflammation, and metabolic syndrome disease were significantly higher in properdin deficient mice compared to properdin wild type mice fed high fat-high sugar diet, and Western diet resulting in immune activation by leading to higher classical and alternative pathway activation in properdin wild type mice. Human serum results showed that highly classical and alternative pathway activation compared to overweight mice and normal people, this is agrees with Vors and colleagues who showed that comparing obese versus lean people, chylomicrons were higher and more enriched with LPS in obese people when compared with lean people (Vors et al., 2015). Chylomicron accelerates C3 tick-over by regulating the role of factor H, leading to the overproduction of ASP resulting in acceleration of alternative pathway activation (Fujita et al., 2007). Our adipose tissue microarray result showed that Lipocalin-2, and IGFB-5 was lower in properdin wild type mice compared to properdin deficient mice. However, they were higher in properdin wild type mice compared to properdin deficient mice (Gauvreau et al., 2012). Fetuin A (Trepanowski et al., 2015), Lipocalin-2, (Wang et al., 2007), IGFBP-6 (Insulin like growth factor binding protein, 6) (Shimasaki and Ling, 1991) are increased in obesity, and diabetic, overweight and NAFLD. All were higher in properdin deficient mice compared to properdin wild type. However, they were not significant differences between properdin wild type and properdin deficient mice (Gauvreau et al., 2012). The differences were detected between our study was the high fat diet content given to mice. The fat percentage in our Western diet and high fat-high sugar diet study were 39.1 % and 59.4 %, while the percentage of fat diet in Gauvreau and his colleagues study was 45 %. The other reason probably was that properdin deficient mice had lower C5L2 mRNA

expression and protein presence compared to properdin wild type, so less lipid clearance occurred in our properdin deficiency mice model. In a study comparing obese versus lean people, chylomicrons were higher and more enriched with LPS in obese people when compared with lean people (Vors et al., 2015). Chylomicron accelerates C3 tick-over by regulating the role of factor H, leading to the overproduction of ASP resulting in acceleration of alternative pathway activation (Fujita et al., 2007). The five week-study provided a meaningful time point in evaluating the development of metabolic changes induced by a high fat diet: Male and female properdin deficient mice given high fat-high sugar diet for five weeks developed NAFLD, the increase of insulin level, NEFA level compared to properdin wild type mice. There are association between elevation of NEFA, obesity, inflammation, dyslipidaemia, and insulin resistance state (Karpe et al., 2011). In five weeks, in male LDLR^{-/-} properdin deficient mice, fed high fat-high sugar diet, led to the increase of insulin resistance possibilities, this was due to high insulin level, high glycated haemoglobin, and low adiponectin level compared to properdin wild type mice. In properdin deficient mice given high fat-high sugar diet had higher metabolic syndrome such as NEFA, TG, and lipid peroxidation compared to properdin wild type. There are association between elevation of NEFA, obesity, inflammation, dyslipidaemia, and insulin resistance stat (Karpe et al., 2011). Our results showed in male properdin deficient mice given high fat-high sugar diet for five weeks developed fatty liver, and metabolic syndrome disease. Interestingly, properdin wild type mice resulted in the less fatty liver disease, and metabolic syndrome. Our results showed that female properdin deficient mice developed NAFLD, and metabolic syndrome disease, and less developed in the presence of properdin. Inflammation marker (IL-6), prediabetic (insulin), and metabolic syndrome such as NEFA were increased in properdin deficient mice compared to properdin wild type mice in LDLR^{+/+} background mice. In LDLR^{-/-}PKO, mice had higher IL-6 compared to properdin wild type mice. The limitation to the results presented herein was clearly time and resources; it is of interest to work out mechanistically the relationship between elevated C5L2 in properdin deficient mice to high triglycerides and greater steatosis, and how this knowledge might be used to revert pathology to the lesser extents observed in wildtype.

Chapter 6 The role of Exercise and Vitamin D on mice induced obesity

6.1 Introduction

Another obvious intervention aside, from dietary supplement (and avoidance of fats and sugars) is exercise. With the gift of an exercise wheel suitable for cages from collaborators at University of Hull, I was able to study the effect of voluntary exercise in groups of mice receiving unhealthy diets. Because there was only one exercise wheel, and the NACWO estimated the floor space to be sufficient only for three mice, the group sizes were limited to three each cage (exercise and normal ventilated cage).

Interestingly, hepatic fibrosis detected histologically by Sirius Red, and alpha smooth muscle actin staining) appeared in the obese state, and was decreased due to the exercise training of HFD mice (Bieghs et al., 2012). A high fat diet can lead to the changing of phenotypic M2 to M1 macrophages in mice. It is obvious that tumour necrosis factor (TNF- α) has a role in enhancing inflammation, but exercise training of mice caused down regulation of TNF- α in adipose tissue (Kawanishi et al., 2012).

Exercise mediated decrease in hepatic steatosis might be due to activation of fuel oxidation by exercising (Alex et al., 2015). Exercise leads to the decrease of obesity by the prevention of fat deposition, and also it prevents cardiovascular disease risks by reducing LDL, and the elevation of HDL (Kraus et al., 2002). Exercise has a significant role in the prevention of inflammation by inhibition of monocyte, and macrophage infiltration into adipose tissue (Kawanishi et al., 2010), and by the reduction visceral fat, and anti-inflammatory cytokines production (Petersen and Pedersen, 2005). There is a strong evidence in reducing risk of diabetes mellitus type 2 when exercising regularly (Gleeson et al., 2011).

According to Kawanishi *et al.* (2010), exercise training improves serum ACT levels, and in addition has a role in the decrease or inhibition of inflammation by switching of M1 macrophage to M2 macrophage. TNF, and F4/80 mRNA expression in adipose tissue mice was reduced a result of the exercise training. A M1 macrophage marker, CD11c, increased in high fat diet; as result, it has decreased mRNA expression in the exercise training high fat diet fed mice. However, CD163, M2 macrophage marker, decreased in high fat diet; while, there was increased mRNA expression in adipose tissue of the exercise mice

training. The mRNA expression of Toll like receptor 4 was decreased in adipose tissue of the exercise training mice.

No study has yet investigated the additional positive effect of voluntary exercise on the beneficial effect of Vitamin D added to our high fat high sugar diet. It is well established that participation in regular exercise improves blood glucose control, prevents type 2 diabetes, and leads to body weight decrease, and the decrease in development of diabetes by up to 58% in high-risk populations (Colberg et al., 2010). Exercise leads the increase of insulin sensitivity in adipocytes and muscle cells which caused by diabetes or obesity related disease (Figure 6.1). Exercise has anti- inflammatory role, it also prevents NAFLD disease (Figure 6.2)

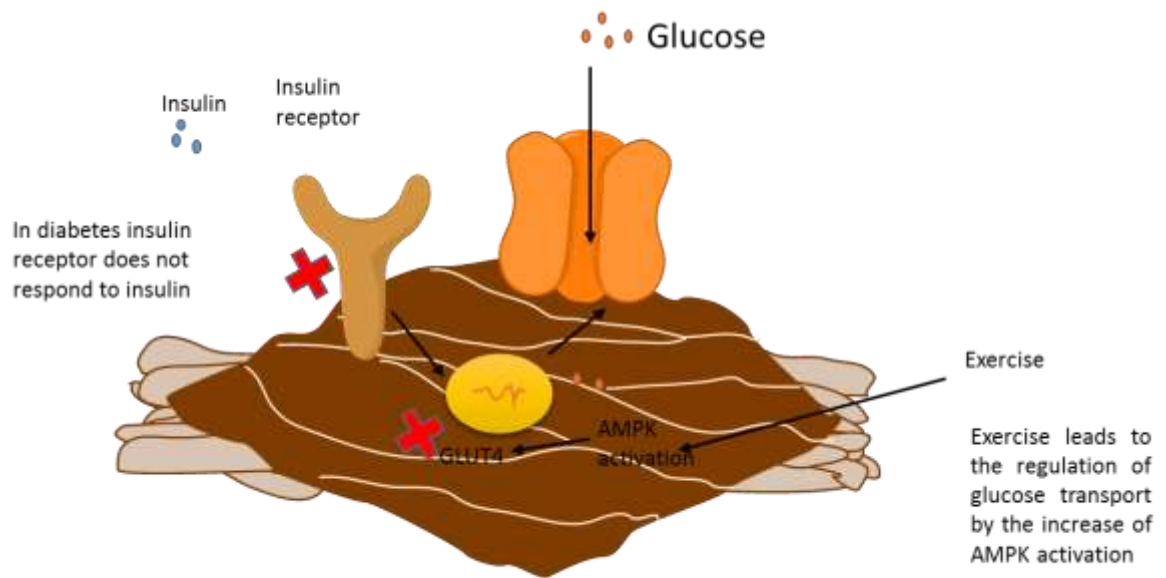


Figure 6.1 Proposed model of action of exercise on muscle cells.

Glucose transporter protein (GLUT4) is the rate limiting step in glucose utilization. GLUT4 is expressed in muscle cells. Insulin, and exercise are most potent activators of GLUT4. High fat–high sugar diet increases the possibility to get diabetes. In diabetes, GLUT4 translocation is impaired, therefore, GLUT4 is not activated by insulin. Vitamin D is beneficial because it can upregulate GLUT 4 activity by increasing AMPK (activated protein kinase) activation.

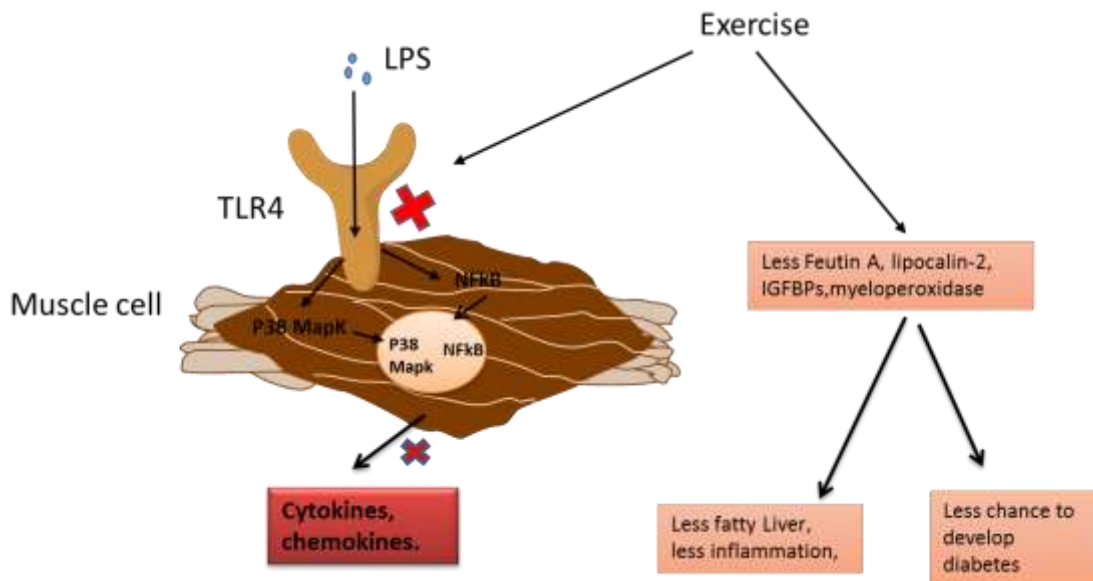


Figure 6-1 Proposed model of action of exercise on muscle cells.

Exercise leads to the decrease of PAMP production so causes the decrease of phosphorylation, and translocation of NFκB, and p38MAPK into the cell nucleus. This antagonises the activity of LPS, which binds to TLR4, signalling via NFκB and p38MAPK. Red crosses indicate the intracellular inhibitory effect of exercise. In addition, exercise decreases Feutin A, Lipocalin-2, IGFBPs, and myeloperoxidase, which is beneficial in decreasing susceptibility to developing liver steatosis and insulin resistance.

6.2 Specific materials and methods

Male C57Bl/6 mice were used for the exercise cage (NACWO) for 5 weeks. Mice were randomised to 4 groups, fed for 5 weeks on the formulated (cholesterol free) diet 58R3 (20% protein, 36% fat, 35% carbohydrate, rich in sucrose) differing in the content of admixed Vitamin D 3 (1 IU/g vs 10 IU/g) (TestDiet). The mice were divided into 4 groups. Group A Exercise wheel (which records revolutions) , n=3, mice were fed with high fat high sugar diet (58R3) with Vitamin D + exercise for 5 weeks only, on PPL 40/3488. At the endpoint, revolutions were recorded, for the three mice (923850*4=3695400) revolutions.

Group B Normal ventilated cage, n=2, (58R3+Vitamin D). Group C, and D as above, without Vitamin D: Group C, n=3, for exercise wheel, Group D, n=2 in normal ventilated cage, diet was 58R3 without Vitamin D. This showed us the positive effect of voluntary exercise on NAFLD developed on the high fat high sugar diet, 58R3. As for Groups A, and B, revolutions were recorded at the endpoint, and averaged for the three mice, but Group C mice revolutions were

not recorded due to technical difficulty. Mice were weighed at the end of study. Mice were bled by cardiac puncture under terminal anaesthesia, and tissues kept for further analyses (muscle for array, liver for histology).

Therefore the aim of this chapter was to investigate the additional effect of voluntary exercise on the beneficial effect of Vitamin D added to our high fat high sugar diet. C57Bl/6 mice were used in the study, where the additional role of exercise was studied. A variety of readouts were used (Body weight, liver histology, ELISA (insulin, IL-6, TNF- α , NEFA, complement activation), and muscle protein array).

6.3 Result

6.3.1 Effect of exercise, and Vitamin D on fatty liver disease

The aim was to see if there was an additional positive effect of voluntary exercise on the beneficial effect of Vitamin D added to our high fat high sugar diet. At the end of five weeks, all four groups mice were bled by cardiac puncture under terminal anesthesia, and tissues kept for further analyses; muscles for array, liver for histology.

In this experiment, only compared 2 groups mice fed the Vitamin D supplemented high fat high sugar diet with, and without access to the exercise, there was not normal diet for this study. Therefore, we cannot comment on diet related body weight gain or liver weight gain. This was meant as a pilot for further studies, we simply looked at the effect of exercise in two dietary situations with a limited number of commercial mice

6.3.1.1 Body Weight measurement

Body weight was measured at final week (week 5) for all experimental mice. It decreased significantly in C57BL/6 mice fed the Vitamin D supplemented high fat high sugar diet with access to the exercise wheel (30.62 ± 0.15) compared to mice fed the Vitamin D supplemented high fat high sugar diet without access to the exercise wheel (Figure 6.3). However, mice fed 58R3 compared in body weight to mice on 58R3, but exercised (Figure 6.3). In the group of mice given 58R3, there was no increase in body weight likely due to increased fighting within this particular group. Taken together, these results suggest that additional exercise to mice fed the Vitamin D supplemented high fat high sugar diet with access to the exercise wheel had a tendency to decrease of body weight compared to mice fed the Vitamin D supplemented high fat high sugar diet without access to the exercise wheel (Figure 6.3).

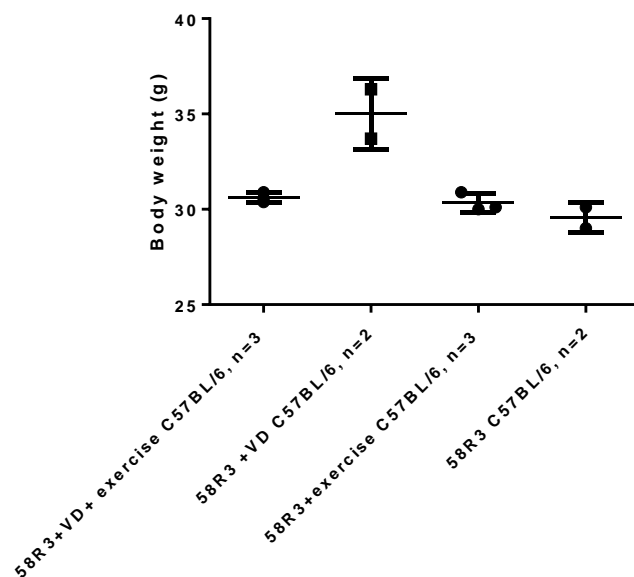


Figure 6-2 The effect of exercise and Vitamin D on body weight measurement. C57BL/6 mice fed high fat high sugar diet for five weeks. comparison were: 58R3+VD+ exercise vs 58R3+VD+ exercise ,and 58R3+exercise vs 58R3.

6.3.1.2 Liver, and end liver % body weight (g) (C57BL/6 mice)

There were not possibility to have significant difference in liver weight between the groups (Figure 3, A), and the percentage of liver weight whichever way expressed (Figure 6.4, B).

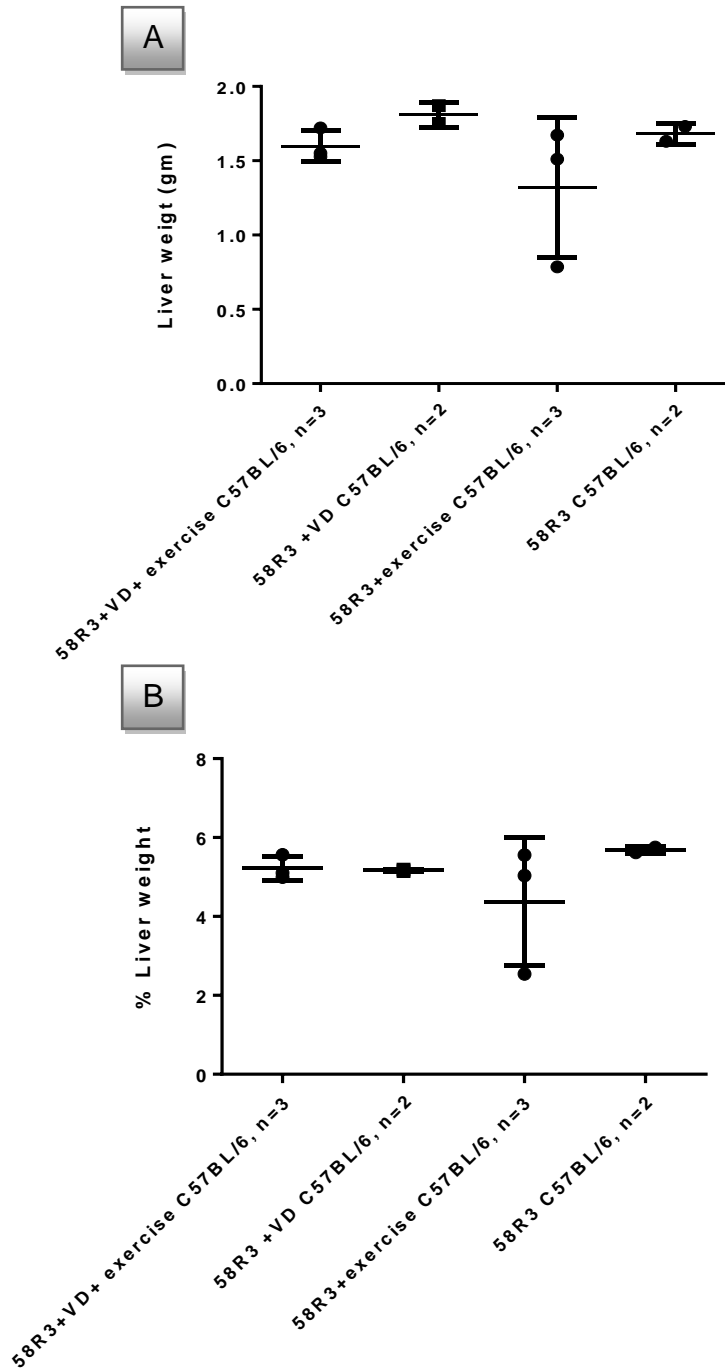


Figure 6-3 The effect of exercise and Vitamin D on liver weight measurement.

C57BL/6 mice fed high fat high sugar diet (58R3) for five weeks. Liver weight (A), and the percentage of liver (B) in C57BL/6 group mice. The comparison were: 58R3+VD+ exercise vs 58R3+VD+ exercise, and 58R3+exercise vs 58R3.

6.3.1.3 Fat pad weight (g)

The mice fed the Vitamin D supplemented high fat high sugar diet with access to the exercise wheel had a tendency to have lower fat pad weight compared the Vitamin D supplemented high fat high sugar diet without access to the exercise wheel (Figure 6.5, A). In mice were given high fat high sugar diet with access to the exercise wheel, there was a tendency to decrease fat pad weight compared to mice were given high fat-high sugar diet without access to the exercise wheel (Figure 6.5, A). The fat pad percentage of body weight had a tendency to have lower in mice fed the Vitamin D supplemented high fat high sugar diet with access to the exercise wheel compared to mice fed the Vitamin D supplemented high fat high sugar diet without access to the exercise. In addition, in mice fed high fat-high sugar diet had a tendency to have lower fat pad percentage of body weight compared to mice fed high fat-high with access to the exercise compared to mice fed high fat high sugar without access to exercise (Figure 6.5, B).

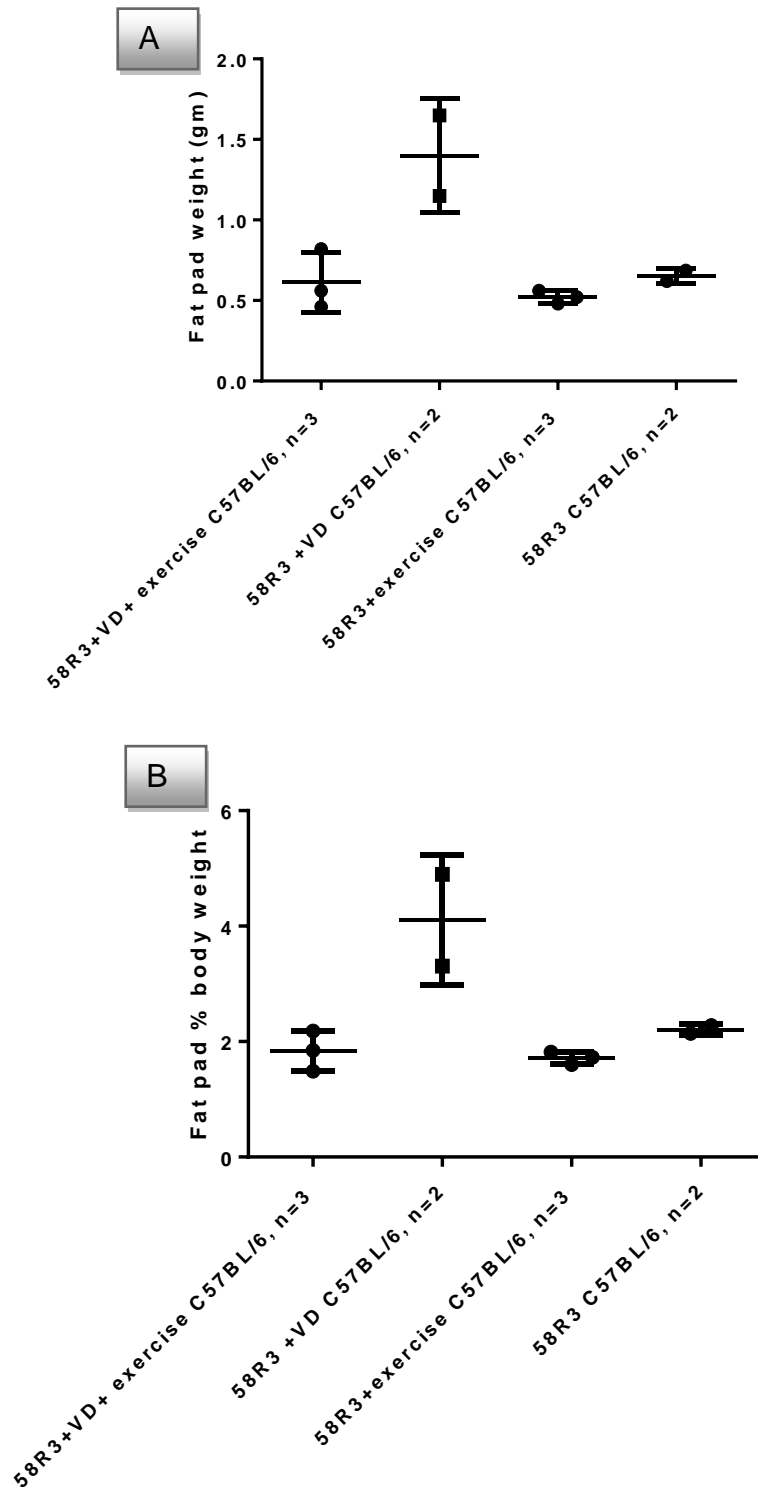


Figure 6-4 The effect of exercise and Vitamin D on epididymal fat pad weight measurement.

C57BL/6 mice fed high fat high sugar diet for five weeks. Epididymal fat pad weight (A), and the percentage of fat pad weight (B) in C57BL/6 mice. The comparison were: 58R3+VD+ exercise vs 58R3+VD+ exercise and 58R3+exercise vs 58R3.

6.3.1.4 Histopathology of livers in C57BL/6 mice fed high fat, and high sucrose diet± Vitamin D ± Exercise

All groups were C57BL/6 mice, sections were prepared from liver, stained with haematoxylin/eosin, and analysed microscopically. Liver steatosis, and inflammation were seen in mice fed high fat-high sugar diet. Vitamin D supplementation with and without exercise led the amelioration of fatty liver changes and inflammation, but the effect was greater and no microvesicular and lobular inflammation in mice fed the Vitamin D supplemented high fat high sugar diet with access to the exercise wheel (Figure 6.7, A) compared to mice fed the Vitamin D supplemented high fat high sugar diet without access to the exercise (Figure 6.7, B) and to mice fed high fat high sugar diet with the exercise (Figure 6.7, C). Macro vesicles were detected in mice fed high fat-high sugar diet, while in the presence of Vitamin D, exercising mice showed micro vesicular lipid inoculations. Lipid accumulation was observed near central vein (zone 3) in mice fed 58R3 diet. (Figure 6.7, D). Pieces of livers of 9 weeks old C57BL/6 mice were fixed, paraffin embedded, and slides were prepared stained with haematoxylin, and eosin. Fatty changes were predominately detected in the livers from mice fed the high fat high sugar diet. There are many microvesicular, and macro-vesicular lipid droplets in livers from mice fed the high fat high sugar diet (Figure 6.7, D). Many inflammatory cells were detected. They might be neutrophilic infiltration or mononuclear cells around portal vein, which are called portal inflammation, or it appears between cells that are called lobular inflammation (Figure 6.7, D).

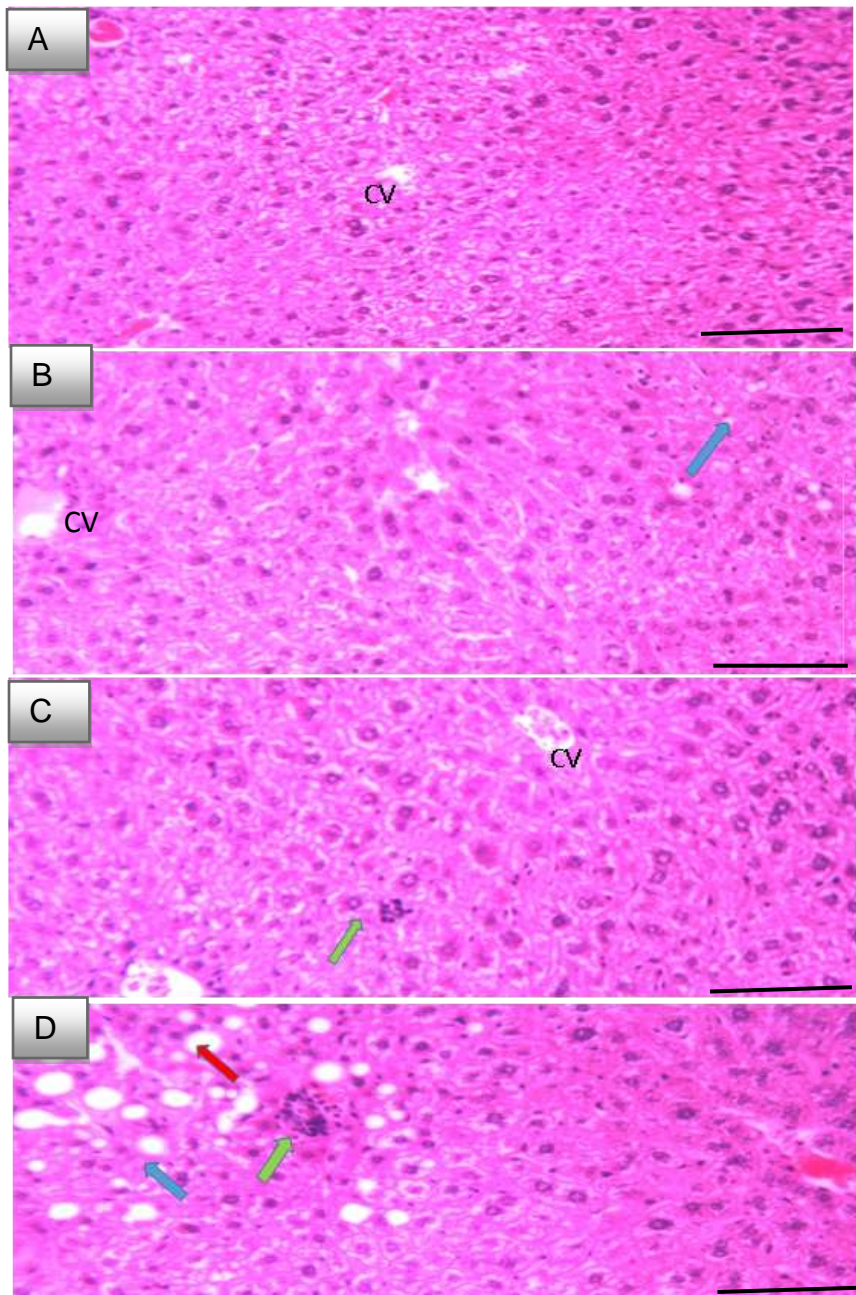


Figure 6-5 Haematoxylin and eosin staining of paraffin embedded liver sections obtained from mice.

Representative images of typical appearance of the livers. No inflammation and steatosis was seen in mice fed the Vitamin D supplemented high fat high sugar diet with access to the exercise (panel, A), microvesicular in mice fed the Vitamin D supplemented high fat high sugar diet without access to the exercise wheel (panel, B) lobular inflammation in mice fed the high fat high sugar diet with access to the exercise wheel (panel, C) Fatty changes in great amount, microvesicular (blue arrows), macrovesicular (red arrows) (steatosis) and inflammation (green-heads) presence of marked fatty changes near CV (zone 3) in middle column in high fat –high sucrose diet (Panel D) CV, central vein 20x. Scale bar represents 100 Micron.

Table 6.1 Scoring system in liver mice fed high fat-high sugar diet for five weeks.

Lobular inflammation scores (A), and steatosis scores (B) in mice fed the Vitamin D supplemented high fat-high sugar diet with access to the exercise wheel compared to mice fed the Vitamin D supplemented high fat high sugar diet without access to the exercise wheel, and also high fat high sugar diet with access to the exercise compared to high fat high sugar without access to exercise.

A

Lobular inflammation score	Meaning (foci per 200X field)	58R3+VD+Exercise	58R3+VD	58R3+Exercise	58R3
0	No foci	2/3	0/2	2/3	1/2
1	Less than 2	1/3	2/2	1/3	1/2
2	2-4	0/3	0/2	0/3	0/2
3	More than 4	0/3	0/2	0/3	0/2

B

Steatosis score	Meaning (parenchymal involvement by steatosis)	58R3+VD+Exercise	58R3+VD	58R3+Exercise	58R3
0	Less than 5%	2/3	1/2	1/3	0/2
1	5-33%	1/3	1/2	2/3	0/2
2	33-66%	0/3	0/2	0/3	0/2
3	More than 66%	0/3	0/2	0/2	2/2

Histological scoring system was performed as described by Kleiner and colleagues (Kleiner et al., 2005). High score (score 3) for steatosis, and lobular inflammation (score 2) was seen in high fat diet-high sugar diet mice. However, no lobular inflammation, and steatosis was documented in mice fed the Vitamin D supplemented high fat high sugar diet with access to the exercise wheel (Table 6.1, A), and lobular inflammation in exercise group ((Table 6.1, A). Steatosis scores (ranges from 0-to 3) show that in mice receiving high fat high sugar diet there are severe fatty change (grade 3), while in groups of mice

receiving Vitamin D supplemented high fat high sugar diet with access to the exercise, no grade three, and two were documented (Table 6.1, B). In addition, microvesicular were detected in Vitamin D group without access to exercise (Table 6.1, B). It appears from Haematoxylin eosin staining that mice fed high fat high sugar diet caused steatosis and inflammation, while in mice receiving Vitamin D supplemented high fat high sugar diet with access to the exercise no steatosis, and inflammation was detected. To further investigate steatosis, and inflammation, measurement of NEFA, and TNF- α , IL-6 were performed.

6.3.1.5 Anti-inflammatory effect on mice fed the Vitamin D supplemented high fat high sugar diet with access to the exercise wheel.

Because obesity induces inflammation (Wellen and Hotamisligil, 2003), and we found inflammation in liver histopathology, TNF- α , and IL-6 ELISA were performed. Candidate inflammatory markers are TNF- α , involved in monocyte attraction, and IL-6 (involved in monocyte attraction (Hursting and Hursting, 2012). TNF- α protein had possibility lower from mice fed the Vitamin D supplemented high fat high sugar diet with access to the exercise wheel compared to the Vitamin D supplemented high fat high sugar diet without access to the exercise wheel (Figure 6.7, A). IL-6 was also had a tendency to have lower from mice fed the Vitamin D supplemented high fat high sugar diet with access to the exercise wheel compared to the Vitamin D supplemented high fat high sugar diet without access to the exercise wheel (Figure 6.7, B). In mice fed high fat high sugar diet with access to the exercise TNF- α protein had a tendency to have lower compared to high fat high sugar without access to exercise (Figure 6.7, A), and also IL-6 protein had possibility lower from mice fed high fat high sugar diet with access to the exercise group mice compared to high fat high sugar without access to exercise (Figure 6.7, B). The current data highlight the importance of supplementary dietary Vitamin D with access to exercise in an anti-inflammatory role, and even more the beneficial effect of exercise (with and without Vitamin D). To study the amelioration of steatosis, and prevention of metabolic syndrome disease level in Vitamin D supplemented high fat high sugar diet with access to the exercise wheel compared to the Vitamin D supplemented high fat high sugar diet without access to the exercise wheel, NEFA was tested in mice sera.

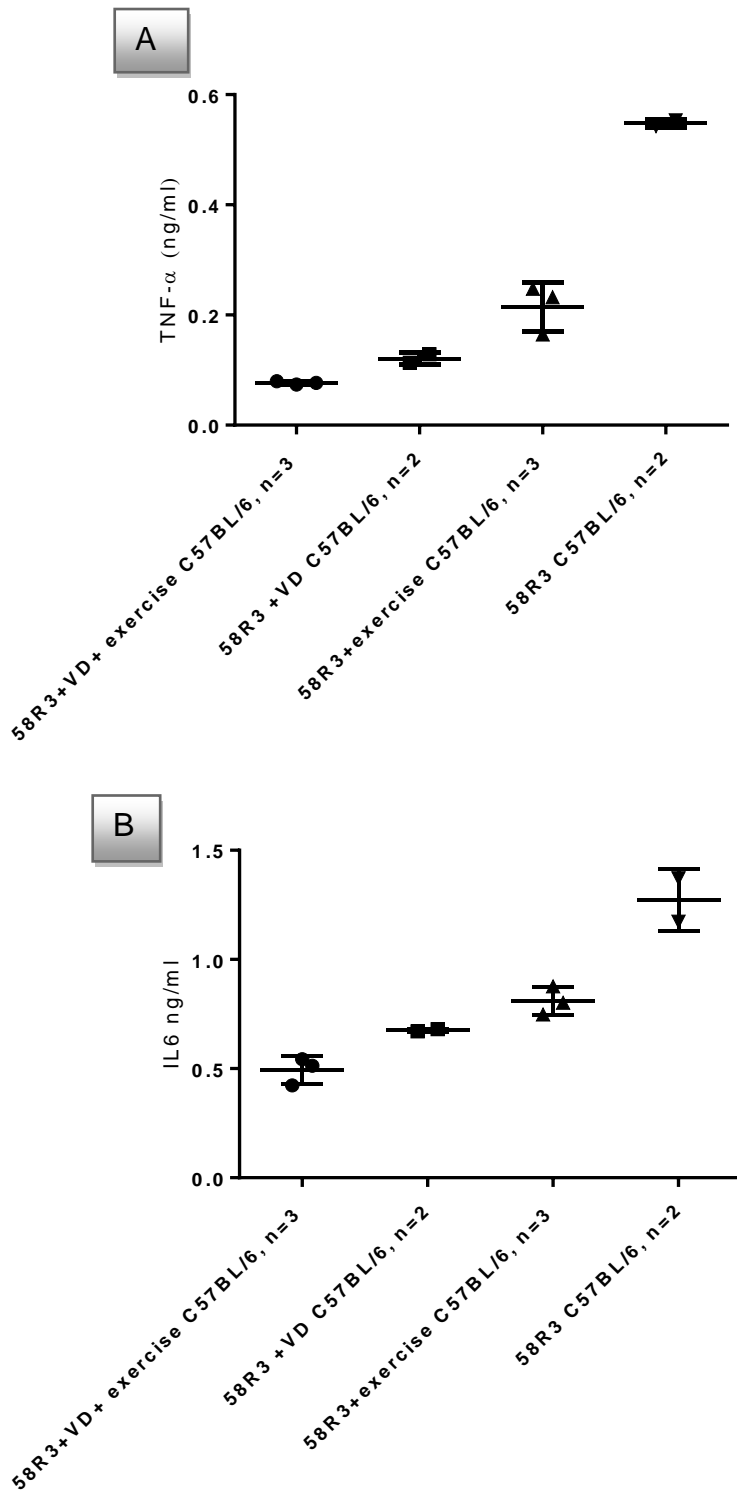


Figure 6-6 The effect of exercise and Vitamin D on TNF- α and IL-6 ELISA.

Mice fed high fat high sugar diet (58R3) for five weeks. TNF- α ELISA (A) and IL-6 ELISA (B) in C57BL/6 mice sera. The comparison were: 58R3+VD+ exercise vs 58R3+VD+ exercise ,and 58R3+exercise vs 58R3.

6.3.1.6 The effect of mice fed the Vitamin D supplemented high fat high sugar diet with access to the exercise wheel on the metabolic syndrome

The increase of non-esterified fatty acids (NEFAs) in obese situation was shown to contribute in the development of various disturbances related to the metabolic syndrome, such as hepatic, and peripheral insulin resistance, and dyslipidaemia (Sarafidis and Bakris, 2007). Because liver histology showed that in high fat diet-high sucrose had steatosis, and no steatosis in treated groups (Vitamin D, and exercised group mice), therefore NEFA was tested in mice sera. NEFA had possibility to have lower in mice fed the Vitamin D supplemented high fat high sugar diet with access to the exercise wheel compared to the Vitamin D supplemented high fat high sugar diet without access to the exercise wheel. In mice fed high fat high sugar diet with access to the exercise group mice had possibility lower NEFA compared to high fat high sugar without access to exercise (Figure 6.8).

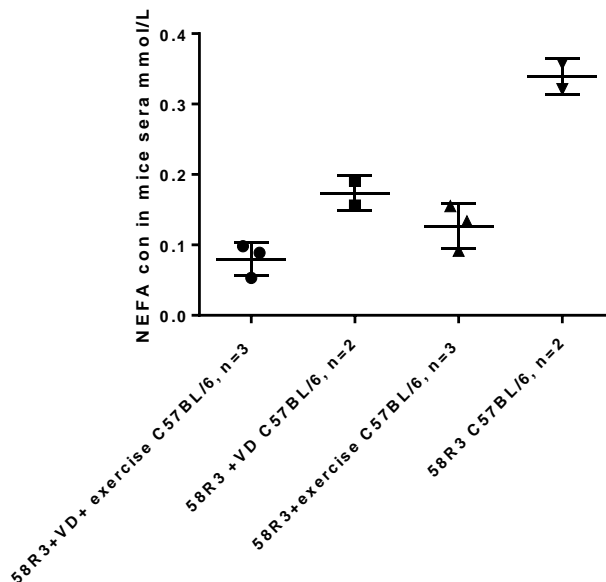


Figure 6-7 The effect of exercise and Vitamin D on NEFA essay in C57BL/6 mice sera. Mice fed high fat high sugar diet (58R3) for five weeks. The comparison were: 58R3+VD+ exercise vs 58R3+VD+ exercise, and 58R3+exercise vs 58R3.

6.3.1.7 Effect of exercise on insulin sensitivity

Insulin levels are increased in circulation in mice given high fat diet compared to control mice ((Ha and Chae, 2010). Mice fed the Vitamin D supplemented high fat high sugar diet with access to the exercise wheel had possibility to have lower insulin levels compared to the Vitamin D supplemented high fat high sugar diet without access to the exercise wheel. In mice fed high fat high sugar diet with access to the exercise group mice, insulin levels had possibility to have lower compared to mice fed high fat high sugar diet without access to the exercise group (Figure 6.9). These findings suggest that the combined effect of exercise and Vitamin D is greater than the individual intervention to reduce insulin. To understand how 58R3 diet causes complement activation, and to see how Vitamin D, and exercise affect the activation, classical and alternative pathway was performed.

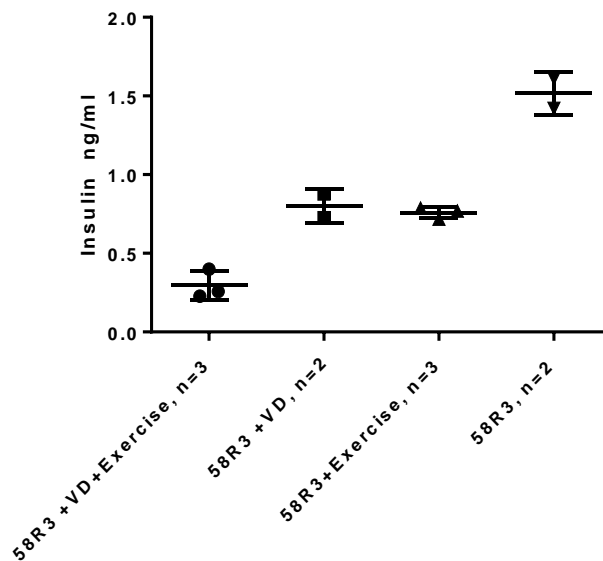


Figure 6-8 The effect of exercise and Vitamin D on Insulin ELISA in C57BL/6 mice sera. Mice fed high fat high sugar diet (58R3) for five weeks. The comparison were: 58R3+VD+ exercise vs 58R3+VD+ exercise ,and 58R3+exercise vs 58R3.

6.3.1.8 Testing functional complement activation (classical, and alternative pathway activation)

In an *in vitro* study, oxidized LDL caused classical complement activation in human serum (Saad et al., 2006), therefore we tested classical pathway activation in serum from mice at the level of C9.

Our results showed that classical pathway complement residual activation (CP) in mice fed 58R3 without exercise had possibility to have lower compared to mice fed 58R3 with exercise (Figure 6.10, A). Mice fed the Vitamin D supplemented high fat high sugar diet with access to the exercise wheel had possibility to have higher residual activity compared to the Vitamin D supplemented high fat high sugar diet without access to the exercise wheel (Figure 6.10, A). It can be said that the increase of residual activity in mice given high fat high sugar diet supplementary Vitamin D with access to exercise, as the result of preserving activity *in vivo*.

In a study of obese versus lean people, chylomicrons were higher, and more enriched with LPS in obese people in compared with lean people (Vors et al., 2015). Fujita et al (2006) reported that chylomicron accelerates C3 tick-over by regulating the role of factor H, leading to the overproduction of ASP; and as a result, it causes acceleration of alternative pathway activation. Our previous results showed that more Triglycerides (TGs), endotoxin levels were showed in high fat –high sucrose compared to mice treated with Vitamin D.

Our results showed that alternative pathway complement residual activation (CP) in mice fed 58R3 without exercise had possibility to have lower compared to mice fed 58R3 with exercise (Figure 6.10, B). Mice fed the Vitamin D supplemented high fat high sugar diet with access to the exercise wheel had a tendency to have higher residual activity compared to the Vitamin D supplemented high fat high sugar diet without access to the exercise wheel (Figure 6.10, panel B). The Vitamin D and exercise interventions are likely to exert their effect on classical and alternative pathway indirectly (via decrease of residual activity in exercise and Vitamin D group compared to the combinations of Vitamin D and exercise group mice, so relatively more *in vivo* activation and consumption of activities).

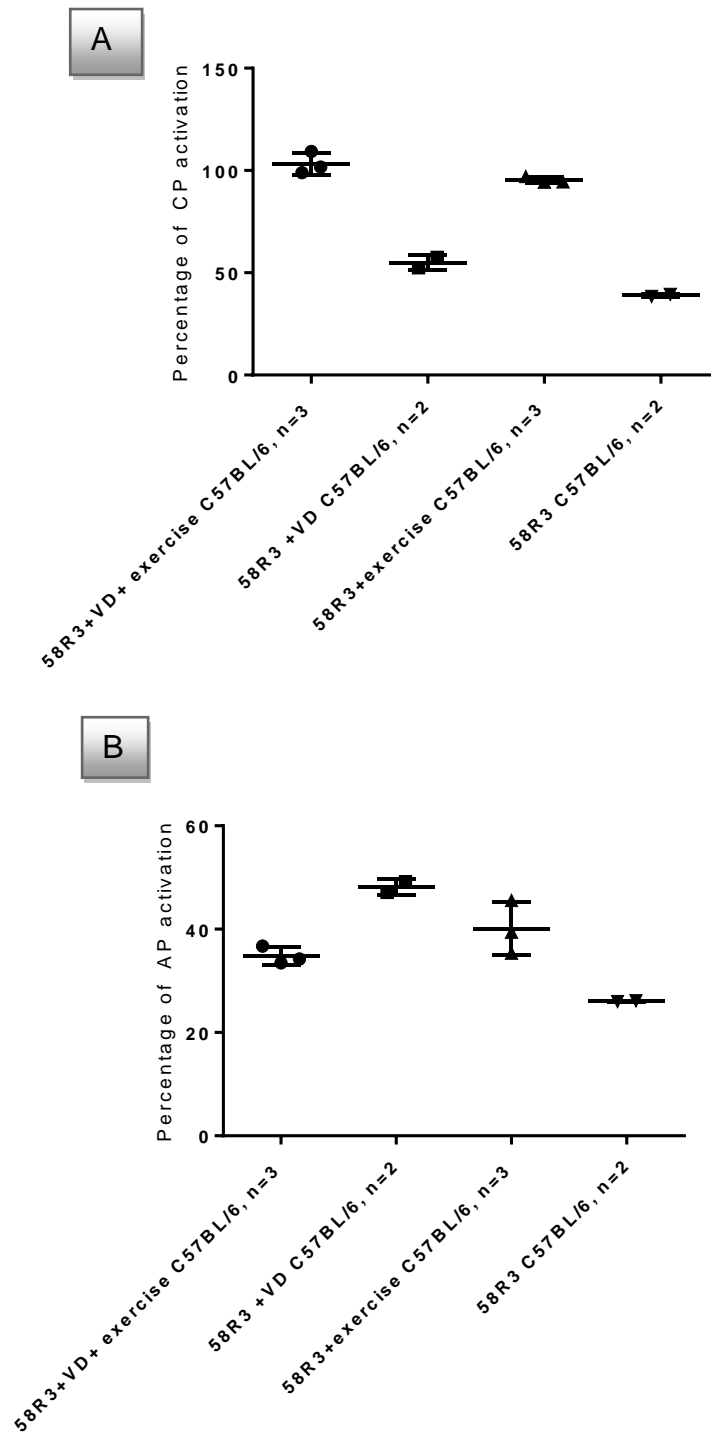


Figure 6-9 The effect of exercise and Vitamin D on functional classical and alternative complement pathway.

Mice fed high fat high sugar diet (58R3) for five weeks. Functional complement residual activities of classical pathway complement (CP) (panel A), and alternative pathway complement (AP) at the level of formation of C9 (panel B). The comparison were: 58R3+VD+ exercise vs 58R3+VD+ exercise and 58R3+exercise vs 58R3.

To further understand the beneficial role of exercise, and Vitamin D together, array proteins were analysed for muscle mice in groups mice given high fat high sugar diet supplementary Vitamin D with, and without access to exercise.

6.3.1.9 Cytokines protein microarray in muscle

Different proteins were expressed in muscle including: cytokines, enzymes, chemokines, and metabolic proteins. Muscle cells express various membrane bound molecules on the cell surface (adhesion molecule, chemokine receptors, and co-stimulatory molecules), especially under inflammatory conditions; in addition, various soluble factors are produced by muscle cells, such as cytokines, chemokines, and matrix metalloproteinases. TLR4 expression in muscle is increased during exercise (Shapiro et al., 2009). PAMPs may be recognised in muscle cells by TLRs (LPS binds TLR4), leading the activation of NF-kB; as the result, different cytokines, and chemokines are produced. However, exercise in mice also leads to the reduction of cytokines, and chemokines due to anabolic effect of exercise. Exercise means increased glucose uptake by muscle, better glycaemic index, counteracts pre-diabetic phenotype.

So far as we know, muscle is a main producer of IL-6 during exercise, and we studied the overall pro inflammatory contributions of muscle as part of our study. Proteins that are linked to inflammation, obesity, diabetes, and metabolic syndrome disease are lower in exercised mice group compared to non-exercised group mice (Figure 6.12). So, the result showed the beneficial significant role of exercise to ameliorate high fat diet –high sucrose induced obesity.

The remainder of proteins are expressed to a lesser extent in muscle from mice receiving high fat high sugar diet with Vitamin D, and access to voluntary exercise.

The main purpose to perform microarray was to see the effect of high fat diet – high sugar diet in the presence, and absence of exercise. Fetuin A (Trepanowski et al., 2015), and Lipocalin-2, (Wang et al., 2007) are increased in obesity and diabetic, overweight and fatty liver disease. IGFBP-3, 5, 6 (Insulin like growth factor binding protein-3,5,6) (Shimasaki and Ling, 1991) and C-

reactive protein (Fronczyk et al., 2014) are elevated during obesity and diabetes. Protein cytokines, and chemokines, enzymes involved in diabetes, steatosis, and inflammation are a tendency to increase in muscle tissue of mice given high fat diet (Figure 6.12). There is a tendency marked decrease of these proteins in exercise of mice given high fat diet plus exercise in addition to Vitamin D (Figure 6.12). Groups of proteins that are not changed on exercise are: CCL12, CD160, Coagulation factor, Chitinase-3-like1, Cystatin, DPPIV, and IGFBP-2.

The increase of endothelial adhesion molecules (VCAM-1, ICAM-1) may lead to atherosclerosis, diabetes, and hypertension in obese people (Ferri et al., 1999). Inflammatory cytokines interleukin-1 beta (IL-1 beta), and tumor necrosis factor-alpha (TNF alpha) plays a role to increase endothelial adhesion molecules (Picchi et al., 2006). Our results showed a tendency to have less cytokines production in exercised group mice and less endothelial adhesion molecules initiation. Our result showed VCAM-1 and ICAM-1 had a tendency to have less in mice fed the Vitamin D supplemented high fat high sugar diet with access to the exercise wheel compared to the Vitamin D supplemented high fat high sugar diet without access to the exercise wheel (Figure 6.12, C,E).

Osteopontin (OPN) is a protein in muscle cells, and infiltrating cells involved in inflammation, fibrosis, and muscle regeneration (Zanotti et al., 2011). It is a multifunctional phosphoprotein, it had a tendency to have less expressed in exercise group mice. It has been reported that high glucose levels cause OPN expression through protein kinase C-dependent pathways (Takemoto et al., 2000). Our result showed had a tendency to have less Osteopontin in mice fed the Vitamin D supplemented high fat high sugar diet with access to the exercise wheel compared to the Vitamin D supplemented high fat high sugar diet without access to the exercise wheel (Figure 6.12, D).

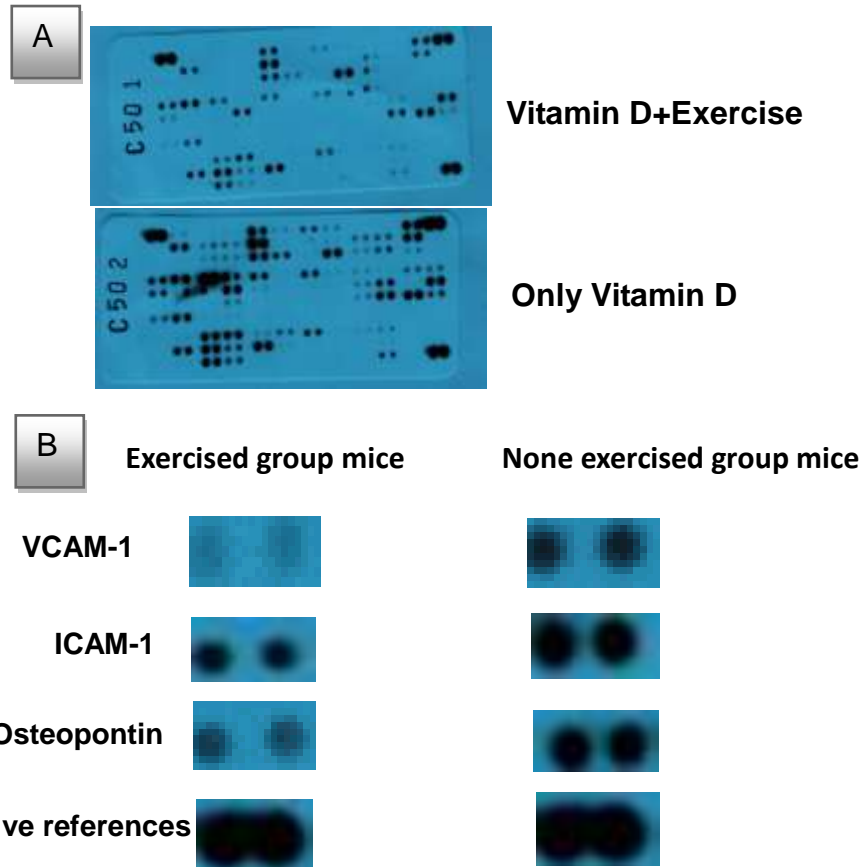


Figure 6-10 Muscle cytokines array protein membrane spots (A) and representative examples (B).

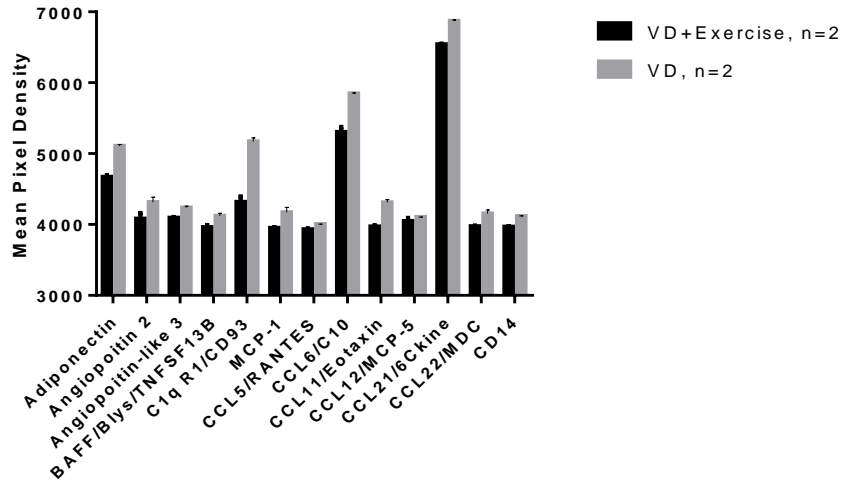
Positive references in mice fed the Vitamin D supplemented high fat high sugar diet with access to the exercise wheel compared to the Vitamin D supplemented high fat high sugar diet without access to the exercise wheel.

Table 6.2 All proteins detected in the microarray.

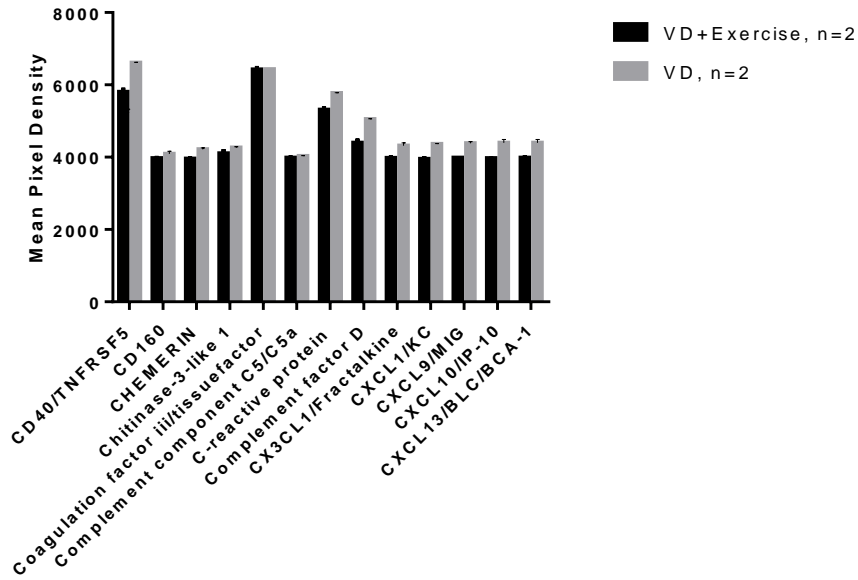
Cytokines	Chemokines	Enzymes	Growth factors	Complement proteins	Adhesion molecules	Insulin family proteins , receptors ,and ligands
BAFF, C-reactive protein, IFN- γ , IL-4, IL-33, IL-1 alfa, osteopontin, RBP4, Resistin, Reg3G	MCP-1, CCL5, CCL6 , (C10), CCL11/Eotaxin, CXCL 1-8, CXL13, Chemerin,CCL12/MCP-5, CCL21/6Ckine, CCL22/MDC, lipocalin 2, LIX	MMP-2: matrix metalloproteinase-2, MMP-3,9, Endostatin, DPPIV/D2, Cystatin C, Myeloperoxidase	Angiopoietin 2, Angiopoietin-like 3 , FGF acidic, EGF, Endoglin	C5/C5a , C1qR1, Factor D	P-selectin, ICAM, Vcam-1	IGFBP-1,2,3,4,4,6, RAGE, LDLR, Gas6,Flt-3 Ligand, Fetuin A, RAGE. and Protein hormone such as adiponectine

Proteins of unknown function in muscle are CD160, R1/CD93. Groups of proteins that were not changed: CCL12, CD160, Coagulation factor, Chitinase-3-like1, Cystatin, DPPIV, and IGFBP-2.

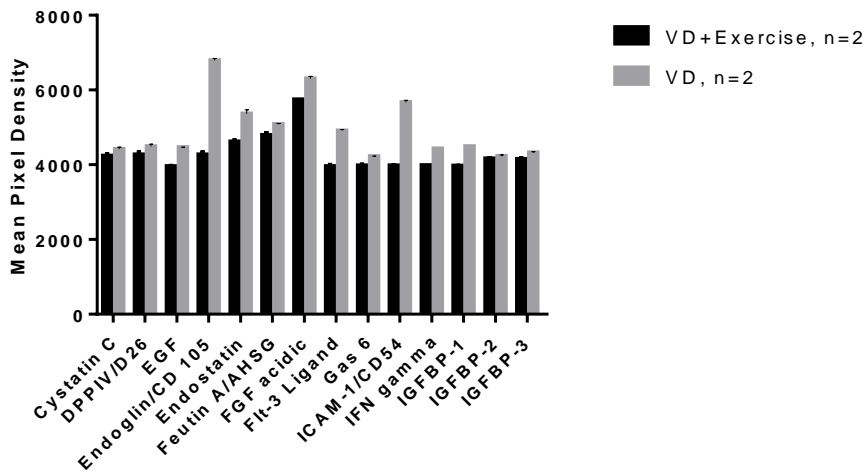
A



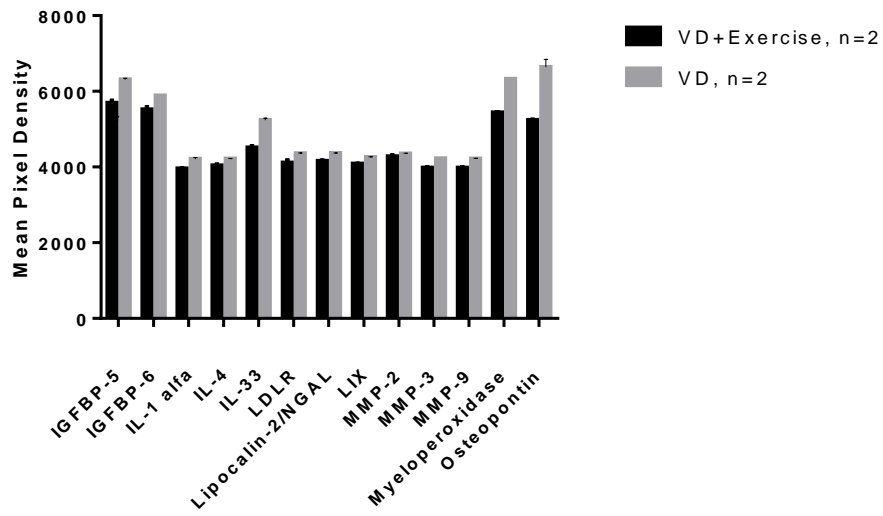
B



C



D



E

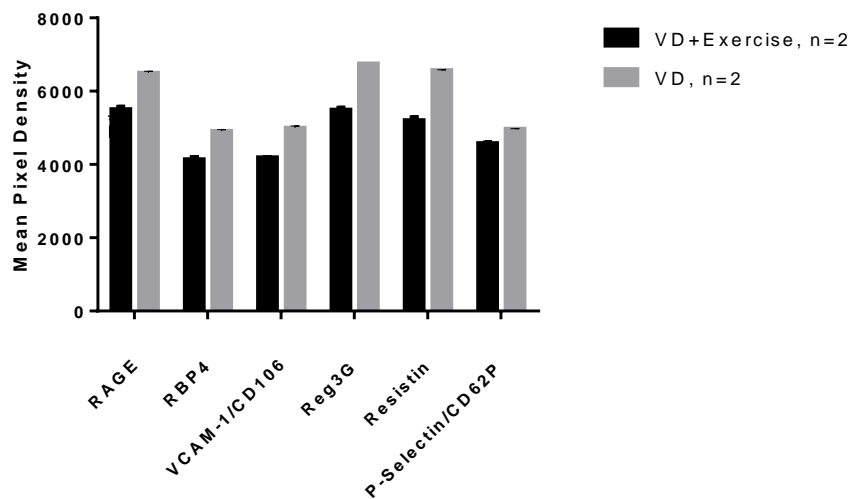


Figure 6-11 Effect of exercise and Vitamin D on muscle cytokines.

All proteins expression from muscle lysate (A-E). Mice fed the Vitamin D supplemented high fat high compared to the Vitamin D supplemented high fat high sugar diet without access to the exercise wheel.

6.4 Discussion

C57Bl/6 mice fed 58R3 were used after 5 weeks high fat diet–high sugar caused the development of liver steatosis. Ten male mice C57BL/6 background were used for this experiment to see the additional effect of exercise on mice fed high fat diet supplemented Vitamin D or not.

Body weight, fat pad weight were measured at the end of study. Mice that were fed high fat-high sugar diet (without additional Vitamin D) did not get body weight increase; this may be because the mice were fighting each other. Body weight, and fat pad weight had a tendency to have lower in mice fed the Vitamin D supplemented high fat-high sugar diet with access to the exercise wheel compared to mice fed the Vitamin D supplemented high fat high sugar diet without access to the exercise wheel. There are many features that related to NASH, such as steatosis, ballooning degeneration, lobular inflammation, and giant mitochondria (Yeh and Brunt, 2007). Liver histology showed that C57BL/6 mice group without access to exercise showed increased steatosis, and inflammation. Microvesicular were seen in mice fed high fat diet supplemented Vitamin D without access to exercise, while no steatosis and inflammation were seen at all in mice fed the Vitamin D supplemented high fat high sugar diet with access to exercise. Alex and colleagues who showed that exercise mediated decrease in hepatic steatosis might be due to activation of fuel oxidation by exercising (Alex et al., 2015). IL-6 had a tendency to have less in mice fed high fat-high sugar diet supplemented Vitamin D with access to exercise, compared to mice fed high fat-high sugar diet supplemented Vitamin D without access to exercise wheel. Our results coincide with Lira *et al.*, (2011), who showed that circulating IL-6 concentrations are highly correlated with percentage of body fat and insulin resistance (Lira *et al.*, 2011). Yeh, and Brunt, (2007) who showed metabolic syndrome features such as obesity, hyperlipidemia, and diabetes are associated with NAFLD/NASH. This means there is a possibility to have diabetes in the case of having NAFLD. Interestingly, in our mice fed mice fed high fat-high sugar diet supplemented Vitamin D without access to exercise, no features of steatosis, inflammation and obesity were seen, and the insulin level elevation had a tendency to have higher in mice fed high fat-high sugar diet

compared supplemented with Vitamin D compared with mice fed high fat-high sugar diet compared supplemented with Vitamin D with access to exercise.

Sarafidis and Bakris (2007) who showed that the increase in non-esterified fatty acids (NEFAs) in obese situation were documented to contribute in the development of various disturbances related to the metabolic syndrome, such as hepatic, and peripheral insulin resistance, and dyslipidaemia. Our results showed a tendency to have less NEFA in mice fed high fat diet supplemented Vitamin D with access to exercise compare to mice fed mice fed high fat diet supplemented Vitamin D without access to exercise.

In general, high fat-high sugar diet caused the increase of insulin resistance. This is due to high insulin level, and was normalised by supplementary dietary Vitamin D containing diet with access to exercise wheel. This is in agreement with Geiger and colleagues who showed that exercise led to the decrease of insulin level (Geiger et al., 2005). Also Forouhi et al, (2008) illustrated that low Vitamin D serum 25-OH Vitamin D may lead to glycaemia, and insulin resistance in non- diabetic subjects.

Oxidized LDL causes classical complement activation in human serum (Saad et al., 2006). Our results showed that Vitamin D group with access to exercise wheel had lower classical pathway residual activity compared to Vitamin D group without access to exercise wheel because Vitamin D less led to the decrease of oxLDL (Oh et al., 2009), and also less oxLDL- is produced in the presence exercise (Vasankari et al., 1998).

Our results showed a tendency to have more alternative pathway residual complement activity in mice fed high fat-high sugar diet without access to exercise wheel compared to mice fed high fat-high sugar diet with access to exercise wheel. Chylomicron accelerates C3 tick-over by regulating the role of factor H, leading to the overproduction of ASP. As a result, it leads to the increase of alternative pathway residual activity (Fujita et al., 2007). Mice fed the Vitamin D supplemented high fat high sugar diet with access to the exercise wheel had a tendency to have less alternative pathway residual activity compared to mice fed the Vitamin D supplemented high fat high sugar diet without access to the exercise wheel.

Muscle array results showed that proteins, which are responsible for obesity, steatosis, inflammation, fibrosis, cardiovascular disease, and diabetes, were decreased in mice fed high fat diet supplemented Vitamin D with access to exercise compared to mice fed high fat diet supplemented Vitamin D without access to exercise. Exercise increases skeletal muscle GLUT4 Glucose transporter type 4 (GLUT 4) expression by increasing AMPK (activated protein kinase) activation (Richter and Hargreaves, 2013). As a result, there is no glucose increasing in the blood circulation, and preventing the development of diabetes. In conclusion it can be said both Vitamin D, and exercise have a beneficial effect, which was additive to dampen inflammatory markers, and metabolic syndrome disease markers (Il-6, NEFA). The clear limitation for this part of the study is the fact that the floor space, as judged by the Unit's NACWOs was compatible only for three mice. Since then, a European company has brought smaller wheels on the market which allow the study of group sizes of five mice. This will be desirable when work as this is repeated.

Chapter 7 General discussion

7.1 Introduction

This thesis applied both *in vitro* and *in vivo* models to studying the effect of immune modulators to cells in culture or to different genotypes of mice. The initial purpose of the work was to pursue the role of properdin in the development of steatohepatitis, based on two clinical studies which showed deposition of complement activation in clinical samples. A model had to be set up first as part of this work and provided a time frame in which to study *in vitro* effects of additional modulators discussed with collaborators at the University of Hull (external supervisor Dr Hobkirk) or identified from the literature. The animal model is one of low intervention and could be further refined as part of this work. The questions analysed were novel and have yielded two publications so far.

7.2 Characteristics of common nutrient additives with beneficial dietary effect

The *in vitro* study was performed to investigate key parameters in a controlled experimental setup before studying a relevant mouse model. J774 (macrophage cell line), and HepG2 (human liver cell line) were used to investigate correlates of steatosis, obesity, and associated complications. Neither DHA, Vitamin D nor Allicin had an impact on cell viability. To study “prevention”, the cells were preconditioned with interventions including Vitamin D, DHA at different concentrations for 1 day, and 5 days, and then stimulated with LPS (100ng/ml). To study “treatment state” the cells were stimulated for 4 hours then treated with interventions for 1, and 5 days (*post hoc*). In addition, FFA were used before, and after treatment with LPS (100ng/ml) as a control, detrimental stimulus (Kheder et al., 2016). The expression of Vitamin D receptor, and TLR4, and insulin receptor was confirmed for J774, and HepG2 cells. A decrease in mRNA expression of insulin receptor after LPS treatment compared to normal indicates a worse, less insulin responsive condition, contrasting with the effect of Vitamin D (Kheder et al., 2016), supplemental data. DHA, and Vitamin D were preconditioned for 5 days, and stimulated for 4 hours and 24 hours with LPS (100ng/ml). The reason for 4 hours and 24 hours stimulation was to know the effectiveness of Vitamin D and DHA at lowering TNF- α in the two different stimulation periods, and also it is established that in 4

hours stimulation of J774 TNF- α mRNA reaches a peak (previous MSc projects in lab). My result showed that DHA led to the decrease of mRNA expression, and protein level of TNF- α . This agrees with Oliver *et al.*, (2012) that showed the anti-inflammatory characteristic of DHA in other studies. Vitamin D was used to investigate the anti-inflammatory role in both J774 and HepG2 cells. The result showed that Vitamin D had a significant anti-inflammatory role, and was most effective in higher concentrations. Therefore, we concluded that Vitamin D has anti-inflammatory role and anti-steatosis (Kheder *et al.*, 2016, Supplementary Figure 3) which agrees with Ning and his colleagues who showed that in diabetic rat models, Vitamin D caused the decrease of inflammation, and steatosis (Ning *et al.*, 2015).

Allicin was also used to investigate its anti-inflammatory role. Allicin has anti-inflammatory role by the inhibition of p38, and JNK pathways, and the expression of NF- κ B in rats given the toxic substance trinitrobenzenesulfonic acid (Li *et al.*, 2015). For the first time Allicin was used as treatment, after stimulation with LPS (100ng/ml) for 4 hours then the cells were treated with Allicin for 1 day. The result showed that Allicin led to the decrease of TNF- α mRNA expression. Therefore the treatment idea was applied to DHA, and Vitamin D interventions (supplementary data in paper)

It can be concluded that Vitamin D, DHA, and Allicin had a significant role in the decrease of inflammation. In addition, Vitamin D caused the prevention of lipid accumulation in HepG2 cells which were stimulated with FFA.

7.3 The effects of Vitamin D3 as a nutraceutical during high fat diets

In *in vivo* studies, NAFLD model was provoked by given LDLR^{-/-} mice 10-12 weeks Western diet (high fat diet). As a result, occasional steatohepatitis (NASH) developed. CD68 positive cells were detected in hepatic sinusoids in high fat diet mice of both genotypes around central vein, and fat droplets. Our results are supported by a study which have presented that high fat and cholesterol diet induces macrophage infiltration, and accumulation in adipose, and liver tissues (Stanton *et al.*, 2011). Positive signals for iNOS (as a feature of NAFLD, and NASH) (Ha and Chae, 2010) were detected between inflammatory groups in Western diet mice. Our C3 immunohistochemistry was positive for most mice; this result coincides with Segers and colleagues who reported that in non-alcoholic steatohepatitis, there was a correlation between increased deposition of C3, lobular inflammation, and an increase of properdin expression. Rensen and colleagues detected C3 in the liver of NAFLD, and related this to steatosis and complement activation, leading to leukocyte infiltration of the liver by C3a, and C5a initiation.

In order to investigate the amount of food eaten by mice giving western diet and low fat diet in both properdin wild type and properdin deficient mice. The result showed that there were no significant differences between mice given Western diet compared with mice given low fat diet. Western diet led to the increase of body weight, fat pad weight, liver weight, triglyceride, and TNF- α compared to low fat diet (5LF2). This showed that Western diet may lead to the development of obesity, and metabolic complications such as NAFLD, NASH, and diabetes. Based on the triglyceride result for liver lysate, we decided to measure triglyceride in serum because during freezing, and thawing, in the tube triglycerides aggregate, and bind to the tube wall which will affect the result. Another reason was a layer of fat/oil after boiling during pipetting a homogenous solution will be added to the wells.

Alician blue staining was used to detect liver cirrhosis, but there was no sign of liver cirrhosis, presumably because the experimental time was not sufficient to initiate liver cirrhosis. Two mice did not even gain body weight. This may relate to diet that caused alteration of gut microbiota, which is termed dysbiosis, which

may cause host cell damage, and immunity consequences. In Western food, which high in protein, leads to abnormality in gastro intestinal tract metabolism, and immune homeostasis because some bacterial enzymes activities increase such as azo reductase and nitro reductase. Dysbiosis also affects weight due to the increase of bactericides species in the gut (Brown et al., 2012).

Liver includes parenchymal, and non-parenchymal cells. The most abundant liver cells are hepatocytes, which is parenchymal cell fraction and represents 90% of the biomass (Crispe, 2016). Hepatocytes are cells in liver which are involved in metabolic, endocrine, and secretory functions (Hindley et al., 2014, Schwen et al., 2016). In the infectious state, local response and immunologically active cells can be developed in non-parenchymal fraction, which includes liver sinusoidal endothelial cells, Kupffer cells, hepatic stellate cells, and trafficking monocytes, dendritic cells (DCs), natural killer cells, natural killer T cells, and diverse varieties of CD4+, and CD8+ T cells (Crispe, 2016).

Liver contributes to the innate immune system as it is a source of protective, and injury tissue proteins (Crispe, 2016). Self-defense at the cellular level: Different receptors are expressed on hepatocytes, including surface receptors (e.g., TLR4), endosomal receptors (e.g., TLR3), and cytoplasmic receptors (e.g., stimulator of IFN genes [STING], retinoic acid inducible gene-1 (RIG-1), and nucleotide-binding oligomerization domain (NOD) family members) (Seki and Brenner, 2008). Microbial products (Vodovotz et al., 2001) and endogenous signals such as heat shock protein 72, via their TLR2, and TLR4 receptors, were responded to directly by isolated hepatocytes (Galloway et al., 2008). In liver injury mediated by a TLR9 ligand, IRF7, and type 1 IFN signalling via the IFN- α R ameliorated liver injury through the action of IL-1ra, an antagonist of IL-1R signalling (Petrasek et al., 2011). There is a relation between signals from intestinal microbiota, and hepatic biology. Therefore, it can be highlighted that high fat diet may change intestinal microbiota diversity, and affect liver inflammation. Besides that, hepatocytes themselves interact with innate immune cells interactions.

LDLR^{-/-} mice were used because of their inherent susceptibility to develop steatosis, and steatohepatitis when fed a high fat, and high cholesterol diet. In LDLR^{-/-} mice were given HFD for 7 and 21 days, there was the development of infiltrating macrophages in liver (Bieggs et al., 2012). While, LDLR^{-/-} mice

developed steatohepatitis after 3 months of high fat high cholesterol (HFC) diet (Bieghs et al., 2012). The present study expands from these analyses. Our diet is less toxic: Here, LDLR^{-/-} and LDLR^{+/+} mice were in parallel fed a high fat -high sugar diet for 10 weeks to develop steatosis, and body weight gain and additionally, in both LDLR^{-/-} and LDLR^{+/+} mice fed high fat high sugar diet the effect of additional Vitamin D was analysed.

There are many features related to NASH, such as steatosis, ballooning degeneration, lobular inflammation, high serum cholesterol, and insulin resistance, and giant mitochondria (Doycheva et al., 2013). Interestingly, high fat -high sugar diet mice had significantly greater body weight, fat pad weight, IL-6 and insulin level compared to mice fed the Vitamin D supplemented high fat high sugar diet. Our results coincide with Lira et al., (2011) , who showed that circulating IL-6 concentrations are highly correlated with percentage of body fat ,and insulin resistance (Lira et al., 2011).

Steatosis was seen in all mice, but greater steatosis (more macrovesicles) were seen in high fat diet-high sugar diet mice, while in the supplementary dietary Vitamin D group less steatosis (microvesicles) and inflammation was detected. In addition, hepatic Srebp-1c, which is regulated by insulin, was increased in high fat -high sugar diet mice compared to mice fed the supplementary diet with Vitamin D. The result is supported support by Yin et al., (2012) who showed that Vitamin D inhibits lipogenesis. In a *vitro* experiment, Vitamin D was used to investigate the role as anti-steatotic molecule. Our results showed that Vitamin D plays a significant role at lowering lipid inclusions, identified by Oil Red O staining. This is supported by a previous study which documented that macrophages derived from peritoneal cavity of obese mice (elicited by intraperitoneal injection of 4% thioglycollate) developed into foam cells, while in the presence Vitamin D less foam cells were found. This is because oxLDL induced cholesteryl ester formation was reduced by Vitamin D (1, 25(OH) 2D3) (Oh et al., 2009). This is the first study to investigate the effect of high fat-high sugar diet on the increase of hepatic damage markers, and this was normalised by supplementary dietary Vitamin D containing diet in LDLR^{-/-} and LDLR^{+/+} mice. This may be how Vitamin D prevents liver damage.

Clinical trials, were unable to establish a benefit of Vitamin D supplementation in enhancing insulin sensitivity (George et al., 2012). However, in our study high

fat -high sugar diet caused the increase of insulin resistance. This was associated with high insulin level and low adiponectin level, and was normalised by supplementary dietary Vitamin D containing diet in LDLR^{-/-} and LDLR^{+/+} mice. Forouhi et al, (2008) had shown that low serum Vitamin D may associate with glycaemia, and insulin resistance in non- diabetic subjects. To investigate the effect of Vitamin D on aortic endothelium and to see the relationship of adhesion molecule expression to initiation factors, and the sites of lesion formation, VCAM-1 (vascular cell adhesion molecule-1) gene expression was performed for aorta of mice fed the Vitamin D supplemented high fat high sugar diet for ten weeks. The result showed that supplementary dietary Vitamin D played a role in the decrease of VCAM-1 gene expression. The findings of this experiment could be used to suggest that Vitamin D prevents atherosclerosis. Prussian blue staining showed that Vitamin D plays an important role in the decrease of M1 macrophage activity and the increase of M2 macrophage activity, as measured by intracellular iron content, a surrogate marker of M1 activity. To investigate M1 and M2 macrophage activity, flow cytometry was used for mice fed high fat-high sugar diet with, and without Vitamin D, F480/CD206 antibodies were used as M2 macrophage markers, but none were detected in spleens. This might be spleen cells for staining F480/CD206 antibodies were not sufficient. To further investigate M1 and M2 macrophages, iNOS, and arginase-1 mRNA expression as M1 and M2 macrophage activity markers (Jablonski et al., 2015). The first time, a reversal of iNOS and arginase-1 expression in the Vitamin D3 treated groups compared to the high fat high sugar diet groups. Hepatic, and splenic mRNA expression of iNOS (as M1 macrophage activity) in high fat -high sugar diet was significantly higher compared to Vitamin D supplemented high fat high sugar diet group, and hepatic Arginase-1 (as M2 macrophage activity) mRNA in Vitamin D supplemented high fat high sugar diet was significantly higher compared to LDLR^{+/+} mice fed high fat -high sugar diet without supplementary Vitamin D. According to Ogura et al., (2009) Vitamin D plays an anti-inflammatory role that coincides with our results, which showed Vitamin D led to the decrease of inflammatory mediators such as TNF- α , and IL-6. This antagonises the activity of LPS which binds to TLR4, signalling via NF κ B, and p38MAPK. The liver reacts in the acute phase response, playing a significant role in innate immune

cells modulation. Acute phase proteins are involved in the elevated several cytokines such as IL-1 α , TNF- α , and IL-6. As a result, coordinated changes in the transcriptional activity of hepatocytes occurs. This leads to the limitation of tissue injury and (Bauer et al., 2013). IL-6 is the so-called master cytokine of the liver in an acute-phase response (Guillen et al., 1996, Castell et al., 1988). IL-6 plays a significant role in the decrease of liver injury, as seen by removing gp130 component of the IL-6R in transgenic mice (Streetz et al., 2003). Antibacterial protein, which is called Lipocalin-2, is produced by liver (Xu et al., 2015). Hepatic mRNA expression of both SR-B1, and HMGCR increased in high fat diet mice (Qiu et al., 2013), compared to Vitamin D supplemented diet group mice in LDLR^{-/-} mice, although in LDLR^{+/+} mice the increase was not significantly different. These results suggest that high fat-high sugar diet caused the increase of genes involved in cholesterol synthesis, and dysregulation of cholesterol, which was prevented by supplementation with Vitamin D. Based on the proteome array, it can be said that proteins involved in fibrosis, steatosis, and inflammation are increased in adipose tissue of mice given high fat diet. There is a marked decrease of these proteins in (pooled) adipose tissue of mice given high fat diet plus Vitamin D. In obese and diabetes individuals, Vitamin D level decreased compared to lean and non-diabetic humans (Zoppini et al., 2013, Park et al., 2015). This agrees with our results, that showed high fat high sugar diet without supplementary Vitamin D had lower Vitamin D levels compared to mice supplemented with Vitamin D in their high fat-high sugar diet.

Saad et al., (2006) who showed that oxidized LDL caused classical complement activation in human serum. Our result showed that the Vitamin D supplemented diet group had increased residual activity of the classical pathway (less classical pathway activation *in vivo*) compared with high fat-high sugar diet mice. This is likely to be due to Vitamin D leading to a decrease of oxLDL (Oh et al., 2009). Our result showed less alternative pathway residual activity (higher alternative pathway activation *in vivo*) in mice fed high fat-high sugar diet. Chylomicron accelerates C3 tick-over by regulating the role of factor H, leading to the overproduction of ASP. As a result it leads to the increase of alternative pathway residual activity (Fujita et al., 2007). In keeping with this, mice fed Vitamin D supplemented high fat high sugar diet had higher alternative

pathway residual activity (lower alternative pathway activation *in vivo*) compared to mice fed high fat high sugar diet without Vitamin D supplementation. Classical pathway, and alternative pathway complement activation were performed on sera from mice. The result demonstrated that mice given high fat-high sugar diet without supplemented Vitamin D had higher classical, and alternative complement activation compared to mice given high fat-high sugar diet with Vitamin D. This is because higher MDA (lipid peroxidation product) was found in mice fed high fat-high sugar diet without Vitamin D compared to mice fed high fat-high sugar diet supplemented with Vitamin D. In addition, the parameters which are associated with obesity, diabetes, and fatty liver disease and inflammation were higher in mice fed high fat high sugar diet without supplemented Vitamin D. This also probably a main reason that classical and alternative pathway had higher activation in mice given high fat high sugar diet without supplemented Vitamin D compared to mice given high fat high sugar supplemented with Vitamin D.

The main reason for performing the diet study in only five weeks was to investigate whether mice get fatty liver disease by this time. This would deliver a study of refinement, following best practice, which could be adopted by others. Megamitochondria, larger than usual mitochondria, are features of fatty liver disease (Ahishali et al., 2010). Electron microscope result showed that megamitochondria were observed in liver of mice fed high fat-high sugar diet, while in mice fed high fat high sugar diet with Vitamin D supplementation only small mitochondria were observed. Megamitochondria are present mostly in hepatocytes with microvesicular steatosis. The reason for this is still poorly understood, but the enlarged organelles may be the result of injury from lipid peroxidation, or may represent an adaptive change (Takahashi and Fukusato, 2014). In obese-state, chronic enrichment of mitochondria–contacted endoplasmic membranes leads to mitochondrial dysfunction (Arruda et al., 2014). Livers from mice fed high fat-high sugar diet appeared to have deformed cell nucleus, and lobular inflammation with sinusoids. Male LDLR^{-/-} mice given high fat-high sugar for five weeks showed an increase of liver transaminases compared to mice given high fat-high sugar diet supplemented with Vitamin D for five weeks. Therefore, the effect of high fat-high sugar diet caused the

increase of hepatic damage markers, and this was normalised by supplementary Vitamin D containing diet for five weeks in male LDLR^{-/-} mice. Lower level of endotoxin, and IL-6 were detected in male LDLR^{-/-} and female LDLR^{-/-} and LDLR^{+/+} mice given high fat-high sugar diet supplemented with Vitamin D compared to mice given high fat-high sugar diet for five weeks. The current data highlight the importance of supplementary dietary Vitamin D in an anti-inflammatory role, and supplementary dietary Vitamin D prevents endotoxin formation in five weeks.

In five weeks, mice fed high fat-high sugar diet developed the increase of insulin resistance. This is demonstrated by high insulin level, high glycated haemoglobin, and low adiponectin level, and was normalised by supplementary dietary Vitamin D containing diet in male LDLR^{-/-} mice. Mice given high fat-high sugar diet had features of developing metabolic syndrome (NEFA, TG, and lipid peroxidation) compared to mice given Vitamin D as early as five weeks.

To summarise, it can be suggested that high fat diet- high sugar diet, given to mice for ten weeks, leads to development of features of metabolic syndrome, and Vitamin D plays an anti-steatosis, anti-inflammatory role, and skewing M1 macrophages to M2 macrophages. Therefore, Vitamin D may prevent liver steatosis, inflammation, and prediabetes phenomenon. Mice given high fat-high sugar diet for five weeks also developed central obesity, fatty liver, and metabolic syndrome disease in male LDLR^{-/-} mice. Consistent with the ten-week-study, high fat diet supplemented with Vitamin D caused the amelioration of fatty liver disease, and metabolic syndrome. Supplementary dietary consumption of Vitamin D for only five weeks plays a significant role in the prevention of steatosis inflammation, insulin resistance, and metabolic syndrome disease in male LDLR^{-/-} mice. Mice given high fat-high sugar diet for five weeks developed fatty liver disease, increased insulin level, and NEFA level, while in Vitamin D supplemented diet groups lower levels were detected in female LDLR^{-/-}, and LDLR^{+/+} mice. All measurements were higher after ten weeks compared to five weeks' diet. The tendency to express inflammation in the development of metabolic syndrome disease was higher in male compared to female LDLR^{-/-} at five weeks' high fat high sugar, based on NEFA, and IL-6 levels.

7.4 The role of properdin in fatty liver disease

Properdin limited the diet induced increase of body weight, fat pad weight, and the increase of NEFA. In murine 3T3-L1 adipocytes, addition of properdin inhibited the insulin-mediated stimulation of fatty acid uptake, and incorporation into TG, but this experiment lacked a control (Gauvreau et al., 2012). Our result showed that female, and male properdin deficient mice on LDLR^{+/+} background fed high sugar-high fat diet background had greater body weight gain, and central obesity compared to properdin wild type. Obesity and associates diseases including type 2 diabetes mellitus, fatty liver disease, atherosclerosis, which are associated with the elevated plasma glucose, fatty acids, cholesterol. As a result they lead to the stimulation of NLRP3 inflammasome expression or activation. The inflammasomes are a family of protein complexes, and a key innate immune system receptors and sensors in response to microbial and endogenous danger signals named DAMP (pathogen-associated molecular patterns (PAMP) and danger-associated molecular patterns (DAMPs) (Guo et al., 2015). It has been found that complement receptors activation, such as C3a and C5a receptors. They causes inflammasome activation which leads to the increase possibility to develop metabolic syndrome diseases (Arbore and Kemper, 2016).

Liver histology showed that female and male LDLR^{+/+}PKO mice fed Western diet and high fat-high sugar diet had greater steatosis, and lobular inflammation compared to LDLR^{+/+}PWT mice. Olive green stain and electron microscopy showed that properdin deficient mice fed Western diet for 10 weeks developed severe steatosis, and all features of fatty liver disease, while in properdin wild type less steatosis was observed. Our result disagree with Phieler et al., (2013) who showed that properdin plays a significant role in complement activation which leads to the development more ASP initiates. As a result, this leads to the increase of triglyceride synthesis, lipid storage in adipocytes and liver through C3a, C5a and C5L2 (Phieler et al., 2013). Acylation stimulating protein (ASP), also known as C3adesArg, has an important role in TG synthesis and energy balance in mice (Steiner et al., 2014).

For further investigation of inflammation, measurement of IL-6, and TNF- α were performed. The current data highlight that male LDLR^{+/+}, and female LDLR^{-/-}

properdin deficiency mice led to the increase of IL-6 compared to properdin wild type mice in mice given high fat high sugar diet. IL-6 level increased during expansion of adipose tissue, which was more obvious in properdin deficient mice. Complement activation in liver led to the increase of pro-inflammatory markers such as IL-6, TNF- α , and IL-8 by activated Kupffer cells (Rensen et al., 2009a). To understand the further effect of properdin on steatosis, strebp-1c mRNA expression as a steatosis marker was performed. The result showed higher strebp-1c mRNA expression in properdin deficient mice compared to wild type mice fed high fat-high sugar diet.

The empirical findings in this study provide a new understanding of properdin that plays a significant role in the prevention of steatosis. This is the first study to analyse liver function tests, to detect properdin effect in mice fed Western diet, and high fat-high sugar diet in both LDLR^{-/-} and LDLR^{+/+} back grounds. The result showed that male properdin deficient mice fed Western diet had higher AST and ALT levels compared to properdin wild type mice. However, ALT level was normal in female LDLR^{-/-} properdin deficient mice fed high fat-high sugar diet, so there might be a sex dependent effect for this observation. Local complement activation is present in patients with NAFLD compared to healthy controls; it therefore appears that complement activation associates with the progression of NAFLD. For example, the cleavage of complement proteins to trigger C5a, and C3a leads to neutrophil infiltration in tissues (Rensen et al., 2009a).

To further understand the role of properdin role in inflammation, endotoxin was measured. Relatively lower levels of endotoxin in wildtype may mean increased properdin dependent clearance of LPS or decreased intestinal permeability, whether of which this study addressed mechanistically. This result concludes that properdin plays a significant role in the prevention of NAFLD, and NASH development, and also showed that Western diet, and high fat-high sugar diet affected the increase of endotoxin in circulation.

According to Steiner et al., (2014), properdin deficient mice had greater M2-macrophage activity profile compared to properdin wild type mice in LDLR^{-/-} background mice, as demonstrated by increased MCP-1.

Classical pathway, and alternative pathway complement activation were performed on serum from mice. The results demonstrated that properdin

deficient mice had higher classical complement activation compared to properdin wild type mice. This is because higher MDA (lipid peroxidation product) was found in properdin deficient mice compared to properdin wild type. Classical pathway, and alternative pathway complement activation were also performed for obese, over weight, and normal people. The result showed that classical, and alternative pathway activation were higher in obese people compare to normal people. The cohort analysed was taken from a published study while ethical approval was valid (investigation of inflammatory markers in sepsis, PI Prof Jonathan Thompson, (Stover, 2015). This is because obese people had higher body mass index (BMI), likely higher MDA, and chylomicrons compared to normal people. Overweight people had higher Classical pathway, and alternative pathway complement activation, but lower than obese people. Properdin deficiency may lead to the increase of cholesterol synthesis, and dysregulation of cholesterol. In addition, the presence of properdin prevented metabolic syndrome disease by the decrease of triglyceride, and NEFA serum level compared to properdin deficient mice. Our results disagree with Stainer et al., (2014), and Gauvreau et al., (2012) who showed higher NEFA in properdin wild type compared to properdin deficient mice (engineered by W. Song). The differences were detected between our study was the high fat diet content given to mice. The fat percentage in our Western diet and high fat-high sugar diet study was 39.1 % and 59.4 %, while the percentage of fat in Stainer and colleagues, Gauvreau and colleagues studies were %16 and 45 % fat consequently.

Insulin, adiponectin and glycosylated haemoglobin were performed to investigate prediabetic features. My results showed that properdin deficient mice fed high fat-high sugar diet, and Western diet are more prediabetic than properdin wild type mice fed high fat-high sugar diet, and Western diet. Complement components could enhance triglyceride (TG) formation by lipolysis inhibition, enhanced glucose, and FFA uptake, and the decrease of FFA release indirectly (Phieler et al., 2013).

It can be observed that proteins involved in fibrosis, steatosis, inflammation, metabolic syndrome disease were higher in properdin deficient mice fed Western diet compared to properdin wild type mice on this diet. Our results showed that Lipocalin-2, and IGFB-5 were lower in properdin wild type mice

compared to properdin deficient mice. In contrast, Gauvreau et al (2012) showed that they were higher properdin wild type mice compared to properdin deficient mice. Fetuin-A, IGFB-2, 6, MCP-1, FGF acidic DPPIV all were higher in properdin deficient mice compared to properdin wild type while they not changed in Gauvreau et al (2012) result. The differences were detected between our study and Gauvreau *and* his colleagues result was that the fat percentage different from high fat diet given to mice between our study and their study. For further investigation the reason why properdin diffidence had higher metabolic syndrome disease parameters. Therefore, C5L2 mRNA expression for adipose tissue was performed. The result showed highly C5L2 mRNA expression in adipose tissue of properdin wild type mice compared to properdin deficient mice. It also to investigate C5L2 protein presence in properdin wild type, and properdin deficient mice, Western blotting was performed on homogenised liver and adipose tissue. Interestingly, the result also showed that C5L2 protein presence in liver, and adipose tissue was higher in properdin wild type mice compared to properdin deficient mice. Noticeably, delayed postprandial TG clearance, and reduced adipocyte size were shown in C5L2-deficient mice fed a diabetogenic diet, and also some insulin resistance features, and inflammation were detected including higher glucose uptake, and lipid deposition in the liver (Paglialunga et al., 2007). It can be determined that C5L2 deficiency may develop the increase of C5a-C5aR which leads to the enhancement of Adipose tissue inflammation, and insulin resistance (Lim et al., 2013). Therefore, it appears that the more complement activation will lead to the increase C5L2 level.

It also noteworthy to mention that C5L2 mRNA and protein level were lower in properdin deficient mice compared to properdin wild type mice. Therefore, it appears from our result that properdin deficient mice may have less lipid clearance therefore properdin deficient mice enhances metabolic syndrome disease.

To investigate the role of properdin in a dietary model, properdin wild type, and properdin deficient mice were given high fat high sugar diet, and western diet for 5 weeks. Mice fed high fat-high sugar diet for 5 weeks also developed fatty liver disease. Properdin wild type mice had less steatosis, and inflammation compared to properdin deficient mice. In five weeks diet mice, in addition to

performing hematoxylin and eosin staining, electron microscopy and MRI were performed on livers to further investigate properdin wild type and properdin deficient mice. Electron microscopy result showed that mega mitochondria were observed in liver male LDLR^{-/-} mice fed high fat-high sugar diet, while in properdin wild type mice fed high fat high sugar diet smaller mitochondria were observed. Liver histology showed that higher fat droplets were seen in properdin deficient mice compared to properdin wild type. Our MRI result showed that fat fraction % was higher in properdin deficient mice compared to properdin wild type in both male and female mice. High fat-high sugar diet, Western diet and low fat diet were different in terms of the percentage of fat fraction, properdin deficient mice fed Western diet had, but in all diets properdin deficient mice had higher fat fraction percentage compared to properdin wild type mice.

There was a higher percentage fat pad weight, and also a tendency to higher body weight percentage in male LDLR^{-/-} properdin deficient mice fed high fat-high sugar diet compared to wild type mice. This agrees with Gauvreau et al., (2012) who showed that properdin deficient mice had higher body weight, and fat pad weight compared to properdin wild type mice. In addition, male LDLR^{+/+} properdin deficient mice fed Western diet had higher fat pad weight, and body weight compared to wild type mice.

The previous ten-week study revealed that properdin deficient mice developed liver damage. In LDLR^{-/-} properdin deficient mice given high fat-high sugar for five weeks, an increase of liver transaminases was detected compared to properdin wild type mice group. In the absence of properdin, hepatic damage markers were increased compared to properdin wild type mice group. A lower level of endotoxin was detected in properdin wild type compared to properdin deficient mice. Properdin wild type mice had lower IL-6, but this was not significantly different compared to properdin deficient mice. The current data highlight the importance of properdin in an anti-inflammatory role, and prevention of intestinal leakage (decreased endotoxin level) in five weeks. Interestingly properdin has been reported to aid in LPS clearance (Kemper and Hourcade, 2008).

In five weeks, in male LDLR^{-/-} properdin deficient mice, fed high fat-high sugar diet, led to the increase of insulin resistance. This was shown by high insulin

level, high glycated haemoglobin, and low adiponectin level compared to properdin wild type mice. Properdin deficient mice given high fat-high sugar diet had higher metabolic syndrome such as NEFA, TG, and lipid peroxidation compared to properdin wild type. There are associations between elevation of NEFA, obesity, inflammation, dyslipidaemia, and insulin resistance stat (Karpe et al., 2011).

Our results showed that male properdin deficient mice given high fat-high sugar diet for five weeks developed fatty liver, and metabolic syndrome disease. Interestingly, properdin wild type mice showed less fatty liver disease, and metabolic syndrome. For further investigation, female mice were used, 11 female mice were fed high fat-high sugar diet LDLR^{+/+} PWT/PKO, and LDLR^{-/-} PWT/PKO for five weeks. The result showed that female properdin deficient mice developed fatty liver disease, and metabolic syndrome disease, and less developed in the presence of properdin. Inflammation marker (IL-6), prediabetic (insulin) ,and metabolic syndrome such as NEFA were increased in properdin deficient mice compared to properdin wild type mice in LDLR^{+/+} back ground mice. Female LDLR^{-/-}PKO, mice had higher IL-6 compared to properdin wild type mice.

To summarise, it can be suggested that high fat diet- high sugar diet and western diet, given to mice for ten weeks and five weeks, leads to development of features of metabolic syndrome in properdin deficient mice compared to properdin wild type mice. Therefore, properdin may prevent liver steatosis, inflammation, and prediabetes phenomenon. The elevation of endotoxin, triglyceride, NEFA, IL-6, MDA, TLR4 mRNA expression low Vitamin D, low C5L2 are associated with obesity and related diseases, which were higher in properdin deficient mice compared to properdin wild type mice.

Properdin deficient mice developed central obesity, fatty liver, and metabolic syndrome disease in mice given high fat-high sugar diet and Western diet for ten and five weeks. All measurements were higher in mice given high fat-high sugar diet for ten weeks compared to mice given high fat-high sugar diet for five weeks.

7.5 The role of Exercise and Vitamin D on mice induced obesity

The exercise study was equally interesting. C57Bl/6 mice fed 58R3 after 5 weeks high fat diet–high sugar developed liver steatosis. Ten male mice C57BL/6 background were used for this experiment to investigate the additional effect of exercise on mice fed high fat diet supplemented Vitamin D or not.

Body weight and fat pad weight had a tendency to have less in mice fed the Vitamin D supplemented high fat high sugar diet with access to the exercise wheel compared to mice fed the Vitamin D supplemented high fat high sugar diet without access to the exercise wheel. C57BL/6 mice group without access to exercise showed increased steatosis and inflammation. Obesity, inflammation, hyperlipidemia, and diabetes are associated with NAFLD, and NASH (Bhatt and Smith, 2015). Interestingly, in our mice fed high fat diet supplemented with Vitamin D without access to exercise, no features of steatosis, inflammation and obesity were seen.

There were no steatosis or inflammation in mice fed the Vitamin D supplemented high fat high sugar diet without access to the exercise wheel. According to Ouchi and his colleagues who showed that several pro inflammatory adipokines such as IL-6, IL-8, IL-1 β , TNF- α and monocyte chemoattractant protein-1 are produced in obese adipose tissue, and they will enter the circulation (Ouchi et al., 2011). In obese rodents, TNF- α was over expressed while in TNF- α receptor deficient rodents, insulin resistance was not developed (Uysal et al., 1997). Insulin resistance can be developed by TNF- α , through modifying adipocyte differentiation and adipocyte lipid metabolism (Cawthorn and Sethi, 2008). Our result showed that mice fed high fat-high sugar diet supplemented with Vitamin D with access to exercise had a tendency to have less TNF- α , and IL-6 protein levels compared to mice fed high fat diet supplemented with Vitamin D without access to exercise. It therefore appears that Vitamin D supplemented with exercise led to the decrease possibility to develop insulin resistance.

Our results showed a tendency to have less NEFA in mice fed mice fed high fat diet supplemented Vitamin D with access to exercise compare to mice fed mice fed high fat diet supplemented Vitamin D without access to exercise. There are

associations between elevation of NEFA, obesity, dyslipidaemia, and insulin resistance state. It is thought that insulin inhibits FFA mobilisation process from adipose tissue. Therefore, lipolysis in adipose tissue is increased in the insulin resistance situation (Karpe et al., 2011). Insulin level had a tendency to have lower in mice fed high fat diet supplemented Vitamin D with access to exercise compare to mice fed mice fed high fat diet supplemented Vitamin D without access to exercise. Exercise caused the decrease insulin level (Geiger et al., 2005), and low Vitamin D serum 25-OH Vitamin D may lead to glycaemia and insulin resistance in non- diabetic subjects (Forouhi et al., 2008). This is due to high insulin level, and was normalised by supplementary dietary Vitamin D containing diet with access to exercise wheel.

Our results showed that Vitamin D group with access to exercise wheel had a tendency to have lower classical pathway residual complement activity compared to Vitamin D group without access to exercise wheel. Our result agrees with Saad et al., (2006) who showed that oxidized LDL caused classical complement activation in human serum, because less oxLDL- is produced in the presence exercise (Vasankari et al., 1998), and low level of Vitamin D developed the decrease of oxLDL (Oh et al., 2009).

Chylomicron accelerates C3 tick-over by regulating the role of factor H, leading to the overproduction of ASP. As a result, it leads to the increase of alternative pathway residual activity (Fujita et al., 2007). Our results showed that mice fed the Vitamin D supplemented high fat high sugar diet with access to the exercise wheel had a tendency to have less alternative pathway residual activity compared to mice fed the Vitamin D supplemented high fat high sugar diet without access to the exercise wheel. In addition, more alternative pathway residual activity in mice fed high fat-high sugar diet without access to exercise wheel compared to mice fed high fat-high sugar diet with access to exercise wheel.

Based on the proteome cytokine array, it can be concluded that proteins involved in fibrosis, steatosis, inflammation, diabetes, obesity, and atherosclerosis are increased in muscle of mice given high fat diet without access to exercise. There is a marked decrease of these proteins in muscle of mice given high fat diet supplemented Vitamin D with access to exercise. In

conclusion, it can be said both Vitamin D, and exercise have a beneficial effect, which was additive to dampen inflammatory markers, and metabolic syndrome disease markers (TNF- α , lipoclin-2, Il-6, NEFA, Feutin-A, IGFB, C- reactive protein). The actual mechanism is that exercise leads to the regulation of glucose transport by the increase of AMPK activation, and it leads to the decrease of PAMP production so causes the decrease of phosphorylation, and translocation of NF κ B, and p38MAPK into the cell nucleus. Therefore, these might be reasons why exercise leads to decrease insulin resistance, decrease of inflammation, obesity, and metabolic syndrome diseases in people.

7.6 Limitations

These studies are limited by the use of cell lines from mouse and human, and could be complemented by FACS analysis for macrophage polarisation and hepatocyte receptor expression.

One limitation of this part of the study might appear to be the small numbers, however, it has to be borne in mind that these mice were bred in house. It was essential in the design of the study to probe mice from the same litters for their reaction to the diet and treatments. It was found that the body weight gain was unequal between litters, so preferably littermates were analysed in this study to ensure more uniformity in diet induced metabolic reaction. All mice were kept in the same barrier unit and were exposed to the same handling and procedures. The Vitamin D dose tested was tenfold higher, as estimated to be nontoxic from the literature. It would be interesting to see a concentration dependent effect, and also, whether this dose is effective in studies longer than ten weeks. This is of particular interest as significant NASH develops later in the disease process. This will require amendment to the existing license. One significant limitation in transferring the data elsewhere is that the microbiome of the mice could not be studied for financial reasons. The experimental unit of three mice per exercise cage can in future be increased when purchasing smaller wheels, which have only recently come onto the market.

7.7 Conclusions

High fat high sucrose diet led to the development NAFLD, and insulin resistance, and this was ameliorated when a tenfold excess of Vitamin D was present in the high fat high sucrose diet in LDLR^{-/-} and LDLR^{+/+} mice. Voluntary exercise further improved the beneficial effect of Vitamin D added to our high fat high sugar diet. Properdin deficient mice were more prone to developing obesity, and metabolic syndrome diseases compared to wildtype mice. This was associated with a distinct regulation of C5L2 in relation to complement activation (Figure). Vitamin D, DHA, and possibly allicin can be used to alleviate fatty liver disease, and obesity associated complications.

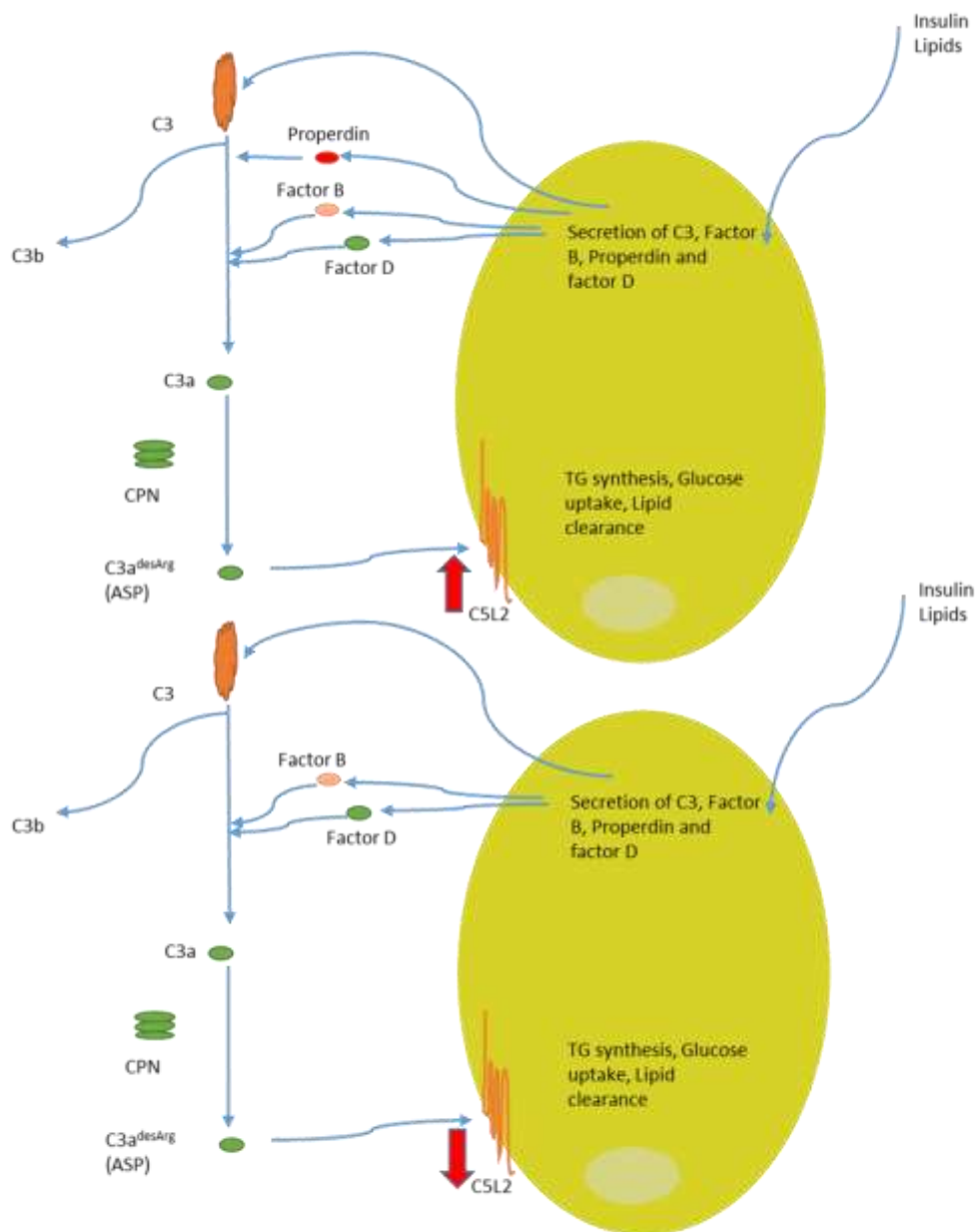


Figure 7-1 Roles of properdin in lipid metabolism.

Properdin leads to the increase of C5L2 expression, as a result, it leads to triglyceride, lipid clearance and glucose uptake increase (Panel A). Properdin deficient caused less C5L2 expression (Panel B)

7.8 Future plan

An obvious future plan is to address the limitations identified as part of this work and to pursue, in particular, the beneficial role of properdin in avoiding severe fatty liver disease. Also, based on present interest in Vitamin D as a nutraceutical for man, it would be of value to investigate a possible beneficial effect of Vitamin D supplements in patients with Type 2 diabetes, based on a recent study. Essentially we will follow a published Iranian clinical trial (Shab-Bidar et al., 2011) which showed that normal consumption of a Vitamin D enrichable yoghurt drink to increase circulating Vitamin D levels ameliorates glucose control, lipid profile and endothelial inflammatory markers in the diabetic probands. We can apply this therapeutic approach in our patients in Iraq and use a popular drink called sheneena (Arabic) and mastao (Kurdish).

Appendix



The role of complement properdin in fatty liver disease

Ramiar Kamal Kheder, Mike Browning, Cordula Stover

Department of Infection, Immunity & Inflammation, University Of Leicester, UK.



Background

Up to a third of people in industrialised countries develop fatty liver disease due to diets rich in fat. A histopathological study of liver specimen diagnosed with non-alcoholic steatohepatitis showed myeloperoxidase positive neutrophils around steatotic hepatocytes, colocalising with complement properdin and C3c. This indicated complement activation in diseased liver. The present study is the first to investigate in a mouse model the role of properdin in diet induced liver disease by comparing properdin deficient (PKO) and wild type mice (PWT) on a C57Bl/6 background.

Aims and Objectives

1. To investigate hepatic and adipose response to Western diet (5TJN) and systemic measures of inflammation.
2. To investigate the role of properdin in dietary fatty liver and possible ensuing

Methods

Body weight, fat pad weight were recorded. Liver histology was performed, qPCR analysis for TNF- α , strep-1c, TLR4. Elisa for serum insulin. Adiponectin and endotoxin. Groups analysed: for PWT/PKO fed high fat diet (5TJN) and low fat diet (5LF2).

Results

Investigate the properdin effect on obesity, body weight, fat pad

The increase of body weight gain in male PKO fed a Western diet (5TJN) compared to male PWT (Figure 1, panel A). In PKO mice fed 5TJN diet significantly higher fat pad weight compared to PWT mice fat pad weight (figure 1, panel B). No significant differences in body weight gain between PWT/PKO in female mice

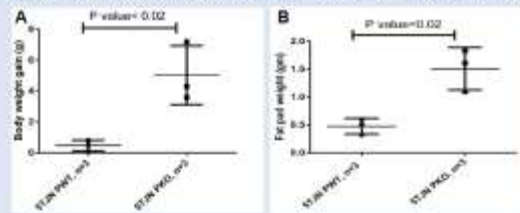


Figure 1: Body weight gain in male PKO fed 5TJN compared to PWT mice, age matched (panel A), fat pad weight in male PKO fed 5TJN compared to properdin wild type mice (panel B).

Endotoxin level in sera and hepatic mRNA expression of TLR4

The western diet leads to translocation of LPS via gut and the hypothesis was that TLR4 expression react to this. The increase of endotoxin in PKO fed 5TJN compared to PWT and 5LF2 fed PKO (Figure 2, panel A). In PKO mice fed 5TJN diet significantly higher TLR4 mRNA expression compared to PKO fed low fat diet (5LF2) (Figure 2, panel B).

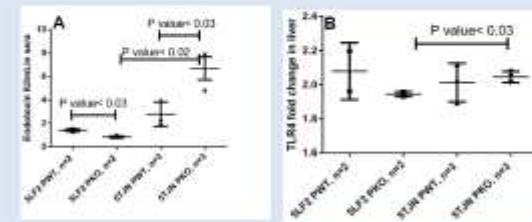


Figure 2: Endotoxin in PKO fed 5TJN compared to PWT and 5LF2, sex and age matched (panel A), Hepatic mRNA expression of TLR4 (panel B).

Hepatic Strep-1c and TNF- α mRNA expression of TLR4

Hepatic mRNA expression of Strep-1c (marker of steatosis) and TNF- α (inflammation marker) to investigate the increased of body weight, fat pad weight and endotoxin in properdin deficient mice. Interestingly, the showed Strep-1c increased in PKO mice compared to PWT mice (figure 3, panel A)

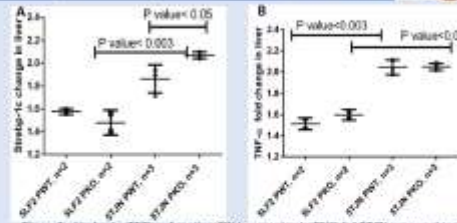


Figure 3: Strep-1c, TNF- α hepatic mRNA expression in PKO fed 5TJN compared to PWT and 5LF2 PKO (panel A and B).

Liver Histology in PWT/PKO mice fed 5TJN and 5LF2 diets

Liver histology was to investigate the role of properdin in fatty liver disease and showed PWT fed 5TJN had same fatty changes (Figure 4, panel C), no steatosis in 5LF2 (panel A and B) and greater steatosis in properdin deficient mice (Figure 4, panel D). Liver function tests were performed but no significant differences between PWT and PKO mice.

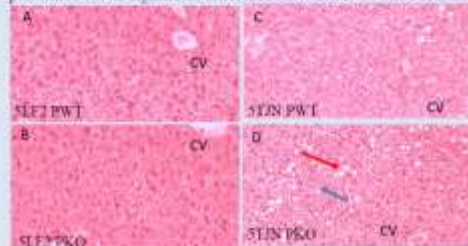


Figure 4: Histomorphology staining of paraffin embedded liver sections obtained from mice (x10). No inflammation and steatosis in control (panel A and B), macrophages (blue arrows), microvesicles (red arrows) (panel C and D), CV, central

Investigate the properdin effect on Insulin resistance

To analyse the development of insulin resistance given the increase in body weight, insulin and Adiponectin was measured. The increase of insulin and decrease of Adiponectin in 5TJN compared 5LF2 diet, no significant differences between PWT and PKO mice (figure 5).

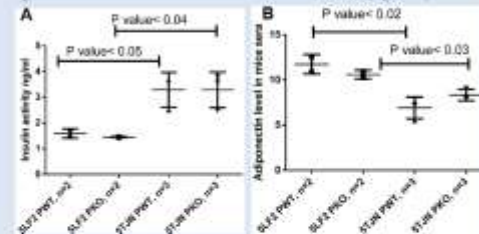


Figure 5: Insulin Elisa and Adiponectin in PWT/PKO fed 5TJN compared to PWT/PKO fed 5LF2.

Conclusions

In the absence of properdin, central obesity is increased in male mice fed a Western diet and circulating endotoxin is significantly elevated. After 10 weeks, diet, there is no indication of insulin resistance compared to wild type mice, though hepatic Strep-1c, which is regulated by insulin, is increased in properdin deficient mice. No properdin role was detected in Insulin and Adiponectin measurements

Future work: Further investigation are needed to see the effect of properdin on fatty liver disease and obesity. To seek the role of properdin on cardiovascular disease. VCAM-1 (vascular cell adhesion molecule-1) gene expression will be performed.

Acknowledgment: Special thanks to Professor Wilhelm Schwaeble (university of Leicester) Dr James Hobkirk (university of Hull) and my sponsor (Kurdish Government of Higher Education)

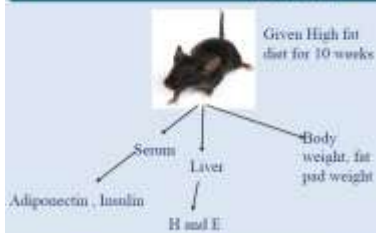
Figure (Appendix I) The 4th European Congress of Immunology (ECI 2015), Austria- Vienna, September 2015 (Appendix I)



Background

Up to a third of people in industrialised countries develop fatty liver disease due to diets rich in fat. The present study is the first to investigate in a mouse model the role of proprotein in diet induced liver disease by comparing proprotein deficient (PKO) and wild type mice (PWT) on a C57BL/6 background. A naturally occurring deletion of exons 7-11 in the nicotinamide nucleotide transhydrogenase gene in C57BL/6 mice from the Jackson Laboratories (C57BL/6J) results in impaired glucose-stimulated insulin secretion (Freeman et al., 2006). This is the reason for not doing glucose tolerance test. This poster summarises our efforts to achieve refinement and reduction.

Methods



Body weight and fat pad weight, Elisa for serum insulin, Adiponectin. Groups analysed to investigate high fat diet induced fatty liver disease and insulin resistance.

Area of refinement

- Comprehensive analysis of each mouse (tissues, bloods, weight)
- Where possible, mice are analysed as complete litters
- Age-and sex matching
- Glucose levels from final blood not from additional tail prick near end of diet
- No glucose tolerance test because of known gene defect (intro)
- Short duration.

Results

Using Body weight, fat pad to investigate fat induced obesity

The increase of body weight gain in male PKO fed a Western diet (5TJN) compared to male PWT (figure 1, panel A). In PKO mice fed 5TJN diet significantly higher fat pad weight compared to PWT mice fat pad weight (figure 1, panel B). No significant differences in body weight gain between PWT/PKO in female mice

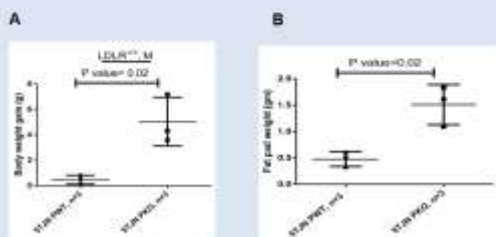


Figure 1: Body weight gain in male PKO fed 5TJN compared to PWT sex, age matched (panel A). Fat pad weight in male PKO fed compared to proprotein wild type mice (panel B).

Liver histology was to investigate the role of proprotein in fatty liver disease and showed PWT fed 5TJN had some fatty changes (Figure 2, panel C), no steatosis in 5LF2 (panel A and B) and less steatosis in proprotein wild type mice (Figure 2, panel C). Liver function tests were performed but no significant differences between PWT and PKO mice.

Using Liver Histology to investigate fat induced obesity in PWT/PKO mice fed 5TJN and 5LF2 diets

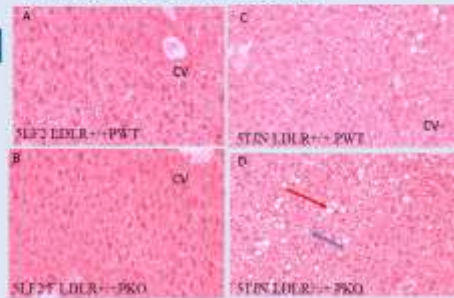


Figure 2: Haematoxylin-eosin staining of paraffin embedded liver sections obtained from mice (LDL). No inflammation and steatosis in control (panel A and B), microvesicles (blue arrows), macrovesicles (red arrows) (panel C and D), CV, central.

Using Sera to investigate insulin resistance by testing Insulin and Adiponectin

To analyse the development of insulin resistance given the increase in body weight, insulin and Adiponectin was measured. There is significance in increase of insulin and in decrease of Adiponectin in 5TJN compared 5LF2 diet, but no significant differences between PWT and PKO mice (figure 3).

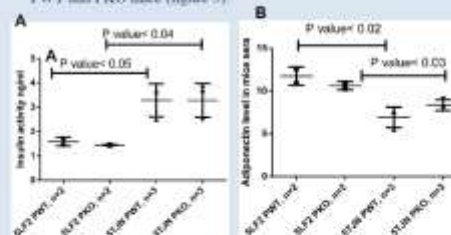


Figure 3: Insulin Elisa and Adiponectin in PWT/PKO fed 5TJN compared to PWT/PKO fed 5LF2.

Conclusions

A fatty liver disease model has been successfully established at Leicester (figure 2). 10-12 weeks are sufficient to have a model in which the metabolic response can be analysed in parallel measurements. Therefore, relatively few mice are needed.

Acknowledgment: Special thanks to DBS staff, Professor Wilhelm Schneble (University of Leicester) and my sponsor (Kurdish Government of Higher Education)

Figure (Appendix II) The 3Rs Conference, Leicester UK. March 2016. Selected as one of the best posters (awarded prize).

The beneficial role of Vitamin D₃ in high fat diet induced fatty liver disease and Obesity

Ramiar Khader,¹ James Hobbs¹, Mike Browning¹, Cordula Stover²
¹ Department of Infection, Immunity & Inflammation, University Of Leicester, UK.
² Department of sport, Health and exercise science, University Of Hull, UK.



Background

Vitamin D is considered as adjuvant therapy in the management of non-alcoholic fatty liver disease (NAFLD). Vitamin D is decreased significantly with increasing body mass index, meaning that low serum levels of Vitamin D are associated with insulin resistance and the development NAFLD. A prospective study showed that women given Vitamin D orally had a lower risk of developing Diabetes mellitus type2 (Bonissova *et al.*, 2003). There is a Vitamin D response element located in the promoter region of the insulin gene.

Aims and Objectives

To define the beneficial effect of dietary Vitamin D₃ in manifestation of diet induced fatty liver disease in LDLR^{+/+} and LDLR^{-/-} mice receiving a high fat high sugar diet by studying histology and biochemical markers.

Material and Methods

Formulated diet was from TestDiet. LDLR^{+/+} and LDLR^{-/-} were taken from colonies held at the University of Leicester. LDLR^{-/-} were used as a model of familial hypercholesterolemia. Liver histology was performed, liver function tests, qPCR analysis for TLR4, Elisa for serum insulin, Adiponectin and endotoxin. Groups fed high fat high sugar with and without Vitamin D (58R3+Vitamin D₃) and low fat diet (5LF2) in LDLR^{-/-} and LDLR^{+/+} mice.
 5LF2: 5.8% fat, 14.3% protein, 0.4% sugar.
 58R3: 35.8% fat, 20.2% protein, 17.4% sugar.
 The extent of (non toxic) Vitamin D supplementation remains undisclosed until after publication.

Results

Dietary Vitamin D₃ leads to the decrease of body weight

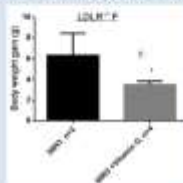


Figure 1: Vitamin D₃ decreased body weight.

Vitamin D₃ significantly improves steatosis

Liver histology showed fatty changes in mice fed high fat high sugar diet (Figure 1, panel A), while there was no steatosis in group receiving Vitamin D (panel B).

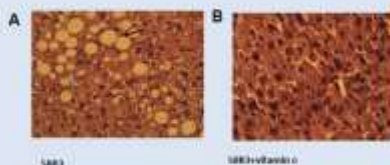


Figure 2: Histopathology (oil) staining of paraffin embedded liver sections obtained from mice LDLR^{+/+} (58R3). No inflammation and steatosis in vitamin D group mice (B). microvesicles (blue arrows), macrovesicles (black arrows) (Panel A).

Vitamin D₃ normalises liver function tests

AST and ALT activities were measured in mouse serum and analysed in dependence of diet. LDLR^{+/+} and LDLR^{-/-} mice were normalised when the diet was supplemented with additional Vitamin D.

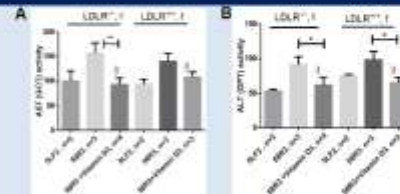


Figure 3: The effect of 58R3 + vitamin D₃ diet on AST (A) and ALT (B) activity

Vitamin D₃ ameliorates endotoxin levels in sera and hepatic mRNA expression of TLR4

Diets high in fat lead to translocation of endotoxins (LPS) from the gut and the hypothesis was that TLR4 expression reacted to this. TLR4 gene expression was increased in LDLR^{-/-} and LDLR^{+/+} fed a diet high in fat and sugar while the group receiving the same diet supplemented with Vitamin D were significantly improved (Panel A). The increase of endotoxin level in high fat high sugar diet groups were significantly decreased when Vitamin D was supplemented, for LDLR^{+/+} and LDLR^{-/-} (panel B).

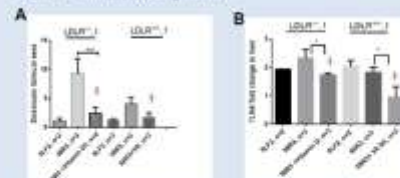


Figure 4: The effect of high fat high sugar diet + vitamin D₃ on endotoxin measurement (A) hepatic gene expression of TLR4 (B).

Vitamin D₃ affects insulin sensitivity favourably

Serum levels of insulin and adiponectin are inversely related measures of developing insulin resistance. Vitamin D causes the increase of insulin sensitivity by increasing Adiponectin and decreasing insulin levels.

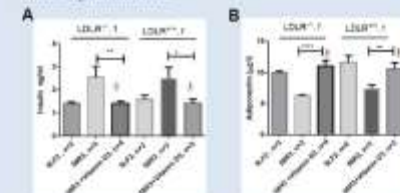


Figure 5: Insulin (A) and Adiponectin (B) were measured in serum samples of LDLR^{+/+} and LDLR^{-/-}.

Conclusions

- 1- Alimentary Vitamin D₃ leads to the decrease of obesity.
- 2- Alimentary Vitamin D₃ improves liver histology and normalises liver function tests.
- 3- Alimentary Vitamin D₃ reduces diet-induced endotoxemia.
- 4- Alimentary Vitamin D₃ normalises insulin sensitivity.

Future work: Further investigation are needed to see the effect of vitamin D₃ on fatty liver disease and obesity in male mice.

Acknowledgment: Biomedical Services University of Leicester; Kurdish Government of Higher Education

Reference: Bonissova, A.M., Todorova, T., Kadir, G., Dzhurkova, L. and Kozucheva, R., 2003. The effect of vitamin D₃ on insulin secretion and peripheral insulin sensitivity in type 2 diabetic patients. *International journal of clinical practice*, 57(10), pp. 258-261.

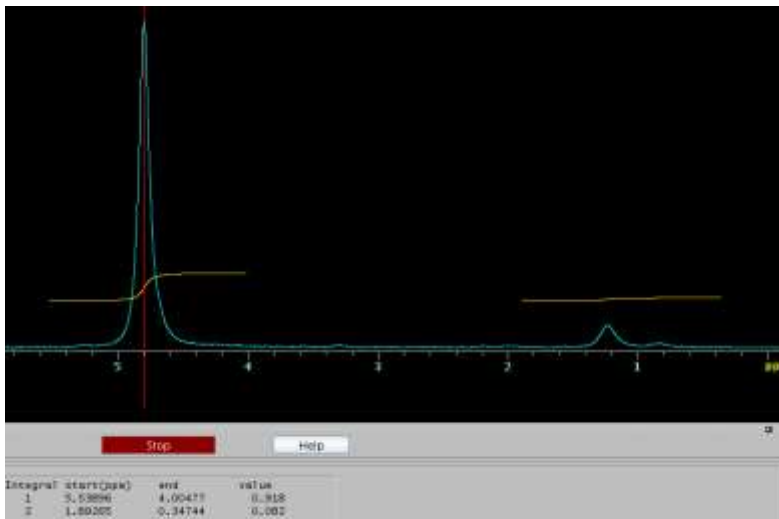


Figure (Appendix III) The 84th European Atherosclerosis Society Congress. 20116. Austria, Innsbruck. May 2016.

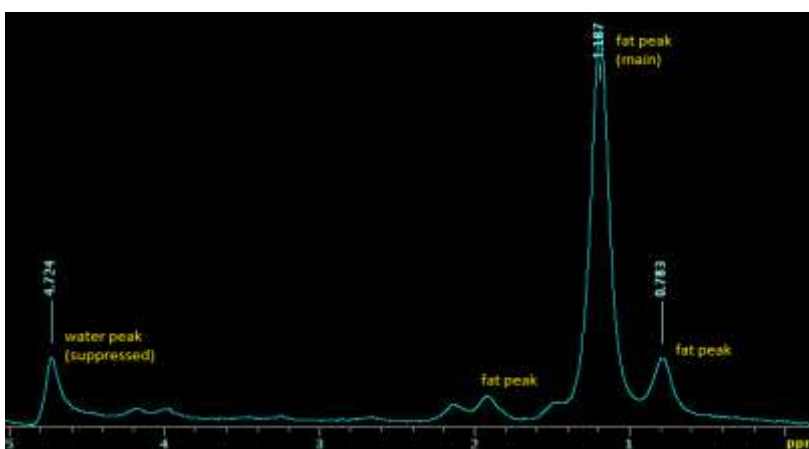
Magnetic resonance imaging (MRI)

Mouse livers were fixed in 10% formal saline, each liver was put in an Eppendorf Tube. The procedure was run by Dr Michael Kelly (preclinical Imaging Manager). The method automatically detects the two peaks, normalizes to the water peak amplitude, and calculates the integrals (in this case, water = 0.918, fat = 0.082 (panel A). Fat reached peak (panel B). % fat fraction = Fat ratio/water ratio so fat fraction = 8.83. The electronic shielding of the protons in the triglyceride molecules of fat is greater than that experienced by protons in water molecules.

A



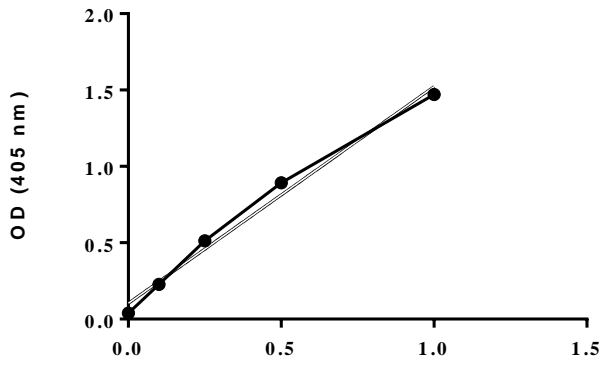
B



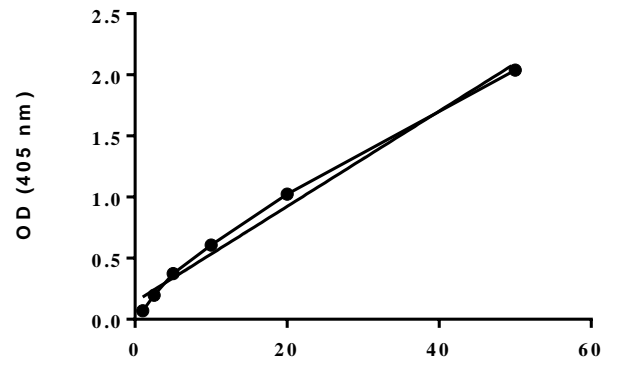
MRI method to detect fat content in liver mice.

In the case of water (panel A), Fat reaches peak (panel B).

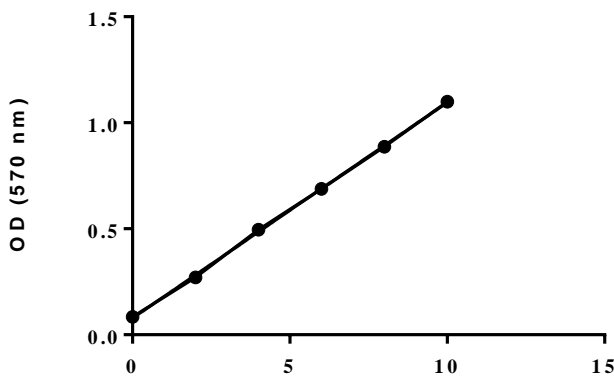
Examples of representative standard curves.



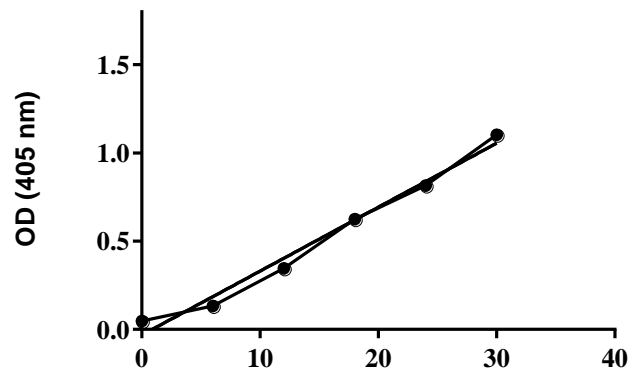
Endotoxin IU/mL



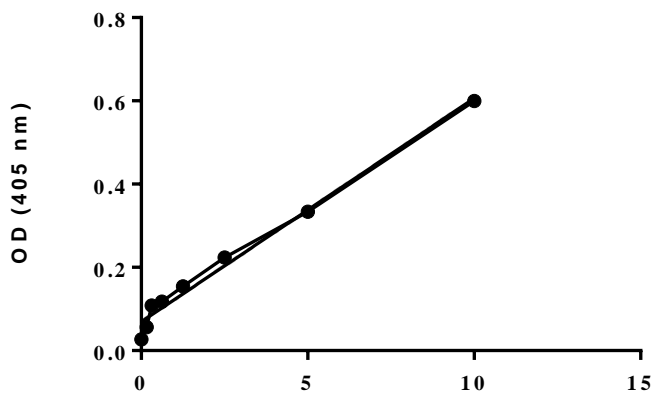
Insulin (ng/mL)



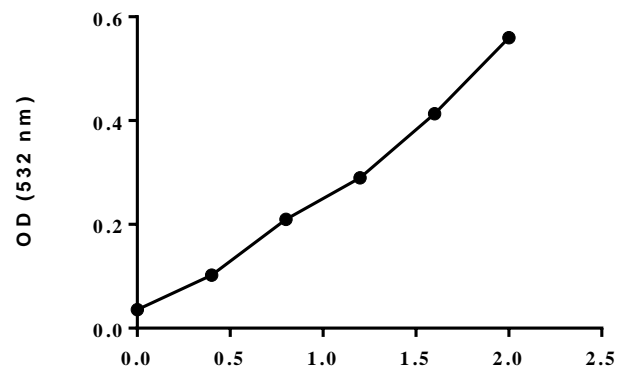
ALT (IU/L)



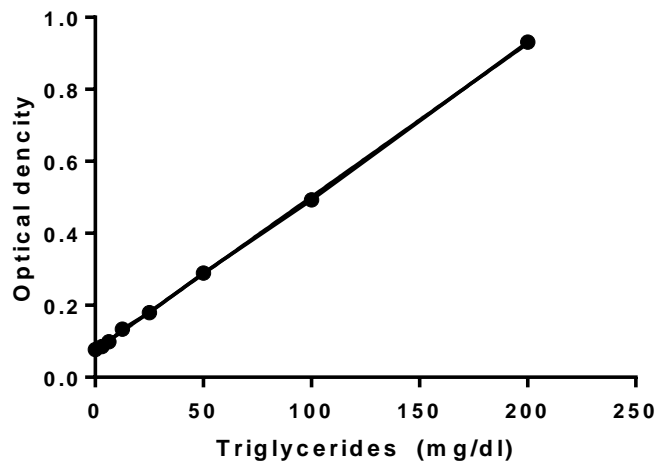
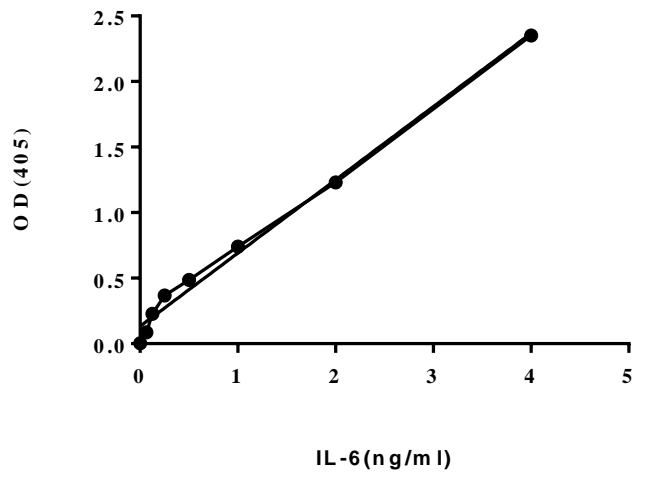
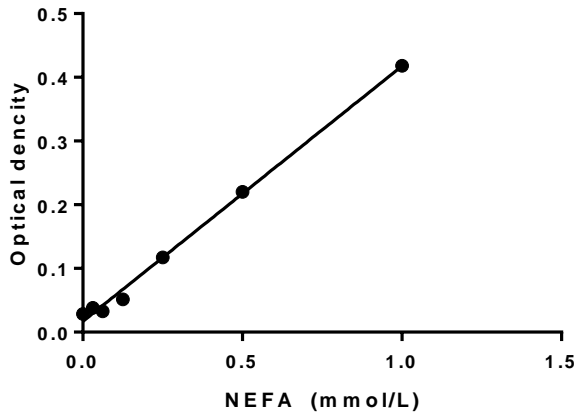
AST (IU/L)



Adiponectin (µg/L)



MDA (µmol/l)



A set of studies was conducted to test the feasibility of the model and the analyses

Weight gain:

Sixteen male mice (8 LDLR^{-/-} PWT, and 8 LDLR^{-/-} PKO) were given high fat diet (HFD) (Western diet) for 12 weeks. In order to further investigate the difference between properdin wild type and properdin knockout mice on HFD mice, some mice were given HFD for 10 weeks as follow: LDLR^{-/-} PWT female (n=5) LDLR^{-/-} PKO female (n=4), this developed because the saturation point of mice was reached peak at 10 weeks during given HFD for 12 weeks.

Body weight was measured once per week (12 weeks). LDLR^{-/-} PWT male mice given HFD for 10 weeks (38.52 ± 7.29 g) had greater body weight when compared to LDLR^{-/-} PWT mice given low fat diet (LFD) (28.65± 2.25 g) but not significantly different compared to male LDLR^{-/-} PKO mice given HFD (33.15 ± 4.29) (Unpaired T-test). Figure 1A shows that line graph increased steadily and reached peak at (week 10) in properdin wild type mice, also in properdin knockout mice, the graph was less steep reaching a plateau at week 10. The food intake was measured once per week by the animal technician for both genotypes as follows: food intake= the amount food was put on the cage minus the amount food remained of the data collected. Only recording for seven mice were reliable due to staff changes in CRF (Central Research Facility), LDLR^{-/-} PWT mice (n=4) was compared to LDLR^{-/-}PKO mice (n=3). The line graph in figure (1 B) shows the amount of food taken for properdin wild type mice reached peak at 4th week then dramatically decreased till the (week 10) while food taken in properdin knockout mice and reached peak at (week 8-9) and then at the three last weeks sharply decreased. There were no significant differences in food intake for LDLR^{-/-} PWT and LDLR^{-/-} PKO mice (figure 1 B), the amount of food taken at (week 1) statistically no differences with the amount of food taken at (week 10). Food intake increased dramatically from week 2 then decreased suddenly till week 3-4 (figure 1 C). Fluctuation was seen till the end of study. This suggests, together with the development of weight gain (panel A) that LDLR^{-/-}PKO mice were saturated at 9/10 weeks, LDLR^{-/-}PWT

kept gaining weight in spite of a reduction in their food intake compared to the first 4 weeks.

Next, female mice were given HFD for 10 weeks as follow: LDLR^{-/-} PWT female (n=5) LDLR^{-/-} PKO female (n=4). Body weight started in LDLR^{-/-} PWT from (19.16 ± 0.54 g) (first week of HFD given) and LDLR^{-/-} PKO (17.58 ± 0.51 g) (first week of HFD given) and no significant differences was seen between them. End body weight of female LDLR^{-/-} PWT (24.66 ± 2.47) mice had not the significant different when compared to end body weight of female LDLR^{-/-} PKO mice given high fat diet (23.83 ± 2.15 g) and increase in body weight over time follows the same increment. During 10 weeks. HFD caused the increase of body weight in LDLR^{-/-} PWT and LDLR^{-/-}PKO mice while HFD mice reached a body weight of (24.66±2.47 g, n=5) (23.83±2.15 g, n=4) at the end of 10 weeks, whereas LFD mice LDLR^{-/-} PWT reached a body weight of (29.93± 0.79, n=6) during 8-9 months age. This means that HFD substantially increases body weight and it a sustainable model to study metabolic adaptation. When age related, it was seen that HFD mice by nearly 4 months age had the body weight of 8 months LFD mice in female LDLR^{-/-} PKO HFD versus LDLR^{-/-} PKO LFD mice. Figure 2A shows that line graph increased steadily and reached peak at (week 8), it fell down dramatically (from week 8 to week 9) skip then it soared from week 9 to week 10. While in properdin knockout mice, the graph reached a plateau at week 9. Additionally, there was a fluctuation between week 5 to week 7 in both female LDLR^{-/-} PWT/PKO mice fed HFD mice, both group 's body weights decreased from week 5 to week 6 then increased steadily till week 8 for female LDLR^{-/-} PWT mice fed HFD and week 9 for female LDLR^{-/-} PKO fed HFD (Figure 2, A). From week 5 –week 7 the body weight mean of Female LDLR^{-/-} PWT increased by 2 grams while female LDLR^{-/-} PKO increased by only 1 gram. The food intake was measured once per week per cage and calculated as food intake per mouse (Figure 2, B). The food intake reached peak at week 2 for female LDLR^{-/-} PWT mice fed HFD and female LDLR^{-/-} PKO mice fed HFD then started dramatically decrease till week 4; they increased slightly from week 4 to week 5. Fluctuation was seen till week 8, in female LDLR^{-/-} PWT mice fed HFD, food intake increased significantly till week 9; this is compatible with that body weight reached peak at week 8 then decreased till week 9, this means in

the case of decreasing body weight, the food intake was increased. In Female LDLR^{-/-} PKO mice fed HFD food intake decreased slightly from week 8 to week 10; this is compatible with that body weight reached peak at week 9.

Body weight drop for WT week 8 to 9, this may be due to technical error. This would represent body weight loss of 8% which is unlikely to normalise the following week. The same group shows an unexpected increase in food intake for the same week (8 to 9). Normal intake is 35g/week/mouse. Male mice took greater food (in some weeks reached nearly 60g/week) (figure 1 B) compared to female mice (only two weeks reached 50 g/day for two mice) (Figure 2, B) and also the body weight of male mice greater (38.52 ± 3.77 , 35.00 ± 1.14) than female body weight (24.66 ± 1.10 , 23.83 ± 1.07) (figure 1 A, 2 A).

Male LDLR^{+/+}PWT and LDLR^{+/+}PKO mice fed HFD were used next and body weight was measured from 1 week to 5 weeks for both genotypes (weight measurement was started from the fifth week of given HFD till the end week). Male LDLR^{+/+}PKO mice given HFD (37.17 ± 1.25 g, n=3) were significantly heavier (p value=0.02) compared to male LDLR^{+/+} PWT mice given HFD (30.33 ± 3.28 g, n=3). Male LDLR^{+/+}PWT mice given HFD (30.33 ± 3.28 g, n=3) had significantly greater body weight (p value=0.03) compared to female LDLR^{+/+} PWT mice given LFD (24.14 ± 1.15 g, n=3).

In male LDLR^{+/+} PKO mice given HFD no fluctuation was detected and increased steadily till week 5 but in LDLR^{+/+} PWT mice caused steady state (nearly same age) from week 1 to 5 (figure 4 A). Food intake increased dramatically from week 5 till week 8 (PWT) (figure 4 B). Fluctuation was seen in LDLR^{+/+}PKO mice from week 5 till week 10. Both genotypes decreased suddenly from week 8 to week 9 then increased from week 9 to week 10 (figure 4 B).

There were no significant differences between liver weights of 8 male LDLR^{-/-} PWT (1.63 ± 0.42 g) and 8 male LDLR^{-/-} PKO mice given HFD (1.35 ± 0.30 g) with male LDLR^{-/-} PWT LFD (1.41 ± 0.15) (age matched). Liver % body weight (g) which was measured as follows: liver mouse weight/body weight mouse *100. There was no sign of dietary induced hepatomegaly (4.19 ± 0.62 and 4.19 ± 1.02 g).

Fat pad weight measurement of 8 male LDLR^{-/-} PWT (1.79 ± 1.04) had not significant differences with 8 male LDLR^{-/-} PKO (1.34 ± 0.63). Fat pad weight measurement of LDLR^{-/-} PWT LFD (0.52 ± 0.36) (7 months) (0.49 ± 0.36) (5 months) had significantly lower than 8 males LDLR^{-/-} PWT mice (1.79 ± 1.04) (4 months). Fat pad weight measurement of LDLR^{-/-}PKO mice given HFD (1.34 ± 0.63) (4 months) had higher measurement compared to LDLR^{-/-} PKO mice given LFD (0.36 ± 0.09) (5 months) but not significantly different between them.

In fat pad % body weight (g) which was measured as follow: fat pad mouse weight/body weight mouse *100. Mean and SEM was (4.07 ± 0.83 and 4.24 ± 0.52 g) significantly no differences between them. Fat pad % body weight measurement of LDLR^{-/-} PWT mice given LFD (1.66 ± 1.07) (5 months) (2.32 ± 0.49) (9 months) had significantly lower than 8 male LDLR^{-/-} PWT mice given HFD mice (4.43 ± 1.88) and also 8 male LDLR^{-/-}PKO mice given HFD (3.59 ± 1.6 g) (4 months) had higher measurement compared to LDLR^{-/-} PKO mice given LFD (1.39 ± 0.27 g) (5 months). Male LDLR^{+/+} PKO mice given HFD (1.51 ± 0.38 g) was significantly greater fat pad weight than LDLR^{+/+} PWT (0.48 ± 0.14) mice. Fat pad % body measurement of LDLR^{+/+} PKO mice given HFD (4.06 ± 0.93) (p value=0.01) was significantly greater than LDLR^{+/+} PWT (1.54 ± 0.18) mice.

To conclude, it can be said that western diet (HFD) causes the increase of body weight, fat pad % body weight in male properdin wild type mice (LDLR^{-/-}PWT) compared to LDLR^{-/-}PWT mice given LFD (central obesity), more LDLR^{-/-}PKO LFD mice are needed to do the statistical analysis and to know whether HFD caused hepatomegaly compare to LFD mice. HFD did not cause the increase of body weight in female LDLR^{-/-}PWT HFD when compared to LDLR^{-/-}PWT LFD mice.

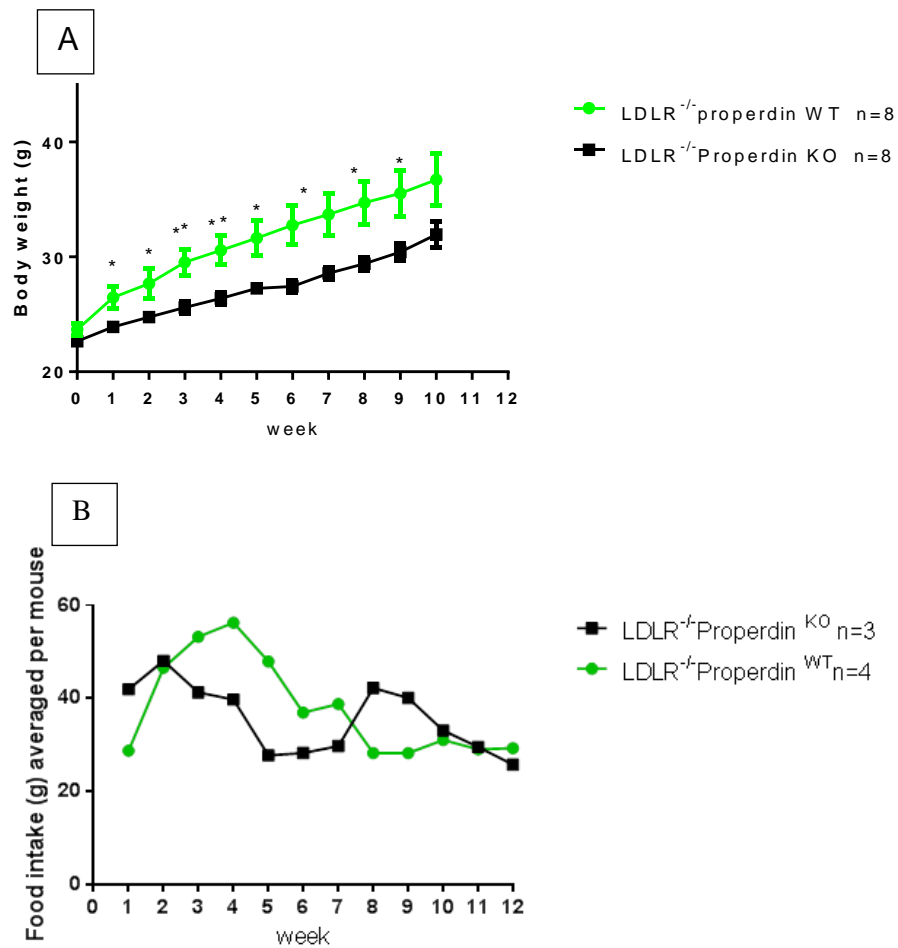


Figure 1: Weight gain and food intake measurement of male LDLR^{-/-} PWT and LDLR^{-/-} PKO HFD mice. Body weight measurement (A). Food intake measurement, 4 properdin wild type mice with 3 mice properdin deficient (B).

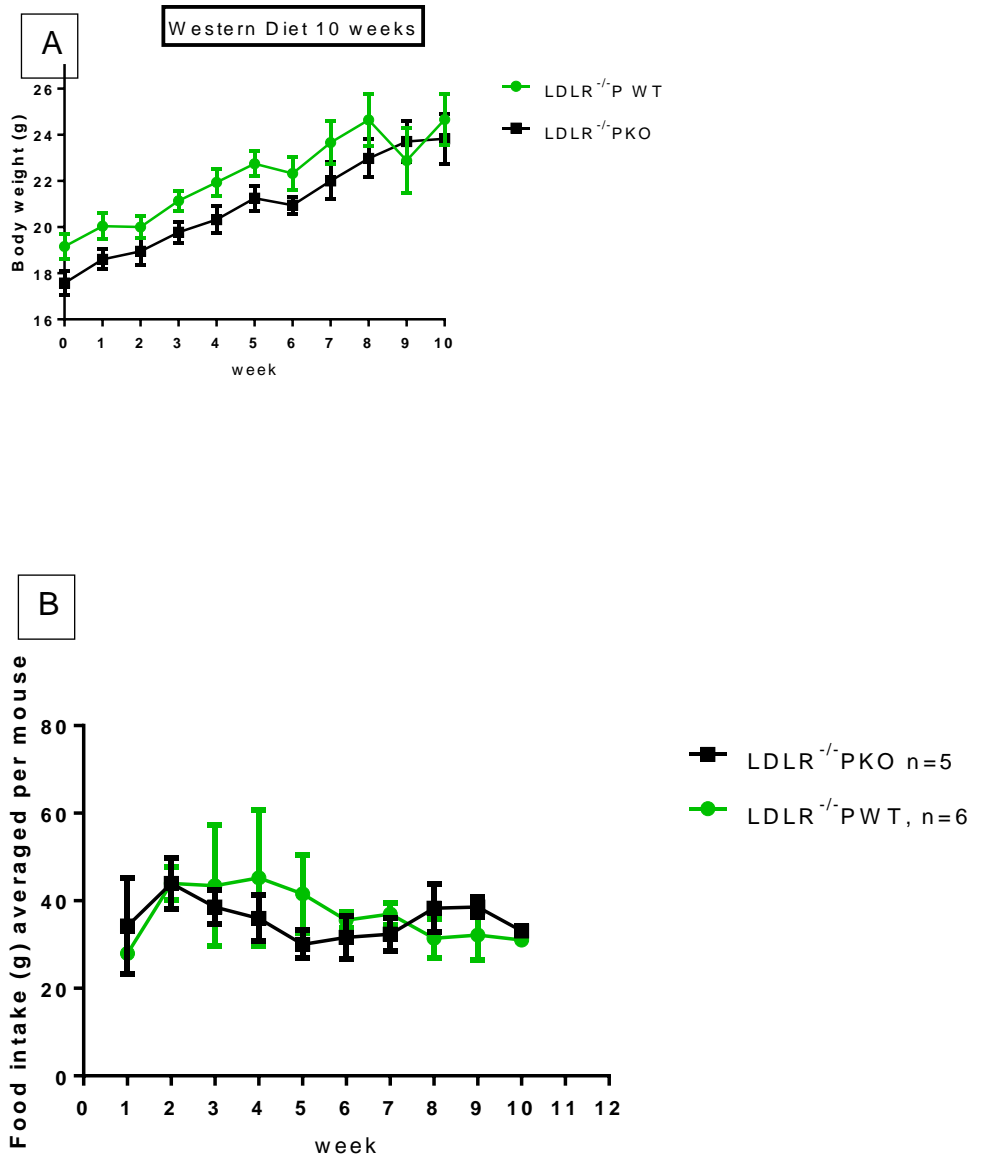


Figure 2: Weight gain and food intake measurement of female LDLR^{-/-} PWT and LDLR^{-/-} PKO mice fed HFD. Body weight measurement (A). Food intake measurement, 4 properdin wild type mice with 3 mice properdin knock out mice (B).

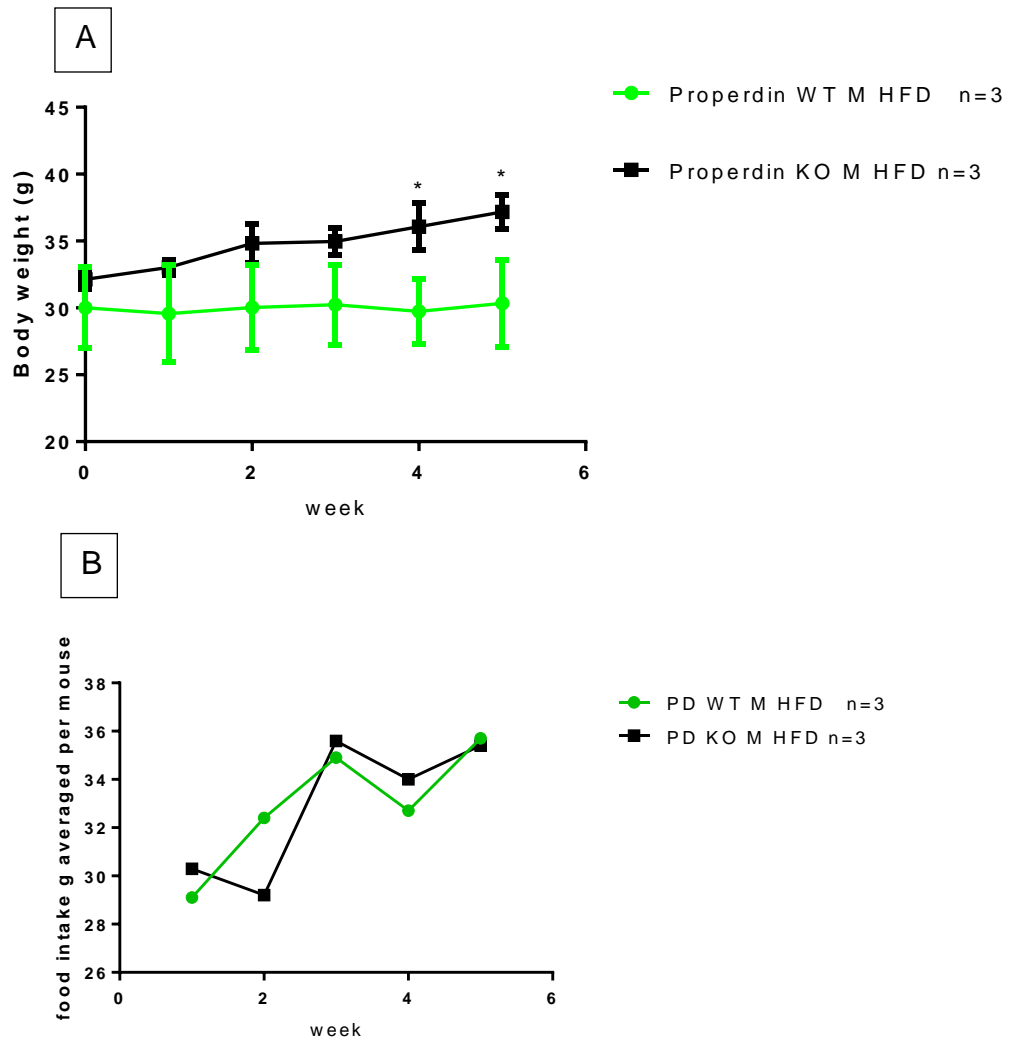


Figure 3: Weight gain and food intake measurement of male PD WT and PD KO HFD mice (10 weeks). Body weight measurement (figure 3 A). Food intake measurement, properdin wild type mice (n=3) with mice properdin knock out mice (n=3), PD=LDLR+/+, (B)

Blood Glucose levels

Hyperlipidemic mice on a HFD may go on to develop insulin resistance (HA and ChA, 2010). Serum samples were measured using a glucose meter. No accurate result were achieved due to hemolysis. The difference in glucose levels between mice fed LFD and HFD obtained in a previous measurement using non hemolysed plasma samples could not be reproduced. Then blood glucose measurement was performed in whole blood from tail pricks in eighth week for LDLR^{-/-} PKO and LDLR^{-/-}PWT female mice fed HFD, LDLR^{-/-} PKO and LDLR^{-/-}PWT male mice given HFD, and LDLR^{+/+}PWT, LDLR^{+/+}PKO mice given HFD in order to investigate the differences between properdin wild type and properdin deficient mice. There were not differences in blood glucose measurement between LDLR^{-/-} PKO female HFD (18.52± 1.52) and LDLR^{-/-} PWT female mice (17.00±0.57) LDLR^{-/-} PKO male HFD (15.70 ± 1.10) and LDLR^{-/-} PWT male HFD mice (18.05± 4.25), LDLR^{+/+}PDWT male (11.77± 1.66) and LDLR^{+/+}PKO male HFD mice (11.40 ± 0.50)

Histological and immunohistochemical characterisation of livers

Sections were prepared from liver, stained with haematoxylin/eosin and analysed microscopically. A piece liver of 16 weeks' male LDLR^{-/-} PKO (6 mice), LDLR^{-/-} PWT (6 mice), were fixed, paraffin embedded and slides were prepared. Microscope was used to document images using a 10x, 40x and 100x objective. Two mice from LDLR^{-/-} PWT mice were excluded due to the absence steatosis and inflammation in histologically sections. In liver sections, we can identify sheets of hepatocytes, sinusoids, branch of hepatic artery portal vein. Four properdin wild type and six properdin deficient in LDLR^{-/-} background were documented and compared with two controls (LFD mice). Big liver changes were detected in HFD mice (figure 5 B, C) compared to mice fed LFD (figure 5 A). There was fatty liver around central vein which led to the development whitish-yellowish background (figure 5 B) due to greater amount of micro vesicular, macro vesicular and also it had the second biggest body weight (48.7g), fat pat weight (3.217g), fat pad % body weight (6.53%), liver weight (2.05g), liver % body weight (4.2%) among properdin wild type mice and also properdin deficient mice. It was positive for C3 IHC, CD 68 IHC and iNOS

IHC and had more steatosis and inflammation. While in mice fed LFD, there was not any variation in color (figure 5 B). In addition, leukocyte infiltration detected between hepatocyte cells (Figure 5 B) and around central vein (Figure 5 C). No leukocyte infiltration in LFD mice around central vein (figure 5 A).

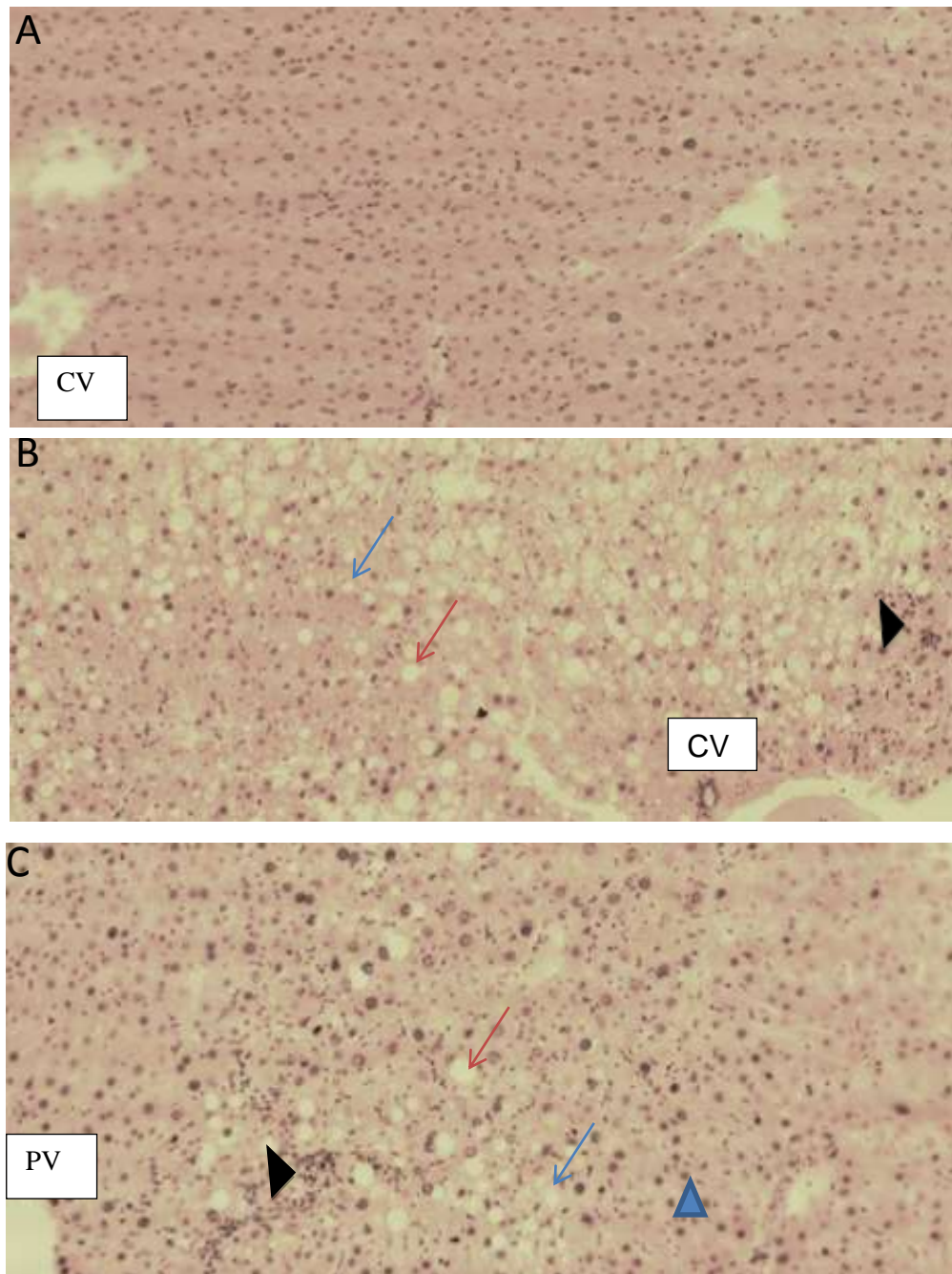


Figure 5: Haematoxylin eosin staining of paraffin embedded liver sections obtained from mice fed high fat diet and low fat diet (x10), representative images. No inflammation and steatosis in mice fed LFD diet (A). Fatty changes in great amount, microvesicular (blue arrows), macrovesicular (red arrows) (steatosis) and inflammation (black- heads) in mice fed HFD (B). Inflammatory cell component, microvesicular (blue arrow), macro vesicular (red arrow) and hepatocyte ballooning in mice fed HFD (panel C) PV, portal vein, CV, central vein.

Contrasting with normal liver (figure 6 panel A), there are many microvesicular and macro-vesicular lipid droplets in HFD liver mice (Figure 6, B, C). In some mice fed HFD, big droplets were detected (Figure 3, B). There are some hepatocyte ballooning and necrosis (Figure 6, C), while no hepatocyte ballooning was seen in normal chow diet.

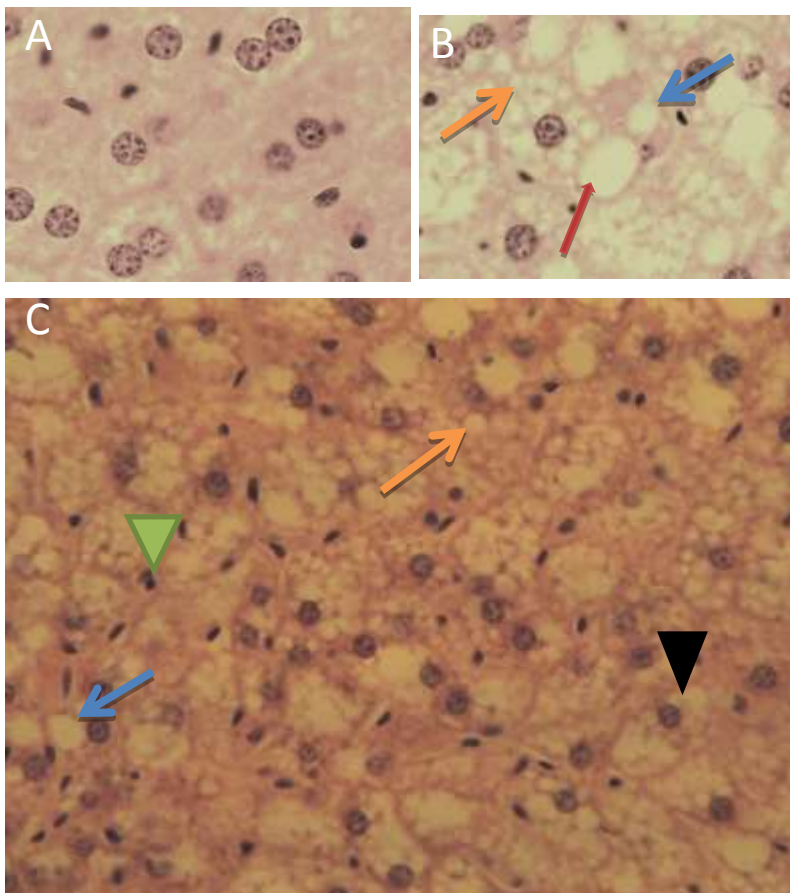


Figure 6: Macro – and microvesicular lipid droplets Macrovesicular (blue arrows) microvesicular (orange arrows) fat droplets (red arrow) 100x (B). Hepatocyte ballooning (black head). Necrosis (green head) 40x (C) (LDLR^{-/-}PWT 5311). (x40).

Many inflammatory groups were detected (Figure 7 panels B and C). Enlarged and irregular nuclei were seen (Nuclear vacuolation) in mice fed HFD (Figure 4 , D) it also had the biggest body weight (49.3g), fat pat weight (3.23g), fat pad % body weight (6.55%), liver weight (2.36g) and liver % body weight (4.75%) among properdin wild type mice and also properdin deficient mice. More steatosis and inflammation and there was positive for C3 IHC, CD68 IHC, iNOS

IHC. While in mice fed LFD, there were not detected enlarged nuclei (Figure 7 panel A).

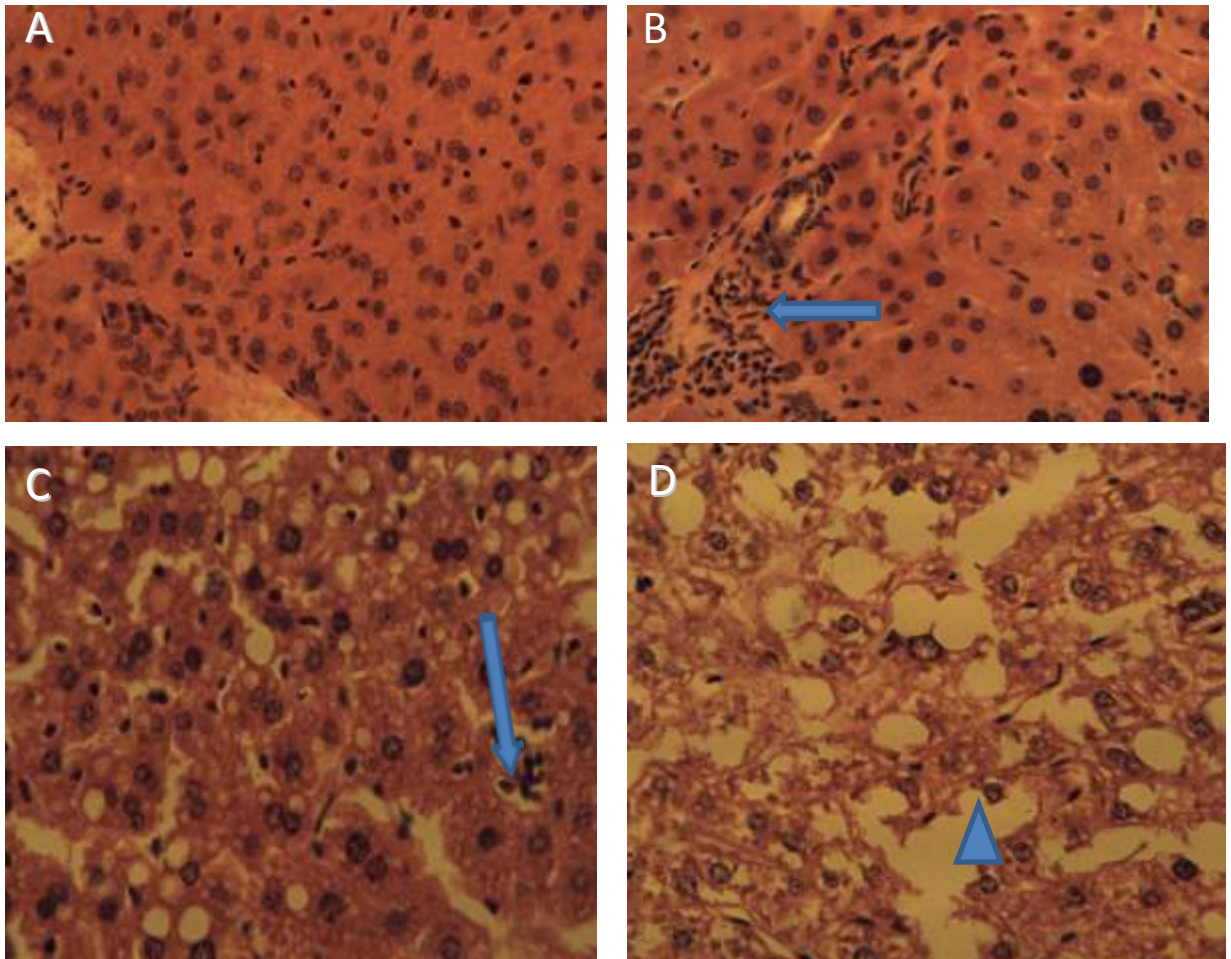


Figure 7: Control mice (LFD) (A). Portal inflammation (LDLR^{-/-}PKO 5322) (B). Lobular inflammation (LDLR^{-/-}PWT 5312) (C). Nuclear vacuolation of hepatocytes (blue head) (LDLR^{-/-}PWT 5310) (D). Haematoxylin eosin staining of paraffin embedded liver sections obtained from LFD (A), high fed mice (B, C, D) (x40).

Hepatocyte ballooning, which is a most feature of NASH (Hubscher, 2006), was detected in HFD mice (figure 8B) while no hepatocyte ballooning was seen in LFD mice (Figure 8, A)

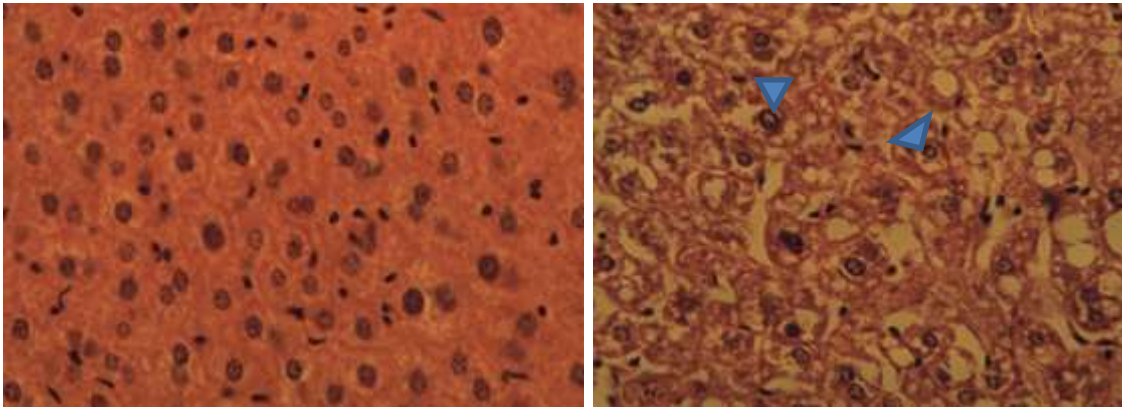


Figure 8: Control mice (LFD) (A). Hepatocyte ballooning (HFD) (B) (blue heads). (x40).

Steatosis was seen in all mice (12 mice) but greater steatosis in 2 properdin wild type mice (LDLR^{-/-}PWT 5310, LDLR^{-/-}PWT 5311), some mice had inflammation (portal and lobular inflammation) (3 LDLR^{-/-}PWT and 3 LDLR^{-/-}PKO mice) and some mice had greater steatosis and inflammation. Triglyceride measurement will be performed to investigate the amount lipid content in hepatocytes. To investigate that inflammation and steatosis, immunohistochemistry was performed as follows:

Previous analysis of liver from LFD fed mice on LDLR^{-/-} background did not get result for CD68 and C3 antibody at paraffin sections and in most publication cryo section was used to perform immunohistochemistry. Therefore, Immunohistochemistry was performed by using cryo sections because Three antibodies were used CD68 (as macrophage marker) (wahr et al., 2014) anti C3 antibody and iNOS (inducible nitrite oxide synthase). The aim is to investigate inflammation (anti-CD 68), complement activation (anti-C3) and characterization of NASH (iNOS) (HA and ChA, 2010).

Monoclonal anti -C3 antibody was used to detect C3, C3b and iC3b (as complement activation), they detected within inflammatory group (Figure 9, A) and also around fat droplets (Figure 9, B). Anti-CD68 antibody was used to detect CD68 (as marker for macrophage). Our result shows CD 68 positive cells were detected in hepatic sinusoids in mice fed HFD of both genotypes around central vein (Figure 9, C) and also was detected around fat droplets (Figure 6, D). Positive signals for iNOS (as a sign of NAFLD and NASH) were detected

between inflammatory groups in mice fed HFD mice (Figure 6, D) and around fat vacuoles.

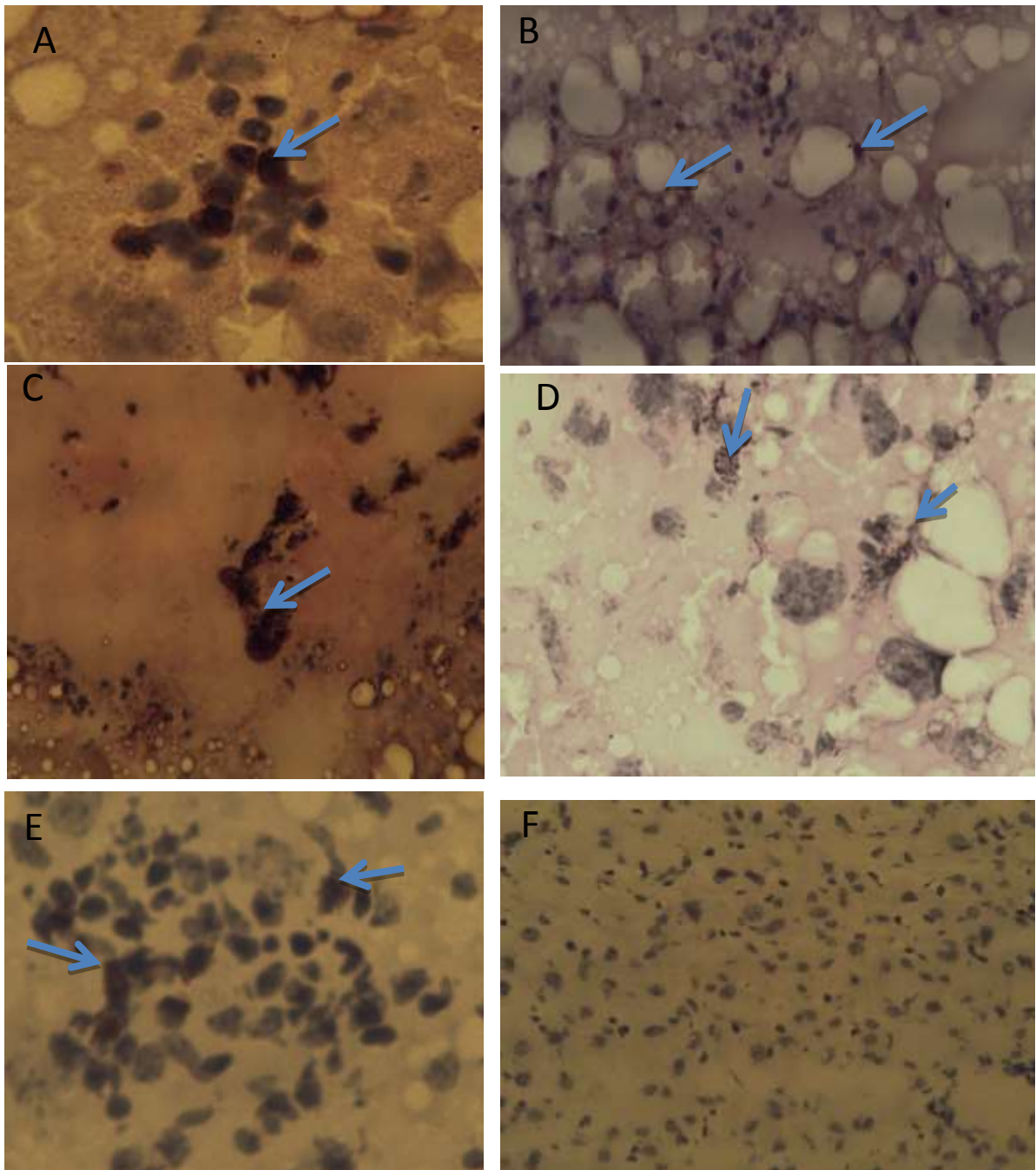


Figure 9: Immunohistochemistry for liver cryo sections of male HFD LDLR^{-/-}PWT/PKO mice, anti-C3 antibody (A, B) , anti CD-68 antibody (C, D) and anti-iNOS antibody (E), Control (no secondary antibody)(F). (x40).

TNF- α measurement in liver lysate

Because of the presence of inflammatory cells in liver histopathology (Figure 5, C), TNF- α for liver of mice fed HFD and LFD was performed. Mice fed HFD had a tendency to have higher TNF- α in liver compared to low fat diet.

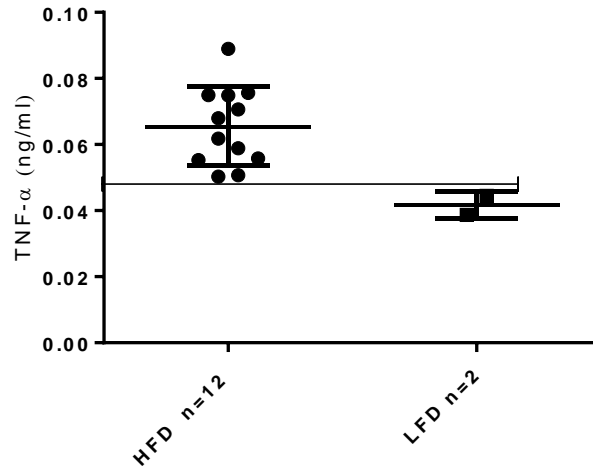


Figure 10: TNF- α measurement in liver male mice fed HFD and LFD diet.

Triglyceride measurement (TG) for liver lysate

Because of the presence of lipid droplet in liver histopathology (Figure 5, B, C). TG for liver of mice fed HFD and LFD was performed. Mice fed Western diet had higher triglycerides in liver compared to low fat diet.

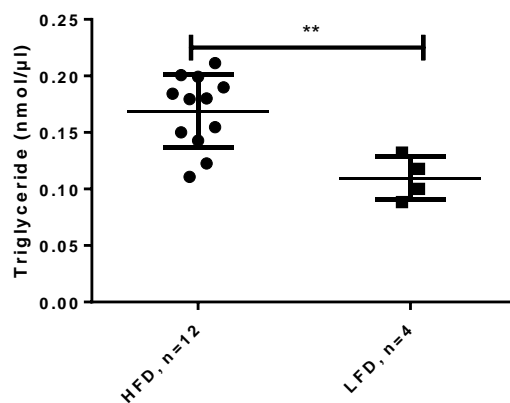


Figure 11: Triglyceride (TG) measurement in liver male mice fed HFD and LFD diet.

References

- AHISHALI, E., DEMIR, K., AHISHALI, B., AKYUZ, F., PINARBASI, B., POTUROGLU, S., IBRISIM, D., GULLUOGLU, M., OZDIL, S., BESISIK, F., KAYMAKOGLU, S., BOZTAS, G., CAKALOGLU, Y., MUNGAN, Z., CANBERK, Y. & OKTEN, A. 2010. Electron microscopic findings in non-alcoholic fatty liver disease: is there a difference between hepatosteatosis and steatohepatitis? *J Gastroenterol Hepatol*, 25, 619-26.
- AHREN, B., HAVEL, P. J., PACINI, G. & CIANFLONE, K. 2003. Acylation stimulating protein stimulates insulin secretion. *Int J Obes Relat Metab Disord*, 27, 1037-43.
- ALEX, S., BOSS, A., HEERSCHAP, A. & KERSTEN, S. 2015. Exercise training improves liver steatosis in mice. *Nutr Metab (Lond)*, 12, 29.
- ANSTEE, Q. M., TARGHER, G. & DAY, C. P. 2013. Progression of NAFLD to diabetes mellitus, cardiovascular disease or cirrhosis. *Nat Rev Gastroenterol Hepatol*, 10, 330-44.
- ARBORE, G. & KEMPER, C. 2016. A novel "complement-metabolism-inflammasome axis" as a key regulator of immune cell effector function. *Eur J Immunol*, 46, 1563-73.
- ARREOLA, R., QUINTERO-FABIAN, S., LOPEZ-ROA, R. I., FLORES-GUTIERREZ, E. O., REYES-GRAJEDA, J. P., CARRERA-QUINTANAR, L. & ORTUNO-SAHAGUN, D. 2015. Immunomodulation and anti-inflammatory effects of garlic compounds. *J Immunol Res*, 2015, 401630.
- ARRUDA, A. P., PERS, B. M., PARLAKGUL, G., GUNEY, E., INOUYE, K. & HOTAMISLIGIL, G. S. 2014. Chronic enrichment of hepatic endoplasmic reticulum-mitochondria contact leads to mitochondrial dysfunction in obesity. *Nat Med*, 20, 1427-35.
- ASRIH, M. & JORNAYVAZ, F. R. 2015. Metabolic syndrome and nonalcoholic fatty liver disease: Is insulin resistance the link? *Mol Cell Endocrinol*, 418 Pt 1, 55-65.

- BABA, S. P., HELLMANN, J., SRIVASTAVA, S. & BHATNAGAR, A. 2011. Aldose reductase (AKR1B3) regulates the accumulation of advanced glycosylation end products (AGEs) and the expression of AGE receptor (RAGE). *Chem Biol Interact*, 191, 357-63.
- BARCHETTA, I., DE BERNARDINIS, M., CAPOCCIA, D., BARONI, M. G., FONTANA, M., FRAIOLI, A., MORINI, S., LEONETTI, F. & CAVALLO, M. G. 2013. Hypovitaminosis D is independently associated with metabolic syndrome in obese patients. *PLoS One*, 8, e68689.
- BAUER, M., PRESS, A. T. & TRAUNER, M. 2013. The liver in sepsis: patterns of response and injury. *Curr Opin Crit Care*, 19, 123-7.
- BHATT, H. B. & SMITH, R. J. 2015. Fatty liver disease in diabetes mellitus. *Hepatobiliary Surg Nutr*, 4, 101-8.
- BIEGHS, V., VAN GORP, P. J., WOUTERS, K., HENDRIKX, T., GIJBELS, M. J., VAN BILSEN, M., BAKKER, J., BINDER, C. J., LUTJOHANN, D., STAELS, B., HOFKER, M. H. & SHIRI-SVERDLOV, R. 2012. LDL receptor knock-out mice are a physiological model particularly vulnerable to study the onset of inflammation in non-alcoholic fatty liver disease. *PLoS One*, 7, e30668.
- BLATT, A. Z., PATHAN, S. & FERREIRA, V. P. 2016. Properdin: a tightly regulated critical inflammatory modulator. *Immunol Rev*, 274, 172-190.
- BOTROS, M. & SIKARIS, K. A. 2013. The de ritis ratio: the test of time. *Clin Biochem Rev*, 34, 117-30.
- BROWN, G. T. & KLEINER, D. E. 2016. Histopathology of nonalcoholic fatty liver disease and nonalcoholic steatohepatitis. *Metabolism*, 65, 1080-6.
- BROWN, K., DECOFFE, D., MOLCAN, E. & GIBSON, D. L. 2012. Diet-induced dysbiosis of the intestinal microbiota and the effects on immunity and disease. *Nutrients*, 4, 1095-119.
- CAPANNI, M., CALELLA, F., BIAGINI, M. R., GENISE, S., RAIMONDI, L., BEDOGNI, G., SVEGLIATI-BARONI, G., SOFI, F., MILANI, S., ABBATE, R., SURRENTI, C. & CASINI, A. 2006. Prolonged n-3 polyunsaturated fatty acid supplementation ameliorates hepatic steatosis in patients with non-alcoholic fatty liver disease: a pilot study. *Aliment Pharmacol Ther*, 23, 1143-51.

- CASTELL, J. V., GOMEZ-LECHON, M. J., DAVID, M., HIRANO, T., KISHIMOTO, T. & HEINRICH, P. C. 1988. Recombinant human interleukin-6 (IL-6/BSF-2/HSF) regulates the synthesis of acute phase proteins in human hepatocytes. *FEBS Lett*, 232, 347-50.
- CAWTHORN, W. P. & SETHI, J. K. 2008. TNF-alpha and adipocyte biology. *FEBS Lett*, 582, 117-31.
- CHAN, D. C., WATTS, G. F., MORI, T. A., BARRETT, P. H., REDGRAVE, T. G. & BEILIN, L. J. 2003. Randomized controlled trial of the effect of n-3 fatty acid supplementation on the metabolism of apolipoprotein B-100 and chylomicron remnants in men with visceral obesity. *Am J Clin Nutr*, 77, 300-7.
- CHOY, L. N., ROSEN, B. S. & SPIEGELMAN, B. M. 1992. Adipsin and an endogenous pathway of complement from adipose cells. *J Biol Chem*, 267, 12736-41.
- COLBERG, S. R., SIGAL, R. J., FERNHALL, B., REGENSTEINER, J. G., BLISSMER, B. J., RUBIN, R. R., CHASAN-TABER, L., ALBRIGHT, A. L. & BRAUN, B. 2010. Exercise and type 2 diabetes: the American College of Sports Medicine and the American Diabetes Association: joint position statement. *Diabetes Care*, 33, e147-67.
- CONARELLO, S. L., LI, Z., RONAN, J., ROY, R. S., ZHU, L., JIANG, G., LIU, F., WOODS, J., ZYCBAND, E., MOLLER, D. E., THORNBERRY, N. A. & ZHANG, B. B. 2003. Mice lacking dipeptidyl peptidase IV are protected against obesity and insulin resistance. *Proc Natl Acad Sci U S A*, 100, 6825-30.
- CRISPE, I. N. 2016. Hepatocytes as Immunological Agents. *J Immunol*, 196, 17-21.
- CUI, W., SIMAAN, M., LAPORTE, S., LODGE, R. & CIANFLONE, K. 2009. C5a- and ASP-mediated C5L2 activation, endocytosis and recycling are lost in S323I-C5L2 mutation. *Mol Immunol*, 46, 3086-98.
- CUI, Y. & JIA, J. 2013. Update on epidemiology of hepatitis B and C in China. *J Gastroenterol Hepatol*, 28 Suppl 1, 7-10.
- DANIEL, D., HARDIGAN, P., BRAY, N., PENZELL, D. & SAVU, C. 2015. The incidence of vitamin D deficiency in the obese: a retrospective chart review. *J Community Hosp Intern Med Perspect*, 5, 26069.

- DAPITO, D. H., MENCIN, A., GWAK, G. Y., PRADERE, J. P., JANG, M. K., MEDERACKE, I., CAVIGLIA, J. M., KHIABANIAN, H., ADEYEMI, A., BATALLER, R., LEFKOWITCH, J. H., BOWER, M., FRIEDMAN, R., SARTOR, R. B., RABADAN, R. & SCHWABE, R. F. 2012. Promotion of hepatocellular carcinoma by the intestinal microbiota and TLR4. *Cancer Cell*, 21, 504-16.
- DONNELLY, K. L., SMITH, C. I., SCHWARZENBERG, S. J., JESSURUN, J., BOLDT, M. D. & PARKS, E. J. 2005. Sources of fatty acids stored in liver and secreted via lipoproteins in patients with nonalcoholic fatty liver disease. *J Clin Invest*, 115, 1343-51.
- DOYCHEVA, I., PATEL, N., PETERSON, M. & LOOMBA, R. 2013. Prognostic implication of liver histology in patients with nonalcoholic fatty liver disease in diabetes. *J Diabetes Complications*, 27, 293-300.
- DUPONT, A., MOHAMED, F., SALEHEN, N., GLENN, S., FRANCESCUT, L., ADIB, R., BYRNE, S., BREWIN, H., ELLIOTT, I., RICHARDS, L., DIMITROVA, P., SCHWAEBLE, W., IVANOVSKA, N., KADIOGLU, A., MACHADO, L. R., ANDREW, P. W. & STOVER, C. 2014. Septicaemia models using *Streptococcus pneumoniae* and *Listeria monocytogenes*: understanding the role of complement properdin. *Med Microbiol Immunol*.
- FABBRINI, E., SULLIVAN, S. & KLEIN, S. 2010. Obesity and nonalcoholic fatty liver disease: biochemical, metabolic, and clinical implications. *Hepatology*, 51, 679-89.
- FARRELL, G. C. & LARTER, C. Z. 2006. Nonalcoholic fatty liver disease: from steatosis to cirrhosis. *Hepatology*, 43, S99-S112.
- FERRI, C., DESIDERI, G., VALENTI, M., BELLINI, C., PASIN, M., SANTUCCI, A. & DE MATTIA, G. 1999. Early upregulation of endothelial adhesion molecules in obese hypertensive men. *Hypertension*, 34, 568-73.
- FISSETTE, A., MUNKONDA, M. N., OIKONOMOPOULOU, K., PAGLIALUNGA, S., LAMBRIS, J. D. & CIANFLONE, K. 2013. C5L2 receptor disruption enhances the development of diet-induced insulin resistance in mice. *Immunobiology*, 218, 127-33.
- FOROUHI, N. G., LUAN, J., COOPER, A., BOUCHER, B. J. & WAREHAM, N. J. 2008. Baseline serum 25-hydroxy vitamin d is predictive of future

- glycemic status and insulin resistance: the Medical Research Council Ely Prospective Study 1990-2000. *Diabetes*, 57, 2619-25.
- FREEMAN, H. C., HUGILL, A., DEAR, N. T., ASHCROFT, F. M. & COX, R. D. 2006. Deletion of nicotinamide nucleotide transhydrogenase: a new quantitative trait locus accounting for glucose intolerance in C57BL/6J mice. *Diabetes*, 55, 2153-6.
- FRONCZYK, A., MOLEDA, P., SAFRANOW, K., PIECHOTA, W. & MAJKOWSKA, L. 2014. Increased concentration of C-reactive protein in obese patients with type 2 diabetes is associated with obesity and presence of diabetes but not with macrovascular and microvascular complications or glycemic control. *Inflammation*, 37, 349-57.
- FUJITA, T., FUJIOKA, T., MURAKAMI, T., SATOMURA, A., FUKU, Y. & MATSUMOTO, K. 2007. Chylomicron accelerates C3 tick-over by regulating the role of factor H, leading to overproduction of acylation stimulating protein. *J Clin Lab Anal*, 21, 14-23.
- GALLOWAY, E., SHIN, T., HUBER, N., EISMANN, T., KUBOKI, S., SCHUSTER, R., BLANCHARD, J., WONG, H. R. & LENTSCH, A. B. 2008. Activation of hepatocytes by extracellular heat shock protein 72. *Am J Physiol Cell Physiol*, 295, C514-20.
- GARG, M., LUBEL, J. S., SPARROW, M. P., HOLT, S. G. & GIBSON, P. R. 2012. Review article: vitamin D and inflammatory bowel disease--established concepts and future directions. *Aliment Pharmacol Ther*, 36, 324-44.
- GAUVREAU, D., ROY, C., TOM, F. Q., LU, H., MIEGUEU, P., RICHARD, D., SONG, W. C., STOVER, C. & CIANFLONE, K. 2012. A new effector of lipid metabolism: complement factor properdin. *Mol Immunol*, 51, 73-81.
- GEIER, A. 2011. Shedding new light on vitamin D and fatty liver disease. *J Hepatol*, 55, 273-5.
- GEIGER, P. C., WRIGHT, D. C., HAN, D. H. & HOLLOSZY, J. O. 2005. Activation of p38 MAP kinase enhances sensitivity of muscle glucose transport to insulin. *Am J Physiol Endocrinol Metab*, 288, E782-8.
- GEORGE, P. S., PEARSON, E. R. & WITHAM, M. D. 2012. Effect of vitamin D supplementation on glycaemic control and insulin resistance: a systematic review and meta-analysis. *Diabet Med*, 29, e142-50.

- GLEESON, M., BISHOP, N. C., STENSEL, D. J., LINDLEY, M. R., MASTANA, S. S. & NIMMO, M. A. 2011. The anti-inflammatory effects of exercise: mechanisms and implications for the prevention and treatment of disease. *Nat Rev Immunol*, 11, 607-15.
- GRAHAM, T. E., YANG, Q., BLUHER, M., HAMMARSTEDT, A., CIARALDI, T. P., HENRY, R. R., WASON, C. J., OBERBACH, A., JANSSON, P. A., SMITH, U. & KAHN, B. B. 2006. Retinol-binding protein 4 and insulin resistance in lean, obese, and diabetic subjects. *N Engl J Med*, 354, 2552-63.
- GRAY, P., DAGVADORJ, J., MICHELSEN, K. S., BRIKOS, C., RENTSENDORJ, A., TOWN, T., CROTHER, T. R. & ARDITI, M. 2011. Myeloid differentiation factor-2 interacts with Lyn kinase and is tyrosine phosphorylated following lipopolysaccharide-induced activation of the TLR4 signaling pathway. *J Immunol*, 187, 4331-7.
- GUILLEN, M. I., GOMEZ-LECHON, M. J., NAKAMURA, T. & CASTELL, J. V. 1996. The hepatocyte growth factor regulates the synthesis of acute-phase proteins in human hepatocytes: divergent effect on interleukin-6-stimulated genes. *Hepatology*, 23, 1345-52.
- GUO, H., CALLAWAY, J. B. & TING, J. P. 2015. Inflammasomes: mechanism of action, role in disease, and therapeutics. *Nat Med*, 21, 677-87.
- GUPTA, A. K., SEXTON, R. C. & RUDNEY, H. 1989. Effect of vitamin D3 derivatives on cholesterol synthesis and HMG-CoA reductase activity in cultured cells. *J Lipid Res*, 30, 379-86.
- GUTIERREZ, D. A., PUGLISI, M. J. & HASTY, A. H. 2009. Impact of increased adipose tissue mass on inflammation, insulin resistance, and dyslipidemia. *Curr Diab Rep*, 9, 26-32.
- GUTTERIDGE, J. M., ROWLEY, D. A. & HALLIWELL, B. 1982. Superoxide-dependent formation of hydroxyl radicals and lipid peroxidation in the presence of iron salts. Detection of 'catalytic' iron and anti-oxidant activity in extracellular fluids. *Biochem J*, 206, 605-9.
- HA, S. K. & CHAE, C. 2010. Inducible nitric oxide distribution in the fatty liver of a mouse with high fat diet-induced obesity. *Exp Anim*, 59, 595-604.
- HARTE, A. L., DA SILVA, N. F., CREELY, S. J., MCGEE, K. C., BILLYARD, T., YOUSSEF-ELABD, E. M., TRIPATHI, G., ASHOUR, E., ABDALLA, M.

- S., SHARADA, H. M., AMIN, A. I., BURT, A. D., KUMAR, S., DAY, C. P. & MCTERNAN, P. G. 2010. Elevated endotoxin levels in non-alcoholic fatty liver disease. *J Inflamm (Lond)*, 7, 15.
- HASHIMOTO, E., TOKUSHIGE, K. & FARRELL, G. C. 2012. Histological features of non-alcoholic fatty liver disease: what is important? *J Gastroenterol Hepatol*, 27, 5-7.
- HINDLEY, C. J., MASTROGIOVANNI, G. & HUCH, M. 2014. The plastic liver: differentiated cells, stem cells, every cell? *J Clin Invest*, 124, 5099-102.
- HOTAMISLIGIL, G. S., SHARGILL, N. S. & SPIEGELMAN, B. M. 1993. Adipose expression of tumor necrosis factor-alpha: direct role in obesity-linked insulin resistance. *Science*, 259, 87-91.
- HOURCADE, D. E. 2006. The role of properdin in the assembly of the alternative pathway C3 convertases of complement. *J Biol Chem*, 281, 2128-32.
- HURSTING, S. D. & HURSTING, M. J. 2012. Growth signals, inflammation, and vascular perturbations: mechanistic links between obesity, metabolic syndrome, and cancer. *Arterioscler Thromb Vasc Biol*, 32, 1766-70.
- JABLONSKI, K. A., AMICI, S. A., WEBB, L. M., RUIZ-ROSADO JDE, D., POPOVICH, P. G., PARTIDA-SANCHEZ, S. & GUERAU-DE-ARELLANO, M. 2015. Novel Markers to Delineate Murine M1 and M2 Macrophages. *PLoS One*, 10, e0145342.
- JESUS CORRAL-CARIDAD, M., MORENO, I., TORANO, A., DOMINGUEZ, M. & ALUNDA, J. M. 2012. Effect of allicin on promastigotes and intracellular amastigotes of *Leishmania donovani* and *L. infantum*. *Exp Parasitol*, 132, 475-82.
- JOHNSON, J. B., SUMMER, W., CUTLER, R. G., MARTIN, B., HYUN, D. H., DIXIT, V. D., PEARSON, M., NASSAR, M., TELLJOHANN, R., MAUDSLEY, S., CARLSON, O., JOHN, S., LAUB, D. R. & MATTSON, M. P. 2007. Alternate day calorie restriction improves clinical findings and reduces markers of oxidative stress and inflammation in overweight adults with moderate asthma. *Free Radic Biol Med*, 42, 665-74.
- JOHSWICH, K., MARTIN, M., THALMANN, J., RHEINHEIMER, C., MONK, P. N. & KLOS, A. 2006. Ligand specificity of the anaphylatoxin C5L2

- receptor and its regulation on myeloid and epithelial cell lines. *J Biol Chem*, 281, 39088-95.
- KADOWAKI, T., YAMAUCHI, T., KUBOTA, N., HARA, K., UEKI, K. & TOBE, K. 2006. Adiponectin and adiponectin receptors in insulin resistance, diabetes, and the metabolic syndrome. *J Clin Invest*, 116, 1784-92.
- KALANT, D., MACLAREN, R., CUI, W., SAMANTA, R., MONK, P. N., LAPORTE, S. A. & CIANFLONE, K. 2005. C5L2 is a functional receptor for acylation-stimulating protein. *J Biol Chem*, 280, 23936-44.
- KANG, T. W., YEVSAA, T., WOLLER, N., HOENICKE, L., WUESTEFELD, T., DAUCH, D., HOHMEYER, A., GEREKE, M., RUDALSKA, R., POTAPOVA, A., IKEN, M., VUCUR, M., WEISS, S., HEIKENWALDER, M., KHAN, S., GIL, J., BRUDER, D., MANNS, M., SCHIRMACHER, P., TACKE, F., OTT, M., LUEDDE, T., LONGERICH, T., KUBICKA, S. & ZENDER, L. 2011. Senescence surveillance of pre-malignant hepatocytes limits liver cancer development. *Nature*, 479, 547-51.
- KARPE, F., DICKMANN, J. R. & FRAYN, K. N. 2011. Fatty acids, obesity, and insulin resistance: time for a reevaluation. *Diabetes*, 60, 2441-9.
- KAWANISHI, N., YANO, H., MIZOKAMI, T., TAKAHASHI, M., OYANAGI, E. & SUZUKI, K. 2012. Exercise training attenuates hepatic inflammation, fibrosis and macrophage infiltration during diet induced-obesity in mice. *Brain Behav Immun*, 26, 931-41.
- KAWANISHI, N., YANO, H., YOKOGAWA, Y. & SUZUKI, K. 2010. Exercise training inhibits inflammation in adipose tissue via both suppression of macrophage infiltration and acceleration of phenotypic switching from M1 to M2 macrophages in high-fat-diet-induced obese mice. *Exerc Immunol Rev*, 16, 105-18.
- KEMPER, C. & HOURCADE, D. E. 2008. Properdin: New roles in pattern recognition and target clearance. *Mol Immunol*, 45, 4048-56.
- KERSTEN, S. 2001. Mechanisms of nutritional and hormonal regulation of lipogenesis. *EMBO Rep*, 2, 282-6.
- KHEDER, R. K., HOBKIRK, J. & STOVER, C. M. 2016. In vitro Modulation of the LPS-Induced Proinflammatory Profile of Hepatocytes and Macrophages- Approaches for Intervention in Obesity? *Front Cell Dev Biol*, 4, 61.

- KILDSCGAARD, J., ZSIGMOND, E., CHAN, L. & WETSEL, R. A. 1999. A critical evaluation of the putative role of C3adesArg (ASP) in lipid metabolism and hyperapobetalipoproteinemia. *Mol Immunol*, 36, 869-76.
- KIM, I., MOON, S. O., KIM, S. H., KIM, H. J., KOH, Y. S. & KOH, G. Y. 2001. Vascular endothelial growth factor expression of intercellular adhesion molecule 1 (ICAM-1), vascular cell adhesion molecule 1 (VCAM-1), and E-selectin through nuclear factor-kappa B activation in endothelial cells. *J Biol Chem*, 276, 7614-20.
- KIM, S. Y., HWANG, J. S. & HAN, I. O. 2013. Tunicamycin inhibits Toll-like receptor-activated inflammation in RAW264.7 cells by suppression of NF-kappaB and c-Jun activity via a mechanism that is independent of ER-stress and N-glycosylation. *Eur J Pharmacol*, 721, 294-300.
- KITSON, M. T. & ROBERTS, S. K. 2012. D-livering the message: the importance of vitamin D status in chronic liver disease. *J Hepatol*, 57, 897-909.
- KLEINER, D. E., BRUNT, E. M., VAN NATTA, M., BEHLING, C., CONTOS, M. J., CUMMINGS, O. W., FERRELL, L. D., LIU, Y. C., TORBENSON, M. S., UNALP-ARIDA, A., YEH, M., MCCULLOUGH, A. J. & SANYAL, A. J. 2005. Design and validation of a histological scoring system for nonalcoholic fatty liver disease. *Hepatology*, 41, 1313-21.
- KOLEV, M. & KEMPER, C. 2017. Keeping It All Going-Complement Meets Metabolism. *Front Immunol*, 8, 1.
- KRAUS, W. E., HOUMARD, J. A., DUSCHA, B. D., KNETZGER, K. J., WHARTON, M. B., MCCARTNEY, J. S., BALES, C. W., HENES, S., SAMSA, G. P., OTVOS, J. D., KULKARNI, K. R. & SLENTZ, C. A. 2002. Effects of the amount and intensity of exercise on plasma lipoproteins. *N Engl J Med*, 347, 1483-92.
- KRUSE, M., SEKI, Y., VUGUIN, P. M., DU, X. Q., FIALLO, A., GLENN, A. S., SINGER, S., BREUHAHN, K., KATZ, E. B. & CHARRON, M. J. 2013. High-fat intake during pregnancy and lactation exacerbates high-fat diet-induced complications in male offspring in mice. *Endocrinology*, 154, 3565-76.
- KUROKAWA, J., NAGANO, H., OHARA, O., KUBOTA, N., KADOWAKI, T., ARAI, S. & MIYAZAKI, T. 2011. Apoptosis inhibitor of macrophage (AIM)

- is required for obesity-associated recruitment of inflammatory macrophages into adipose tissue. *Proc Natl Acad Sci U S A*, 108, 12072-7.
- LADE, A., NOON, L. A. & FRIEDMAN, S. L. 2014. Contributions of metabolic dysregulation and inflammation to nonalcoholic steatohepatitis, hepatic fibrosis, and cancer. *Curr Opin Oncol*, 26, 100-7.
- LAFDIL, F., MILLER, A. M., KI, S. H. & GAO, B. 2010. Th17 cells and their associated cytokines in liver diseases. *Cell Mol Immunol*, 7, 250-4.
- LANG, A., LAHAV, M., SAKHNINI, E., BARSHACK, I., FIDDER, H. H., AVIDAN, B., BARDAN, E., HERSHKOVIZ, R., BAR-MEIR, S. & CHOWERS, Y. 2004. Allicin inhibits spontaneous and TNF-alpha induced secretion of proinflammatory cytokines and chemokines from intestinal epithelial cells. *Clin Nutr*, 23, 1199-208.
- LAU, J. K., ZHANG, X. & YU, J. 2017. Animal models of non-alcoholic fatty liver disease: current perspectives and recent advances. *J Pathol*, 241, 36-44.
- LEE, M. S., KIM, I. H., KIM, C. T. & KIM, Y. 2011. Reduction of body weight by dietary garlic is associated with an increase in uncoupling protein mRNA expression and activation of AMP-activated protein kinase in diet-induced obese mice. *J Nutr*, 141, 1947-53.
- LEWIS, R. D., PERRY, M. J., GUSCHINA, I. A., JACKSON, C. L., MORGAN, B. P. & HUGHES, T. R. 2011. CD55 deficiency protects against atherosclerosis in ApoE-deficient mice via C3a modulation of lipid metabolism. *Am J Pathol*, 179, 1601-7.
- LI, C., LUN, W., ZHAO, X., LEI, S., GUO, Y., MA, J. & ZHI, F. 2015. Allicin alleviates inflammation of trinitrobenzenesulfonic acid-induced rats and suppresses P38 and JNK pathways in Caco-2 cells. *Mediators Inflamm*, 2015, 434692.
- LIM, J., IYER, A., SUEN, J. Y., SEOW, V., REID, R. C., BROWN, L. & FAIRLIE, D. P. 2013. C5aR and C3aR antagonists each inhibit diet-induced obesity, metabolic dysfunction, and adipocyte and macrophage signaling. *FASEB J*, 27, 822-31.
- LIM, J. S., MIETUS-SNYDER, M., VALENTE, A., SCHWARZ, J. M. & LUSTIG, R. H. 2010. The role of fructose in the pathogenesis of NAFLD and the metabolic syndrome. *Nat Rev Gastroenterol Hepatol*, 7, 251-64.

- LIRA, F. S., ROSA, J. C., CUNHA, C. A., RIBEIRO, E. B., DO NASCIMENTO, C. O., OYAMA, L. M. & MOTA, J. F. 2011. Supplementing alpha-tocopherol (vitamin E) and vitamin D3 in high fat diet decrease IL-6 production in murine epididymal adipose tissue and 3T3-L1 adipocytes following LPS stimulation. *Lipids Health Dis*, 10, 37.
- LIU, Z., PATIL, I. Y., JIANG, T., SANCHETI, H., WALSH, J. P., STILES, B. L., YIN, F. & CADENAS, E. 2015. High-fat diet induces hepatic insulin resistance and impairment of synaptic plasticity. *PLoS One*, 10, e0128274.
- MAMANE, Y., CHUNG CHAN, C., LAVALLEE, G., MORIN, N., XU, L. J., HUANG, J., GORDON, R., THOMAS, W., LAMB, J., SCHADT, E. E., KENNEDY, B. P. & MANCINI, J. A. 2009. The C3a anaphylatoxin receptor is a key mediator of insulin resistance and functions by modulating adipose tissue macrophage infiltration and activation. *Diabetes*, 58, 2006-17.
- MARTINS, F., CAMPOS, D. H., PAGAN, L. U., MARTINEZ, P. F., OKOSHI, K., OKOSHI, M. P., PADOVANI, C. R., SOUZA, A. S., CICOGNA, A. C. & OLIVEIRA-JUNIOR, S. A. 2015. High-fat Diet Promotes Cardiac Remodeling in an Experimental Model of Obesity. *Arq Bras Cardiol*, 105, 479-86.
- MATOUSKOVA, P., BARTIKOVA, H., BOUSOVA, I., HANUSOVA, V., SZOTAKOVA, B. & SKALOVA, L. 2014. Reference genes for real-time PCR quantification of messenger RNAs and microRNAs in mouse model of obesity. *PLoS One*, 9, e86033.
- MCARDLE, M. A., FINUCANE, O. M., CONNAUGHTON, R. M., MCMORROW, A. M. & ROCHE, H. M. 2013. Mechanisms of obesity-induced inflammation and insulin resistance: insights into the emerging role of nutritional strategies. *Front Endocrinol (Lausanne)*, 4, 52.
- MELI, R., MATTACE RASO, G., IRACE, C., SIMEOLI, R., DI PASCALE, A., PACIELLO, O., PAGANO, T. B., CALIGNANO, A., COLONNA, A. & SANTAMARIA, R. 2013. High Fat Diet Induces Liver Steatosis and Early Dysregulation of Iron Metabolism in Rats. *PLoS One*, 8, e66570.

- MERLE, N. S., CHURCH, S. E., FREMEAUX-BACCHI, V. & ROUMENINA, L. T. 2015. Complement System Part I - Molecular Mechanisms of Activation and Regulation. *Front Immunol*, 6, 262.
- MIN, H. K., KAPOOR, A., FUCHS, M., MIRSHAHI, F., ZHOU, H., MAHER, J., KELLUM, J., WARNICK, R., CONTOS, M. J. & SANYAL, A. J. 2012. Increased hepatic synthesis and dysregulation of cholesterol metabolism is associated with the severity of nonalcoholic fatty liver disease. *Cell Metab*, 15, 665-74.
- MIURA, K., YANG, L., VAN ROOIJEN, N., OHNISHI, H. & SEKI, E. 2012. Hepatic recruitment of macrophages promotes nonalcoholic steatohepatitis through CCR2. *Am J Physiol Gastrointest Liver Physiol*, 302, G1310-21.
- MORI, T. A. & BEILIN, L. J. 2004. Omega-3 fatty acids and inflammation. *Curr Atheroscler Rep*, 6, 461-7.
- MUNKONDA, M. N., LAPOINTE, M., MIEGUEU, P., ROY, C., GAUVREAU, D., RICHARD, D. & CIANFLONE, K. 2012. Recombinant acylation stimulating protein administration to C3^{-/-} mice increases insulin resistance via adipocyte inflammatory mechanisms. *PLoS One*, 7, e46883.
- MUSSO, G., GAMBINO, R. & CASSADER, M. 2009. Recent insights into hepatic lipid metabolism in non-alcoholic fatty liver disease (NAFLD). *Prog Lipid Res*, 48, 1-26.
- MUTT, S. J., HYPONEN, E., SAARNIO, J., JARVELIN, M. R. & HERZIG, K. H. 2014. Vitamin D and adipose tissue-more than storage. *Front Physiol*, 5, 228.
- NEWMARK, H. L., YANG, K., LIPKIN, M., KOPELOVICH, L., LIU, Y., FAN, K. & SHINOZAKI, H. 2001. A Western-style diet induces benign and malignant neoplasms in the colon of normal C57Bl/6 mice. *Carcinogenesis*, 22, 1871-5.
- NING, C., LIU, L., LV, G., YANG, Y., ZHANG, Y., YU, R., WANG, Y. & ZHU, J. 2015. Lipid metabolism and inflammation modulated by Vitamin D in liver of diabetic rats. *Lipids Health Dis*, 14, 31.
- NUTTALL, F. Q. 2015. Body Mass Index: Obesity, BMI, and Health: A Critical Review. *Nutr Today*, 50, 117-128.

- OGURA, M., NISHIDA, S., ISHIZAWA, M., SAKURAI, K., SHIMIZU, M., MATSUO, S., AMANO, S., UNO, S. & MAKISHIMA, M. 2009. Vitamin D3 modulates the expression of bile acid regulatory genes and represses inflammation in bile duct-ligated mice. *J Pharmacol Exp Ther*, 328, 564-70.
- OH, J., WENG, S., FELTON, S. K., BHANDARE, S., RIEK, A., BUTLER, B., PROCTOR, B. M., PETTY, M., CHEN, Z., SCHECHTMAN, K. B., BERNAL-MIZRACHI, L. & BERNAL-MIZRACHI, C. 2009. 1,25(OH)₂ vitamin d inhibits foam cell formation and suppresses macrophage cholesterol uptake in patients with type 2 diabetes mellitus. *Circulation*, 120, 687-98.
- OLIVER, E., MCGILLICUDDY, F. C., HARFORD, K. A., REYNOLDS, C. M., PHILLIPS, C. M., FERGUSON, J. F. & ROCHE, H. M. 2012. Docosahexaenoic acid attenuates macrophage-induced inflammation and improves insulin sensitivity in adipocytes-specific differential effects between LC n-3 PUFA. *J Nutr Biochem*, 23, 1192-200.
- OUCHI, N., PARKER, J. L., LUGUS, J. J. & WALSH, K. 2011. Adipokines in inflammation and metabolic disease. *Nat Rev Immunol*, 11, 85-97.
- PADIDAR, S., FARQUHARSON, A. J., WILLIAMS, L. M., KEARNEY, R., ARTHUR, J. R. & DREW, J. E. 2012. High-fat diet alters gene expression in the liver and colon: links to increased development of aberrant crypt foci. *Dig Dis Sci*, 57, 1866-74.
- PAGLIALUNGA, S., FISETTE, A., YAN, Y., DESHAIES, Y., BROUILLETTE, J. F., PEKNA, M. & CIANFLONE, K. 2008. Acylation-stimulating protein deficiency and altered adipose tissue in alternative complement pathway knockout mice. *Am J Physiol Endocrinol Metab*, 294, E521-9.
- PAGLIALUNGA, S., SCHRAUWEN, P., ROY, C., MOONEN-KORNIPS, E., LU, H., HESSELINK, M. K., DESHAIES, Y., RICHARD, D. & CIANFLONE, K. 2007. Reduced adipose tissue triglyceride synthesis and increased muscle fatty acid oxidation in C5L2 knockout mice. *J Endocrinol*, 194, 293-304.
- PAREKH, S. & ANANIA, F. A. 2007. Abnormal lipid and glucose metabolism in obesity: implications for nonalcoholic fatty liver disease. *Gastroenterology*, 132, 2191-207.

- PARK, J. M., PARK, C. Y. & HAN, S. N. 2015. High fat diet-Induced obesity alters vitamin D metabolizing enzyme expression in mice. *Biofactors*, 41, 175-82.
- PASCHOS, P. & PALETAS, K. 2009. Non alcoholic fatty liver disease and metabolic syndrome. *Hippokratia*, 13, 9-19.
- PEAKE, P. W., SHEN, Y., WALTHER, A. & CHARLESWORTH, J. A. 2008. Adiponectin binds C1q and activates the classical pathway of complement. *Biochem Biophys Res Commun*, 367, 560-5.
- PERRY, R. J., SAMUEL, V. T., PETERSEN, K. F. & SHULMAN, G. I. 2014. The role of hepatic lipids in hepatic insulin resistance and type 2 diabetes. *Nature*, 510, 84-91.
- PETERSEN, A. M. & PEDERSEN, B. K. 2005. The anti-inflammatory effect of exercise. *J Appl Physiol (1985)*, 98, 1154-62.
- PETERSEN, S. V., THIEL, S., JENSEN, L., STEFFENSEN, R. & JENSENIUS, J. C. 2001. An assay for the mannan-binding lectin pathway of complement activation. *J Immunol Methods*, 257, 107-16.
- PETRASEK, J., DOLGANIUC, A., CSAK, T., KURT-JONES, E. A. & SZABO, G. 2011. Type I interferons protect from Toll-like receptor 9-associated liver injury and regulate IL-1 receptor antagonist in mice. *Gastroenterology*, 140, 697-708 e4.
- PHIELER, J., GARCIA-MARTIN, R., LAMBRIS, J. D. & CHAVAKIS, T. 2013. The role of the complement system in metabolic organs and metabolic diseases. *Semin Immunol*, 25, 47-53.
- PICCHI, A., GAO, X., BELMADANI, S., POTTER, B. J., FOCARDI, M., CHILIAN, W. M. & ZHANG, C. 2006. Tumor necrosis factor-alpha induces endothelial dysfunction in the prediabetic metabolic syndrome. *Circ Res*, 99, 69-77.
- PREISS, D. & SATTAR, N. 2008. Non-alcoholic fatty liver disease: an overview of prevalence, diagnosis, pathogenesis and treatment considerations. *Clin Sci (Lond)*, 115, 141-50.
- QIU, Y., LIU, S., CHEN, H. T., YU, C. H., TENG, X. D., YAO, H. T. & XU, G. Q. 2013. Upregulation of caveolin-1 and SR-B1 in mice with non-alcoholic fatty liver disease. *Hepatobiliary Pancreat Dis Int*, 12, 630-6.

- RENSEN, S. S., SLAATS, Y., DRIESSEN, A., PEUTZ-KOOTSTRA, C. J., NIJHUIS, J., STEFFENSEN, R., GREVE, J. W. & BUURMAN, W. A. 2009a. Activation of the complement system in human nonalcoholic fatty liver disease. *Hepatology*, 50, 1809-17.
- RENSEN, S. S., SLAATS, Y., NIJHUIS, J., JANS, A., BIEGHS, V., DRIESSEN, A., MALLE, E., GREVE, J. W. & BUURMAN, W. A. 2009b. Increased hepatic myeloperoxidase activity in obese subjects with nonalcoholic steatohepatitis. *Am J Pathol*, 175, 1473-82.
- RICHTER, E. A. & HARGREAVES, M. 2013. Exercise, GLUT4, and skeletal muscle glucose uptake. *Physiol Rev*, 93, 993-1017.
- RICKLIN, D., HAJISHENGALLIS, G., YANG, K. & LAMBRIS, J. D. 2010. Complement: a key system for immune surveillance and homeostasis. *Nat Immunol*, 11, 785-97.
- SAAD, A. F., VIRELLA, G., CHASSEREAU, C., BOACKLE, R. J. & LOPES-VIRELLA, M. F. 2006. OxLDL immune complexes activate complement and induce cytokine production by MonoMac 6 cells and human macrophages. *J Lipid Res*, 47, 1975-83.
- SALTIEL, A. R. & KAHN, C. R. 2001. Insulin signalling and the regulation of glucose and lipid metabolism. *Nature*, 414, 799-806.
- SARAFIDIS, P. A. & BAKRIS, G. L. 2007. Non-esterified fatty acids and blood pressure elevation: a mechanism for hypertension in subjects with obesity/insulin resistance? *J Hum Hypertens*, 21, 12-9.
- SCHENK, S., SABERI, M. & OLEFSKY, J. M. 2008. Insulin sensitivity: modulation by nutrients and inflammation. *J Clin Invest*, 118, 2992-3002.
- SCHONTHAL, A. H. 2012. Endoplasmic reticulum stress: its role in disease and novel prospects for therapy. *Scientifica (Cairo)*, 2012, 857516.
- SCHWEN, L. O., HOMEYER, A., SCHWIER, M., DAHMEN, U., DIRSCH, O., SCHENK, A., KUEPFER, L., PREUSSER, T. & SCHENK, A. 2016. Zonated quantification of steatosis in an entire mouse liver. *Comput Biol Med*, 73, 108-18.
- SCORLETTI, E. & BYRNE, C. D. 2013. Omega-3 fatty acids, hepatic lipid metabolism, and nonalcoholic fatty liver disease. *Annu Rev Nutr*, 33, 231-48.

- SEGERS, F. M., VERDAM, F. J., DE JONGE, C., BOONEN, B., DRIESSEN, A., SHIRI-SVERDLOV, R., BOUVY, N. D., GREVE, J. W., BUURMAN, W. A. & RENSEN, S. S. 2014. Complement alternative pathway activation in human nonalcoholic steatohepatitis. *PLoS One*, 9, e110053.
- SHALHOUB, J., FALCK-HANSEN, M. A., DAVIES, A. H. & MONACO, C. 2011. Innate immunity and monocyte-macrophage activation in atherosclerosis. *J Inflamm (Lond)*, 8, 9.
- SHAPIRO, H., SINGER, P. & ATTAL-SINGER, J. 2009. Comment on: Reyna et al. (2008) Elevated toll-like receptor 4 expression and signaling in muscle from insulin-resistant subjects. *Diabetes* 57:2595-2602. *Diabetes*, 58, e5; author reply e6-7.
- SHARDA, D. R., YU, S., RAY, M., SQUADRITO, M. L., DE PALMA, M., WYNN, T. A., MORRIS, S. M., JR. & HANKEY, P. A. 2011. Regulation of macrophage arginase expression and tumor growth by the Ron receptor tyrosine kinase. *J Immunol*, 187, 2181-92.
- SHI, H., KOKOEVA, M. V., INOUE, K., TZAMELI, I., YIN, H. & FLIER, J. S. 2006. TLR4 links innate immunity and fatty acid-induced insulin resistance. *J Clin Invest*, 116, 3015-25.
- SHIMASAKI, S. & LING, N. 1991. Identification and molecular characterization of insulin-like growth factor binding proteins (IGFBP-1, -2, -3, -4, -5 and -6). *Prog Growth Factor Res*, 3, 243-66.
- SIMOPOULOS, A. P. 2002. Omega-3 fatty acids in inflammation and autoimmune diseases. *J Am Coll Nutr*, 21, 495-505.
- SINGHANIA, N., PURI, D., MADHU, S. V. & SHARMA, S. B. 2008. Assessment of oxidative stress and endothelial dysfunction in Asian Indians with type 2 diabetes mellitus with and without macroangiopathy. *QJM*, 101, 449-55.
- SOLEIMANI, D., PAKNAHAD, Z., ASKARI, G., IRAJ, B. & FEIZI, A. 2016. Effect of garlic powder consumption on body composition in patients with nonalcoholic fatty liver disease: A randomized, double-blind, placebo-controlled trial. *Adv Biomed Res*, 5, 2.
- STAUFFER, J. K., SCARZELLO, A. J., JIANG, Q. & WILTROUT, R. H. 2012. Chronic inflammation, immune escape, and oncogenesis in the liver: a unique neighborhood for novel intersections. *Hepatology*, 56, 1567-74.

- STEIN, E. M. & SHANE, E. 2011. Vitamin D in organ transplantation. *Osteoporos Int*, 22, 2107-18.
- STEINER, T., FRANCESCUT, L., BYRNE, S., HUGHES, T., JAYANTHI, A., GUSCHINA, I., HARWOOD, J., CIANFLONE, K., STOVER, C. & FRANCIS, S. 2014. Protective role for properdin in progression of experimental murine atherosclerosis. *PLoS One*, 9, e92404.
- STOVER, C. M. 2015. Editorial: Antimicrobial Peptides and Complement - Maximising the Inflammatory Response. *Front Immunol*, 6, 491.
- STOVER, C. M., LUCKETT, J. C., ECHTENACHER, B., DUPONT, A., FIGGITT, S. E., BROWN, J., MANNEL, D. N. & SCHWAEBLE, W. J. 2008. Properdin Plays a Protective Role in Polymicrobial Septic Peritonitis. *The Journal of Immunology*, 180, 3313-3318.
- STREETZ, K. L., WUSTEFELD, T., KLEIN, C., KALLEN, K. J., TRONCHE, F., BETZ, U. A., SCHUTZ, G., MANNIS, M. P., MULLER, W. & TRAUTWEIN, C. 2003. Lack of gp130 expression in hepatocytes promotes liver injury. *Gastroenterology*, 125, 532-43.
- SUGANYA, N., BHAKKIYALAKSHMI, E., SURIYANARAYANAN, S., PAULMURUGAN, R. & RAMKUMAR, K. M. 2014. Quercetin ameliorates tunicamycin-induced endoplasmic reticulum stress in endothelial cells. *Cell Prolif*, 47, 231-40.
- TAKAHASHI, Y. & FUKUSATO, T. 2014. Histopathology of nonalcoholic fatty liver disease/nonalcoholic steatohepatitis. *World J Gastroenterol*, 20, 15539-48.
- TAKEMOTO, M., YOKOTE, K., NISHIMURA, M., SHIGEMATSU, T., HASEGAWA, T., KON, S., UEDE, T., MATSUMOTO, T., SAITO, Y. & MORI, S. 2000. Enhanced expression of osteopontin in human diabetic artery and analysis of its functional role in accelerated atherogenesis. *Arterioscler Thromb Vasc Biol*, 20, 624-8.
- THACKER, S. G., ROUSSET, X., ESMAIL, S., ZARZOUR, A., JIN, X., COLLINS, H. L., SAMPSON, M., STONIK, J., DEMOSKY, S., MALIDE, D. A., FREEMAN, L., VAISMAN, B. L., KRUTH, H. S., ADELMAN, S. J. & REMALEY, A. T. 2015. Increased plasma cholesterol esterification by LCAT reduces diet-induced atherosclerosis in SR-BI knockout mice. *J Lipid Res*, 56, 1282-95.

- TIMLIN, M. T. & PARKS, E. J. 2005. Temporal pattern of de novo lipogenesis in the postprandial state in healthy men. *Am J Clin Nutr*, 81, 35-42.
- TINIAKOS, D. G., VOS, M. B. & BRUNT, E. M. 2010. Nonalcoholic fatty liver disease: pathology and pathogenesis. *Annu Rev Pathol*, 5, 145-71.
- TOSELLO-TRAMPONT, A. C., LANDES, S. G., NGUYEN, V., NOVOBRANTSEVA, T. I. & HAHN, Y. S. 2012. Kupffer cells trigger nonalcoholic steatohepatitis development in diet-induced mouse model through tumor necrosis factor-alpha production. *J Biol Chem*, 287, 40161-72.
- TREPANOWSKI, J. F., MEY, J. & VARADY, K. A. 2015. Fetuin-A: a novel link between obesity and related complications. *Int J Obes (Lond)*, 39, 734-41.
- UYSAL, K. T., WIESBROCK, S. M., MARINO, M. W. & HOTAMISLIGIL, G. S. 1997. Protection from obesity-induced insulin resistance in mice lacking TNF-alpha function. *Nature*, 389, 610-4.
- VASANKARI, T. J., KUJALA, U. M., VASANKARI, T. M. & AHOTUPA, M. 1998. Reduced oxidized LDL levels after a 10-month exercise program. *Med Sci Sports Exerc*, 30, 1496-501.
- VODOVOTZ, Y., LIU, S., MCCLOSKEY, C., SHAPIRO, R., GREEN, A. & BILLIAR, T. R. 2001. The hepatocyte as a microbial product-responsive cell. *J Endotoxin Res*, 7, 365-73.
- VON HURST, P. R., STONEHOUSE, W. & COAD, J. 2010. Vitamin D supplementation reduces insulin resistance in South Asian women living in New Zealand who are insulin resistant and vitamin D deficient - a randomised, placebo-controlled trial. *Br J Nutr*, 103, 549-55.
- VONGHIA, L., MICHELSEN, P. & FRANQUE, S. 2013. Immunological mechanisms in the pathophysiology of non-alcoholic steatohepatitis. *Int J Mol Sci*, 14, 19867-90.
- VORS, C., PINEAU, G., DRAI, J., MEUGNIER, E., PESENTI, S., LAVILLE, M., LAUGERETTE, F., MALPUECH-BRUGERE, C., VIDAL, H. & MICHALSKI, M. C. 2015. Postprandial Endotoxemia Linked With Chylomicrons and Lipopolysaccharides Handling in Obese Versus Lean Men: A Lipid Dose-Effect Trial. *J Clin Endocrinol Metab*, 100, 3427-35.

- WANG, Y., LAM, K. S., KRAEGER, E. W., SWEENEY, G., ZHANG, J., TSO, A. W., CHOW, W. S., WAT, N. M., XU, J. Y., HOO, R. L. & XU, A. 2007. Lipocalin-2 is an inflammatory marker closely associated with obesity, insulin resistance, and hyperglycemia in humans. *Clin Chem*, 53, 34-41.
- WANG, Y. C., MCPHERSON, K., MARSH, T., GORTMAKER, S. L. & BROWN, M. 2011. Health and economic burden of the projected obesity trends in the USA and the UK. *Lancet*, 378, 815-25.
- WANG, Z., YAN, J., LIN, H., HUA, F., WANG, X., LIU, H., LV, X., YU, J., MI, S., WANG, J. & HU, Z. W. 2013. Toll-like receptor 4 activity protects against hepatocellular tumorigenesis and progression by regulating expression of DNA repair protein Ku70 in mice. *Hepatology*, 57, 1869-81.
- WEISBERG, S. P., MCCANN, D., DESAI, M., ROSENBAUM, M., LEIBEL, R. L. & FERRANTE, A. W., JR. 2003. Obesity is associated with macrophage accumulation in adipose tissue. *J Clin Invest*, 112, 1796-808.
- WELLEN, K. E. & HOTAMISLIGIL, G. S. 2003. Obesity-induced inflammatory changes in adipose tissue. *J Clin Invest*, 112, 1785-8.
- WESTERBACKA, J., LAMMI, K., HAKKINEN, A. M., RISSANEN, A., SALMINEN, I., ARO, A. & YKI-JARVINEN, H. 2005. Dietary fat content modifies liver fat in overweight nondiabetic subjects. *J Clin Endocrinol Metab*, 90, 2804-9.
- WILCOX, G. 2005. Insulin and insulin resistance. *Clin Biochem Rev*, 26, 19-39.
- WOUTERS, K., VAN GORP, P. J., BIEGHS, V., GIJBELS, M. J., DUIMEL, H., LUTJOHANN, D., KERKSIEK, A., VAN KRUCHTEN, R., MAEDA, N., STAELS, B., VAN BILSEN, M., SHIRI-SVERDLOV, R. & HOFKER, M. H. 2008. Dietary cholesterol, rather than liver steatosis, leads to hepatic inflammation in hyperlipidemic mouse models of nonalcoholic steatohepatitis. *Hepatology*, 48, 474-86.
- XU, M. J., FENG, D., WU, H., WANG, H., CHAN, Y., KOLLS, J., BORREGAARD, N., PORSE, B., BERGER, T., MAK, T. W., COWLAND, J. B., KONG, X. & GAO, B. 2015. Liver is the major source of elevated

- serum lipocalin-2 levels after bacterial infection or partial hepatectomy: a critical role for IL-6/STAT3. *Hepatology*, 61, 692-702.
- XU, W., BERGER, S. P., TROUW, L. A., DE BOER, H. C., SCHLAGWEIN, N., MUTSAERS, C., DAHA, M. R. & VAN KOOTEN, C. 2008. Properdin binds to late apoptotic and necrotic cells independently of C3b and regulates alternative pathway complement activation. *J Immunol*, 180, 7613-21.
- YEH, M. M. & BRUNT, E. M. 2007. Pathology of nonalcoholic fatty liver disease. *Am J Clin Pathol*, 128, 837-47.
- YIN, K., YOU, Y., SWIER, V., TANG, L., RADWAN, M. M., PANDYA, A. N. & AGRAWAL, D. K. 2015. Vitamin D Protects Against Atherosclerosis via Regulation of Cholesterol Efflux and Macrophage Polarization in Hypercholesterolemic Swine. *Arterioscler Thromb Vasc Biol*, 35, 2432-42.
- YIN, Y., YU, Z., XIA, M., LUO, X., LU, X. & LING, W. 2012. Vitamin D attenuates high fat diet-induced hepatic steatosis in rats by modulating lipid metabolism. *Eur J Clin Invest*, 42, 1189-96.
- ZANOTTI, S., GIBERTINI, S., DI BLASI, C., CAPPELLETTI, C., BERNASCONI, P., MANTEGAZZA, R., MORANDI, L. & MORA, M. 2011. Osteopontin is highly expressed in severely dystrophic muscle and seems to play a role in muscle regeneration and fibrosis. *Histopathology*, 59, 1215-28.
- ZHANG, H., DELLSPERGER, K. C. & ZHANG, C. 2012. The link between metabolic abnormalities and endothelial dysfunction in type 2 diabetes: an update. *Basic Res Cardiol*, 107, 237.
- ZOPPINI, G., GALLETTI, A., TARGHER, G., BRANGANI, C., PICHIRI, I., NEGRI, C., STOICO, V., CACCIATORI, V. & BONORA, E. 2013. Glycated haemoglobin is inversely related to serum vitamin D levels in type 2 diabetic patients. *PLoS One*, 8, e82733.